BABCOCK PROPERTY HOLDINGS, L.L.C.

17837 Murdock Circle Port Charlotte, Florida 33948

July 27, 2012

VIA FEDEX

Janette Knowlton, County Attorney Charlotte County Attorney's Office 18500 Murdock Circle Port Charlotte, FL 33948-1094

Michael D. Hunt, County Attorney Lee County Attorney's Office 2115 Second Street, 6th Floor P.O. Box 398 Fort Myers, FL 33902-0398

RE: August 11, 2009 Settlement Agreement

Modeling Report and Analysis

Dear Ms. Knowlton and Mr. Hunt:

On August 11, 2009 we entered into the attached Settlement Agreement ("Agreement") in which Babcock Property Holdings, LLC ("Babcock") committed to undertake certain surface water and ground water modeling. Specifically, pursuant to Sections 6(c)(i) & (ii), Babcock was to create a "Calibrated Model," a "Post Community Conditions Model," and a "Natural Conditions Model," all as described in the Agreement. Since entering into the Agreement, we have undertaken and completed these three models.

Over the last three years, Babcock has invested significant time, money, and resources in the development of these three models. This modeling effort, which encompasses over 310 square miles, was unprecedented, extensive and complex. The models are based on appropriate data, sound scientific and engineering assumptions, and principals, and have been subject to quality control and assurance.

For your reference, we have attached a copy of the report and executive summary of the modeling process and results. This report identifies the process undertaken, the data utilized, and the results of the modeling effort, including a comparison of the three models. As demonstrated therein, the Post-development Conditions will help to mitigate changes in groundwater recharge, decrease average daily rates during storm events, and increase the wetland hydroperiods within the Babcock Ranch Community ("BRC") as compared to the Current Conditions. Moreover, the Post-development Conditions simulation showed that no adverse impacts to downstream receiving bodies or environmental features would occur. When the three conditions are fully analyzed and compared, the model demonstrates that the Post-development Conditions

RECEIVED BY

1:39

Janette Knowlton, County Attorney, Charlotte County Attorney's Office Michael D. Hunt, County Attorney, Lee County Attorney's Office July 27, 2012
Page 2

effectuates progress towards historic flow rates and hydroperiods of certain freshwater marsh wetlands that would have been expected under Natural Conditions.

With this, the modeling efforts are completed. In accordance with the Agreement, Babcock will consider the results of the three models in the preparation of future Construction ERP's for site development design and restoration activities.

Sincerely yours,

Thomas J. Danahy

President

Enclosures

cc: Mr. Roland Ottolini (w/encl.)

Donna Marie Collins, Esq. (w/encl.)

Luna E. Phillips, Esq. (w/encl.)

Brian M. Seymour, Esq. (w/encl.)

Mr. Gary Nelson (w/encl.)

Commissioner Bob Starr, Charlotte County, District 1 (w/o encl.)

Worky

Commissioner Christopher Constance, Charlotte County, District 2 (w/o encl.)

Commissioner Robert Skidmore, Charlotte County, District 3 (w/o encl.)

Commissioner Stephen R. Deutsch, Charlotte County, District 4 (w/o encl.)

Commissioner Tricia Duffy, Charlotte County, District 5 (w/o encl.)

Commissioner John E. Manning, Lee County, District 1 (w/o encl.)

Commissioner Brian Bigelow, Lee County, District 2 (w/o encl.)

Commissioner Ray Judah, Lee County, District 3 (w/o encl.)

Commissioner Tammy Hall, Lee County, District 4 (w/o encl.)

Commissioner Frank Mann, Lee County, District 5 (w/o encl.)

SETTLEMENT AGREEMENT

Petitioner, Lee County Florida, a political subdivision of the State of Florida ("Lee County"), Respondent, Charlotte County, Florida a political subdivision of the State of Florida ("Charlotte County"), and Intervener, Babcock Property Holdings, LLC ("Babcock") stipulate and agree to the following in settlement of all matters which have been or could have been raised in the case of Lee County v. Charlotte County, Case #08-174CA, pending in the Circuit Court of the Twentieth Judicial Circuit in and for Charlotte County, Florida (the "Lawsuit").

RECITALS

- A. Lee County filed the Lawsuit against Charlotte County on January 11, 2008 alleging inconsistencies between the Master DRI DO (as defined below) and various provisions of the Charlotte County Comprehensive Plan.
- B. Babcock intervened in the Lawsuit and maintains all rights as a party thereto.
- C. Lee County, Charlotte County, and Babcock desire to settle the Lawsuit.
- D. This Settlement Agreement is being entered into in order to settle contested disputes over multiple issues, the resolution of which is uncertain, and regarding which the Parties have differences of opinion. Regardless of these differences, the Parties acknowledge that these are matters of interpretation and recognize the strength with which the other party holds such opinions. None of the provisions set forth in this Settlement Agreement constitute admissions by any of the parties. The purpose of this Settlement Agreement is to resolve and settle all claims in the Lawsuit.

- E. Babcock and Charlotte County entered into the <u>Development Agreement Between Board of County Commissioners of Charlotte County, Florida, and MSKP III, Inc. on April 20, 2006 ("Charlotte DA"). The Charlotte DA addresses the provision of various infrastructure facilities which may be required to mitigate impacts of development undertaken pursuant to Babcock's Master Development of Regional Impact Development Order adopted by Charlotte County on December 13, 2007 ("Master DRI DO").</u>
- F. Babcock and Lee County entered into the <u>Babcock Ranch Community Road Planning Agreement Regarding the Charlotte County Babcock Ranch Overlay District Amendments</u> on May 23, 2006 ("Lee Road Agreement"). The Lee Road Agreement addresses various road facility improvements which may be required to mitigate the impacts in Lee County of development undertaken pursuant to Babcock's Master DRI DO on roads in Lee County. A Memorandum of Understanding was executed by Babcock and Lee County pursuant to approval by the Lee County Commission on September 23, 2008 ("Memorandum of Understanding") in furtherance of the Lee Road Agreement. The Charlotte DA, the Lee Road Agreement, and the Memorandum of Understanding may be referred to collectively as the "Agreements".
- G. In the Lawsuit, Lee County has alleged transportation inconsistencies which can generally be characterized as follows: (1) the Master DRI DO does not require that the traffic analysis for the Increments be done cumulatively, thereby potentially underestimating the project impacts at each Incremental stage; (2) the full impact to roads in Lee County are not considered and mitigated because the buildout analysis used for the Master DRI DO was based on a model that was not approved and

accepted by the reviewing agencies, as required by the Charlotte DA and Lee Road Agreement; (3) the Master DRI DO does not include as a condition of approval satisfaction of the terms of the Lee Road Agreement; and (4) Map H of the approved Master DRI DO is inconsistent with BROD Map 11e of the Charlotte County Comprehensive Plan. Charlotte County and Babcock do not agree with these alleged transportation inconsistencies; however, they have agreed to settle the litigation in accordance with the following terms.

Now, therefore for good and valuable consideration and the mutual promises set forth herein, the parties agree to the following:

1. The Recitals and all exhibits attached hereto are incorporated herein and made a part hereof.

TRAFFIC

2.

(a) Babcock, Charlotte County and Lee County agree that the Florida Department of Transportation ("FDOT") Regional Travel Demand Model (2008 D1 Districtwide Model) with the addition by FDOT of the existing plus committed ("E+C") roadway network, which is acceptable for use by Babcock, is hereby accepted as the model contemplated by the Charlotte DA, the Lee Road Agreement, and the Memorandum of Understanding for use in the initial Master Traffic Study and revisions thereto as contemplated by and updated in accordance with the Master DRI DO and for the Incremental traffic studies undertaken thereto. Future updates of the Master Traffic Study also may be based on adjustments of the 2008 D1 Districtwide Model pursuant to

professionally accepted techniques applicable to communities of the size, location, mix of uses, and design of Babcock or other travel demand modeling techniques and data that reflect the size, location, mix of uses, and "smart growth" design of the Project, as determined at the traffic methodology meetings required before the updates commence.

- (b) Charlotte County and Lee County, through their designated representatives, will be invited to participate in the traffic methodology meeting(s) for the Master Traffic Study revision(s) and shall provide any comments on or objections to the methodology in writing to the other parties hereto within ten (10) business days of said methodology meeting(s). If a county has no comment or objection, then it shall provide a letter so stating within the same ten (10) business day period. Any revisions proposed by Babcock to the methodology shall be provided to each county in writing and each county shall provide any written comments or objections within ten (10) business days of receipt. If a county has no comment or objection, it shall provide a letter so stating within the same ten (10) business day period. Failure of a party to respond in writing within the required ten (10) business day period shall constitute no objection and no comment.
- (c) The same process described in provision 2(b) above shall be used with respect to the Master list of road improvements to be generated by Babcock in accordance with the Master DRI DO, based upon the use of the 2008 DI District-wide Model and E+C roadway network as referenced in provision 2(a) above.

(a) In order to address the concerns of the Florida Department of Community Affairs and Lee County about a cumulative traffic analysis Charlotte County adopted on June 17, 2008 an amendment to the language in the Babcock Master DRI DO, which revised Section 5.C.(1) and the findings of fact and conclusions of law as follows:

Section 5.C.(1)(f)

Each Increment will constitute a separate DRI, and each subsequent Incremental traffic study will include the any previously evaluated and mitigated Increment as background Project traffic consistent with Sections 380.06(21)(b) and 380.0651, F.S., and 9J-2.045, F.A.C. Phases of an Increment that alone do not constitute a DRI will be aggregated with previous or subsequent phases and analyzed cumulatively as a DRI. Mitigation provided by any previously evaluated Increment shall be credited to the overall impact of the Project.

Findings of Fact and Conclusions of Law

- 5. The Developer proposes to develop Babcock Charlotte in accordance with the Babcock Master Concept Plan (Map "H" in the AMDA) attached hereto as Exhibit "B" attached hereto and made a part hereof. Map "H" will be further revised as part of each Incremental development order. Map "H", and as further revised in each Increment, constitutes the revised Master Plan for the Babcock Ranch Overlay District in the County's Comprehensive Plan and the revised Exhibit C-1 in the Charlotte Development Agreement. The development program authorized by this development order is as follows ("Development Program" or "Project")
- (b) The intent of the language in Section 5.C.(1) as revised above, is that as each increment is submitted for review, the transportation analysis for that increment will include the traffic from previous increments as Project traffic so that the cumulative impacts of Project traffic can be determined and addressed. The overall mitigation obligation for combined increments will be calculated and then

there will be an offset for the value of mitigation paid for previous increments (e.g., cash payments, dedications, equipment and construction). The balance of the mitigation obligation will reflect the mitigation for the subject increment, as well as any unaddressed cumulative impacts to the road network from Project traffic. If previously provided mitigation results in additional roadway capacity that is reflected in the E+C network for a subsequent increment, the value of the mitigation that resulted in the improved network will not be included in the credit calculation for that increment By way of one "pipelining" example, if in the first increment, the developer elects with the proper county concurrence, to "pipeline" his proportionate share obligation into a specific improvement, and the developer benefits from the added road capacity in the analysis of subsequent increments, the cash value of that pipelined improvement from the previous increment will not be included in the offset/credit against the cumulative proportionate share obligation for subsequent increments.

- (c) The parties agree that in no event will the Babcock Ranch Community receive "double credit" or be "double charged" for traffic mitigation. The specific details of traffic mitigation, including credits, will be addressed in the Incremental traffic methodology meeting memoranda and will be reflected in the Incremental Development Orders and associated developer agreements.
- 4. The methodology for the use of the 2008 D1 Districtwide Model in the various Incremental traffic studies will be consistent with the methodology contained within the Master DRI DO and further refined as part of the traffic methodology for the first Application for Incremental Development Approval ("AIDA"). Any changes to the

methodology proposed thereafter by Babcock shall be subject to comments and objections by Charlotte County and Lee County as set forth in (2)(b) above.

5. In order to address Lee County's concerns about the inconsistencies between the Charlotte Plan BROD Map 11-e and Map H of the Master DRI DO, Charlotte County agrees to schedule for public hearing the amendment of the maps in the Charlotte County Comprehensive Plan at the earliest convenient opportunity to be consistent with the Master Concept Plan (Map H) approved for the Babcock AMDA. At the same public hearing, Babcock will request and Charlotte County will consider the following amendment to Section 5.C(1) of the Master Babcock DRI MDO as follows:

Section 5.C.(1)

...The traffic study in support of each Increment will estimate the trips external to the Property for that Incremental development program and may will include the following...

WATER

6. (a) Babcock, Lee County, and Charlotte County recognize that certain existing man-made changes in the general area of the Babcock Ranch Community property as described in the Master DRI DO ("Community" or "Project") and the Caloosahatchee River have resulted in alterations to the water regime in those areas. In some cases, returning that water regime to the conditions that existed prior to those man-made changes may create unacceptable and adverse impacts on other properties and, therefore, may not be desirable or permittable under the applicable regulations. Man-made changes within the Community, and on lands adjacent thereto, have affected wetlands and habitat conditions. The removal by Babcock of certain man-made features, such as Big Island Dike, Big Island Canal, the Curry Lake Canal, and SR31

may not be reasonable or practicable. However, modifications by Babcock to some of these features may be reasonable and practicable.

- (b) Babcock, Lee County, and Charlotte County desire to achieve the objectives set forth in provisions 6(b)(i) and (ii) to the reasonable extent practicable, recognizing that in some instances balance between objectives will be necessary to obtain a feasible outcome. For the purposes of this provision 6, the term "practicable" means capable of being done with the means at hand and the circumstances as they are taking into account legal permissibility, cost/benefit, and the physical impacts on persons and property both within and outside the Community.
- (i) Babcock desires to improve the current management of surface waters within the Community including, but not limited to, and where practicable, decreasing downstream flooding, increasing base flows in the dry season, sustaining, or improving where impaired, the quality of water leaving the Community, increasing the detention time of stormwater over that of pre-Community conditions (thereby effectuating progress towards flow rates more reflective of natural conditions), providing selected water control structures intended for the improvement of associated flowways and the restoration, re-hydration, and connectivity of certain wetlands. Such improvement will be achieved without material adverse effect to lands outside of the Community located within Charlotte County and within Lee County south to the Caloosahatchee River.
- (ii) Lee County desires to restore and enhance wetlands and natural waters, reduce flooding, restore/improve wetland hydroperiod, and improve water quality outside the Community where practicable.

- (c) In an effort to advance, to the degree reasonably practicable, the objectives set forth in provisions 6(b)(i) and (ii), Babcock, Lee County, and Charlotte County agree as follows:
- (i) Babcock will develop a calibrated continuous simulation integrated surface water and groundwater model for the sub-basins delineated on Exhibit #1. The detailed calibration is to be determined based on the list of primary parameters (attached as Exhibit #2), and accompanying Data Set (attached as Exhibit #3). The model simulation time period will be verified to insure a representative sampling of average and extreme wet and dry periods. Stream flow and stage data for this analysis will be obtained from the Telegraph Cypress Water Management District (TCWMD) records from 1987 to 2005 and other verified applicable data sets. The model will be calibrated and verified using two forms of data. The first form of data (quantitative) such as the stages, water levels, and flows from the TCWMD records, other applicable data sets, and additional data gathered by Babcock from the second quarter of 2006 through the third quarter of 2008 will be used to calibrate the model. The second form of data (qualitative) such as available permits, studies, onsite observations and wetland indicators, will be used to verify the calibrated model. The model report will explain how these data compare to the model output. The model will be calibrated to pre-Community conditions ("Calibrated Model"). Upon completion of the Calibrated Model, Babcock will then develop a second model by modifying the Calibrated Model to reflect the proposed development conditions as shown on the Conceptual Environmental Resource Permit ("ERP") application ("post-Community Conditions") pending before the SFWMD (Application Number 070330-5), including the proposed environmental

enhancement conditions ("ERP Model" or "Post-Community Conditions Model"). The Lee County Division of Natural Resources ("DNR"), Charlotte County and Babcock will confer during the development of the models. Babcock will provide the following model development deliverables to Lee County and Charlotte County for review and comment: Model domain and input and calibration data; Regional Modflow/GSFLOW model setup and scenario details; Modflow/GSFLOW model calibration results; GSFLOW scenario results. The models will be based on sound scientific and engineering assumptions and principles and best available data, and will be subjected to quality control and quality assurance in accordance with normal industry accepted standards, in order to assure an accurate calibrated and verified model. A list of guidances/guidelines for evaluating hydrologic and hydraulic models is provided in Exhibit #4 as references for sound scientific and engineering principles.

(ii) Additionally, Babcock will develop a third model to be known as the "Natural Conditions Model." The Natural Conditions Model will estimate historic water levels, flow rates, and patterns of flow across the Community south to the Caloosahatchee River. The Natural Conditions Model will initially be based upon the Calibrated Model described in 6(c)(i) recognizing, however, the absence of natural conditions data to calibrate and verify the Natural Conditions Model. The Natural Conditions Model will simulate the elimination of the current man-made ditches, weirs, dikes, roads, berms, mines, canals, farm field detention, farm fields, and pastures shown on Exhibit #5, and will include natural habitats instead of farm fields and pastures. Upon completion of the Natural Conditions Model, Babcock will compare the Natural Conditions Model results to the pre-Community and post-Community

hydroperiod conditions for the area shown on Exhibit #5. The results of all three models will be considered by Babcock in the preparation of each of its Construction ERP's for site development design and restoration activities in an effort to effectuate progress toward historic flow rates and hydroperiods of certain freshwater marsh wetlands more reflective of natural conditions, taking into account the practical consequences to the development of the Community and to the areas outside of the Community. The parties acknowledge that the intent of this provision may require modification of the conceptual ERP plan approved by the SFWMD in the Conceptual ERP permit, and/or the Master Plan adopted in the Master DRI DO.

- (iii) Extended hydroperiods for the freshwater marsh wetlands will be determined by the ERP post-Community Model results for the three (3) assessment validation sites shown on Exhibit #6. Babcock will endeavor to effectuate progress towards hydroperiods of certain freshwater marsh wetlands more reflective of natural conditions.
- (iv) The parties acknowledge and agree that the SFWMD is the entity responsible for monitoring compliance with the Conceptual ERP.
- (v) Babcock will provide Lee County and Charlotte County with all surface water and groundwater data it collects and the analytical results of such data, including, but not limited to, data provided to the SFWMD for the Conceptual ERP application. In addition, Babcock will provide Lee County and Charlotte County with copies of the compliance reports submitted to the SFWMD pursuant to conditions in the Conceptual ERP. Data will be submitted in the most current version of Access, Excel or

in text file format, suitable for import into the referenced programs. The referenced reports will be submitted as Adobe pdf files in addition to printed copy.

- (d) Surface water conveyances carry water from the Community into Lee County. Babcock and Lee County will discuss the ERP Model results with regard to whether different quantities of water, different flow rates, and different schedules could reasonably be made available through those conveyances to properties in Lee County without a material adverse impact on meeting the provisions in 6(b)(i). One objective is to reduce downstream flooding. Flow rates and volumes will be evaluated at all outfalls from the Community for the pre-Community, post-Community, and Natural conditions for average annual, 5 year, 25 year and 100 year storm events. These flow rate and volume analyses will be conducted one time as part of the initial model runs for each of these three Conditions.
- (e) The Community's hydrology contributes to the hydrology for the downstream Lee County areas. The Water Quality Monitoring Plan, attached hereto as Exhibit #7, is being implemented and the resulting data made available as described in 6(c)(v). The Water Quality Monitoring Plan has been developed and is being implemented in accordance with the State of Florida Department of Environmental Protection's Standard Operating Procedures for Field Activities, most recent edition. Parameters tested will be as detailed in Exhibit #7 at the locations shown in Exhibit #7.
- (f) A portion of Babcock's property is located in Lee County immediately south of the Community ("Babcock-Lee Property"). Babcock and Lee are contemplating the sale of a portion of the Babcock-Lee Property to Lee County. That sale may occur with one closing or with multiple closings on portions over a period of time. In the event

the sale occurs, the surface and groundwater monitoring well locations situated on the Babcock-Lee Property within the area(s) purchased and as shown on Exhibit 7d-1, attached hereto, will be relocated to Charlotte County with respect to the area(s) purchased upon closing in accordance with the pertinent locations shown on Exhibit 7d-2, attached hereto.

IMPASSE MEDIATION

- 7. In the event an impasse arises under either provision 2, 3, 4, 5, or 6 of this Settlement Agreement, Charlotte County, Lee County, and Babcock ("Dispute Parties") agree to use the following dispute resolution procedures:
- (a) First, a Dispute Party which believes that an impasse exists shall have its designee notify the other Dispute Parties' designees in writing of the nature of the dispute or impasse. Within fourteen (14) calendar days of receipt of said notice, the Dispute Parties shall confer in person in an effort to resolve the impasse (the "Conference Period").
- (b) Second, in the event that the dispute or impasse is not resolved within the Conference Period, the Dispute Parties will mediate the impasse under the statutes and rules governing mediation in the State of Florida. If the Dispute Parties cannot agree on a mediator within five (5) business days of the end of Conference Period, then the Dispute Parties shall seek the assistance of the Florida Conflict Resolution Consortium (the "FCRC") located at Florida State University in selecting a mediator by mutually requesting that FCRC provide a list of potential mediators. Any mediator selected, or sought to be appointed as provided below, must be a mediator certified by the Supreme Court of the State of Florida to mediate civil cases, unless otherwise

agreed to by the Dispute Parties, and must have substantial experience in land use and environmental matters. If the Dispute Parties cannot agree on a mediator within five (5) business days following receipt of the list from FCRC, they will then request that the FCRC select a mediator. The Dispute Parties agree to accept the mediator as selected by the FCRC. The costs of obtaining the appointment of a mediator and the fees and expenses of the mediation shall be borne equally by the Dispute Parties, unless otherwise agreed. Each Dispute Party will bear the cost of its own attorney fees, consultant fees, and any other costs or fees associated with its participation in the mediation. Any mediation will be conducted as expeditiously as possible and the Dispute Parties agree to use all reasonable efforts to facilitate an expeditious mediation.

(c) In the event that the Dispute Parties do not resolve the particular dispute or impasse after employing the mediation procedures set forth in this provision, the parties may then avail themselves of any remedies available to them at law or in equity in the courts in the State of Florida.

MISCELLANEOUS

8. Upon execution of this Settlement Agreement, the parties hereto agree to file a joint motion in this lawsuit requesting that the Court approve this Settlement Agreement and incorporate it into a final judgment dismissing the lawsuit with prejudice, but retaining jurisdiction to enforce the terms of this Settlement Agreement. If the Court does not accept this Settlement Agreement, it shall be null and void as though never executed and will not be admissible as evidence in this or any other lawsuit or administrative proceeding.

- 9. Lee County agrees that if the Court accepts this Settlement Agreement, the lawsuit shall be dismissed with prejudice.
- 10. Each party shall bear its own costs, including attorney fees, incurred in connection with the Lawsuit and this Settlement Agreement.
- 11. All parties to this Settlement Agreement are deemed to have participated in its drafting. In the event of any ambiguity in the terms of this Settlement Agreement, the parties agree that such ambiguity shall be construed without regard to which of the parties drafted the provision in question.
- 12. This Settlement Agreement contains the entire agreement between the parties and no verbal or written assurance or promise relating to the subject matter hereof is effective or binding unless included in this document.
- 13. Each county, by executing this Settlement Agreement, confirms by its signature hereto that this Settlement Agreement has been approved and executed pursuant to all required procedures.
- 14. This Settlement Agreement may be executed in any number of originals, all of which evidence one agreement, and only one of which need be produced for any purpose.

In witness whereof, the parties hereto have caused this Settlement Agreement to be executed by their undersigned officials as duly authorized.

ATTEST:

BARBARA T. SCOTT, CLERK OF CIRCUIT

COURTAND EX-OFFICIO CLERK OF THE

BOARD OF COUNTY COMMISSIONERS

3Y:

7.28-09 DEPUTY CLERK

Attest: Charlie Green, Ex-Officio Clerk

By: Marcia Mulson
Deputy Clerk

For: Charlotte County

By: July Chairperson, Board of County Commissioners

AS TO FORM AND LEGAL SUFFICIENCY BY:

County Attorney

LR 08-120

For: Lee County

By: _______ Chairperson, Board of County
Commissioners

AS TO FORM AND LEGAL SUFFICIENCY BY:

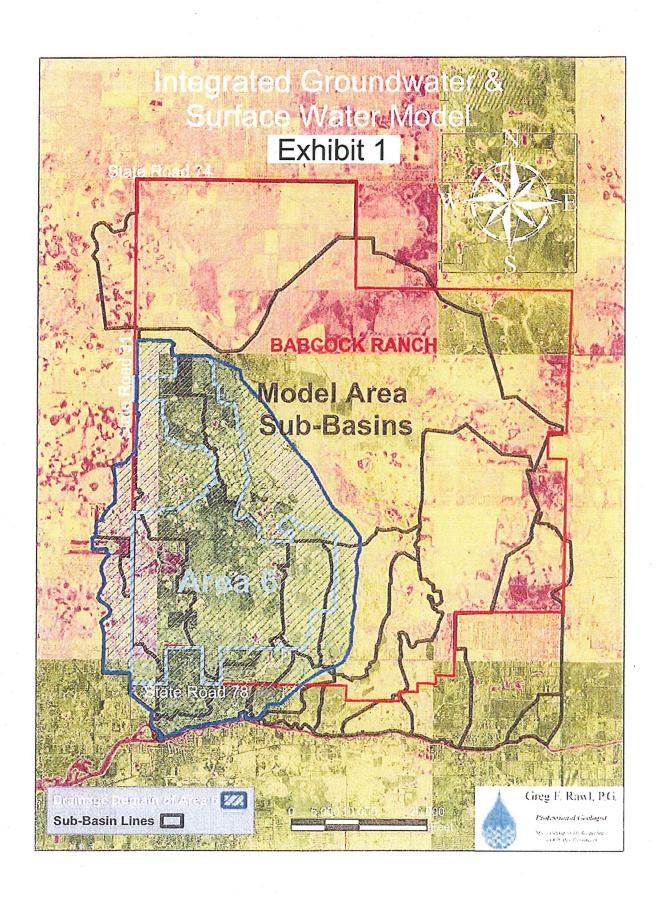
County Attorney

For: Babcock Property Holdings, LLC

By: President

STATE OF FLORIDA COUNTY OF CHARLOTTE

- July, 2009	cknowledged before me this 28 day of by Patricia M. Duffy, as Charlotte County. The above named person as identification.
STATE OF FLORIDA COUNTY OF LEE	Signature of Notary Public Printed Name of Notary Public My Commission Expires: BONNIE S. STONER MY COMMISSION # DD 894423 EXPIRES: July 6, 2013 Bonded Thru Notary Public Underwriters
personally known to me or has produced_	knowledged before me this // day of by Ammusioner Hall , as Lee County. The above named person is as identification.
	Printed Name of Notary Public Rosama Kyrevn My Commission Expires: ROSANNA HERRERA Notary Public - State of Florida Commission Expires Aug 24, 2009 Commission # DD465488 Bonded By National Notary Assn.
, <i>TULY</i> , 2009	knowledged before me this <u>13th</u> day of by <u>THOMAS J. DANAHY</u> , as sabcock Property Holdings, LLC. The above ne or has produced as
F N	Printed Name of Notary Public ELNABETH A. ANDRE My Commission Expires: My Commission Expires: MY COMMISSION # DD 663677 EXPIRES: April 16, 2011 Bonded Thru Budget Notary Services



Below is a list of primary parameters and data needs for modeling effort.

Model Parameters (Assumptions)

Aquifer thickness

Aquifer elevations

Aquifer hydraulic conductivities

Aquifer storativity

Aquifer leakance

Aquifer boundary conditions

ET coefficients by land use type

Pumpage rates and distribution

Stream/canal bed conductance

Rainfall data

JEI gages

RainOne (Lee County)

DBHydro (SFWMD)

Surface water basin delineation

Stream/Canal properties

JEI

Lee County

SWFFS (SFWMD)

Topography (DEM)

Kitson Lidar Survey

JEI Survey data

SWFFS (SFWMD)

Overland flow parameters

Water control structures (weirs, culverts, etc.)

JEI

Lee County NRM

SWFFS (SFWMD)

Roads (berms, dikes, etc.)

Land uses (spatial distribution)

Soils (spatial distribution)

<u>Data Sets</u> (list of data sets we will utilize and how they will be utilized for the modeling – calibration/validation of model)

Water level data JEI piezometers Lee County NRM piezometers USGS JEI non-surfical DBHydro (SFWMD) **SWFFS** JEI well inventory Stream flow data JEI Lee County NRM DBHydro (SFWMD) SWFFS Stream stage data JEI Lee County NRM DBHydro (SFWMD) SWFFS

Partial List of Guidance/Guidelines for Evaluating Hydrologic and Hydraulic Models

Guidelines for Evaluating Ground-Water Flow Models, U.S. Geological Survey Scientific Investigations Report 2004-5038—Version 1.01, by Thomas E. Reilly and Arlen W. Harbaugh,

http://pubs.usgs.gov/sir/2004/5038/PDF/SIR20045038 ver1.01.pdf

ASTM D6025 - 96(2002) Standard Guide for Developing and Evaluating Ground-Water Modeling Codes, http://www.astm.org/Standards/D6025.htm Referenced Documents under the ASTM links

<u>D5447</u> Guide for Application of a Ground-Water Flow Model to a Site-Specific Problem

<u>D5490</u> Guide for Comparing Ground-Water Flow Model Simulations to Site-Specific Information

<u>D5609</u> Guide for Defining Boundary Conditions in Ground-Water Flow Modeling <u>D5610</u> Guide for Defining Initial Conditions in Ground-Water Flow Modeling <u>D5718</u> Guide for Documenting a Ground-Water Flow Model Application <u>D653</u> Terminology Relating to Soll, Rock, and Contained Fluids

Effective Groundwater Model Calibration: With Analysis of Data, Sensitivities, Predictions, and Uncertainty by Mary C. Hill (Author), Claire R. Tiedeman (Author)

GSFLOW—Coupled Ground-Water and Surface-Water Flow Model Based on the Integration of the Precipitation-Runoff Modeling System (PRMS) and the Modular Ground-Water Flow Model (MODFLOW-2005), Techniques and Methods 6–D1, U.S. Department of the Interior, U.S. Geological Survey by S.L. Markstrom, R.S. Regan, et al, 2008.

A Modular Three-Dimensional Finite-Difference Ground-Water Flow Model: U.S. Geological Survey Techniques of Water-Resources Investigations, Book 6, Chapter A-1, 586 p. by McDonald, M.G., and Harbaugh, A.W., 1988.

Precipitation-Runoff Modeling System - User's Manual: U.S. Geological Survey Water-Resources Investigations Report 83-4238, 203 p. Leavesely, G.H., Lichty, R.W., Troutman, B.M., and Saindon, L.G., 1983,

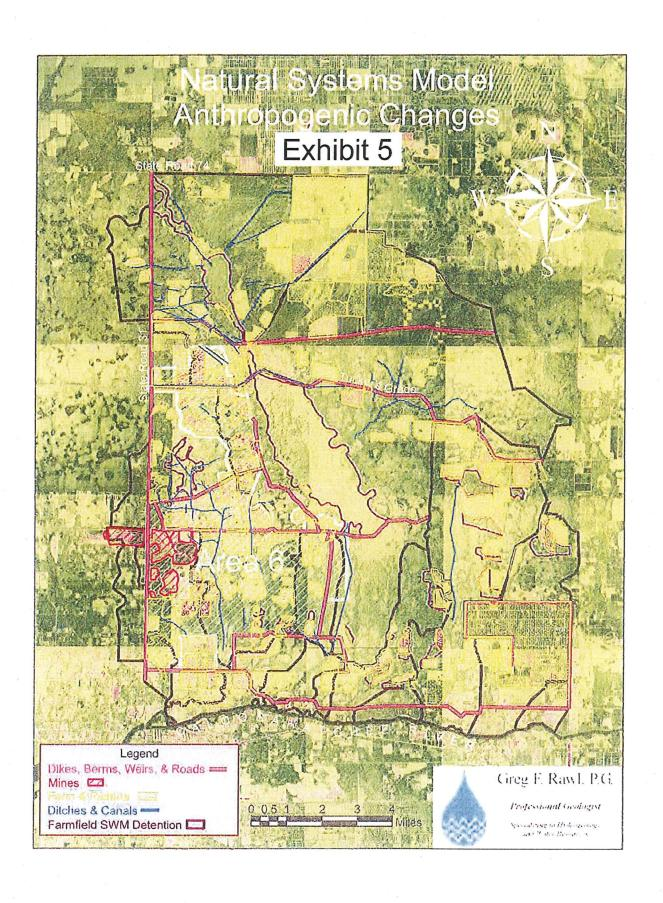
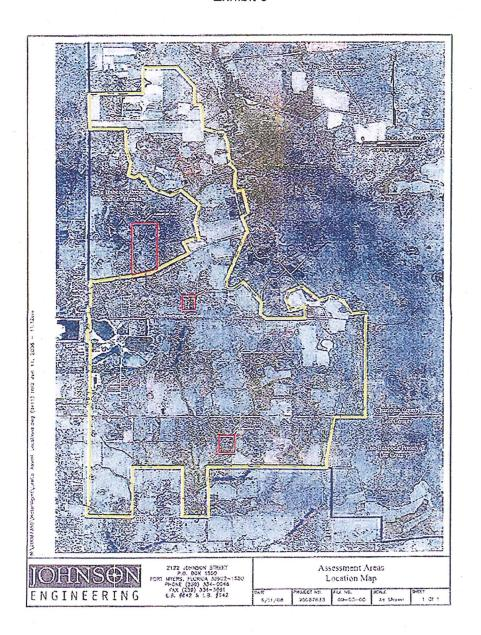


Exhibit 6



BABCOCK RANCH COMMUNITY WATER QUALITY MONITORING PLAN

OBJECTIVE:

To evaluate any potential impact to surface water and ground

water quality at the Babcock Ranch Community project site.

This proposed monitoring plan is divided into six (6) items as follows:

- 1. Surface Water Quality Monitoring
- 2. Ground Water Quality Monitoring
- 3. Sediment Monitoring
- 4. Site Location Data
- 5. Water Quality Data Reporting
- 6. Water Quality Monitoring Plan Revisions

SURFACE WATER QUALITY MONITORING

Six (6) surface water samples locations will monitor up gradient and down gradient surface water conditions. The surface water sample locations are shown on the attached map. Surface water samples will be collected monthly when water is flowing and will be analyzed for the parameters listed in Table 1.

In addition to the parameters listed in Table 1, surface water samples will be laboratory analyzed semiannually (during the dry season and the rainy season) for constituents. shown in Table 4 that are currently used on the site. A one-time test will be conducted for items shown in Table 5. The surface water samples will be collected by qualified personnel in accordance with Florida Department of Environmental Protection (FDEP) Standard Operating Procedures (SOP) 001/01 or current version. Each sampling event will include an equipment blank and a field duplicate sample. The surface water samples will be laboratory analyzed by a State of Florida NELAC certified environmental laboratory. If the one-time sampling done for parameters shown in Table 5 yields positive findings, the test found positive shall be continued in conjunction with those specified in Table 1, at the same frequency.

GROUND WATER QUALITY MONITORING

Seven (7) existing water table ground water monitor wells will monitor up gradient and down gradient ground water conditions. The ground water monitor well locations are shown on the attached map. Each well will be outfitted with an electronic water level datalogger that will record water levels at six (6) hour intervals. The water level data will be downloaded quarterly. The ground water monitor wells will be sampled semiannually (during the dry season and the rainy season) and analyzed for the parameters listed in Table 2.

Ground water samples from each of the monitor wells will be collected by qualified personnel in accordance with Florida Department of Environmental Protection (FDEP) Standard Operating Procedures (SOP) 001/01 or current version. Each sampling event will include an equipment blank and a field duplicate sample. The ground water samples will be laboratory analyzed by a State of Florida NELAC certified environmental laboratory.

SEDIMENT MONITORING

Sediments shall be monitored at all six (6) surface water sites initially for a background determination during the dry season. Subsequent monitoring shall be annually (during the dry season) at the three (3) major outfalls (Owl Creek East Branch, Trout Creek, and Strickland Creek). Testing is to be for the metals listed in Table 3 and in accordance with the most recent FDEP Interpretive Tool for Assessment of Metal Enrichment in Florida Freshwater Sediment. The sediment samples will also be laboratory analyzed for the herbicides/pesticides shown in Table 4. A one-time sampling will be done for the parameters shown in Table 5. If the one-time sampling done for parameters shown in Table 5 yields positive findings, the test found positive shall be continued in conjunction with those specified in Table 1, at the same frequency.

SITE LOCATION DATA

The following site data will be reported:

- Latitude and Longitude and State Plane 1983 Northing and Easting of the surface water sampling locations and ground water monitor wells
- Aerial maps of the surface water sample locations and ground water monitor wells
- Monitor well information including: top-of-casing elevations referenced to NAVD, total depths, slotted screen depths, construction materials

WATER QUALITY DATA REPORTING

Water quality data will be reported in accordance with FAC 62-160, and submitted annually in electronic format.

WATER QUALITY MONITORING PLAN REVISIONS

This water quality monitoring plan shall be re-evaluated by Babcock Property Holdings, LLC and Lee County and modified as necessary on an annual basis, depending on findings, land use changes, etc.

Babcock Ranch Community Water Quality Monitoring Parameters

Table 1 – Surfa	Table 1 - Surface Water Parameters
temperature	total nitrogen
pH	total Kjeldahl nitrogen
specific conductance	total ammonia nitrogen
dissolved oxygen	nitrite
salinity	nitrate
turbidity	total phosphorus
total suspended solids	dissolved orthophosphate
chlorophyll-a	enterococci
color	fecal coliform
iron	flow

Table 2 - Ground	Table 2 - Ground Water Parameters
temperature	biochemical oxygen demand
pH	chloride
specific conductance	nitrite
dissolved oxygen	nitrate
turbidity	total ammonia nitrogen
total dissolved solids	sulfate
color	Florida PRO
iron	water table elevation

Table 3 - Sediment Parameters		Lead	ic Mercury		lum	lium Zinc
	Aluminum	Iron	Arsenic	Barium	Cadmium	Chromium

Table 5
One Time Test Pesticide/Herbicide

Atrazine desethyl	pesticide	surface water	sediment	pesticide	surface water	sediment	
2,4,5-T X X 2,4,5-TP (silvex) X X Urea herbicides and imidacloprid diuron X	chlorinated (phenoxy acid) herbicides			organochlorine pesticides			
Application	2,4-D	X	X	aldrin) x	X	
Deta BHC	2,4,5-T	X	X	alpha BHC	1		
	2,4,5-TP (silvex)	X	X				
diuron	urea herbicides a	nd imidacloprie	d	delta BHC	X	******	
linuron X X X imidacloprid X - chlorodane X	diuron	X	X	gamma BHC (lindane)	X		
organophosphorus and nitrogen pesticides alacinlor X	linuron	X	X			~~~	
chlorothalonil X X X and p.p. DDD X X X X p.p. DDD X X X X p.p. DDD X X X X x x x x x x x x x x x x x x	imidacloprid	Х	-	chlordane	X	Х	
A	organophosphorus and	i nitrogen pest	icides	chlorothalonil	X		
Atrazine X	alachlor] x	X	cypermethrin	X	-	
Atrazine desethyl	ametryn	Х	X	p.p'-DDD	Х	X	
atrazine desisopropyl X - dicofol (kelthane) X X X dicofol (kelthane) X X X dicofol (kelthane) X X X A dicofol (kelthane) X X X X dicofol (kelthane) X X X X A dicofol (kelthane) X X X X X X X X X X X X X X X X X X X	atrazine	X	X	p,p'-DDE	х	Х	
azinphos methyl (guthion) X	atrazine desethyl	X	-	p.p'-DDT	х	Х	
bromacil X X X butylate X - beta endosulfan X X X chlorpyrifos ethyl X X X endosulfan Sulfate X X X endosulfan Sulfate X X X endosulfan Sulfate X X X demeton X X X endrin A Sulfate X X X demeton X X X endrin A Sulfate X X X disulfoton X X X heptachlor X X X heptachlor X X X endrin A Sulfate X X X endrin A Sulfate X X X endrin A Sulfate X X X demethon X X X heptachlor Sulfate X X X endrin A Sulfate X X X ender A Sulfate X X X Ended X X X X Ended X Ended X X X Ended X Ended X X X Ended X	atrazine desisopropyl	X	-	dicofol (kelthane)	Х	Х	
butylate X - beta endosulfan X X X endosulfos ethyl X X X endosulfos endosulfos X X X endrin eldenyde X X X endosulfos endosulfos endosulfos X X X endosulfos endosulfos X X X endosulfos endosulfos endosulfos X X X endosulfos endosul	azinphos methyl (guthion)	X	X	dieldrin	х	X	
chlorpyrifos ethyl X X X endosulfan sulfate X X X endrin ladehyde X X X lendre ton X X X lendre ton X X X lendre ton X X X lendrin aldehyde X X X lendrin ladehyde X X X lendrin ladehy	bromacil	X	×	alpha endosulfan	х	Х	
chlorpyrifos ethyl X X X endosulfan sulfate X X X endrin aldehyde X X X x disulfoton X X X heptachlor X X X heptachlor X X X heptachlor epoxide X X X ethion X X X methoxychlor X X X endronen X X X methoxychlor X X X endronen X X X permethrin X - fonophos X X X formethoxychlor X X X permethrin X - fonophos X X X formethoxychlor X X X permethrin X - fonophos X X X formethoxychlor X X X permethrin X X X permethoxychlor X X X permethrin X X X permethrin X X X permethrin X X X permethrin X X X permethagilar in X X X permethrin X X X x permethrin X X X permethrin X X X permethrin X X X x permethrin X X X permethrin X X X permethrin X X X x x x x x x x x x x x x x x x x	butylate	X	-	beta endosulfan	X	Х	
demeton X X diazinon X X disulfoton X X disulfoton X X dethion X X ethion X X <tr< td=""><td>chlorpyrifos ethyl</td><td>X</td><td>X</td><td>endosulfan sulfate</td><td>х</td><td></td></tr<>	chlorpyrifos ethyl	X	X	endosulfan sulfate	х		
A	chlorpyrifos methyl	X	X	endrin	х	X	
A	demeton	Х	X	endrin aldehyde	х	Х	
Mathematics	diazinon	X	X	heptachlor	X	X	
Milestand Mile	disulfoton	X	X	heptachlor epoxide	Х	X	
Permethrin X	ethion	X	X			Х	
Toxaphene	ethoprop	X	X	mirex	Х	Х	
Description	fenamiphos	X	X	permethrin	Х	•	
malathion X X metalaxyl X - methamidophos X' X methamidophos X' X metolachlor X X metribuzin X X metribuzin X X mevinphos X X monocrotophos X' X monocrotophos X' X morflurazon X X parathion ethyl X X	fonophos	X	X	toxaphene	х	X	
Maretalaxyl	hexazinone	Х	Х	PCB-1016	Х	X	
methamidophos X' X PCB-1242 X X X metolachlor X X X PCB-1248 X X X metribuzin X X X PCB-1254 X X X mevinphos X X X PCB-1254 X X X monocrotophos X' X X PCB-1260 X X X monocrotophos X' X X monocrotophos X X X X X Monocrotophos X X X X X Monocrotophos X X X X X X Monocrotophos X X X X X Monocrotophos X X X X X Monocrotophos X X X X X X Monocrotophos X X X X X X Monocrotophos X X X X X X X X X X X X X X X X X X X	malathion	X	X	PCB-1221	X	X	
metolachlor X X X PCB-1248 X X X metribuzin X X X PCB-1254 X X X mevinphos X X X PCB-1260 X X X monorcotophos X X X Triffuralin X X X monorcotophos X X X X monorflurazon X X X Triffuralin X X X monorflurazon X X X Triffuralin X X X monorflurazon X X X Triffuralin X X X X Triffuralin X X X X X X Triffuralin X X X X X X X X X X	metalaxyl	Х	-	PCB-1232	Х	X	
metribuzin X X X mevinphos X X X monocrotophos X X X X m	methamidophos	X*	Х	PCB-1242	X	Х	
mevinphos X X X PCB-1260 X X X monocrotophos X X X T trifluralin X X X naled X X X norflurazon X X X T not analyzed parathion ethyl X X X	metolachlor	X	X	PCB-1248	Х	Х	
PCB-1260 X X X	metribuzin	X	X			Х	
monocrotophos X, X triffuralin X X naled X X norflurazon X X parathion ethyl X X	mevinphos	Х	X	PCB-1260	Х		
norflurazon X X - not analyzed parathion ethyl X X	monocrotophos	X,	X	trifluralin	X		
parathion ethy! X X	naled	Х	X			-	
parathion ethyl X X	norflurazon	X	X		- not analyzed	1	
parathion methyl X X	parathion ethyl	Х	X		=		
	parathion methyl	X	Х				

Compounds in italics have a Surface Water Quality Class I or III criterion (FAC 62-302)

X

X

Х

phorate

prometryn

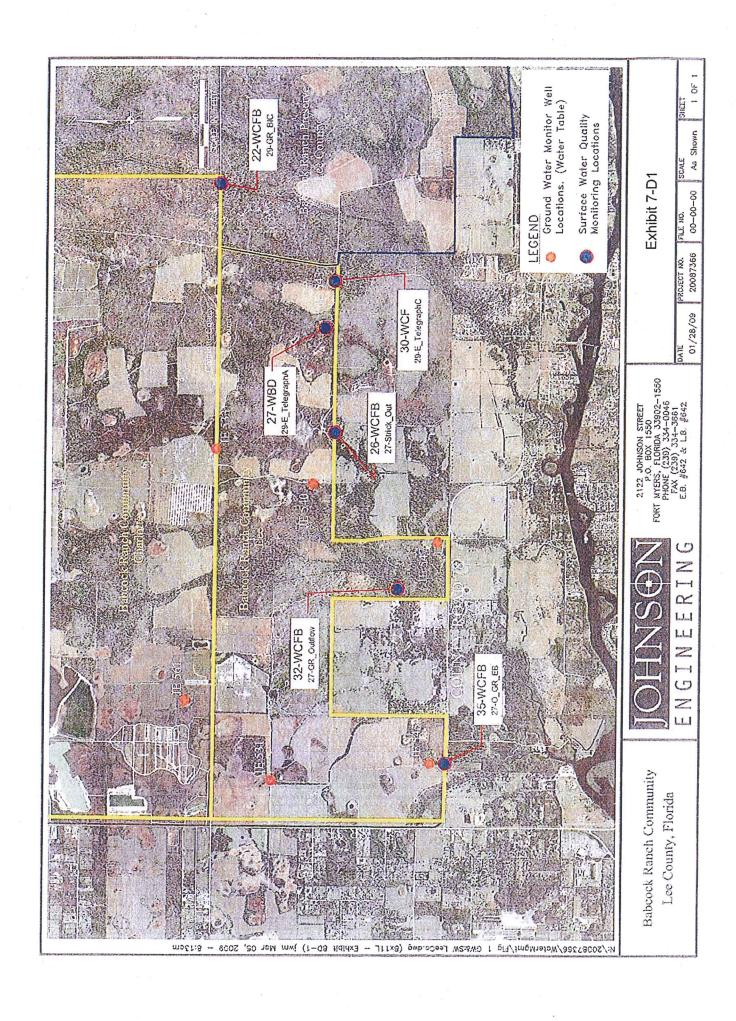
simazine

Reference: South Florida Water Management District - Jacksonville District, U.S. Army Corps of Engineers CERP Guidance Memorandum, CGM Number Revision: 42.00, dated 06/27/2005

X

X

Χ



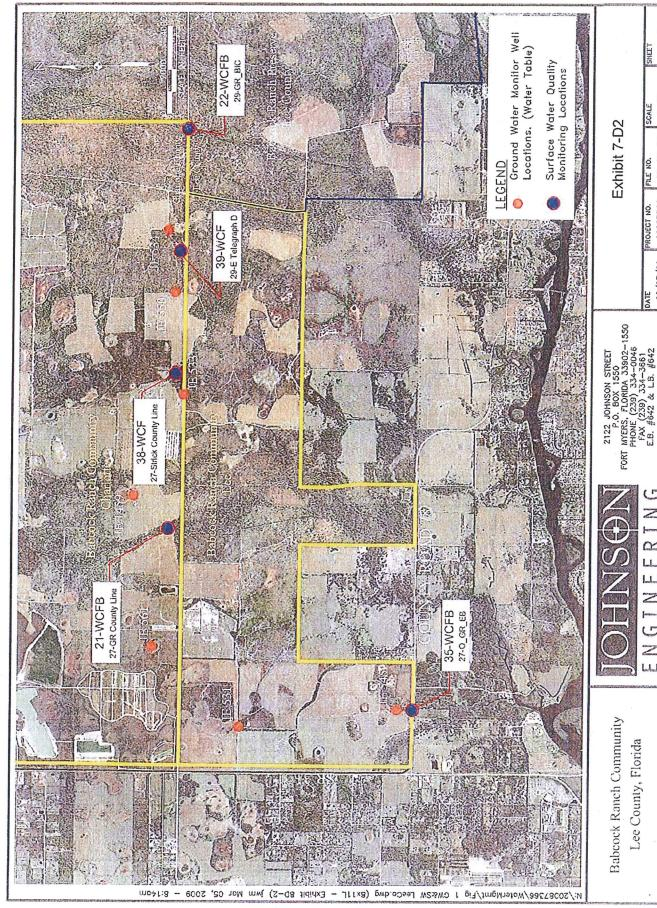


Exhibit 7-D2

FILE NO.

DATE 02/27/09

Z

0 Ш Ш 2

|----|

9 LLI

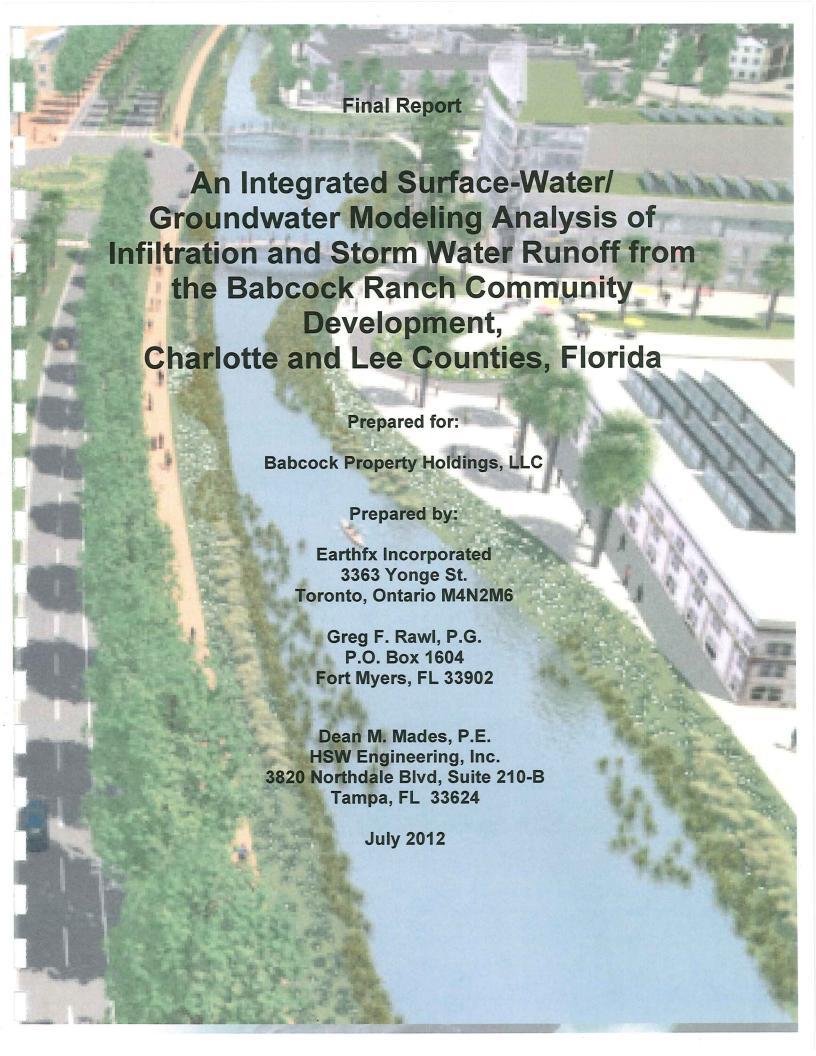
Lee County, Florida

PROJECT NO. 20087366

00-00-00

As Shown

9



Executive Summary

Background

This report culminates a unique, extensive, and complex modelling analysis associated with the Babcock Ranch Community (BRC). The modelling analysis was undertaken in accordance with the Settlement Agreement entered into between Lee County, Charlotte County and Babcock Property Holdings (BPH) in August 2009 (Settlement Agreement).

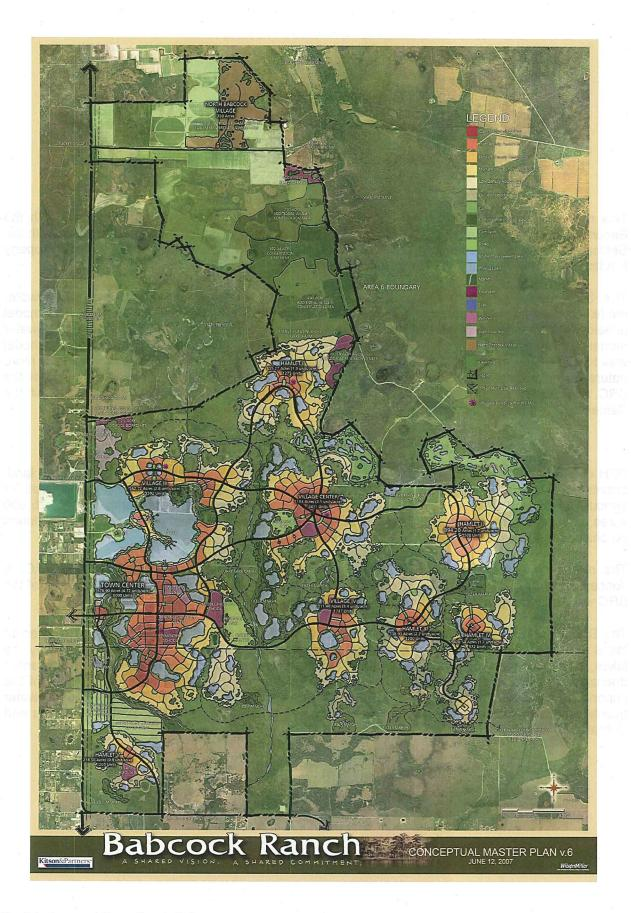
The Settlement Agreement required BPH to conduct an integrated surface and groundwater modelling analysis within certain parameters as set forth in the Settlement Agreement. The model developed and calibrated for this study was a continuous integrated surface water/groundwater model that represented flow in the BRC and surrounding area. The purpose of the integrated model was to allow BPH to evaluate whether the development was effectuating progress towards a more natural or historic wetland conditions and discharge of water as it exited the southern end of the BRC and flowed toward Lee County. This modelling report completes that requirement of the Settlement Agreement and includes the conclusions derived from the modelling analysis.

The Babcock Ranch Community Development

BPH owns approximately 17,780 acres of property that was originally part of a larger tract of land, approximately 92,000 acres historically known as the Babcock Ranch, which was primarily used for agricultural purposes. When BPH purchased the Babcock Ranch, it sold approximately 75,000 acres, collectively, to Lee County and the State of Florida in the largest public conservation lands purchase conducted by the State.

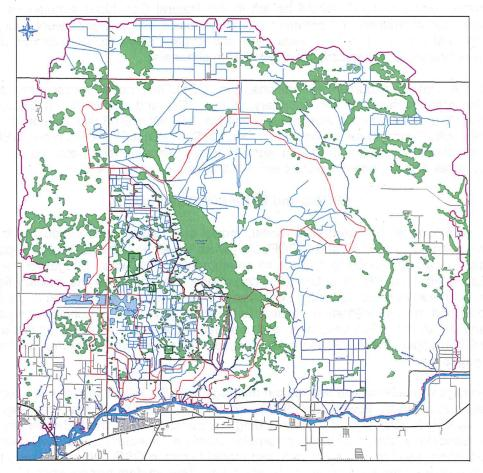
The remaining approximately 17,780 acres owned by BPH will be developed into the BRC. A conceptual plan of the BRC is depicted in the figure on the following page. Over 9,000 acres of the BRC will be limited to conservation, greenways, flow ways, and agriculture.

The BRC's surface water management (SWM) system is composed of a series of interconnected lakes and constructed water quality treatment marshes. Stormwater runoff will be captured by the lakes, which will have the capacity to attenuate the larger of 1.5 inches of runoff from the entire drainage area or the equivalent volume of 3.75 of inches of rainfall multiplied by the area of the impervious surfaces. A portion of the intercepted water will be treated and discharged to the water quality treatment marshes for additional detention before discharging to the existing channels and ultimately offsite.



The GSFLOW Integrated Surface and Ground Water Model

In accordance with the Settlement Agreement, the integrated model evaluated three conditions: the Pre-development Condition (Current Conditions), the "Natural Conditions" (historic) and the Post-development Conditions (with the BRC development as permitted by the South Florida Water Management District) for the BRC. To accurately model the three conditions, a large area surrounding the BRC was considered in the model simulations. The model boundaries encompassed three watersheds within the vicinity of the BRC development, Telegraph Watershed, Trout Creek Watershed, and Owl Creek Watershed and extended to cover 310 square miles in southern Charlotte County and northern Lee County north of the Caloosahatchee River in southwest Florida (well beyond the boundaries of the BRC development). The study area extends about 4.2 miles west from State Route 31, 16.5 miles east from State Route 31, and about 3 miles north of County Road 74. The study area includes all of the sub-basins outlined in the Settlement Agreement (figure below depicts the boundaries of the BRC, the three watersheds discussed above, and the model extent.)



The model considered numerous factors related to hydrologic conditions as set forth in Exhibits 2 and 3 of the Settlement Agreement. Factors considered in the model include climatologic, topographic, geologic, soil, land-use, land cover, and groundwater and surface water data. Continuous flow data, wetland stage data, and groundwater level data from a large number of observation points inside and outside the BRC were used in model calibration.

The integrated surface and groundwater model was built using the U.S. Geological Survey's Coupled Groundwater and Surface-water Flow Model (GSFLOW). It is an open source, internally-coupled, distributed surface water and groundwater model. GSFLOW represents the integration of the two widely-recognized USGS models: the Precipitation Runoff Modelling System (PRMS)

(Leavesly and other, 1983) and the modular groundwater flow model MODFLOW (Harbaugh, 2005). Use of the GSFLOW model was set forth in Exhibit 4 of the Settlement Agreement.

The Three Conditions (Current, Post Development and Natural)

The GSFLOW model was calibrated using surface and groundwater data from mid-2006 through mid-2010 to match Current Conditions. A good calibration was achieved to the Current Conditions and, therefore, the model provided a dependable platform from which to simulate the Natural and Post-development Conditions.

To develop the Natural Condition, the GSFLOW model was modified by removing historic anthropogenic features, such as roads, ditches, dikes, berms and water control structures which affected the routing of overland runoff and surface water flows. Removing these man made features from the model was intended to simulate, to the extent reasonably possible, the historical flow of surface and groundwater. It was stipulated in the Settlement Agreement that the Caloosahatchee River, otherwise known as C-43, would be left in the Natural Conditions simulations as it exists today. Historic documentation and previous scientific studies and analyses were researched and considered to best represent historic vegetation and stream channels (included in place of the existing ditches and anthropogenically-modified stream channels).

To develop the Post-development Conditions, the GSFLOW model represented the Current Conditions for areas outside of the boundary of the BRC and added the hydrologic features permitted under the Environmental Resource Permit No. 08-00004-S-05 (Application No. 070330-5) issued by the South Florida Water Management District (SFWMD) for the BRC project (ERP Permit). The model simulated all of the proposed surface water management water control structures, conveyances, lakes and treatment marshes permitted as authorized in the ERP Permit.

The PRMS and MODFLOW Submodels

To facilitate calibration of the integrated model, model construction was conducted in stages, in which the two submodels (PRMS and MODFLOW) were developed and calibrated separately. The PRMS submodel was developed to analyze all components of the water budget for the BRC on a daily time-step basis. The PRMS submodel incorporates information on the spatial distribution of precipitation, temperature, solar radiation, soil properties, vegetation and land use to yield outputs of estimated overland runoff, infiltration, evapotranspiration (ET) and groundwater recharge and discharge, and streamflow. Soil, vegetation and land use properties were assigned to classes based on available GIS mapping in the PRMS model process. The model was calibrated against observed flows at the gages.

Estimated average wet season and dry season recharge from the PRMS model was used as input to a steady-state groundwater flow model developed for the study area. The groundwater system consisted of eight hydrostratigraphic units including the surficial sands, the Ochopee Limestone, the Peace River Sandstone, the Mid-Hawthorn aquifer (Arcadia Limestone) and the Lower Hawthorn aquifer. The surficial sand unit was split into two model layers in GSFLOW simulations to allow the upper layer to represent the shallow wetlands and lakes. The aquifers are separated by three semiconfining units (aquitards). Hydraulic conductivity of the aquifer and aquitard layers BRC were adjusted in the calibration to best match the average wet season and average dry season groundwater levels.

GSFLOW Model Calibration

Data sets from the two sub-models were then combined into a single data set for simulations with the GSFLOW code. GSFLOW includes additional simulation methods specifically related to the coupling and integration of the models, the most important being a cascading overland flow algorithm that routes Hortonian flow, Dunnian flow, and interflow through individual cells and

ultimately to the streams and wetlands. The PRMS submodel simulated the soil moisture processes while the MODFLOW submodel was run under transient conditions using a daily time step and simulated groundwater flow as well as flow, stage, and groundwater interaction in the wetland and streams. The GSFLOW model was used to simulate and analyze the groundwater and surface water flow on an integrated basis in the BRC and the study area, per the requirements of the Settlement Agreement.

Because the groundwater and surface water systems are tightly connected in the study area, significant effort was expended in further calibrating the integrated GSFLOW model. Model parameters were adjusted within reasonable ranges to match the observed streamflow at 10 continuous-recording gages, observed wetland stage, and observed heads at 165 continuous observation wells. Hydrographs and maps were produced for comparison and good correlations were achieved at the BRC gages, as well as at the off-site gages including those listed in Exhibit 2. Good correlations were also achieved with most of the observation wells. Hydroperiods for the wetlands were estimated from the daily stage data.

The GSFLOW Model was then modified as discussed above to simulate the Natural Conditions and the Post-development Conditions. The results of each model simulation were compared to determine the long-term hydrologic impacts of the anthropogenic changes that resulted in the Current Conditions and in the proposed hydrologic regime of the permitted Post-development Conditions. Specifically, the model predicted changes in daily streamflow, wetland stage, and groundwater heads at points in the study area using the same climatic data for the five-year period.

Three design storm events were simulated using the GSFLOW model for each of the three conditions. The integrated model facilitated a comparison of daily average discharge rates for the surface water basins that included the effects of the storms on both the groundwater and surface water systems. The design storm events used were those generally mandated in water resource permitting by the SFWMD, that is, the 100-year 3 day event, the 25-year 3-day event, and the 5-year 1-day event. The three watersheds were modelled for all three storm events and for each of the three conditions as required by the Settlement Agreement. The chart below summarizes the results for all of these discrete modelling storm events.

	100 Year, 3-Day Storm			25 Year, 3-Day Storm			5 Year, 1-Day Storm		
Basin	Cur- rent	Post- Develop- ment	Natural	Cur- rent	Post- Develop- ment	Natural	Cur- rent	Post- Develop- ment	Natural
Trout Creek	2,432	1,697	1,196	1,748	1,245	856	693	513	1,212
Owl Creek	440	372	332	328	265	242	166	119	110
Telegraph Creek	2,046	1,973	829	1,419	1,367	587	448	.442	236

It is recognized that these results differ slightly from previous modelling efforts using the US Army Corps of Engineers Hydrologic Modeling System (HEC-HMS) and River Analysis System (HEC-RAS) models which focussed on predicting peak flow rates in specific storm events. The results differ because the instant model accounts for a larger land mass and assess the introduction of ground water and surface water. The previous modelling efforts were for purposes of determining an allowable discharge only. Both modelling effects are reliable and robust and similar in their conclusions. The results of the HEC-HMS modelling were described in the Allowable Discharge Report for BRC and were used to further verify the calibrated GSFLOW model in the Current Conditions, prior to running the Post-development and Natural Conditions simulations.

Summary of GSFLOW Modelling Results

A comparison of the three conditions clearly demonstrates that the Post-development Conditions will help to mitigate changes in groundwater recharge (through leakage from the proposed stormwater management lakes), decrease average daily discharge rates during storm events, and increase the wetland hydroperiods within the BRC as compared to the Current Conditions. Moreover, the Post-development Conditions simulation demonstrated that no adverse impacts to downstream receiving water bodies or environmental features would occur. When the three conditions are fully analyzed and compared, the model demonstrates that the Post-development Conditions effectuates progress towards historic flow rates and hydroperiods that would have been expected under Natural Conditions.

CERTIFICATION

The undersigned attest that the analyses contained herein are in conformance with the standards of the industry.



Greg F. Rawl, P.G. Florida License PG479 Greg F. Rawl, P.G. P.O. Box 1604 Fort Myers, FL 33902-1604



Dean M. Mades, P.E. Florida License PE48742 HSW Engineering, Inc. 3820 Northdale Blvd, Suite 210-B Tampa, FL 33624 COA 0005971



E.J. Wexler, P.Eng.
Ontario License 100132311
Earthfx Inc.
3363 Yonge Street
Toronto, Ontario M4N 2M6
GANADA

Table of Contents

1	INTRO	DUCTIO	N	17
	1.1		ound	
	1.2		s Studies	
2	Physica	al Settin	g of the Study Area	19
	2.1	Climate		10
	2.2	Land S	urface Topography	10
	2.3	Soil Da	tata	18
	2.4		se	
	2.5			
	2.5	2.5.1	ogic Setting	20
			Streamflow Monitoring	21
	0.0	2.5.2	Streamflow Calculation Methods	23
	2.6		ic Setting	
	2.7		ic Layers	
	2.8	Hydros	tratigraphy	25
	2.9		Properties	
	2.10	Ground	water Monitoring	26
	2.11	Ground	water Flow Patterns	26
	2.12		Jse	
3		cal Mod	elling	28
	3.1	GSFLC	W Model Overview	28
	3.2	PRMS	Sub-model	31
			PRMS Operation	
		3.2.2	PRMS Model Data	34
	3.3	PRMS	Model Results	37
			Current Conditions	
			Natural Conditions	
			Post-Development Conditions	38
4	MODFL	OW Mo	odel Development and Steady-State Calibration	39
•	4.1		water Flow Equation	
	4.2		OW Model Grid	
	1.2	4.2.1	Model Layers	
	4.3		Boundary Conditions	
			Specified Head Boundaries	
			No-Flow Boundaries	
	4.4		Head Dependent Discharge Boundaries (Lakes and Streams)	
		Ground	water Recharge	4/
	4.5		water Model Parameters	
_	4.6		Results	
5		VV IVIOd	el Simulations	49
	5.1	GSFLO	W Model Parameters	49
	5.2		W Model Calibration and Discussion of Results	
		5.2.1	Streamflow Maps and Hydrographs	51
		5.2.2	Potentiometric Maps and Hydrographs	52
		5.2.3	Natural Conditions Simulations	52
		5.2.4	Post Development Simulations	53
	5.3	Hydrop	eriod Analysis	54
	5.4	Design	Storm Simulations	55
		5.4.1	Design Storms under Current Conditions	
		700 000 0	Design Storms under Natural Conditions	
		100010110110100000	Design Storms under Post Development Conditions	
6	Summa		Conclusions	
7			50101030113	
8				
•				00
- WILLIIM	aire	· City I	Γο	1900

63
66
230
231
231
245
246

List of Tables

Table 1: Summary of streamflow monitoring station information Table 2: Geologic, hydrogeologic, and groundwater model layer in study area (modified from Rawl	and
others, 2005). Table 3: Simulated flows at Trout, Owl, and Telegraph Creek in response to design storms under Curl	rent,
Post-development, and Natural Conditions	
00002-W	246
Table 5: Water use withdrawal facilities with pumping data for permitted users.	247
List of Figures	
Figure 1: Study area showing Babcock Ranch Community and model extents	67
Figure 2: Sub-basins and model assessment areas discussed in the Settlement Agreement	68
Figure 3: Land surface topography (NGVD).	69
Figure 4: Monthly average rainfall at S-79 (Franklin Lock) based on 1991 to 2010 data	
Figure 5: Annual precipitation at S-79 (Franklin Lock)	
Figure 6: Monthly potential evapotranspiration at S79 (Franklin Lock).	
Figure 7: Annual potential evapotranspiration at S79 (Franklin Lock).	73
Figure 8: Land use mapping based on FLUCCS data for 2000	/4
Figure 10: Stream gages and surface water features represented in Current Condition simulations	/5
Figure 11: Wells in the study area with lithologic information	
Figure 12: Interpolated top of the Ochopee Limestone (in feet above NGVD).	78
Figure 13: Interpolated top of the upper Peace River clay (bottom of the Ochopee limestone) (in	feet
above NGVD).	79
Figure 14: Interpolated top of the Peace River sandstone (in feet above NGVD)	80
Figure 15: Interpolated top of the basal Peace River clay (bottom of Peace River sandstone) (in	
above NGVD).	81
Figure 16: Interpolated top of the Arcadia limestone (in feet above NGVD).	
Figure 17: Interpolated top of the Mid-Hawthorn confining unit (in feet above NGVD).	83
Figure 18: Interpolated top of the Lower Hawthorn unit of the Floridan aquifer (in feet above NGVD)	84
Figure 19: Northeast-Southwest geologic section through the study area showing principal aquifers aquitards	and
Figure 20: Hydraulic conductivity of the surficial sand as estimated from soils mapping.	oo
Figure 21: Hydraulic conductivity of the Ochopee limestone	80 87
Figure 22: Hydraulic conductivity of the Peace River sandstone	88
Figure 23: Hydraulic conductivity of the Arcadia limestone.	89
Figure 24: Location of observation wells	90
Figure 25: Average observed heads in the surficial aquifer and interpolated heads (in ft above NGVD).	
Figure 26: Location of pumping wells simulated in the model.	92
Figure 27: NEXRAD rainfall (daily sum in inches) for August 10, 2006	
Figure 28: Average daily NEXRAD rainfall versus observed rainfall at S-79 (Franklin Lock)	
Figure 29: Monthly NEXRAD rainfall versus observed monthly rainfall at S-79 (Franklin Lock)	
Figure 30: Gridded daily potential evapotranspiration (PET) rates (inches) for August 10, 2006	95
Figure 31: Slope values (decimal fraction) used in the PRMS model.	
Figure 32: Cascading flow network in the southern part of the BRC – Current Conditions	
Figure 33: Cascading flow network in the southern part of the BRC – Post-development Conditions Figure 34: Percent imperviousness under Current Conditions	
Figure 34. Percent imperviousness under Current Conditions	
Figure 36: Soil Conservation Service (SCS) curve number (CN) values (AMC II) assigned based	
combinations of soil type and Current Conditions land use. Wetland areas have no CN assigned.	
Figure 37: Soil Conservation Service (SCS) curve number (CN) values (AMC II) assigned based	
	102

assigned. 103 Figure 39: Observed monthly precipitation (inches) in November 2007
Figure 41: Monthly evaporation from canopy interception and detention storage (inches) in August 2008 under Current Conditions
Figure 41: Monthly evaporation from canopy interception and detention storage (inches) in August 2008 under Current Conditions. 107 Figure 42: Monthly overland runoff (inches) in August 2008 under Current Conditions. 107 Figure 43: Monthly cascade flows (inches) for August 2008 (inches/month) under Current Conditions. Cascade flows include runoff generated and passing through each cell. 108 Figure 44: Monthly infiltration (inches) in August 2008 under Current Conditions. 109 Figure 45: Monthly infiltration (inches) in November 2007 under Current Conditions. 110 Figure 46: Monthly actual ET (inches) in August 2008 under Current Conditions (note change in scale). 111 Figure 47: Monthly potential evapotranspiration (inches) in August 2008 under Current Conditions. 112 Figure 48: Monthly groundwater recharge (Infiltration - AET) in August 2008 under Current Conditions. 113 Figure 49: Monthly evaporation from canopy interception and detention storage (inches) in August 2008 under Natural Conditions. 114 Figure 50: Monthly runoff (inches) in August 2008 under Natural Conditions. 115 Figure 51: Monthly runoff (inches) in August 2008 under Natural Conditions. 116 Figure 52: Monthly groundwater recharge (Infiltration - AET) in August 2008 under Natural Conditions. 116 Figure 53: Monthly groundwater recharge (Infiltration - AET) in August 2008 under Natural Conditions. 117 Figure 54: Monthly evaporation from canopy interception and detention storage (inches) in August 2008 under Post-development Conditions. 119 Figure 55: Monthly water budget parameters near well Jel-526 under Post-development Conditions. 121 Figure 56: Monthly runoff (inches) in August 2008 under Post-development Conditions. 121 Figure 57: Monthly water budget parameters near well Jel-526 under Current Conditions. 122 Figure 68: Monthly water budget parameters near well Jel-526 under Current Conditions. 124 Figure 69: Monthly water budget parameters near well Jel-526 under Post-development Conditions. 124 Figure 69: Monthly water budget parameters near
under Current Conditions
Figure 42: Monthly overland runoff (inches) in August 2008 under Current Conditions
Figure 43: Monthly cascade flows (inches) for August 2008 (inches/month) under Current Conditions. Cascade flows include runoff generated and passing through each cell. 108 Figure 44: Monthly infiltration (inches) in August 2008 under Current Conditions. 110 Figure 45: Monthly actual ET (inches) in November 2007 under Current Conditions. 111 Figure 46: Monthly actual ET (inches) in August 2008 under Current Conditions (note change in scale). 111 Figure 47: Monthly potential evapotranspiration (inches) in August 2008 under Current Conditions. 112 Figure 48: Monthly groundwater recharge (Infiltration - AET) in August 2008 under Current Conditions. 113 Figure 49: Monthly evaporation from canopy interception and detention storage (inches) in August 2008 under Natural Conditions. 114 Figure 50: Monthly runoff (inches) in August 2008 under Natural Conditions. 115 Figure 51: Monthly infiltration (inches) in August 2008 under Natural Conditions. 116 Figure 52: Monthly actual ET (inches) in November 2007 under Natural Conditions. 117 Figure 53: Monthly groundwater recharge (Infiltration - AET) in August 2008 under Natural Conditions. 118 Figure 54: Monthly evaporation from canopy interception and detention storage (inches) in August 2008 under Post-development Conditions. 119 Figure 55: Monthly runoff (inches) in August 2008 under Post-development Conditions. 119 Figure 56: Monthly runoff (inches) in August 2008 under Post-development Conditions. 120 Figure 57: Monthly groundwater recharge (Infiltration - AET) in August 2008 under Post-development Conditions. 121 Figure 58: Monthly groundwater recharge (Infiltration - AET) in August 2008 under Post-development Conditions. 122 Figure 58: Monthly groundwater recharge (Infiltration - AET) in August 2008 under Post-development Conditions. 123 Figure 59: Monthly water budget parameters near well JEI-526 under Current Conditions. 124 Figure 61: Monthly water budget parameters near well JEI-526 under Post-development Conditions. 125 Figure 63: Boundary cond
Cascade flows include runoff generated and passing through each cell
Figure 44: Monthly infiltration (inches) in August 2008 under Current Conditions
Figure 45: Monthly actual ET (inches) in November 2007 under Current Conditions. 110 Figure 46: Monthly actual ET (inches) in August 2008 under Current Conditions (note change in scale). 111 Figure 47: Monthly potential evapotranspiration (inches) in August 2008 under Current Conditions. 112 Figure 48: Monthly groundwater recharge (Infiltration - AET) in August 2008 under Current Conditions. 113 Figure 49: Monthly evaporation from canopy interception and detention storage (inches) in August 2008 under Natural Conditions. 114 Figure 50: Monthly runoff (inches) in August 2008 under Natural Conditions. 115 Figure 51: Monthly infiltration (inches) in August 2008 under Natural Conditions. 116 Figure 52: Monthly groundwater recharge (Infiltration - AET) in August 2008 under Natural Conditions. 117 Figure 53: Monthly groundwater recharge (Infiltration - AET) in August 2008 under Natural Conditions. 117 Figure 54: Monthly evaporation from canopy interception and detention storage (inches) in August 2008 under Post-development Conditions. 119 Figure 55: Monthly runoff (inches) in August 2008 under Post-development Conditions. 120 Figure 56: Monthly infiltration (inches) in August 2008 under Post-development Conditions. 121 Figure 57: Monthly actual ET (inches) in November 2007 under Post-development Conditions. 122 Figure 58: Monthly groundwater recharge (Infiltration - AET) in August 2008 under Post-development Conditions. 122 Figure 59: Monthly groundwater recharge (Infiltration - AET) in August 2008 under Post-development Conditions. 124 Figure 60: Monthly water budget parameters near well JEI-526 under Current Conditions. 124 Figure 61: Monthly water budget parameters near well JEI-526 under Post-development Conditions. 124 Figure 62: Model grid and boundary conditions in upper layers. 126 Figure 63: Boundary conditions in Layer 6 to represent inflow in northeast 127 Figure 64: Southwest-Northeast section through study area showing MODFLOW models layers. 128 Figure 65: Simulated wet season steady-state heads (ft abo
Figure 46: Monthly actual ET (inches) in August 2008 under Current Conditions (note change in scale). 111 Figure 47: Monthly potential evapotranspiration (inches) in August 2008 under Current Conditions
Figure 47: Monthly potential evapotranspiration (inches) in August 2008 under Current Conditions
Figure 47: Monthly potential evapotranspiration (inches) in August 2008 under Current Conditions
Figure 47: Monthly potential evapotranspiration (inches) in August 2008 under Current Conditions
Figure 48: Monthly groundwater recharge (Infiltration - AET) in August 2008 under Current Conditions. 113 Figure 49: Monthly evaporation from canopy interception and detention storage (inches) in August 2008 under Natural Conditions. 114 Figure 50: Monthly runoff (inches) in August 2008 under Natural Conditions. 115 Figure 51: Monthly infiltration (inches) in August 2008 under Natural Conditions. 116 Figure 52: Monthly actual ET (inches) in November 2007 under Natural Conditions. 117 Figure 53: Monthly groundwater recharge (Infiltration - AET) in August 2008 under Natural Conditions. 118 Figure 54: Monthly evaporation from canopy interception and detention storage (inches) in August 2008 under Post-development Conditions. 119 Figure 55: Monthly runoff (inches) in August 2008 under Post-development Conditions. 120 Figure 56: Monthly infiltration (inches) in August 2008 under Post-development Conditions. 121 Figure 57: Monthly actual ET (inches) in November 2007 under Post-development Conditions. 122 Figure 58: Monthly groundwater recharge (Infiltration - AET) in August 2008 under Post-development Conditions. 123 Figure 59: Monthly water budget parameters near well JEI-526 under Current Conditions. 124 Figure 60: Monthly water budget parameters near well JEI-526 under Natural Conditions. 124 Figure 61: Monthly water budget parameters near well JEI-526 under Post-development Conditions. 125 Figure 63: Boundary conditions in Layer 6 to represent inflow in northeast. 126 Figure 63: Boundary conditions in Layer 6 to represent inflow in northeast. 127 Figure 64: Southwest-Northeast section through study area showing MODFLOW models layers. 128 Figure 65: Simulated wet season steady-state heads (ft above NGVD) in the surficial aquifer. 130 Figure 67: Scattergram comparing observed and simulated wet season surficial aquifer heads (ft above NGVD).
Figure 49: Monthly evaporation from canopy interception and detention storage (inches) in August 2008 under Natural Conditions
Figure 49: Monthly evaporation from canopy interception and detention storage (inches) in August 2008 under Natural Conditions
under Natural Conditions
Figure 50: Monthly runoff (inches) in August 2008 under Natural Conditions
Figure 51: Monthly infiltration (inches) in August 2008 under Natural Conditions
Figure 52: Monthly actual ET (inches) in November 2007 under Natural Conditions
Figure 53: Monthly groundwater recharge (Infiltration - AET) in August 2008 under Natural Conditions. 118 Figure 54: Monthly evaporation from canopy interception and detention storage (inches) in August 2008 under Post-development Conditions. 119 Figure 55: Monthly runoff (inches) in August 2008 under Post-development Conditions. 120 Figure 56: Monthly infiltration (inches) in August 2008 under Post-development Conditions. 121 Figure 57: Monthly actual ET (inches) in November 2007 under Post-development Conditions. 122 Figure 58: Monthly groundwater recharge (Infiltration - AET) in August 2008 under Post-development Conditions. 123 Figure 59: Monthly water budget parameters near well JEI-526 under Current Conditions. 124 Figure 60: Monthly water budget parameters near well JEI-526 under Natural Conditions. 124 Figure 61: Monthly water budget parameters near well JEI-526 under Post-development Conditions. 125 Figure 62: Model grid and boundary conditions in upper layers. 126 Figure 63: Boundary conditions in Layer 6 to represent inflow in northeast. 127 Figure 64: Southwest-Northeast section through study area showing MODFLOW models layers. 128 Figure 65: Simulated wet season steady-state heads (ft above NGVD) in the surficial aquifer. 129 Figure 66: Simulated dry season steady-state heads (ft above NGVD) in the surficial aquifer. 130 Figure 67: Scattergram comparing observed and simulated wet season surficial aquifer heads (ft above NGVD).
Figure 54: Monthly evaporation from canopy interception and detention storage (inches) in August 2008 under Post-development Conditions
under Post-development Conditions
Figure 55: Monthly runoff (inches) in August 2008 under Post-development Conditions
Figure 56: Monthly infiltration (inches) in August 2008 under Post-development Conditions
Figure 57: Monthly actual ET (inches) in November 2007 under Post-development Conditions
Figure 58: Monthly groundwater recharge (Infiltration - AET) in August 2008 under Post-development Conditions
Conditions
Figure 59: Monthly water budget parameters near well JEI-526 under Current Conditions
Figure 60: Monthly water budget parameters near well JEI-526 under Natural Conditions
Figure 61: Monthly water budget parameters near well JEI-526 under Post-development Conditions 125 Figure 62: Model grid and boundary conditions in upper layers
Figure 62: Model grid and boundary conditions in upper layers
Figure 63: Boundary conditions in Layer 6 to represent inflow in northeast
Figure 64: Southwest-Northeast section through study area showing MODFLOW models layers
Figure 65: Simulated wet season steady-state heads (ft above NGVD) in the surficial aquifer
Figure 65: Simulated wet season steady-state heads (ft above NGVD) in the surficial aquifer
Figure 67: Scattergram comparing observed and simulated wet season surficial aquifer heads (ft above NGVD)
Figure 67: Scattergram comparing observed and simulated wet season surficial aquifer heads (ft above NGVD)
NGVD)131
- I game and a control of the contro
NGVD)
Figure 69: Simulated steady-state dry season heads (ft above NGVD) in the Ochopee Limestone 132
Figure 70: Simulated dry season steady-state heads (ft above NGVD) in the Peace River Sandstone133
Figure 71: Simulated dry season steady-state heads (if above NGVD) in the Arcadia Limestone134
Figure 72: Simulated dry season steady-state heads (it above NGVD) in the Lower Hawthorn aquifer 135
Figure 73: NEXRAD rainfall (inches) for August 19, 2008
Figure 74: Simulated accumulated Hortonian flow (inches) for August 19, 2008
Figure 75: Simulated accumulated Dunnian flow (inches) for August 19, 2008
Figure 76: Simulated infiltration (inches) for August 19, 2008.
Figure 77: Precipitation and infiltration (inches) at cell 62969 (row 228, col. 97) near JEI-527, for July
through October 2008
Figure 78: Upslope and downslope Hortonian and Dunnian flows (inches) at cells 62969 for July through
October 2008
Figure 79: Simulated streamflow (cfs) for August 18, 2008 under Current Conditions
Figure 80: Simulated streamflow (cfs) for August 19, 2008 under Current Conditions
Figure 81: Simulated and observed daily flow (cfs) at gage JEI-567
Figure 82: Simulated and observed daily flow (cfs) at gage JEI-569
Earthfx Inc. and Greg Rawl, P.G. Page 12

Figure 83: Simulated and observed daily flow at gage JEI-570	
Figure 84: Simulated and observed daily flow (cfs) at gage JEI-1471.	
Figure 85: Simulated and observed daily flow (cfs) near gage JEI-564 and JEI-565 (no observed flow	
gages)	145
Figure 86: Simulated and observed daily flow (cfs) at gage JEI-1495.	
Figure 87: Simulated and observed daily flow (cfs) at gage JEI-1497.	146
Figure 88: Simulated and observed daily flow (cfs) at the USGS Telegraph Creek gage (0229291)	
Figure 89: Simulated and observed daily flow (cfs) at JEI-1518	
Figure 90: Simulated and observed daily flow (cfs) at gage JEI-1508:	
Figure 91: Simulated and observed daily flow (cfs) at gage JEI-1514.	
Figure 92: Simulated heads (ft above NGVD) at the end of the 2003 dry season.	149
Figure 93: Simulated heads (ft above NGVD) at the end of the 2003 wet season	150
Figure 94: Simulated heads (ft above NGVD) at the end of the 2004 dry season.	151
Figure 95: Simulated heads (ft above NGVD) at the end of the 2004 wet season	152
Figure 96: Simulated heads (ft above NGVD) at the end of the 2005 dry season.	153
Figure 97: Simulated heads (ft above NGVD) at the end of the 2005 wet season.	
Figure 98: Simulated heads (ft above NGVD) at the end of the 2006 dry season.	155
Figure 99: Simulated heads (ft above NGVD) at the end of the 2006 wet season.	156
Figure 100: Simulated heads (ft above NGVD) at the end of the 2007 dry season.	157
Figure 101: Simulated heads (ft above NGVD) at the end of the 2007 wet season.	158
Figure 102: Simulated heads (ft above NGVD) at the end of the 2008 dry season.	150
Figure 103: Simulated heads (ft above NGVD) at the end of the 2008 wet season.	160
Figure 104: Simulated heads (ft above NGVD) at the end of the 2009 dry season.	161
Figure 105: Simulated heads (ft above NGVD) at the end of the 2009 wet season.	160
Figure 106: Simulated heads (ft above NGVD) at the end of the 2010 dry season.	162
Figure 107: Wells along transects through the study area.	
Figure 108: Simulated and observed heads (ft above NGVD) at JEI-1466.	
Figure 109: Simulated and observed heads (ft above NGVD) at JEI-1468.	
Figure 110: Simulated and observed heads (ft above NGVD) at JEI-1465.	
Figure 111: Simulated and observed heads (ft above NGVD) at JEI-1476.	
Figure 112: Simulated and observed heads (ft above NGVD) at JEI-1505.	
Figure 113: Simulated and observed heads (ft above NGVD) at JEI-500.	
Figure 114: Simulated and observed heads (ft above NGVD) at JEI-502.	
Figure 115: Simulated and observed heads (ft above NGVD) at JEI-612	
Figure 116: Simulated and observed heads (ft above NGVD) at JEI-1506.	
Figure 117: Simulated and observed heads (ft above NGVD) at JEI-1507	
Figure 118: Simulated and observed heads (ft above NGVD) at JEI-558.	
Figure 119: Simulated and observed heads (ft above NGVD) at JEI-504	
Figure 120: Simulated and observed heads (ft above NGVD) at JEI-505	
Figure 121: Simulated and observed heads (ft above NGVD) at JEI-507	
Figure 122: Simulated and observed heads (ft above NGVD) at JEI-1475	172
Figure 123: Simulated and observed heads (ft above NGVD) at JEI-556.	172
Figure 124: Simulated and observed heads (ft above NGVD) at JEI-555	173
Figure 125: Simulated and observed heads (ft above NGVD) at JEI-514	173
Figure 126: Simulated and observed heads (ft above NGVD) at JEI-554.	
Figure 127: Simulated and observed heads (ft above NGVD) at JEI-1517	174
Figure 128: Simulated and observed heads (ft above NGVD) at JEI-1510	
Figure 129: Simulated and observed heads (ft above NGVD) at JEI-1512	
Figure 130: Simulated and observed heads (ft above NGVD) at JEI-516.	
Figure 131: Simulated and observed heads (ft above NGVD) at JEI-520A.	
Figure 132: Simulated and observed heads (if above NGVD) at JEI-521.	
Figure 133: Simulated and observed heads (if above NGVD) at JEI-553.	
Figure 134: Simulated and observed heads (it above NGVD) at JEI-533.	
Figure 135: Simulated and observed heads (it above NGVD) at JEI-1519.	
Figure 136: Simulated and observed heads (it above NGVD) at JEI-1319.	
Figure 137: Simulated and observed heads (it above NGVD) at JEI-325.	
Figure 138: Simulated and observed heads (it above NGVD) at JEI-1457. Figure 138: Simulated and observed heads (ft above NGVD) at JEI-1457.	
Figure 139: Simulated and observed heads (ft above NGVD) at JEI-528.	
Earthfx Inc. and Greg Rawl, P.G. Page	13

Figure 140: Simulated and observed heads (ft above NGVD) at JEI-529	31 32 33 33 34 34
Figure 149: Simulated and observed heads (ft above NGVD) at JEI-1498	35 36 36 37 37
Figure 154: Surface water features represented in Natural Conditions simulations	al 39 ns 90
Figure 157: Simulated infiltration (inches) for August 19, 2008 under Natural Conditions	in 92
through October 2008 under Current and Natural conditions)8 93
Figure 162: Simulated daily flow (cfs) at gage JEI-567 under Current and Natural Conditions	95 95 96
Figure 166: Simulated accumulated Hortonian flow (inches) for August 19, 2008 under Post-developme Conditions	nt 98 nt
Conditions	00 01 is.
Figure 171: Simulated daily flow (cfs) at gage JEI-569 under Current and Post-development Condition	is. 02
Figure 172: Simulated daily flow (cfs) at gage JEI-570 under Current and Post-development Condition)3
Figure 173: Wetland stage observation points)5)5)6
Figure 177: Simulated stage (ft above NGVD) in upper Curry Lake near JEI-557	07 07 08
Figure 181: Simulated stage (ft above NGVD) in wetland near JEI-518	09 09 10
Figure 185: Simulated stage (ft above NGVD) in wetland near JEI-562. 21 Figure 186: Simulated stage (ft above NGVD) in wetland near JEI-1520. 21 Figure 187: Simulated stage (ft above NGVD) in wetland near JEI-562. 21 Farthfy Inc. and Greg Rawl, P.G.	11

Figure 188: Simulated stage (ft above NGVD) in Assessment Area 1 (Curry Lake) under Current, Natural,
and Post-development Conditions.
Figure 189: Simulated stage (ft above NGVD) in Assessment Area 2 under Current, Natural, and Post-
development Conditions
development Conditions
Figure 191: Simulated hydroperiod, in average days per year, in the BRC under Current Conditions214
Figure 192: Simulated hydroperiod, in average days per year, in the BRC under Natural Conditions 215
Figure 193: Simulated hydroperiod, in average days per year, in the BRC under Post-development
Conditions
Figure 194: Increase in simulated hydroperiod (Post-development – Current Conditions) in the BRC217
Figure 195: Decrease in simulated hydroperiod (Post-development – Current Conditions) in the BRC. 218
Figure 196: Average days per year with simulated flow under Post-development Conditions
Figure 197: Simulated flow (cfs) versus time for 5-yr, 25-yr, and 100-year storms at JEI-567 under Current
Conditions
Conditions
Conditions
Conditions
Figure 200: Simulated flow versus time for 5-yr, 25-yr, and 100-year storms at JEI-567 under Natural
Conditions
Figure 201: Simulated flow versus time for 5-yr, 25-yr, and 100-year storms at JEI-569 under Natural
Conditions
Figure 202: Simulated flow versus time for 5-yr, 25-yr, and 100-year storms at JEI-570 under Natural
Conditions 222
Figure 203: Simulated flow versus time for 5-yr, 25-yr, and 100-year storms at JEI-567 under Post-
development Conditions
Figure 204: Simulated flow versus time for 5-yr, 25-yr, and 100-year storms at JEI-569 under Post-
development Conditions
development Conditions
Figure 206: Simulated flow versus time for the 5-yr storm at JEI-567 under Current, Natural, and Post-
development Conditions.
Figure 207: Simulated flow versus time for the 25-yr storm at JEI-567 under Current, Natural, and Post-
development Conditions
Figure 208: Simulated flow versus time for the 100-yr storm at JEI-567 under Current, Natural, and Post-
development Conditions
Figure 209: Simulated flow versus time for the 5-yr storm at JEI-569 under Current, Natural, and Post-
development Conditions
Figure 210: Simulated flow versus time for the 25-yr storm at JEI-569 under Current, Natural, and Post-
development Conditions 226
Figure 211: Simulated flow versus time for the 100-yr storm at JEI-569 under Current, Natural, and Post-
development Conditions
development Conditions
Figure 213: Simulated flow versus time for the 25-yr storm at JEI-570 under Current, Natural, and Post-
development Conditions.
Figure 214: Simulated flow versus time for the 100-year storm at JEI-570 under Current, Natural, and
Post-development Conditions. 228
Figure 215: Location of points for measuring simulated flows at the downstream ends of Trout, Owl, and
Telegraph Creeks for design storms under Current, Natural, and Post-development Conditions229
Figure 216: Rating curves for JEI-567.
Figure 217: Rating curve for JEI-569.
Figure 218: Rating curve for JEI-570.
Figure 219: Rating curve for JEI-1471
Figure 221: Rating curve for JEI-1495
Figure 222: Rating curve for JEI-1497
Earthfx Inc. and Greg Rawl, P.G. Page 15

Figure 223: Rating curve for JEI-1502.	243
Figure 224: Rating curve for JEI-1508.	
	244
Figure 226: Regression Analysis of Big Island (BI) Canal Discharge at BI Dike and County Line	244

AN INTEGRATED SURFACE-WATER/GROUNDWATER FLOW MODEL ANALYSIS OF INFILTRATION AND STORM WATER RUNOFF FROM THE BABCOCK RANCH COMMUNITY DEVELOPMENT, CHARLOTTE AND LEE COUNTIES, FLORIDA

1 INTRODUCTION

1.1 Background

Babcock Property Holdings, LLC (BPH) s developing 17,780 acres of property that was a part of a larger tract of land historically known as the Babcock Ranch. The remainder of the lands were sold to Lee County and the State of Florida in the largest public conservation lands purchase conducted by the State. These lands will be maintained and managed as preservation lands in perpetuity.

The 17,780 acres owned by BPH will be known as the Babcock Ranch Community (BRC). The BRC (shown in Figure 1) is bounded by State Road 31 to the west and County Road 78 to the south. The land has historically been used for agricultural operations. A limestone mining operation (Earthsource Mine) is located in the west-central part of the BRC near State Road 31 and Cook Brown Road.

The BRC mixed-use development will consist of several "development pods" of mixed uses. The mixed uses are organized in a town center, three villages, and four hamlets linked with a series of pathways for the use of alternative vehicles and pedestrians. Over 9,000 acres of the BRC will have usage limited to conservation, greenways, flow ways, and agriculture.

The BRC surface water management (SWM) system is composed of a series of interconnected lakes and constructed scrubber marshes. Stormwater runoff will be captured by the lakes which will have the capacity to attenuate the larger of 1.5 inches of runoff from the entire drainage area or the equivalent volume of 3.75 of inches of rainfall multiplied by the area of the impervious surfaces. A portion of the intercepted water will be treated and discharged to the scrubber marshes for additional treatment before discharging to the existing natural channels or offsite.

In August 2009, Lee County, Charlotte County, and Babcock Property Holdings, LLC entered into a Settlement Agreement to address concerns raised by Lee County regarding the development of the BRC. As a Point of Agreement of this Settlement Agreement, Babcock Property Holdings, LLC agreed to develop a calibrated continuous-simulation integrated surface water/groundwater model for the BRC and surrounding area. The model would be calibrated to simulate Current Conditions (pre-BRC) and calibrated to observed groundwater levels, stage, and flows from 2006 to 2008. A second model would be completed by modifying the input data to represent Post-development Conditions as authorized in the Environmental Resource Permit (ERP) Modification issued by SFWMD for the development (Permit #08-00005-S-05, Application #0703305). Finally, a third model would be developed to simulate, as reasonably as possible, the Natural Conditions by eliminating existing man-made features such as roads, ditches, weirs, dikes, roads, berms, canals, farm fields and farm field detention, and pastures (as identified in the Settlement Agreement) and replacing them with reasonable representations of natural habitat.

Earthfx and Greg Rawl P.G. have worked in consultation with Dean Mades, P.E. to develop a calibrated continuous-simulation integrated surface water and groundwater flow model using the new U.S. Geological Survey GSFLOW code. The model domain includes the sub-basins and model assessment areas specified in the Settlement Agreement (shown in Figure 2) and extends further to the west and north (Figure 1). The model area encompasses approximately 310 square miles. The

model was used to simulate surface water and groundwater flow and calibrated to match observed groundwater levels, stage, and discharge over an extended simulation period (October 2002 to July 2010). The simulation period encompassed an extreme dry year (WY2007) and an extreme wet years (WY 2003). The model then simulated future Post-development Conditions and Natural Conditions, as defined in this report. Comparisons were made between the hydrologic response at observation points and in the model assessment areas.

The models were developed using sound scientific and engineering assumptions and principles and best available data, and were subject to internal review for quality control and quality assurance in accordance with normal industry accepted standards to assure an accurate calibrated and verified model.

1.2 Previous Studies

Johnson Engineering Incorporated (JEI) developed the conceptual plans for the BRC (JEI, 2007a). The plans provide mappings of topography, soils, and drainage as well as detailed plans for the lakes, scrubber marshes, and wetland preserves. A second JEI report (JEI, 2007b) describes the SWM system and reports on results of the Interconnected Pond Routing Model (ICPR) used to predict response of the SWM system to the 5-year (1 day), 25-year (3 day), and 100-year (3 day) design storm events. Also described in this report is the hydraulic model developed by JEI for each of the major streams flowing through the site (i.e., Telegraph Creek, Trout Creek, and Owl Creek). The model was developed using the U.S. Army Corps of Engineers Hydraulic Engineering Center River Analysis System (HEC-RAS). The models were used to compare peak stage under existing and proposed conditions.

In 2008, Earthfx and Greg Rawl P.G conducted additional hydrologic modelling to independently determine the existing condition design storm discharge for the BRC. Two models, one based on the HEC-HMS Hydraulic Engineering Center Hydrologic Modeling System (HEC-HMS) and the other based on the USGS Precipitation Runoff Modeling System (PRMS) were used to simulate flows generated by the 5-year (1-day), 25-year (3-day) and 100-year (3-day) design storms. The models were calibrated to observed storm flows for 2006 and 2007 in the Trout Creek watershed which extends through the center of the BRC and receives the majority of the runoff from the area.

The study area has been included in a number of modelling studies commissioned by the SFWMD. Portions of the current study area fall within the western part of the Freshwater Caloosahatchee River Basin (C-43) model developed by the Danish Hydrologic Institute in 2004 (DHI and Stanley Consultants Inc., 2005). Other portions of the current study area fall within the eastern portion of the Tidal Caloosahatchee River Basin model also developed in 2004 by Camp Dresser and McKee Inc. (CDM, 2006). These models are relatively large in scale and are too generalized for the local-scale analysis needed. These models were combined with other sub-regional models into an even larger regional model for the Southwest Florida Feasibility Study (SWFFS) in a study by SDI Environmental Services, Inc. (SDI and others, 2008). In a study commissioned by Lee County, DHI developed the Lee County Groundwater Model (DHI, 2009) which focused on the central part of Lee County.

2 Physical Setting of the Study Area

The study area is located in northern Lee County and southern Charlotte County north of the Caloosahatchee River in southwest Florida. The study area extends about 4.2 miles west from State Route 31, 16.5 miles east from State Route 31, approximately 3 miles north of County Road 74, and about 3 miles south of the BRC. The study area includes all the sub-basins outlined in the Settlement Agreement (see Figure 2).

2.1 Climate

Climate in the study area is considered to be subtropical and is strongly influenced by its proximity to the Gulf of Mexico. The area has short, mild winters and long, hot summers. Monthly average daily high temperatures range from a low of 75 °F in January to a high between 91 and 92 °F in June through September. Monthly average daily low temperatures range from a low of 54 °F in January to a high of about 75 °F in June through September.

There is a pronounced seasonal variation in rainfall. Monthly average rainfall at Station S-79 at Franklin Lock (based on 20 years of record) ranges between 8.4 to 9.7 inches in the June through September wet season. Monthly average rainfall ranges between 1.9 to 3.4 inches in the dry season from October to May (Figure 4). Annual rainfall at S-79 is about 54.2 inches per year (in/yr) with a standard deviation of about 9.1 inches. A graph of annual rainfall by water years (Figure 5) shows that amounts vary from year-to-year with recent dry years having occurred in WY2007 and WY2009 and wet years in WY2003, WY2004, and 2005.

Daily values for potential evapotranspiration (PET) were calculated by SFWMD based on climate data measured at S-79 for 2001 to 2011. Monthly averages, based on the data for the period of record are shown in Figure 6. PET rates are highest in April and May (about 5.9 in) and lowest in December (2.9 in). PET values vary from year to year (Figure 7) and averages about 52.1 in/yr.

2.2 Land Surface Topography

Land surface topography has a strong influence on surface water processes such as runoff and infiltration. The study area is characterized by low topographic relief, high water tables and poorly drained soils. Baseline topography for the study area, as shown in Figure 3, was determined based on a mix of LIDAR data and a gridded 100-foot digital elevation model (DEM) obtained from the South Florida Water Management District and was utilized for the South West Florida Feasibility Study (SWFFS). The BRC topography information was updated with LIDAR-based datasets developed by AIM Engineering and Surveying, Inc. and the Surdex Corporation based upon aerial photogrammetry flown from October 13, 2007 to November 3, 2007. The SFWMD base topography south of the Lee-Charlotte County line was based upon Lee County derived LIDAR data. On the west side of Telegraph Swamp, the land slopes gently from north to south towards the Caloosahatchee River although locally it slopes east-west towards the creeks and swales that drain the area. Higher elevations (over 75 ft above sea level) occur in the north on the east side of Telegraph Swamp. Steeper slopes occur in the central part of the study area with gentler slopes to the south. Several anomalous areas of higher elevations occur, for example in the vicinity of the Earthsource mines. These areas are associated with temporary stockpiles of granular material. The DEM was revised to remove these anomalous values before use in developing the model.

2.3 Soil Data

Soils in the study area are primarily sandy but are classified as "poorly drained" because of the shallow depth to water table. Muck soils occur in the wetland areas. A simplified soil map for the study area is shown in Figure 9 based on data obtained from SFWMD. The number of soil types shown was reduced to eight general categories:

- (1) Sand;
- (2) Sand (depressional)
- (3) Fine Sand;
- (4) Fine Sand (depressional);
- (5) Loam
- (6) Muck
- (7) Urban Land Complex; and
- (8) Organic.

As can be seen from the mapping, most of the BRC and surrounding area is covered by fine sand with the remainder mainly depressions filled with muck soils.

2.4 Land Use

Historically, land use in the study area was primarily for cattle ranching, agriculture, silviculture, and citrus groves in the first half of the twentieth century. Babcock Ranch was a large cattle ranch; the Four Corners area (at the intersection of Lee, Charlotte, Hendry and Glades County in the southeast of the study area) contains a large citrus grove. The initial alteration of lands involved the clearing of native vegetation. A significant amount of ditching has been done within the study area to improve drainage and facilitate agricultural development.

Residential land development became a major economic driving force in Lee and Charlotte County in recent history. Canals were dredged and natural surfaces were disturbed by the removal of native vegetation. Impervious surfaces were also created. This major alteration not only affected the land surface, but also had an impact by altering the natural flows of both surface and groundwater. Residential development is limited within the study area and has occurred mainly in the southern part of the study area between North River Road and the Caloosahatchee River and in the southwest between Interstate 75 and SR 31. Rock mining for road fill and concrete aggregate has occurred on the BRC and to the immediate west across SR 31.

Detailed mapping of current (2000) land use in the study area based on the Florida Land Use, Cover and Forms Classification System was obtained from SFWMD. A simplified version, in which subclasses have been merged, is shown in Figure 8. The simplified land use data were used in conjunction with soils data to partition runoff and infiltration in the PRMS sub-model.

2.5 Hydrologic Setting

The purpose of this section is to introduce the hydrologic setting and discuss continuous streamflow data that have been collected across the study area since 2006. These data, along with groundwater level data, form the principal calibration targets for the GSFLOW model.

The BRC is located within three watersheds – Telegraph Creek, Trout Creek, and Owl Creek. The most significant surface water features in the study area include: Telegraph Swamp located in the center of the study area, a large wetland complex along the west boundary included within the Cecil Webb State Wildlife Management Area; and another large wetland complex in the northeast.

Telegraph Creek watershed, which includes Telegraph Swamp, has the largest drainage area and includes a small portion of the BRC. Owl and Trout Creeks, make up the majority of the BRC. Approximately 67% of the BRC is located in the Trout Creek watershed, 5% in the Owl Creek watershed, and about 28% in the Telegraph Creek watershed. Numerous other wetland complexes and streams, most notably Jacks Branch which receives flow from the wetland complex in the northeast, are found within the study area (east and west of the BRC).

Drainage from the BRC and the western part of the study area (Popash, Stroud, Palm, Owl, Trout, Otter, and Telegraph Creeks) discharges to the tidal reaches of the Caloosahatchee River. The eastern part of the study area (Fitchers Branch, Cypress Creek, Millers Gully, and Jacks Branch) discharge to the freshwater part of the Caloosahatchee River upstream from Franklin Lock. Historically, all of the above-referenced tributaries discharged to the tidal reaches of a narrow meandering Caloosahatchee River. In the 1950's and 1960's, the Caloosahatchee River was channelized and deepened and the Franklin Lock control structure was constructed upstream of Telegraph Creek. The deepening of the Caloosahatchee River intersected higher hydraulic conductivity limestone units thereby affecting the regional groundwater hydrology.

Natural flow in the study area is generally from north to south. Ditches redirect runoff locally and vary in size from small perimeter ditches around fields to large conveyances such as Curry Lake Canal and Big Island Canal.

2.5.1 Streamflow Monitoring

Stream monitoring was initiated in 2006 by JEI on behalf of BPH. Continuous records of water level (stage) and monthly measurements of stream velocity were collected by JEI and used to calculate stream discharge. These data were provided to Earthfx and Greg Rawl, P.G. for use in calibrating the GSFLOW model. Station information is provided in Table 1; locations are shown in Figure 10. The USGS maintains a streamflow station on lower Telegraph Creek. Earlier data collected by the Telegraph Creek Water Management District were also compiled and reviewed.

Each JEI station is equipped with a continuous recording, pressure transducer and data logger installed in a protective PVC pipe affixed in a stationary position in the channel. The data loggers are programmed to record stream stage at 4-hour intervals. Data logger records are downloaded during the monthly site inspections and subsequently archived at the office. The USGS maintains a streamflow station on tidally influenced Telegraph Creek (022929176), and the station is equipped with a stage sensor and acoustic Doppler velocity meter.

Stream-gaging records collected from March 2006 through July 2010 at the JEI stations were analyzed to determine daily average discharge at the three sites within the BRC (JEI-567, JEI-569 and JEI-570) and the eight additional stations. Methods used to determine daily discharge for the JEI stations are described in this section and in Appendix 1. Raw data collected at USGS station 022929176 are post-processed by the USGS using a statistical filter to remove tidal influence in the flow record. Daily records of "tidally-filtered" discharge are published by the USGS and can be used to estimate freshwater runoff from the watershed.

Recorder JEI-567, Curry Lake Canal at Hercules Grade, Trout Creek Watershed: Station JEI-567 is located on the upstream side of two parallel thirty-inch diameter culverts at a road known locally as Hercules Grade. The station is at the southern end of the State Preserve portion of Curry Lake and represents the headwaters of Curry Lake Canal and Trout Creek. Flow can be regulated by placing timber stop logs in the risers on the upstream side of each culvert, although there is no record of this activity.

Recorder JEI-569, Curry Lake Canal near County line, Trout Creek Watershed: JEI-569 is located approximately 19,400 ft downstream of JEI-567. The gage is located in an open incised

channel section of Curry Canal north of the convergence of Curry Lake Canal with the headwaters of Trout Creek, just north of the Lee/Charlotte County Line.

Recorder JEI-570, Trout Creek near State Road 78, Trout Creek Watershed: JEI-570 is located at the southern extent of Trout Creek south of the confluence of Trout Creek and Curry Canal. It is in roughly the same relative location as that of the original Trout Creek stage recorder that was installed in the early 1990's by the Telegraph Cypress Water Management District.

Recorder JEI–1471: Telegraph Creek at Babcock Ranch Headquarters, Telegraph Creek Watershed: JEI-1471 is on the upstream side of a 140-ft. wide concrete low-water control (LWC) weir structure located 600 ft northeast of the ranch headquarters office (now in the State Preserve). The structure includes eight 6-ft wide by 3-ft high bays for timber stop logs (i.e., removable boards), and the remainder is a fixed (concrete) crest of relatively constant elevation, 3 ft above the LWC sill. The stop logs are typically in place, although any number of logs can be removed at the direction of the SFWMD to maintain an upstream stage or meet downstream flow demands. They are removed during high flow to minimize upstream flooding. Few records of board settings were available, thus making it difficult to construct a record of historic discharges.

Recorders JEI-564 and JEI-565: Big Island Canal at Big Island Dike, Telegraph Creek Watershed: There are three LWC structures constructed on Big Island Dike. The dike spans the entire width of Telegraph Swamp approximately 2 miles north of the Lee-Charlotte County line. The gages are located at the western LWC structure. The west structure is a 100-ft wide, fixed-crest dam with two 4-ft high by 2.5-ft wide vertical-lift slide gates (also referred to as screw gates), one on each downstream side wall. A road crossing consisting of a concrete armoured earthen dam with three culverts is located parallel to the fixed dam about 50 ft downstream. Discharges past the dam flow through the culverts and, at higher flows, over the culverted road crossing as well. JEI-564 is located on the upstream side of the fixed dam; JEI-565 is located in the tailwater section, immediately downstream from the fixed dam and upstream from the culverted road crossing. Discharge past this structure flows downstream in Big Island Canal to a stream gaging station located near the Lee County line. Few records of gate opening were available, thus making it difficult to construct a record of historic discharges at this structure.

The central and eastern structures on Big Island Dike are concrete LWC structures constructed similar to the LWC structure at gage JEI-1471. The central structure is 100-ft wide and includes five 6-ft wide by 3-ft high bays for timber stop logs. The remainder is a fixed crest wall of relatively constant elevation, 3 ft above the LWC structure's sill. The eastern structure is 200-ft wide and includes eight 6-ft wide by 3-ft high bays for timber stop logs. The remainder is a fixed crest of relatively constant elevation, 3 ft above the LWC structure sill. The upstream pool at these structures is hydraulically connected to, and presumably similar or the same as, the upstream pool at JEI-564. However, the downstream pools at these structures are likely separated except during periods of high flow. Discharge past the central and eastern structures flows downstream in Telegraph Creek to a gage on a timber bridge. There are no data loggers or active stream gaging at the middle and eastern structures. Few records of board settings or stream discharge were available for use in determining discharge at these two structures.

Additional gages, discussed below, are not located in the BRC. They provided useful information used in model calibration in the portions of the study area outside the BRC.

Recorder JEI–1495 - Big Island Canal at County Line, Telegraph Creek Watershed: JEI-1495 is located in an open channel section of Big Island Canal about 2 miles downstream from JEI-565 and about 1.5 miles upstream of the canal convergence with Telegraph Creek.

Recorder JEI–1497 - Telegraph Creek at Timber Bridge, Telegraph Creek Watershed: JEI-1497 is located at a timber bridge approximately 2,200-ft upstream of the mouth of Big Island Canal.

Station 022929176 - Telegraph Creek at State Highway at Olga, Telegraph Creek Watershed: The USGS maintains a continuous recording stream-gaging station on an open section of Telegraph Creek about 600 feet downstream from the State Road 78 bridge and 2,700 feet upstream from the mouth at the Caloosahatchee River.

Recorder JEI–1518 - South Lightered Canal at Cypress Head, Cypress Creek Watershed: JEI-1518 is located in an open channel section of South Lightered Canal about 9,500 feet east-northeast from the east terminal end of Big Island Dike.

Recorder JEI-1502 - Cypress Creek Outflow, Cypress Creek Watershed: JEI-1502 is located in an open channel section of Cypress Creek approximately 2.4 miles upstream from the creek mouth at the Caloosahatchee River.

Recorder JEI-1508 - Jacks Branch Inflow, Jacks Branch Watershed: JEI-1508 is located in an open channel section of Jack' Branch about 8.5 miles due east from Babcock Ranch Headquarters station JEI-1471.

Recorder JEI-1514 - Jacks Branch Outflow, Jacks Branch Watershed: JEI-1514 is located on the upstream side of the County Road 720 bridge. Water is conveyed under CR720 via three rectangular, concrete culverts, each 12-ft wide by 5-ft high.

2.5.2 Streamflow Calculation Methods

Stream discharge at the JEI gages was calculated using two methods. A conventional stream-gaging approach based on stage-discharge ratings was used for all stations except JEI-564/565 on Big Island Dike. An empirical approach based on hydrograph comparison was used for JEI-564/565 because insufficient operational data regarding the position of stop logs and gates were available to support the calculation of discharge based on standard ratings for hydraulic structures. Specific information on the rating methods are provided in Appendix 1.

2.6 Geologic Setting

The lateral movement of groundwater from the northern part of the study area to the Caloosahatchee River occurs primarily through the carbonate rocks. This section of the report describes the geology, hydrostratigraphy, and the hydraulic characteristics of the area.

Southwest Florida is comprised of sedimentary rocks of Cenozoic age. These rocks are of a relatively young age (geologically), from 56 million years ago to the present (Berggren et al, 1995), as shown below.

Geologic Time Scale					
Era Period		Epoch	Approximate duration (10 ⁶ years)	Approximate number of years ago (10 ⁶ years)	
randowy di	Oustornan	Holocene	.01	0	
Cenozoic	Quaternary	Pleistocene	1.8	.01	
	nes Differens	Pliocene	3.5	1.8	
		Miocene	18.5	5.3	
	Tertiary	Oligocene	10.1	23.8	
	general a	Eocene	22	33.7	
	50)	Paleocene	9.5	56	

The exposed landmass of Southwest Florida was formed during the Pleistocene Epoch with the advances and declines in sea level 1.8 million to 8,000 years ago. The underlying limerock formations are also of more recent Cenozoic age, with the Suwannee Limestone formed in the Oligocene, 36 to 25 million years ago. These rocks are primarily carbonates (limestones) in the lower portion with clastics (sand and clay) in the upper part.

Geologic units in southwestern Florida generally consist of, in ascending order, the Suwannee Limestone of Oligocene age, Hawthorn Group (Arcadia and Peace River Formations) of Oligocene to Pliocene age, Tamiami Formation of Pliocene age, and undifferentiated sediments of Holocene to Pleistocene age. These formations are shown in Table 2.

The Suwannee Limestone is composed of fossiliferous, calcarenitic, limestone with minor amounts of quartz sand. The thickness of the limestone varies widely, and is found at depths greater than 500 ft in Lee and Collier Counties. The basal Suwannee Limestone generally contains fine-grained, phosphatic, clastic material with interbeds of micrite and clay (Reese, 2000).

The Hawthorn Group is divided into the Arcadia Formation and the Peace River Formation. The Arcadia Formation, which unconformably overlies the Suwannee Limestone, consists of fine-grained carbonate sediments as well as sandy limestone, shell beds, dolomite, phosphatic sand and carbonate, sand, silt, and clay. The predominantly clastic Peace River Formation has a highly irregular erosional and karstic surface. The contact with the overlying Tamiami Formation appears to be unconformable in some areas but indistinct in other areas. The sediments of the Peace River Formation consist of interbedded, fine- to coarse-grained quartz sand, quartz silt, gravel, clay, carbonate, and phosphatic sand (Reese, 2000).

The Tamiami Formation overlies the Peace River Formation and consists of varying amounts of silt, sandy clay, micritic limestone, sandy and shelly limestone, calcareous sandstone, and quartz sand. The lithology of the Tamiami Formation varies greatly because of the complex nature of the depositional environment. The limestone is well indurated to un-indurated, slightly phosphatic, variably sandy, and fossiliferous. The sand facies varies from well sorted, clean sand with abundant shells and traces of silt-size phosphate, to clayey sand with sand-size phosphate, clay-size carbonate in the matrix, and abundant well-preserved mollusc shells (Knapp and others, 1986; Reese and Cunningham, 2000).

The undifferentiated sediments of Holocene to Pleistocene age overlie the Tamiami Formation at land surface (Reese, 2000). These deposits mainly consist of quartz sand with minor amounts of shell and clay, and contain limestones, sandstones, and shell beds. With increasing elevation inland, the sand becomes thicker and less calcareous. The sand facies varies from fine to coarse grained, non-integrated to poorly indurated, and non-clayey to slightly clayey. Included in this group are marine terrace sediments, Aeolian sand dunes, fluvial deposits, freshwater carbonates, peats, and clay beds.

2.7 Geologic Layers

The regional geology of the study area was mapped and analyzed three dimensionally using a geologic data management and analysis software package called VIEWLOG-GIS (Version 4.0, www.viewlog.com). VIEWLOG was also utilized to analyze groundwater level data and aquifer properties for the study area. This software was developed by and applied by Earthfx for the Southwest Florida Feasibility Study (SWFFS). The program interfaces with a Microsoft Access hydrogeologic database developed for the BRC and surrounding area. The database contains information on well construction, lithologic units, hydrogeologic parameters and groundwater level data. Data were interrogated and interpolated to form a three-dimensional geologic model and a

hydrostratigraphic model for the study area. Surfaces of the hydrostratigraphic model were used directly in the groundwater model.

The lithologic information stored in the database contains interpretative information pertaining to the elevations of the top and bottom of the various geologic and hydrostratigraphic units described in the previous section for each well from which data have been obtained. The lithologic database initially consisted of 1,080 wells extracted by Earthfx from a Water Resource Solutions (WRS) report prepared for the SFWMD. Addition lithologic information, as well as aquifer property data and water level information, were added to the database by Greg Rawl, P.G. to extend the areal coverage to the adjacent counties. This facilitated the analysis of regional trends and provided geologic control for the portions of the model in Charlotte County. The data include information from a variety of sources, including the USGS, Lee County Division of Natural Resources, mining operations, water supply investigations, and various geotechnical reports. Locations of wells with lithologic information are shown on Figure 11.

Geologic "picks" (i.e., the interpreted contact elevation for the top or bottom of a particular unit) were extracted from the database and used to create a surface by interpolating the information to a regular grid using the kriging method. Unit thicknesses were determined by using VIEWLOG to subtract the gridded top of each unit from the bottom. Rules were then applied to ensure that interpolated surfaces did not cross in areas where data were limited. The thickness of the upper unit (i.e., the Holocene sediments) was determined by subtracting the top of the Pliocene from the DEM.

Figure 12 through Figure 18 display the tops of the principal aquifers and aquitards represented in the model. A southwest to northeast geologic cross section was generated across the study area to show the area geology (Figure 19) and the eight geologic units represented in this modelling study. The location of the cross section is shown in Figure 11.

2.8 Hydrostratigraphy

The hydrogeologic units correspond to the geologic units as shown in Table 2. The three main water-producing aquifers that are underlying the study area are the Floridan Aquifer System, the Intermediate Aquifer System and the Surficial Aquifer System.

Floridan Aquifer: The Floridan Aquifer System is one of the most productive aquifers in the world, according to the United States Geological Survey (USGS). It underlies an area of over 100,000 square miles and is a source of water for many major cities in Georgia and Florida. The recharge area for this aquifer is in North-Central Florida. The Floridan Aquifer includes water-bearing rock of the Lower Hawthorn and Suwannee Formations. The water in the Floridan aquifer beneath the study area typically contains water with a total dissolved solids (TDS) concentration above recommended potable drinking water standard of 500 mg/L and requires treatment for potable use. However, it is commonly used for irrigation especially in coastal areas of Lee County where other aquifers are unavailable for use. This aquifer is used for public water supplies in Lee County where the other shallower aquifers are not productive or have been degraded by salt water intrusion.

Intermediate Aquifer: The Intermediate Aquifer System contains both the Sandstone and the Mid-Hawthorn Aquifers, along with the confining basal layers that underlie each within the Hawthorn Group. The Intermediate Aquifer System extends beneath a twelve-county area in Southwest and West-central Florida. This system contains water under confined conditions; that is, the aquifer is underlain and overlain by confining layers. It is of great significance in the study area.

Available information used to assess the Intermediate Aquifer was typically collected as a result of permit applications to one of the regulatory agencies. Water level, water quality, and aquifer performance test (APT) data are used by scientists and engineers to determine the quantity and quality of water available. Water level data were used to show seasonal differences in the aquifer or

changes as the result of pumping of the well or nearby wells. When data are available from a network of wells, water level contour mapping will show the water table over a larger spatial area. Water quality data are used to show trends in water quality of the aquifer.

Surficial Aquifer: The Surficial Aquifer System is comprised of one aquifer in the study area - the Water Table Aquifer. Throughout the study area, it consists of varying thicknesses of unconsolidated sand/silt and somewhat discontinuous limestone units

2.9 Aquifer Properties

The hydrogeologic parameters or aquifer coefficients contained within the database cover the same area as described for the lithologic information. Hydrogeologic parameters were determined for each unit simulated in the model and include hydraulic conductivity, storativity and leakance. These values were derived from previous studies by the USGS, SFWMD, Florida Geological Survey, and others (e.g., Boggess and Watkins, (1986), Wedderburn, *et al*, 1982, FGS (2001), BEM (2003), Rawl (2005), Ardaman & Associates (2005), JEI (2001), JEI(2006)).

These values formed the initial estimates of hydraulic properties used in the MODFLOW sub-model. The values were adjusted slightly during the model calibration process. Figure 20 shows the final hydraulic conductivity distribution for the surficial sands. The values were assigned to the soil classes described earlier. Figure 21 through Figure 23 show the hydraulic conductivity distributions for the Ochopee limestone, Peace River sandstone, and Arcadia limestone, respectively. The Lower Hawthorn was assigned a uniform transmissivity value equal to 0.0486 ft²/s (4,200 ft²/d).

2.10 Groundwater Monitoring

Observation wells were drilled across the BRC site and in the surrounding area starting in 2006. Each well is equipped with a continuous recording, pressure transducer and data logger. Water level data were collected and processed by JEI. A total of 203 observation wells (including wells installed by JEI, the USGS, Lee County, SFWMD and others), with 173 of them screened in the surficial aquifer, were available for use in calibrating the GSFLOW model. Well locations are shown in Figure 24

2.11 Groundwater Flow Patterns

Water levels measured in the observation wells are a measure of the hydraulic head (also referred to as potential or head) in the aquifer in which the well is screened. Observed heads recorded between 1997 and 2010 in observation wells in the BRC and in the surrounding area were averaged over time and plotted in Figure 25. Not all wells in the study area are shown because monitoring at these wells was discontinued during the study period or there were temporal gaps in their records.

Contours of interpolated heads were generated from the observation data for use in describing generalized patterns of groundwater flow. Because groundwater flows from areas of higher heads to lower in a direction perpendicular to the equipotential lines, it can be inferred that regional groundwater flow is from the north and northeast towards the Caloosahatchee River. The bending of the contours around Telegraph Swamp indicates that groundwater is discharging to this feature. Similar bending of contours can be seen in the vicinity of streams in the BRC indicating that the streams are also points of groundwater discharge. Although the general flow patterns will remain consistent, heads in the aquifer vary seasonally (i.e., during the wet and dry seasons) and the rates and directions of flow will vary accordingly. Heads will also change in response to year to year variations in rainfall (i.e., wet years and dry years). Groundwater extraction for irrigation can affect flow patterns locally.

2.12 Water Use

Surface water and groundwater use data for the study area were obtained from the South Florida Water Management District (SFWMD). Pumping rates are reported regularly by permitted users as required by the Water Management Districts. Data are stored in databases maintained by the District.

Information was obtained regarding all water use permits issued by SFWMD. Once the permits were identified, the withdrawal facilities (groundwater wells or surface water pumps) were located and the aquifer being tapped was identified. The monthly reported pumping for each facility was summarized in a database for access by the GSFLOW model. Withdrawal facility summary information is provided in Appendix 2. Well locations are shown in Figure 26.

3 Numerical Modelling

The primary objective of this study was to develop an integrated groundwater and surface-water model capable of addressing the specific requirements of the Settlement Agreement. A multi-stage model development and calibration approach was followed in which:

- insights and parameter values obtained from an earlier "PRMS-only" surface water model calibrated to observed streamflow were used to develop the input data sets for the updated PRMS sub-model in GSFLOW;
- a separate "MODFLOW-only" groundwater model was calibrated to steady-state (average wet season and average dry season) conditions to verify aquifer property estimates; and
- an integrated transient calibration was done with the two sub-models coupled in GSFLOW.

This stepwise process was needed because of the complexity of coupling the surface water and groundwater systems, the differences in the type and density of data, and the difference in characteristic time scales.

As noted earlier, the PRMS calibration built on earlier work by Earthfx in developing a PRMS and HEC-HMS model for the BRC. The MODFLOW work built on earlier hydrogeologic investigations and groundwater modelling of the region by the USGS, SFWMD, Greg F. Rawl P.G., and Earthfx.

3.1 GSFLOW Model Overview

The U.S. Geological Survey GSFLOW code (Markstrom and others, 2008) was developed specifically to simulate coupled groundwater and surface-water flow. GSFLOW represents an integration of the two widely-recognized USGS models: the Precipitation Runoff Modelling System (PRMS) (Leavesly and other, 1983) and the modular groundwater flow model MODFLOW (Harbaugh, 2005). In addition to the PRMS and MODFLOW sub-models, GSFLOW includes additional simulation methods and options specifically related to the coupling and integration of the models.

The MODFLOW code is extremely well-suited for modelling transient groundwater flow in multi-layered aquifer systems and can easily account for irregular boundaries, complex stratigraphy, and variations in hydrogeologic properties. MODFLOW uses the finite-difference method and requires that the study area be subdivided vertically into several layers, where each layer can represent a hydrogeologic unit or subunit (such as the Ochopee Limestone or the upper part of the surficial sands). The study area must also be subdivided horizontally into a grid of small rectangular cells. Aquifer properties, such as top and bottom elevations for each layer, hydraulic conductivity, and storage coefficients are assigned to each cell. Boundary conditions are specified for cells that lie along lines corresponding to the physical boundaries of the flow system. The model is primarily employed to solve for groundwater heads in the saturated zone below the water table. Application of the MODFLOW code to the study area is described further on in Section 4.

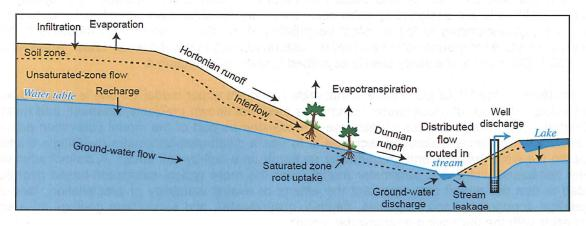
One limitation of the MODFLOW code is that recharge to the upper model surface is specified as an input value. The rate of groundwater recharge is often not known precisely, however, and must be estimated. The initial estimates of recharge are adjusted as part of the model calibration process. An alternative to simply estimating recharge is to use a distributed-parameter hydrologic model to compute the water balance and groundwater recharge on a cell-by-cell basis. A distinct advantage of the cell-based distributed parameter model (over the more typical catchment-based hydrologic model) is that the model can represent the effects of spatial variability of precipitation, land-use, vegetation, topography, soil properties, depth-to-groundwater, and subsurface geology on a scale compatible with the underlying groundwater model.

In earlier work, Earthfx and Greg F. Rawl, P.G. (2008) used a version of the PRMS code to simulate response to precipitation events and estimate surface water discharge in the study area. The study area was divided into grid of square cells, each with unique values for characteristics such as slope, aspect, elevation, vegetation type, soil type, and land use. Water and energy balances were computed daily for each cell using climate data inputs of spatially distributed precipitation along with temperature and pan evaporation data from nearby stations. The model produced cell-based estimates of evapotranspiration (ET), evaporation from canopy interception and detention storage (referred to as depression storage in the PRMS model documentation), runoff, infiltration, percolation and daily average groundwater recharge. The PRMS model was calibrated by adjusting model parameters to best match observed response to observed flows in the local streams.

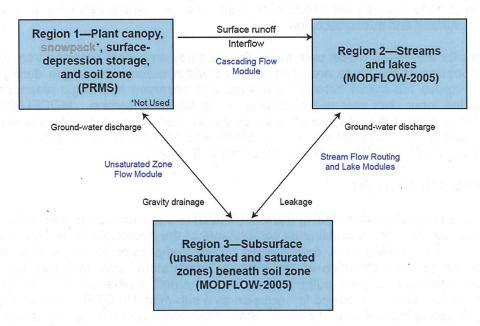
One limitation to calculating recharge with an independent hydrologic model is that there is no feedback between the groundwater and surface water systems. For example, the rate of ET (and, ultimately, the rate of groundwater recharge) as calculated by the hydrologic model is affected by depth to the water table. At the same time, the depth to the water table is determined by the groundwater model based on the rate of recharge. Similarly, the exchange of water between the shallow aquifer and surface water features such as wetlands and streams affects both groundwater flow and surface water flows. The strong coupling between the physical systems, especially in areas such as the BRC, is better simulated using a linked groundwater/surface water model such as GSFLOW which integrates hydrologic processes on a continuous basis and allows for feedback between the groundwater and surface water systems.

GSFLOW incorporates a new version of the PRMS code with a number of enhancements to the methods for computing the soil water balance. The PRMS sub-model simulates all surface processes including precipitation, evaporation, canopy interception, snow accumulation and snowmelt, the partitioning of throughflow between runoff and infiltration, interflow, and ET from the soil zone. The PRMS sub-model can compute water balances on a catchment basis but for this study, the model was used to compute the soil water balance on a cell-by-cell basis. Snow accumulation and snowmelt simulation are an important component of the PRMS code, but are obviously irrelevant to the hydrology of the study area.

A new module unique to GSFLOW routes overland flow (also referred to as surface runoff) and interflow as it cascades from cell to cell until it reaches a stream, lake (or wetland), or surface depression (swale). The cascade algorithm allows overland flow from multiple upslope cells to enter a cell and then either infiltrate or contribute to overland flow to down-slope cells. For these analyses, a one-to-one relationship was used, where the maximum slope determined the down-slope cell. The first schematic below (from Markstrom and others, 2008) shows the processes simulated within GSFLOW; with PRMS and the cascading flow module simulating all processes above the soil zone (dashed line on figure). The soil zone is typically defined by the average rooting depth of the predominant vegetation.



The MODFLOW sub-model, based on the MODFLOW-2005 version of the code, was designed primarily to solve for groundwater potentials in the saturated zone below the water table. The model can readily simulate flow in a multilayered aquifer system such as the one that underlies the study area. Add-on modules to the MODFLOW code are used to simulate additional processes such as flow in the unsaturated flow, groundwater interaction with the streams and lakes, and pumping. The second schematic (modified from Markstrom and others, 2008) shows where interaction between the PRMS and MODFLOW sub-models occurs and the modules (in blue text) used to simulate groundwater/surface water interaction.



The unsaturated zone flow (UZF) package (Niswonger, 2005) is incorporated into GSFLOW to simulate the percolation of excess moisture (infiltration minus I evapotranspiration) from the soil zone to the water table, groundwater ET processes, and the return of excess infiltration to the surface. The UZF module handles the particularly complex problem of the saturated zone rising into the soil zone which is a common occurrence in the study area. For example, water stored in the unsaturated zone is added to the saturated zone as the water table rises and water is removed from the saturated zone and retained in the unsaturated zone as the water table declines.

Another MODFLOW add-on incorporated into GSFLOW is the SFR2 stream flow routing module (Niswonger and Prudic, 2005) which calculates stream stage, seepage between the groundwater and surface water systems, and the routing of flow. Stream stage in each reach is calculated based on upstream inflows, precipitation, evaporation, and overland flow to the reach. Seepage to or from the aquifer is then calculated based on the difference between stream stage and the head in the underlying aquifer. Net outflow from each reach is routed to a downstream segment. The segments can terminate in a lake or wetland or exit the model area. SFR2 allows unsaturated flow beneath streams perched above a deep water table but this option was not implemented in these simulations due to the shallow depth to water in the study area.

The lake simulation (LAK) module (Merritt and Konikow, 2000) is also incorporated into GSFLOW and was used in this study to represent the shallow wetlands and proposed storm water lakes in the study area. The module computes a separate water balance for each lake or wetland based on computed inflows (e.g., precipitation, runoff, and incoming stream discharge) and outflows (e.g., evaporation, groundwater seepage, and outgoing stream discharge). Lake stage is calculated daily using a stage-storage relationship. Seepage to or from the aquifer is calculated based on the difference between lake stage and the head in the underlying aquifer. Discharge from the lake is calculated by the SFR2 package with rates determined by a specified stage-discharge relationship for each outlet channel or structure.

The hydrologic processes simulated in PRMS are driven by climate inputs (rainfall, air temperature, and solar radiation) supplied to the model. GSFLOW operates on a daily time step and employs the daily-mode option of the PRMS sub-model. Similarly, MODFLOW is constrained to operate using uniform one-day (24-hour) time steps and stress periods. Changes in the groundwater stress (e.g., pumping) can be supplied on a daily basis. The MODFLOW module routes streamflow on a daily basis and calculates average daily stream flow, stream stage, and lake stage, discharge, and storage. GSFLOW can readily simulate groundwater-surface water response over extended time periods and be used to evaluate the effects of land-use change, climate variability, and groundwater withdrawals on surface and subsurface flow.

Initial estimates for the PRMS model parameters for the study area were obtained from the previous PRMS-only modelling of the study area and adjusted within reasonable ranges during the model calibration to improve the match between simulated and observed hydrologic responses. PRMS operation and the input data sets are discussed in the following section. MODFLOW data sets needed to represent the study area, steady-state model calibration, and model results are discussed further on in Section 4. The linking of the PRMS and MODFLOW sub-models, the transient calibration, and GSFLOW model results are discussed in Section 5.

3.2 PRMS Sub-model

The USGS Precipitation-Runoff-Modelling-System (PRMS) is a sub-model included within GSFLOW. It is an open-source code for calculating all components of the hydrologic cycle on a watershed or sub-watershed scale. PRMS is a deterministic, distributed-parameter model that incorporates information on the spatial distribution of precipitation, temperature, solar radiation, soil properties, vegetation, and land use to yield outputs of estimated runoff, infiltration, ET, and groundwater recharge. The code has been modified for inclusion as a sub-model in GSFLOW such that its use is primarily for calculating the soil water balance. Streamflow processes can be simulated when doing PRMS-only model runs but these are now handled by MODFLOW add-on modules in GSFLOW. The code is well documented in Leavesly et al. (1983) and in the GSFLOW manual (Markstrom and others, 2008).

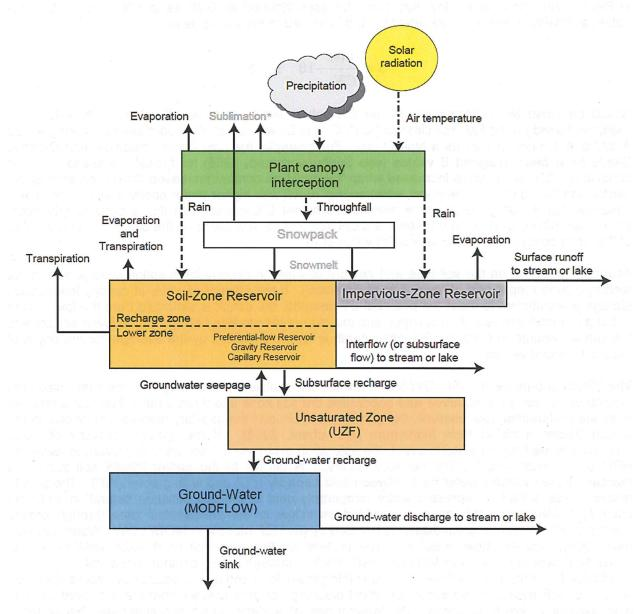
The PRMS code computes water balances for a set of Hydrologic Response Units (HRUs) on a daily basis. HRUs are defined as areas with uniform hydrologic properties and can represent a catchment or part of a catchment with a dominant soil type and land use. For this GSFLOW modelling study, a direct correspondence between the HRUs and MODFLOW model cells was established and the terms can be used interchangeably. A small cell size was selected (generally 300 ft by 300 ft) so that values associated with land use classes, soil types, and surface water features (i.e., wetlands and lakes) could be mapped to the cells with reasonable accuracy.

3.2.1 PRMS Operation

A schematic flow chart (modified from Markstrom and others, 2008) describing the operation of the PRMS sub-model is shown below. Each of the boxes in the diagram represents a "storage reservoir" in a single HRU. The arrows represent the transfer of water from one reservoir to another or to an ultimate point of discharge (e.g., the atmosphere or a stream or lake). Processes related to snowpack accumulation and snowmelt were bypassed in simulations of the study area.

The model tracks the volume of water in each storage reservoir as well as the flows between reservoirs each day. Each HRU can contain pervious and impervious surfaces and the water balance for each area is computed separately. For impervious areas, the model first computes capture of precipitation by canopy interception (if any) and detention storage (e.g., water captured on flat roofs or puddles in parking lots). If the impervious-zone reservoir storage capacity is exceeded, the surplus is assumed to run off. Water is removed from canopy and detention storage by

evaporation. Total detention storage was assumed to be small due to the limited amount of impervious surface area under Current Conditions.



For pervious areas, the model first computes canopy interception. The amount intercepted depends on the vegetation type and winter/summer vegetation cover density. Water is removed from the canopy by evaporation.

The PRMS model uses a "contributing-area" method to estimate the Hortonian flow component of overland runoff from each HRU. Earthfx added the option of using a U.S. Soil Conservation Service (SCS) curve number technique. The SCS runoff curve number is based on the concept that the volume of runoff is small for small storm events but increases with the size of the rainfall event. The volume of runoff depends on the soil class and land use (SCS, 1972). The runoff volume, R, is given by:

$$R = \frac{(P - I_a)^2}{(P - I_a) + S}$$
 Eq. 1

where $(P-I_a)$ is the effective precipitation after initial abstraction of evaporation from canopy interception and detention storage and other similar terms. Initial abstraction is calculated explicitly in PRMS rather than assuming that it can be approximated as 0.2S as is often done. S is the potential maximum soil moisture retention and is related to the CN value by:

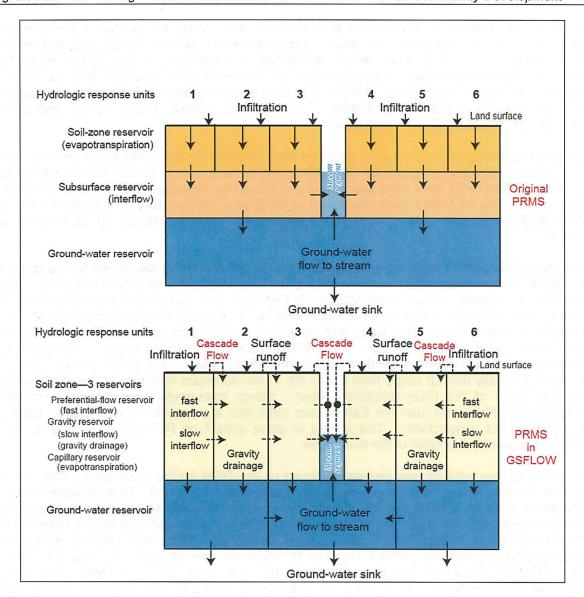
$$S = \frac{1000}{CN} - 10$$
 Eq. 2

Based on these two relationships, higher CN values yield higher runoff values. CN values are assigned based on the four soil classes (A, B, C, and D) with a well-drained clean sand being a type A soil and a muck or clay as a type D soil. For example, the Eau Gallie, Wabasso and Oldsmar Sands have been assigned B values (see Suphunvorranop, 1985) for typical dry-season drained conditions. CN values were increased when the moisture content increased (based on antecedent rainfall and the position of the water table) so that runoff was higher under poorly-drained conditions. Land use types that generate more runoff have higher CN values such that a good quality forest (more than 50% cover) on type B soil has a CN value of 55, row crops on the same soil have a value of 78, while commercial areas have a CN value of 92.

Actual ET depends on the soil type and amount of water in canopy interception storage and in the recharge zone (upper part of the soil zone reservoir). If the amount of water in canopy interception storage is insufficient to meet the potential ET demand, the deficit is extracted from the lower zone but at a reduced rate based on soil type and the ratio of the storage capacity of the lower soil zone to the current volume in storage. Soil zone depth is typically defined by the average rooting depth of the predominant vegetation.

The PRMS sub-model in GSFLOW has a revised soil moisture accounting that limits the maximum volume of the soil zone reservoir and subdivides the soil zone into three smaller reservoirs referred to as the preferential flow reservoir, the gravity reservoir, and the capillary reservoir, as shown in the sketch below (modified from Markstrom and others, 2008). If the storage capacity of these reservoirs is filled during a storm event, the saturation excess in the soil zone is allowed to leave the HRU as Dunnian runoff. The capillary reservoir is similar to the earlier PRMS soil zone and represents the available water held between field capacity (FC) and wilting point (WP). The gravity reservoir was added to represent water temporarily held in the soil between saturation and field capacity. Water from this zone is provided as inflow to the unsaturated zone through gravity drainage. Percolation to groundwater is handled by the UZF module in MODFLOW. Water can also move downslope as "slow" interflow. The preferential flow reservoir represents additional water above field capacity that is available for "fast" interflow through large openings in the soil.

In addition to runoff due to infiltration excess (Hortonian flow) and due to saturation excess (Dunnian flow), the UZF package also simulates direct discharge of groundwater from the saturated zone to land surface in low-lying areas. All three forms of surface runoff are schematic below (from Markstrom and others, 2008). Inflows from upstream cells are combined with net precipitation and can either contribute to infiltration or cascade further downslope until it reaches a stream, lake (or wetland), or surface depression (swale). One advantage of this method is that infiltration can occur along the flow path such that runoff from upland areas with poorly drained soils can re-infiltrate in areas with sandier soils and then re-emerge as groundwater discharge or interflow to streams. Once entering the streams, the water is routed downstream along the stream network using the SFR2 module. Groundwater can seep into the streams in reaches where the stage is lower than the groundwater heads. Water can seep out of the stream where the groundwater heads are low but this occurs infrequently in the study area. Streams and groundwater can discharge to wetlands and lakes.



3.2.2 PRMS Model Data

Climate Data: Key climate data inputs into the model are precipitation, potential evapotranspiration, and minimum and maximum air temperature. For this study, we used daily temperature data for October 2006 to July 2010 from the FPWX (Flint Pen Strand) weather station (latitude 26° 25' 57", longitude 81° 43' 24").

NEXRAD radar-based precipitation data were obtained from SFWMD for 2002 to 2010. These data are based on a 2 x 2 kilometer (km) grid that covered the entire study area. To prepare the rainfall input data sets, the 15-minute data were processed to create a continuous time series of daily rainfall values for the NEXRAD grid. These data were then re-sampled to create a corresponding time series for each model cell for each water year. An example of the gridded rainfall for August 10, 2006 (Figure 27) shows that daily rainfall varied spatially, from 0.0 to 1.8 inches, over the study area.

Observed rainfall at S-79 (Franklin Lock) for October 2002 through June 2010 was compared against the daily NEXRAD data for the 2 x 2 km cell containing the station. A scatterplot of the daily data is shown in Figure 28. Values generally compare well although some variation is expected

because of the distance of the radar station from the study area, the possibility that the rainfall (measured at higher altitudes by the radar) evaporates before striking the ground, and drifting of rainfall caused by wind. A comparison of monthly data is presented in Figure 29 and shows better correlation. Comparisons were made between the NEXRAD generated rainfall data, three Lee County rain gages, the USACOE/SFWMD rainfall data from S-79 and the four onsite rain gages that were maintained by Johnson Engineering. The NEXRAD generated data agreed well with the County and SFWMD/USACOE rainfall data.

Potential evapotranspiration data were obtained from SFWMD for the entire study area for 2005 to 2010. These data were computed by SFWMD on the same 2 x 2-km grid as the NEXRAD rainfall data. The SFWMD PET data were was calculated using the Priestley-Taylor method (Priestly and Taylor, 1972). The PET data were processed to produce a gridded daily time series for the study area for each water year. An example of the gridded PET data for August 10, 2006 is shown in Figure 30.

Parameters Related to Topography: A digital elevation model (DEM) developed for the study area (see Figure 3) was interpolated to the model grid. Observed data for shortwave solar radiation received on a horizontal surface were adjusted in PRMS for land surface slope and slope aspect as well as time of year prior to their use in ET calculations. This allows a north-facing slope to get less solar radiation than a south-facing slope and will therefore have lower potential ET rates. Slope and aspect values were calculated from the DEM by Earthfx using a five-point finite-difference approximation and provided as gridded data to the PRMS model. Figure 31 shows that natural slopes are generally flat but range from 0.1 to 2% in the northeast quadrant of the study area and along the banks of the Caloosahatchee River. Steep, man-made slopes occur north of the Caloosahatchee River and near the Earthsource mine and are associated with dredge spoils and material stockpiles, respectively. The effects of slope aspect on PET are small due to the low latitude and generally low relief of the study area.

The cascading flow network was generated based on the DEM for the study area. The maximum slope was used to determine the down-slope cell that received the runoff. Thus, multiple cells could contribute to a single downslope cell. Each local cascade network ended when it intercepted a mapped feature such as a stream or wetland or it entered a closed depression (swale) where surface runoff tends to accumulate and infiltrate over time. Map lines showing smaller-scale features such as ditches and berms were used to modify the cascade network. Figure 32 shows a portion of the cascading flow network generated for the study area. As can be seen from the figure, the number of connections to any given point is relatively small due to the large number of surface water features that intercept runoff. There are also a large number of swales in the study area.

For the Natural Conditions simulations, all mapped man-made changes to topography in the study area were removed by locally adjusting and smoothing the DEM. These included berms, dikes, roadways, and dredge spoil areas. Slopes and slope aspect were re-calculated using the adjusted, Natural Conditions DEM and the cascading flow network was rebuilt for these simulations.

For Post-development Conditions simulations, an algorithm was developed to approximate the final grading associated with the Modified ERP. The algorithm iteratively adjusted the DEM such that all runoff within each development area was redirected to the storm-water lakes as per the design of the SWM system. Slopes and slope aspect were then re-calculated using the adjusted Post-development Conditions DEM and the cascading flow network was rebuilt for these simulations. Topography outside the BRC was not changed in the Post-development Condition simulations from that of the Current Conditions simulations.

Parameters related to Land Cover: Land cover type can have a strong influence on the water balance. Evaporation from canopy interception and ET are directly influenced by vegetation type and cover density which, in turn, affects surface runoff and infiltration rates. Conversion of natural to non-natural land use generally increases the amount of impervious cover and decreases vegetative cover leading to increased surface runoff. At the same time, however, ET and evaporation from Earthfx Inc. and Greg Rawl, P.G.

Page 35

canopy interception storage are decreased, so the net effect on groundwater recharge is more complex.

Land use data were obtained from SFWMD as discussed earlier. Parameters such as percent impervious, summer and winter cover density, canopy interception storage, and detention storage were estimated initially from map data and available literature and assigned to each land use type. Imperviousness in the study area under Current Conditions is shown in Figure 34 and is very low except in the southwest and along and south of the Caloosahatchee River.

Although there is likely a range of values within each land class type, the use of uniform properties for each land class type across the study area was adopted to achieve a measure of parsimony in assigning parameter values. Thus lands classified as "row crops" in the southeast of the study area were treated the same as lands classed as "row crops" in the northwest of the study area. Initial estimates for model parameter values were based on those from the previous PRMS modelling and found to need only minor adjustment during model calibration.

For Natural Conditions simulations, all areas of urban and agricultural activities were remapped as areas with natural vegetation based upon mapping compiled by Mike Duever of the SFWMD in 2009. The natural vegetation map developed as part of the SWFFS, was used to assign natural vegetation classes. Parameters used in the Current Conditions model for similar vegetation types were applied to these areas.

For Post-development Conditions simulations, the planning documents developed by JEI were used to re-map land use classes within the developed areas, assign vegetative cover, and assign percent imperviousness. Imperviousness in the BRC under Post-development Conditions is shown in Figure 35. Land cover outside the BRC was not changed from that of the Current Conditions model. The Post-development Conditions simulations did not consider application of Low Impact Designs (LIDs).

Parameters related to Soil Cover: Soil properties have a significant influence on hydrological processes as they control the amount of water that can infiltrate and be transmitted to the water table as well as how much water is lost to ET. Soil water movement is controlled by two main factors: 1) the ability of the soil to transmit water (hydraulic conductivity), and 2) the gravity and suction forces acting on the soil water. Both sets of properties vary as a function of the moisture content of the soil. These processes are simulated for the shallow soil zone in the PRMS code.

Soil classification systems provided generalized information about the nature and properties of local soils. Detailed soil mapping was obtained from Lee County, SFWMD, and USGS websites. For modelling purposes, the number of soil types was reduced to eight general categories, as discussed earlier. Most of the BRC is covered by fine sand with part of the area having depressions filled with muck soils. Consistent parameter values were assigned to each general soil type. Hydraulic conductivities for the soils were initially estimated from literature values and refined as part of the earlier PRMS calibration process.

Soil properties were not changed for the Natural Conditions and Post-development Conditions simulations.

Combined Soil Type/Land Use Parameters: A pre-processor function was written to assign CN values to each cell based on the land use and soil type as previously mapped to the cell. Standard tables developed by the SCS (SCS, 1972) and soil classifications for Florida (e.g., Suphunvorranop, 1985) were used in assigning initial values. These were adjusted slightly during model calibration. The distribution of CN values in the study area in the Current Conditions model is shown Figure 36.

Adjusting CN values was a primary means of representing the effects of land use change in the PRMS sub-model. Land cover classification was changed across the study area for the Natural Conditions simulations and within the BRC for the Post-development Conditions simulations, as described above. Soil properties did not change. Combined soil type/land-use parameters were Earthfx Inc. and Greg Rawl, P.G.

Page 36

updated and CN values were assigned to the remapped land-use and soil type combinations using the pre-processor. A general lowering of CN values in the study area under Natural Conditions can be seen in Figure 37. A general increase in CN values within the BRC under Post-development Conditions can be seen in Figure 38.

Other Parameters: Other parameters must be specified for the PRMS model, such as threshold values (e.g., the temperatures at which precipitation is assumed to be either all snow, all rain, or a rain/snow mix), correction factors (e.g., lapse rates for elevation-based temperature correction) and critical dates (e.g., dates for starting and ending ET). Some parameters are irrelevant to South Florida. Other parameter values were estimated directly from known or measurable basin characteristics. Default parameter values were used where reasonable. These parameters values were set for the Current Conditions model and were not changed for the Natural Conditions and Post-development Conditions simulations.

3.3 PRMS Model Results

3.3.1 Current Conditions

The PRMS code produced outputs for all water balance components on a daily basis. Results are best illustrated by contouring the gridded results and creating animations showing the changes in the daily values. Select animations for the GSFLOW model results are presented in a digital appendix to this report. Daily results were accumulated to produce monthly and annual summaries for the simulation period. General patterns in the monthly and annual results were checked for reasonableness as part of the quality assurance process. Color-contoured maps of select water budget results and general findings of the PRMS simulations are discussed below.

Figure 39 shows monthly precipitation for November 2007, one of the driest months in the simulation period; while Figure 40 shows the monthly average precipitation for August 2008, one of the wettest months in the simulation. Local variation is due to spatial variability in rainfall that is captured in the NEXRAD data. Figure 41 shows simulated monthly evaporation of water from the canopy interception and detention storage reservoirs. The patterns shown are strongly influenced by land use distribution which control the assignment of vegetative cover type and cover density.

Figure 42 shows the spatial distribution of simulated monthly overland runoff for August 2008. The primary influence on the values appears to be the distribution of rainfall and the variation in land use and soil type (through the CN values). Figure 43 shows the distribution of simulated cascading flows which tends to increase from the upper portions of each subcatchment to their discharge points at a wetland or stream. The sizes of the subcatchments are relatively small due to the large number of ditches, streams and wetlands. The effect of berms and dikes can be seen where runoff is directed parallel to the feature. Figure 44 shows the complex patterns of simulated monthly infiltration for August 2008. Higher values occur at the downstream ends of the cascade network flow paths where greater amounts of water are available for infiltration.

Figure 45 presents the spatial distribution of simulated actual ET (AET) values for November 2007. As might be expected, rates are low due to lower PET for that period and the limited rainfall which decreases the amount of soil water available to plants. Evaporation rates are high within the larger wetlands and even in the smaller ones west of Telegraph Swamp. Curry Lake, however, shows lower AET rates, because it is simulated as being "dry" for much of the month. Subtle variations in AET are apparent due to the variation in rainfall, vegetative cover, soil type, depth to water, and overland runoff and infiltration patterns. AET for August 2008 is much higher, as expected, but also more uniform and nearly identical to the potential ET values for the month (shown in Figure 47) because soil water is not limiting. Finally, Figure 48 shows simulated net groundwater recharge for August 2008. Patterns are similar to that of infiltration but the rates are reduced primarily due to ET.

It should be noted that these figures are primarily for comparative analysis with similar figures for the Natural Conditions and Post-development Conditions simulations. The primary means of PRMS sub-model calibration was through comparing simulated and observed daily streamflow. To avoid duplication in this report, the comparison of observed and simulated daily flows and groundwater levels are discussed further on in the sections describing the GSFLOW model calibration.

3.3.2 Natural Conditions

Precipitation for the study period did not change for the Natural Conditions PRMS simulations. Figure 49 shows simulated monthly evaporation from canopy interception for August 2008 which increased from Current Conditions due to greater forest cover; evaporation from detention storage on impervious areas went to zero because there were no impervious surfaces. Figure 50 shows simulated monthly overland runoff for August 2008 which decreased over much of the area because of the lower CN values (relative to Current Conditions) while Figure 51 shows that infiltration for the same month increased despite the increase in evaporation from canopy interception. Average potential ET was unchanged but Figure 52 shows that AET in November 2007 increased over much of the area due to greater vegetation cover and an increase in the available soil water. AET in August 2008 (not shown) did not increase significantly because it was already close to PET. Finally, Figure 53 shows that groundwater recharge for August 2008 generally increased over the study area due to increased infiltration and unchanged AET.

3.3.3 Post-Development Conditions

Monthly precipitation for the study period did not change for the Post-development Conditions. Figure 54 shows monthly evaporation from canopy interception and detention storage for August 2008. Results were unchanged outside the BRC and evaporation from canopy interception generally decreased from Current Conditions in the BRC due to greater impervious cover while evaporation from detention storage on impervious areas increased due to the increased impervious cover. Figure 55 shows monthly overland runoff for August 2008 which increased within the development pods in the BRC where per-cent imperviousness increased. These flows are directed to the to the stormwater lakes for attenuation and treatment. Figure 56, however, shows that infiltration generally decreased across all of the BRC. Average potential ET was unchanged but Figure 57 shows that AET in November 2007 decreased in the central part of the BRC due to decreased vegetation. AET in August 2008 did not decrease significantly because a water surplus still existed. Finally, Figure 58 shows net groundwater recharge in August 2008 which decreased over most of the BRC primarily due to the decrease in infiltration.

The results shown are just from one month out of the nearly eight-year simulation period. Hydrographs of the various water budget components under the three scenarios (Figure 59 through Figure 61) for a location near well JEI-526 in the center of the BRC show that the relative changes discussed above are generally consistent from year to year. Initial CN value at that location increased from 68 to 74 (for lawns) and the percent imperviousness increased from 0 to 58.7%.

The net impact of the BRC development cannot be assessed solely from the PRMS results as increased runoff is redirected in GSFLOW to the storm water lakes where it helps to recharge the aquifer and where some excess flows are diverted to scrubber marshes and to existing wetlands to increase hydroperiod. These results are better seen by the changes in simulated flows, groundwater heads, wetland stage and hydroperiod computed by GSFLOW and discussed further on.

4 MODFLOW Model Development and Steady-State Calibration

A conceptual groundwater flow model is a simplified representation of the complex physical, hydrologic and hydrogeological processes and factors that affect the rates and direction of groundwater flow. These processes and factors relate to physical characteristics of the study area and include:

- stratigraphy (i.e., the bedrock and overburden stratigraphic layers, stratigraphic correlations, unit top and bottom elevations, lateral extent of the formations and their thickness);
- hydrostratigraphy (i.e., descriptions of the aquifers and aquitards in the study area, their top and bottom surface elevations, and their lateral extent, thickness, and degree of continuity;
- aquifer and aquitard properties (i.e., estimated hydraulic conductivity, anisotropy, saturated thickness, storativity and transmissivity);
- inputs to the hydrologic system (i.e., rates of groundwater recharge and discharge and the underlying processes that affect these rates);
- properties of the surface-water system and factors controlling groundwater/surface water interaction;
- anthropogenic inputs and outputs from the groundwater system (pumping rates and irrigation return flows); and
- other significant features (e.g., surficial geology, soil properties, and topographic features, such as depressional wetlands and breaks in slope) that may affect recharge, discharge, and groundwater flow).

The conceptual groundwater flow model was developed based on a synthesis of this diverse information as presented earlier in this report. The conceptual model was refined over the course of this study as the understanding of the study area and the behaviour of the groundwater system and its response to changes in stress improved. Key features of the conceptual model have been presented in the previous report sections. This section primarily describes features of the conceptual model directly related to the construction of the numerical groundwater flow model.

4.1 Groundwater Flow Equation

Groundwater flow is governed by Darcy's Law, which states that flow is proportional to the hydraulic gradient and to the hydraulic conductivity of the aquifer material and is given by:

$$q = -K \cdot \nabla h$$
 (Eq. 3)

where q is the specific discharge or rate of flow per unit area, K is the hydraulic conductivity, and ∇ h is the hydraulic gradient (change in hydraulic head per unit length in each direction). Groundwater flow is also governed by the Law of Conservation of Mass which states that all inflows to an area must be balanced by outflows and/or by a change in aquifer storage. When the mass balance equation is combined with Darcy's Law, it yields the governing equation for three-dimensional groundwater flow.

$$\frac{\partial}{\partial x} \left(K_{xx} \frac{\partial h}{\partial x} \right) + \frac{\partial}{\partial y} \left(K_{yy} \frac{\partial h}{\partial y} \right) + \frac{\partial}{\partial x} \left(K_{zz} \frac{\partial h}{\partial z} \right) = S_o \frac{\partial h}{\partial t} \quad (Eq. 4)$$

where: K_{XX} = hydraulic conductivity in the x direction;

K_{VV} = hydraulic conductivity in the y direction;

 K_{77} = hydraulic conductivity in the z direction;

h = hydraulic head; S₀ = specific storage

Hydraulic conductivity is a measure of how easily water can pass through the pores in the geologic unit. Specific storage is a measure of how much water is released from aquifer storage per unit decline in aquifer head per unit volume of aquifer. Water is released from confined storage when the head decreases due to expansion of the water and due to compression of the pore structure by the increase in intergranular stress. The intergranular stress increases as the water pressure decreases because total stress due to the weight of the overburden remains constant.

In the hydraulic approach to aquifer flow (see Bear, 1979), Eq. 4 can be simplified by integrating over the thickness of the aquifer. The resulting equation for two-dimensional flow in a confined aquifer of thickness B with recharge, discharge, and leakage from above and below, and negligible storage in the confining units can be written mathematically (Bear, 1979) as:

$$\frac{\partial}{\partial x} \left(T_{xx} \frac{\partial h}{\partial x} \right) + \frac{\partial}{\partial y} \left(T_{yy} \frac{\partial h}{\partial y} \right) + \left[\frac{K_o'}{B_o'} (H_o - h) \right] + \left[\frac{K_u'}{B_u'} (H_u - h) \right] + N + \sum_{i=1}^{Nw} Q_i' = S \frac{\partial h}{\partial t} \quad (Eq. 5)$$

where: T_{xx} = transmissivity in the x direction (where $T_{xx} = K_{xx}B$);

 T_{VV} = transmissivity in the x direction (where $T_{XX} = K_{XX}B$);

B = aquifer thickness:

K' = vertical hydraulic conductivity of an overlying (or underlying) confining unit

B' = thickness of the overlying (or underlying) confining unit;

H = head in the aguifer layer overlying/underlying the confining unit;

N = rate of groundwater recharge;

Q'_i = pumping rate (per unit area) at well i

S = storativity or storage coefficient (where $S = S_0B$)

A similar equation can be written for each aquifer in a layered sequence of aquifers and confining units. When an aquifer layer is unconfined, the transmissivity terms T_{XX} and T_{YY} are replaced by the effective transmissivity, equal to K_{XX} (h-b) and K_{YY} (h-b), where b is the elevation of the base of the aquifer. The storage coefficient for an unconfined aquifer is usually replaced with the specific yield, S_Y , which is used to represent water "released from storage" due to the draining of the pore space above the water table as the water table drops. S_Y is generally several orders of magnitude large than compressive storage.

Eq. 5 is a differential equation which forms the basis of the mathematical model developed for the study area. The equation is "solved" to determine aquifer heads at all points and all times in the model area. Information in the form of aquifer properties, recharge and discharge rates, and conditions along the study area boundaries, are provided as input to the model to make the solution unique to the study area. Numerical methods are needed to solve Eq. 5 because study area boundaries are irregular and aquifer/aquitard properties, aquifer geometry (stratigraphy), and rates of recharge and discharge vary spatially within the study area.

If the variation of head over time is considered to be small, for example, when considering equilibrium or long-term average conditions, the term on the right hand side of Eq. 5 is set to zero. This yields the steady-state form of the groundwater flow equation. The steady-state equation is often solved first because it provides information on aquifer hydraulic conductivity properties independent of the aquifer storage properties. Once the hydraulic properties are known, then the transient form can be solved to determine the storage properties of the aquifer.

The U.S. Geological Survey (USGS) MODFLOW code was developed to solve Eq. 5 using the finite-difference method. The first step in the method is to subdivide the hydrostratigraphic system vertically into a series of layers each representing an aquifer or an aquitard or a subunit within these. Next the area is divided horizontally into a grid of small square or rectangular cells. The finite-difference method uses an algebraic approximation to the equation and solves for the heads at points in the center of each cell. An alternative way of viewing the method is that it solves a mass balance equation for each grid cell where the inflows are determined by hydraulic properties and the difference in head between the center of each cell and all adjacent cells. Aquifer properties, such as top and bottom elevations for each layer, hydraulic conductivity, and recharge and discharge rates, are assigned to each cell in the grid. Boundary conditions are specified for cells that lie along lines corresponding to the physical boundaries of the flow system. Grid design, property assignment and boundary conditions are discussed below.

4.2 MODFLOW Model Grid

A model grid was designed for the MODFLOW simulation with the cell size in the center of the study area set to 300 by 300 ft. This provided the resolution needed to represent critical surface water features while keeping the computational effort at a reasonable level (about 1.5 hours per year of simulated time). Cells in the periphery of the model were set at 600 by 600 ft. The model grid consists of 318 rows and 300 columns and contains a total of 572,400 grid cells in six layers. This grid, shown in Figure 62, was used for all steady state MODFLOW and GSFLOW simulations. The 318 row by 300 column grid was also used for the PRMS analysis.

MODFLOW works in a local, grid coordinate system based on row and column numbers. The VIEWLOG™ GIS MODFLOW pre-processor was used to translate geo-referenced map data into MODFLOW input. The local origin for the model grid is at Florida East State Plan Coordinates 385700 E and 497000 N. All digital maps and point data for the study area were transformed to the Florida East (NAD83) coordinate system and used NGVD 1929 as the vertical datum. An adjustment of 1.2 ft was used to convert survey data in NAVD to NGVD.

4.2.1 Model Layers

As discussed in the previous section, the groundwater system is represented by eight hydrostratigraphic model layers. These include the surficial sands and four limestone/sandstone aquifers, the Ochopee Limestone, the Peace River Sandstone, the Mid-Hawthorn aquifer (Arcadia Limestone) and the Lower Hawthorn aquifer (see Table 2). The surficial sand unit was split into two model layers in GSFLOW simulations to allow the upper layer to represent the shallow wetlands and lakes as will be discussed further on. The aquifers are separated by three semi-confining units (aquitards): the upper and lower Peace River clays and the basal Mid-Hawthorn aquitard. The Bonita Springs Marl, which separates the surficial sands from the Ochopee Limestone in most of Lee County, is not present in the study area.

Figure 64 shows a southwest-northeast cross section through the study area showing the layers represented in the groundwater model. The location of the cross section is shown in Figure 11.

4.3 Model Boundary Conditions

The physical boundaries of the study area must be represented mathematically in the numerical model. Three boundary condition types were used in this analysis.

4.3.1 Specified Head Boundaries

A specified-head condition is applied where the simulated head is held at a constant, known value. Specified-heads were used along the north bank of the Caloosahatchee River in the upper three model layers. Specified head values were determined from average stage values at USGS gage S79 and set to 1.2 ft (above NGVD) below Franklin Locks and at 3.25 ft above the locks. Tidal fluctuations in the lower reaches of the river were not represented in the model.

A constant head was specified along the north and northeast border of the study area in Layer 6 (Lower Hawthorn aquifer) as shown in Figure 63 to allow underflow into the model area.

4.3.2 No-Flow Boundaries

No-flow boundaries were specified along the remainder of the lateral model boundaries. These generally conformed to flow lines along inter-stream divides. It was assumed that any lateral flow into the model area across these flow lines is insignificant. These boundaries are also quite distant from the BRC, the focus of the modelling study. Portions of the finite-difference grid outside these boundaries are designated as "inactive" and heads were not determined for these cells. The base of the modeled area (i.e., below Layer 6) was also assumed to behave as a no-flow boundary, indicating the little groundwater flow is being contributed from the lower portions of the Floridan aquifer.

4.3.3 Head Dependent Discharge Boundaries (Lakes and Streams)

A third type of boundary condition (head-dependent discharge boundary) was used extensively to represent groundwater/surface water interaction processes within the active model area. Flow was assumed to be exchanged as "leakage" across a lake or stream bed assumed to be of lower hydraulic conductivity compared to the underlying aquifer. The rate of flow is determined based on Darcy's Law where:

$$Q_{Leak} = \frac{K'}{B'} A_L (H_L - h)$$
 (Eq. 6)

where: Q_{LEAK} = volumetric flow rate between aquifer and stream or lake;

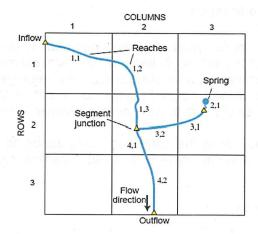
K' = vertical hydraulic conductivity of the stream or lake bed;

B' = thickness of the stream or lake bed; A_L = wetted area of the stream or lake;

H_L = stream or lake stage; and

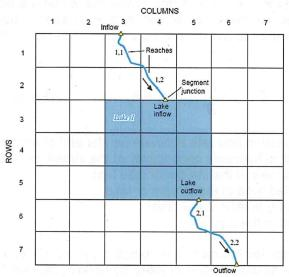
h = head in the aquifer

As noted earlier, stream-aquifer interaction is handled by the SFR2 module. To use the SFR2 module, a dendritic stream network is first created by defining stream "segments" and junctions at the confluence of two or more tributary segments as in the sketch below. Segments are numbered from upstream to lowest downstream and in such a way that all upstream flows are calculated when two sub-networks join at a junction (for example, Reach 3 of Segment 1 in the sketch joins Reach 2 of Segment 3 at a junction and the confluent flow moves downstream to Reach 1 of Segment 4).



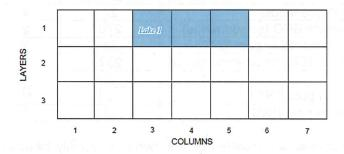
Stream reaches are defined by overlaying the model grid on the stream segment network. Reaches are numbered in downstream order. Stream properties can be defined on a reach basis or on a segment basis. In this study we used a combination, where stream cross-section, roughness, and streambed hydraulic conductivity were defined on a segment-by-segment basis. The hydraulic conductivity of the streambed material was set to 4 feet per day (ft/d) for all streams. Stream slope was defined on a reach-by-reach basis and determined from the DEM.

Stream stage in each reach is calculated based on the inflow from upstream, precipitation, evaporation, and overland flow to the reach. Leakage to or from the aquifer is then calculated based on the difference between calculated stream stage and the head in the underlying aquifer. Net outflow (i.e., sum of all inflows plus the leakage) from each reach is routed to the next downstream reach. Stream segments can terminate in a lake or wetland (as shown in the schematic below) or exit the model area.

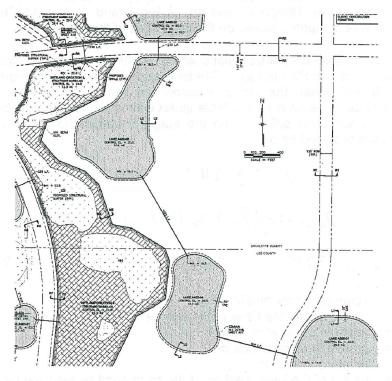


The input data for the stream simulation can be quite large when using mapped stream networks rather than the simplified stream networks such as that used in the previous HEC_HMS simulations. VIEWLOG was used to construct the stream network topology (including assigning reach and segment numbers, defining junctions, and assigning segment based properties) and overlay the stream network on the model grid to determine the length of each reach and slope. Maps of the existing stream and wetlands were obtained from a USGS hydrography layer. Some of the line work was updated based on the interpretation of recent airphotos to account for changes since the USGS data were compiled. All of the natural drainage and most of the anthropogenic ditching is represented in the model.

The lake simulation (LAK) module (Merritt and Konikow, 2000) is also included in GSFLOW and was used to represent the shallow wetlands, mining lakes, and proposed storm water lakes in the study area. The module computes a separate water balance for each lake or wetland based on computed inflows (e.g., precipitation, runoff, and incoming stream discharge) and outflows (e.g., evaporation, groundwater leakage, and outgoing stream discharge). Lakes are represented as occupying part of the volume of the model as shown in the sketch above and in the associated cross-section view below.



Lake areas were defined in VIEWLOG by overlaying the polylines representing the wetlands and lakes (from the USGS hydrography coverage) over the model grid. Shape files provided by JEI showing the locations of the proposed storm water lakes, wetlands, and scrubber marshes, were imported into the VIEWLOG project to provide lake information for the Post-development Conditions. Many of the storm water lakes are connected by buried pipes (as shown in the drawing below) which would tend to equalize lake stage over most of the year. The pipe-connected lakes were represented by assigning the cells the same lake ID number and a single stage value was computed for the lake chain. The number of 300 x 300 ft cells mapped to each lake closely approximated the area for the larger lakes but small differences occurred for the smaller and irregularly shaped lakes. All lakes were contained in the uppermost model layer for these simulations.



Lake stage is calculated daily using a stage-storage relationship which is established based on the number of cells occupied by the lake and the elevation of the lake bottom. Initial lake stage was

established by examining the DEM around each lake. Lake bottoms were defined by adjusting the top of Layer 2 (the lower part of the surficial sands) such that the difference between the initial lake stage and the top of Layer 2 represented the average lake depth. Average lake depths were assigned as indicated in the table below. Some adjustments were needed locally to better represent the bathymetry of some of the larger wetlands.

Feature	Number Represented in Model	Average Depth (ft)	Conduc- tance (ft/d/ft)\
Larger wetlands (all scenarios)	22	4	0.004 to 0.01
Small wetlands outside BRC (all scenarios)	270	2	0.02
Wetlands in BRC (removed in post-BRC)	38	2	0.02
Wetland Preserves in BRC (in all simulations)	282	2	0.02
Mining lakes	9	35	0.5
Storm water lakes (in post-BRC)	130	15	0.05
Scrubber marshes (in post-BRC)	12	4	0.02

Leakage to or from the aquifer is calculated by the model on a daily basis based on the difference between lake stage and the head in the underlying aquifer. Lake bed hydraulic conductivity for the larger wetlands was assigned based on the mapped soil properties and the conductance (i.e., hydraulic conductivity divided by sediment thickness) ranged from 0.004 ft/d/ft for areas mapped as muck to 0.01 ft/d/ft for fine sandy soils. Smaller wetlands, storm-water lakes, and scrubber marshes (in Post-development Conditions simulations), were assigned uniform values as shown in the table above. The mining lakes were assumed to be in good hydraulic connection with the underlying aquifer and were assigned a higher conductance value.

Discharge from the lake is calculated by the SFR package with rates determined by a specified lake stage versus discharge relationship. For most outlets, the relationship was established based on the properties of the downstream stream segment. Where control structures exist, such as at the downstream side of the Upper Telegraph swamp, at Big Island Dam, and Curry Lake, a stage discharge relationship was computed based on the properties of the structure.

The ability to calculate stage-discharge relationships for three additional types of lake outlet structures was added to the SFR2 package. These included a simple rectangular weir, an orifice (which behaves as a weir when the stage is below the top of the orifice), and a compound rectangular weir (which behaves as a simple rectangular weir when the stage is below the top of the lower section and as a weir and orifice when the stage is above the top of the lower section). Governing equations are provided below:

$$\begin{split} Q_{\rm rect,weir} &= 3.2 \ W \ H^{3/2} \quad \text{(Eq. 7)} \\ Q_{\rm orifice} &= 0.6 \sqrt{2g} \ W \ h \sqrt{(H-h/2)} \quad \text{(Eq. 8)} \\ Q_{\rm comp.weir} &= 3.2 \ W \ H^{3/2} + 0.6 \sqrt{2g} \ W_1 \ h_1 \sqrt{(H-h_1/2)} \quad \text{(Eq. 9)} \end{split}$$

where: Q = volumetric flow rate in (cfs);

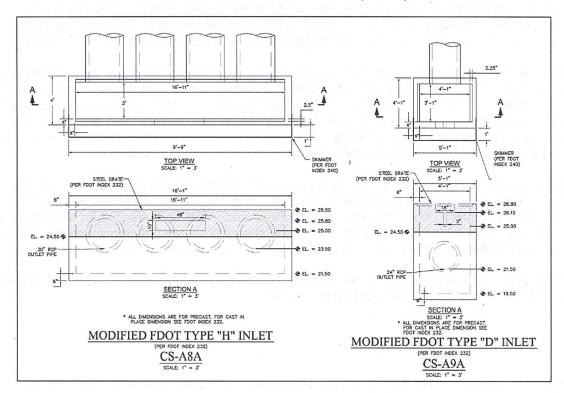
H = height above the base of the weir or orifice;

W = width of the weir or orifice; g = gravitational acceleration; h = height of the orifice;

h₁ = height of the lower section of the compound rectangular weir; and

 W_1 = width of the lower section of the compound rectangular weir.

These relationships were used to represent existing control structures and the 121 new control structures added to the BRC storm-water lakes (see table below). For example, control structure CS-A8A, shown below, has a 10 in by 48 in orifice with a control elevation of 26.2 ft (NGVD) to control flow, while CS-A9A is a compound weir with a 3 in rectangular lower weir at the same control elevation that widens to an 18 in weir at an elevation of 27.3 ft (NGVD).



Location	Number Represented in Model	Simple Weirs	Orifices	Compound Weirs
Area A	23	4	11	8
Area B	15	9	1	5
Area C	11	2	3	6
Area D	11	6	0	5
Area E	16	10	1	5
Area F	15	6	0	9
Area G	9	4	1	4
Area H	11	9	19119 . 1	2
Areas I and J	TA BOOT DISTRIB	1	2	
In-Stream	7	6	0.02	
Existing	5	19211	1	4

It is recognized that simulating the wetlands as MODFLOW lakes is a simplification because neither the slope of the water surface nor the velocity variation within the wetland are calculated. For some of the larger wetlands, especially those oriented in a north-south direction, simulating the entire wetland as one reservoir with a single stage value would have been a poor approximation for the variation of stage along the direction of flow. To improve the representation, the larger wetlands were subdivided into a series of cascading lakes. Flows between the lakes were simulated with the SFR2 package.

The lake module has an option to lag the calculation of stage by one time step (explicit method). Although this might be reasonable for large deep lakes, the rapid changes in daily stage in the shallow wetlands required stage to be calculated implicitly but at the cost of increased numerical instability and computational effort.

Maps of existing wetlands were obtained from a USGS hydrography layer. All of the wetlands in the BRC and all the connected wetlands outside the BRC are represented. Some of the smaller, non-connected wetlands were not simulated explicitly but were treated as swales in the GSFLOW model.

To simulate Natural Conditions, all man-made ditching and the mining lakes were represented as being removed. Some of the wetlands were left connected to simulate natural slough system that likely preceded the ditching. The line work to map Natural Condition streams was developed by adjusting the Current Conditions line work based on aerial photography and estimates of the pre-existing developed in the SWFFS study. The sloughs were simulated to be wide but shallow whereas the agricultural drainage ditches were generally narrower but deeper.

For Post-Development Conditions simulations, the planning documents developed by JEI were used to map changes to the existing streams in the BRC. Stormwater management system lakes were added in and boundary condition, lake conductance, and initial lake stage, and vegetative cover input data sets were edited as necessary. Information on the control structures was assembled and used as input to the SFR2 package to calculate stage-dependent lake outflows.

Storm water lakes were simulated to be 15 ft deep on average and assigned a conductance of 0.05 ft/d/ft. Conditions outside the BRC were not changed.

4.4 Groundwater Recharge

Groundwater recharge rates for the steady-state calibration were estimated from the average of annual recharge rates from the PRMS-only simulations. Wet season and dry season recharge rates were estimated as percentages of the total recharge. The split was modified as part of the calibration process. The calibrated model determined that 67% of the recharge is contributed in the four-month wet season. The average annual rates were used in the initial steady-state simulation that was done in all GSFLOW runs to establish starting conditions for the daily simulations.

4.5 Groundwater Model Parameters

A considerable amount of effort was spent to calibrate the groundwater model. Initial estimates for aquifer properties were taken from the Lee County model study and other investigations in the area. Hydraulic properties were adjusted within reasonable ranges to better match local observed average dry-season and wet-season water levels. The results of these simulations provided estimates for average recharge and average hydraulic conductivities of the hydrostratigraphic units. The final calibrated values of hydraulic conductivity that were used in the steady-state model and in subsequent GSFLOW model runs are shown in Figure 20 through Figure 23.

4.6 Model Results

Simulated heads in the wet season are shown in Figure 65 along with the observed water levels averaged over June through September. Simulated heads in the dry season are shown in Figure 66 along with the observed water levels averaged over the dry season months. A scattergram comparing the observed and simulated wet season heads in the surficial aquifer is shown in Figure 67 and indicates that the match is quite good. A similar figure for the dry season heads is shown in

Figure 68. Although the match is still quite good, the simulated heads tend to be slightly lower than the observed. This is not unexpected as the steady-state model does not account for storage in the aguifer that can help reduce the decline in water levels during the dry period.

Four calibration statistics were used to assess, and ultimately demonstrate, model accuracy: the mean error (ME), mean absolute error (MAE), and root mean squared error (RMSE), and correlation coefficient (r²). These are given by Anderson and Woessner (1992) as:

$$\operatorname{Mean Error} = \frac{1}{n} \sum_{n=1}^{nwell} (h_o - h_s)_n \qquad \text{(Eq. 10)}$$

$$\operatorname{Mean Absolute Error} = \frac{1}{n} \sum_{n=1}^{nwell} |(h_o - h_s)|_n \qquad \text{(Eq. 11)}$$

$$\operatorname{Root Mean Square Error} = \sqrt{\frac{1}{n} \sum_{n=1}^{nwell} (h_o - h_s)_n^2} \qquad \text{(Eq. 12)}$$

$$r^2 = \frac{n \sum h_o h_s - \sum h_o \sum h_s}{\sqrt{n \sum h_o^2 - (\sum h_o)^2} \sqrt{n \sum h_s^2 - (\sum h_s)^2}} \qquad \text{(Eq. 13)}$$

where:

Observed head:

Simulated head; and,

n Number of observation wells.

Calibration statistics for the simulated heads in the surficial aquifer are presented in the table below.

Simulation	No. of Observations	Mean Error (ft)	Mean Absolute Error (ft)	Root Mean Squared Error (ft)	r²
Wet Season - Surficial	155	0.21	0.93	1.36	0.98
Dry Season - Surficial	155	0.96	1.41	1.96	0.96

The magnitudes of the absolute error, in ft, are relatively small and the positive signs on the ME values indicates that, on average, simulated values are generally lower than the observed values. The ME and MAE are estimates of the average magnitude of the difference between the observed and simulated values. The RMSE is a measure of the variability of the differences. If the differences are normally or near-normally distributed, approximately two-thirds of the simulated heads will fall within one RMSE value from the observed heads.

Values for MAE and RMSE are often compared to the overall response of the model (Anderson and Woessner, 1992). The total range for hydraulic head in the model area is about 70 ft. The RMSE as a percent of range varied between 1.9% for the wet season and 2.8% for the dry season which is less than 5% and generally considered to be a good calibration.

Simulated and observed dry season heads for the other principal aquifers are shown in Figure 69 through Figure 72. Differences between the observed wet season and dry season heads in the deeper layers were not significant indicating that storage effects and attenuating effects of the confining units mutes the seasonal variation in heads. Calibration statistics are not presented for the deeper layers as there were insufficient numbers of observations in each layer to be statistically significant.

5 GSFLOW Model Simulations

As noted earlier, the GSFLOW calibration methodology was based on a staged approach whereby the individual MODFLOW and PRMS models were constructed, calibrated and tested prior to the final simulations with GSFLOW. The initial PRMS calibration provided estimates of soil properties and other parameters needed to calculate recharge and runoff in the study area while the steady-state MODFLOW calibration to wet season and dry season conditions provided assurance that the model could reasonably match regional flow patterns and seasonal response. However, because of the close linkage between the surface water and groundwater systems in the study area, a final calibration was needed to account for the feedback mechanisms and better match the observed transient response in water levels and flows. Because the independent PRMS and MODFLOW models have already been described in preceding sections, the following discussion focuses on model parameters and features unique to GSFLOW.

5.1 GSFLOW Model Parameters

Data preparation for GSFLOW runs involved creating a mix of PRMS and MODFLOW data sets along with a number of GSFLOW-specific operation control parameters. All data preparation was facilitated by a GSFLOW pre-processor developed for VIEWLOG. Few changes were needed to the parameterization of the PRMS model for use in the GSFLOW model; primarily related to replacing the linear groundwater reservoir that is used in PRMS in place of MODFLOW. With regards to MODFLOW data sets, the transient groundwater flow model required additional information on time step size, time-dependent stresses, time-dependent boundary conditions, and aquifer storage properties. Time step size is one-day in GSFLOW.

Pumping for crop irrigation, the primary time-dependent stress, was simulated by applying the wet season and dry season water withdrawals. Time-dependent boundary conditions, specifically the change in recharge rates and changes in stream and wetland stage, are calculated internally in GSFLOW from climate data inputs rather than being estimated external to the model. This allows feedback mechanisms related to the rise of the water table into the soil zone and leakage to and from lakes and streams to be fully represented. Canopy interception, ET, and overland runoff to streams, wetlands, and lakes are all calculated internally within GSFLOW.

Aquifer storage properties were derived from values used in previous modelling studies (e.g., Rawl and others, 2005) which, in turn, were interpolated from aquifer tests conducted in the study area. There are little data on the local variation in storage properties so values were applied uniformly across the study area and adjusted through model calibration. Final values ranged between 0.00001 and 0.0002. The specific yield for the surficial sands was set at 0.1.

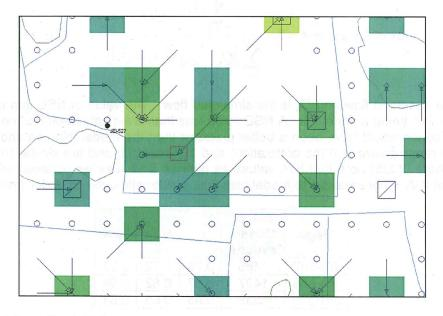
The steady-state simulations discussed previously used the MODFLOW recharge (RCH) module which directly applies the specified recharge to the water table. The RCH module is not supported in GSFLOW and, instead, one-dimensional unsaturated zone flow is simulated in GSFLOW with a version of the MODFLOW-2005 UZF flow package (Niswonger, et al., 2006). Because of the shallow depth to groundwater over the study area, an option in the UZF package which allows soil moisture entering the unsaturated zone to reach the water table within the time step was employed. Other features of the UZF package that were implemented included the calculation of head-dependent groundwater discharge to the soil surface when heads are predicted to rise into the soil zone and the calculation of excess rainfall when the infiltration rate exceeds hydraulic conductivity. Both surface discharge and excess rainfall are added to the runoff volumes and routed to adjacent cells and eventually to streams and wetlands.

5.2 GSFLOW Model Calibration and Discussion of Results

The GSFLOW data sets were generated and the model was calibrated to any eight-year period from October 2002 to July 2010 (WY2003-WY2010). The calibration period covers an extreme wet year (WY2003) an extreme dry year (WY2007). Because the bulk of the observation data was collected after 2005, the calibration focussed on WY2006 to WY2010. Model results were compared to quantitative observed groundwater levels and streamflow for this period as discussed in the following sections. Results were also compared to earlier tidal-influenced gage data from the Telegraph Creek Water Management District as a qualitative check.

GSFLOW model results are similar to those generated for the PRMS and MODFLOW sub-models but with a number of significant enhancements. For example, up to 86 different water budget components can be output on a cell-by-cell basis each simulation day. These include PRMS sub-model flow volumes such as observed (interpolated) precipitation, canopy interception, potential ET, actual ET, lake evaporation, Dunnian (saturation excess) and Hortonian (infiltration excess) overland runoff, and infiltration. System state variables are also generated on a cell-by-cell basis and include the volumes of water in canopy interception storage, detention storage, and in the various soil zone reservoirs. Precipitation, accumulated Hortonian flow, accumulated Dunnian flow, and infiltration for August 19, 2008 are shown in Figure 73 through Figure 76, respectively, and reflect the spatial variability in flows generated by a large (greater than 3 inches) rainfall event. The accumulated flows represent the inflows from the upstream cell into each cell shown and, as can be seen, increase in the downslope direction.

Model output is also presented as hydrographs by extracting the daily values for a single cell from the model output. Figure 77 shows the precipitation and infiltration for cell 62969 (row 228, column 97) for July through October 2008. The cell is located in the center of the BRC near surficial monitoring well JEI-527 (note the red square in the map below). Infiltration values are less than the precipitation for most of the period. However, values are higher around August 19, 2008 and for several days following. This can be explained by looking at a second set of hydrographs (Figure 78) showing the upslope Hortonian and Dunnian flow (i.e., runoff into the cell) from the five contributing cells. The upslope Hortonian and Dunnian flow for the adjacent cell to the west is also shown as this represents runoff leaving cell 62969. Net runoff (i.e., the difference between Dunnian and Hortonian flow and Dunnian and Hortonian flow out) provides some of the extra water that infiltrates in the cell. Also contributing and included in the model, but not shown, is the net interflow from upstream cells. This example shows the importance of factoring in the accumulation of cascading overland flow in the calculation of infiltration.



5.2.1 Streamflow Maps and Hydrographs

Output from GSFLOW includes information on groundwater heads and drawdowns, unsaturated flow components (e.g., rejected recharge, infiltration from the soil zone, discharge to the soil zone. ET from groundwater and the unsaturated zone, discharge to the soil surface, and net groundwater recharge), streamflow and stage, lake stage and a complete lake water balance (inflows from streams, precipitation, overland flow, evaporation, groundwater leakage to and from the lake, and change in storage). Additional post-processing was done to sum up volumes of groundwater discharge and overland flow along the stream network to calculate the cumulative volumes at each point. Total stream flow, including upstream inflow, overland runoff and groundwater discharge, are reported for each stream reach.

Figure 79 shows cumulative stream flow for August 18, 2008 along all streams and ditches simulated in the model. The flows are plotted on a log scale to highlight the lower flow values. Total flows are relatively low with the higher flows (greater than 10 cfs) seen in the lowest reaches of the major streams. Figure 80 shows the high stream flows on August 19, 2008 along most of the reaches of the major streams and in the larger ditches and drains due to the large storm on that day.

Comparisons of simulated flows at all gages with the available stream flow observations were done as part of the GSFLOW calibration. Figure 81 through Figure 83 compare the simulated daily streamflow with the observed average daily flow at the three gages in the Trout Creek watershed; JEI-567, JEI-569, and JEI-570. Flows match very well in the two upstream gages but peak flows are under-predicted at JEI-570. The model captures the shape of the rising limb and the recession curves quite well in all cases.

In addition to the coefficient of determination, r2, two common statistics for testing the quality of transient simulations were used: the Nash-Sutcliffe (1970) efficiency (NSE), the index of agreement (IOA). These are given by:

Nash Sutcliffe Efficiency =
$$1 - \frac{\sum\limits_{n=1}^{nobs}(Q_o - Q_s)^2}{\sum\limits_{n=1}^{nobs}(Q_o - \overline{Q}_o)^2}$$
 (Eq. 14)

Nash Sutcliffe Efficiency =
$$1 - \frac{\sum_{n=1}^{nobs} (Q_o - Q_s)^2}{\sum_{n=1}^{nobs} (Q_o - \overline{Q}_o)^2}$$
 (Eq. 14)
$$\frac{\sum_{n=1}^{nobs} (Q_o - \overline{Q}_o)^2}{\sum_{n=1}^{nobs} (|Q_s - \overline{Q}_o| + |Q_o - \overline{Q}_o|)^2}$$
 (Eq. 15)

where Qo is the observed flow and Qs is the simulated flow. The value of NSE can range from 1 to minus infinity with 1 being a perfect fit. A NSE value less than 0 indicates that the mean value of the observed time series would have been a better predictor than the model (Krause and others, 2005). Values for IOA range between 0 (no correlation) and 1 (perfect fit) and are similar to the r² statistic. Krause and others (2005) note that IOA values as high as 0.65 may be obtained with poorly fitted models and that IOA is not sensitive to model bias (i.e., systematic over- or under-prediction).

Gage	No. of Observations	r ²	NSE	IOA
JEI-567	1466	0.76	0.72	0.93
JEI-569	1497	0.87	0.82	0.94
JEI-570	1533	0.85	0.65	0.84

The calibration statistics indicate that good matches were achieved and that the best visual match, JEI-569, also has the best statistical properties.

Hydrographs for the other gages are presented in Figure 84 through Figure 91. Overall, matches to gages outside the BRC are good with some exceptions. For example, simulated flows at JEI-1470 (Figure 84) tend to be lower than observed. This may be due to underestimating the connectivity and flows from the smaller wetlands to the west and north. Similarly, JEI-1508 has higher flows than simulated, most likely due to the contribution from smaller wetlands and the agricultural drains to the northeast that were not included in the model.

5.2.2 Potentiometric Maps and Hydrographs

The primary outputs from the MODFLOW sub-model are the simulated heads in the aquifers and the stage in the wetlands (which is output along with the heads in Layer 1). Figure 92 through Figure 106 show the end of wet season and dry season heads and wetland stage for each year in the simulation. The overall change in head between wet and dry season is less than five ft so the maps do not show large shifts in the water levels with time.

Hydrographs of simulated heads for 43 wells along several transects across the study area were compared against observed water levels at the monitoring wells. Well locations are shown in Figure 107. The hydrographs are shown in Figure 108 through Figure 150. The matches between the observed and simulated are quite good in general with a few exceptions. Local variations in properties are the likely explanation for the differences. Gaps in the data, measurement error, and instrument drift may account for some discrepancies as well.

Simulated heads in the Peace River Sandstone tended to be lower than observed. Patterns in the simulated seasonal response agreed reasonably well with the observed, however, as seen in the comparisons of relative simulated heads versus relative observed heads shown in Figure 151 though Figure 153.

5.2.3 Natural Conditions Simulations

Simulations were carried out to examine the behavior of the groundwater and surface water systems under Natural Conditions. Changes in watershed characteristics prescribed for the simulated Natural Conditions were discussed earlier in this report and were applied to the entire study area. These include the simulated change in agricultural and urban land use classes to natural land cover types with the associated decrease in imperviousness, changes in vegetative cover type and density, and adjustment of CN values. Limited changes were made to DEM to remove berms and features such as dredge spoil areas. Significant changes were also made to the stream network. The mining lakes and agricultural drainage ditches were removed as shown in Figure 154. Some of the wetlands were left connected to simulate natural, pre-existing slough systems.

The Natural Conditions model was run with the time-series of data climate data for October 2002 to June 2010. Example results from the PRMS sub-model, shown as maps of the spatial distribution of simulated monthly rates for evaporation from canopy interception and detention storage, runoff, infiltration, AET, and groundwater recharge under Natural Conditions for August 2008, are presented in Figure 49 through Figure 53. Maps showing the daily variation in water budget components were also prepared. For example, the spatial distribution of simulated Hortonian flow, Dunnian flow, and infiltration under Natural Conditions for August 19, 2008 are shown in Figure 155 through Figure 157, respectively. These results can be compared by subtracting the gridded values for the Current Conditions (shown in Figure 73 through Figure 76) from the gridded values for Natural Conditions. As an example, Figure 158 shows the difference in simulated infiltration on August 19, 2008 between Natural Conditions and Current Conditions in the BRC. The greatest decrease (blue

shading) occurs in the vicinity of the mining lakes which do not exist in the Natural Conditions model and therefore should not be considered. Decreases in infiltration across the remainder of the BRC are due to the higher CN values used in the Current Conditions simulation to represent the areas that switched from natural vegetation to agriculture. The decrease is not uniform and there are areas within the BRC that show a net increase in infiltration (red areas in Figure 158).

A similar type of analysis was done at select locations and time periods. Figure 159 shows the simulated evaporation from canopy interception for cell 62969 (row 228, column 97), located in the center of the BRC, for June through October 2008 for Current Conditions and Natural Conditions. Canopy Interception is higher under Natural Conditions. Figure 160 shows the simulated infiltration for cell 62969 for Current Conditions and Natural Conditions. Infiltration values are generally higher under Natural Conditions for the higher rainfall events but are lower for the low rainfall events. The higher infiltration rates under Natural Conditions are due to the lower CN value which decreases Hortonian runoff from the cell and allows more water to infiltrate. The reversal under low rainfall events is because the increase in ET and evaporation from canopy interception in the cell under Natural Conditions is more important in low rainfall events. Changes in canopy interception, ET, surface runoff, and infiltration in the five cells that contribute overland flow and interflow to cell 62969 also affect the local rates of infiltration.

Map views of cumulative stream discharge were created for comparison with Current Conditions. Figure 154 shows cumulative stream flow for August 19, 2008 along all streams simulated in the model. The flows are plotted on a log scale to highlight the lower flow values. Comparing this figure with Figure 80 shows that the simulated Natural Conditions flows are generally lower than under Current Conditions due to higher infiltration and the absence of ditches and drains that intercept surface runoff and groundwater.

Streamflow hydrographs were also generated for comparison with Current Conditions. Figure 162 through Figure 164 compare the simulated daily streamflow under Natural Conditions with simulated flow under Current Conditions at JEI-567, JEI-569, and JEI-570. As can be seen, simulated flows under Natural Conditions are much lower than those under Current Conditions.

5.2.4 Post Development Simulations

Changes in the watershed characteristics prescribed for Post-development Conditions were discussed earlier in this report and were applied only within the BRC. These included changes in land use class within the development pods and the associated increase in imperviousness, changes in vegetative cover, and changes in local topography and the cascading flow network. Most notable were changes introduced by the construction of storm water lakes and their associated control structures, construction of scrubber marshes and their control structures, re-routing of the streams and construction of new weirs and flow blocks in existing streams, and the removal of berms and agricultural drainage ditches, as shown in Figure 165. Input data sets for the PRMS submodel and the LAK and SFR2 modules were modified to represent these changes.

The Post-development Conditions model was run with the time-series of climate data for October 2002 to June 2010. Results from the PRMS sub-model, shown as maps of the spatial distribution of simulated monthly rates of evaporation from canopy interception and detention storage, surface runoff, infiltration, ET, and groundwater recharge for August 2008 under Post-development Conditions are presented in Figure 54 through Figure 58.

Maps showing the daily variation in water budget components were also prepared. The spatial distribution of simulated Hortonian flow, Dunnian flow, and infiltration under Post-development Conditions for August 19, 2008 are shown in Figure 166 through Figure 168, respectively. These results were compared by subtracting the gridded values for the Current Conditions (shown in Figure 73 through Figure 76) from the gridded values for the Post-development Conditions. Infiltration

generally increased despite the higher CN values and imperviousness. The greatest increase on infiltration occurs on the east side of Trout Creek. Localized areas of decrease in infiltration can also be seen.

Map views of cumulative stream discharge were created for comparison with Current Conditions. Figure 154 shows cumulative streamflow for August 19, 2008 along all streams simulated in the model. The flows are plotted on a log scale to highlight the lower flow values. Comparing this figure with Figure 80 shows that the simulated flows outside the BRC are unchanged. Flows within the main stream channels are generally lower than under Current Conditions due to the removal of agricultural ditches and drains that intercept runoff and groundwater and due to the SWM system which is designed to attenuate and retain storm water.

Streamflow hydrographs were also generated for comparison with Current Conditions. Figure 170 through Figure 172 compare the simulated daily streamflow under Post-development Conditions with simulated flow under Current Conditions at JEI-567, JEI-569, and JEI-570. The graph for JEI-567 shows that flow volumes are roughly the same but the peak discharges for larger storms are higher in the Post-development Conditions. The similarity in flow volumes is expected because the area contributing flow to Curry Lake is largely unaffected by development in the BRC. The structure at Curry Lake, which was modified to increase storage upstream, results in less attenuation of the higher flows because less storage is available. The graphs for JEI-569 and JEI-570 show that simulated flow volumes and peak flows are reduced within the BRC in the Post-development Conditions as compared to simulated flows under Current Conditions.

5.3 Hydroperiod Analysis

The LAK module uses the cells in Layer 1 within the lake outline to store output of simulated lake stage. Hydrographs of wetland stage were prepared by plotting the simulated head in Layer 1 over the simulation period in Figure 174 through Figure 187. The observed water level in nearby wells or gauges and the land surface elevation at the measuring point are shown for reference. Figure 179 shows the stage in the Curry Lake wetland for the simulation period versus the observed stage at JEI-567. Simulated wet season water levels are very close to observed. The observed dry season stage is able to drop below the simulated because the gage is located in an excavated channel within the wetland. Figure 180 shows the simulated stage in upper Telegraph Swamp versus water level at a nearby observation well JEI-1516. Simulated stage in the lower part of Telegraph Swamp is compared against a nearby well, JEI-564 (Figure 182). The agreement between the simulated and observed stage in Telegraph Swamp is also very good at the higher stage values in the wet season. The recession in dry season stage is not as steep as the recession in the nearby groundwater well (JEI-1516). The observed dry season stage at JEI-564 is able to drop below the simulated because this gage is also located in a channel. Good matches to observed water levels were obtained for most of the other smaller wetlands.

A post-processing routine was written to examine simulated lake stage and calculate average hydroperiod over the eight-year simulation period. For the purposes of this study, days with a water depth above the estimated bottom were considered to be inundated. Figure 191 shows the map of simulated average hydroperiod, in days, for each wetland in the study area under Current Conditions. Hydroperiods within the BRC, based on this definition, vary from as little as 10 days to 365 days. Figure 192 shows the map of simulated hydroperiod under Natural Conditions. Almost all wetlands in the BRC show an increase in simulated hydroperiod between Current Conditions and Natural Conditions. Figure 193 shows the map of simulated hydroperiod under Post-development Conditions. Curry Lake and many of the pre-existing wetlands in the southern part of the BRC show an increase in hydroperiod (Figure 194). A few show a net decrease (Figure 195). Some of these include isolated wetlands that were located in the development pods.

The response of the wetlands to the Post-development Conditions is complex. On the one hand, berms around the development pods and directing overland flow to the SWM lakes decrease overland flow to the wetlands. On the other hand, groundwater leakage from the SWM lakes raise groundwater levels in the development pods and compensates for the increase in imperviousness. In most cases, the local increase in heads areas is sufficient to counter the loss of overland runoff and most wetlands show increased hydroperiod. Discharge of treated and attenuated stormwater also helps to increase wetland stage and increase Post-Development hydroperiod. Figure 196 shows the average number of days during a water year with flow in the streams under Post-development Conditions and indicates that flow from the SWM lakes to the adjacent wetlands occurs with varying frequency across the BRC.

5.4 Design Storm Simulations

The rainfall data for the study area were edited to create time series inputs for the 5-yr (1-day), 25-year (3-day), and 100-year (3-day) storm event simulations. The data set for WY2006 was copied and the values for August 25, 2006 to August 27, 2006 were adjusted according to the table below. The start date for the storm event simulations was chosen because it was determined to represent an average annual wet season condition based upon long-term monitoring well data. The model was started in October 2005 to set reasonable starting conditions prior to the storm. Rainfall was set to zero for the remaining days in the water year so that the recession after the storm event could be simulated.

	Design Storm Daily Rainfall								
Day	Date	5-yr 1-day (in)	25-yr 3-day (in)	100-yr 3-day (in)					
1	8/25/06	5.40	1.20	1.53					
2	8/26/06	ii Suit at	1.76	. 2.22					
3	8/27/06	.746W po	8.24	10.45					
Total	111111111111111111111111111111111111111	5.40	11.2	14.2					

5.4.1 Design Storms under Current Conditions

Design storms were simulated using the GSFLOW model under with all model parameters set for Current Conditions. Results for the 5-yr, 25-yr, and 100 year storm are shown as hydrographs for each gage in the BRC. Figure 197 shows the simulated flows at JEI-567, Figure 198 shows the simulated flows at JEI-569, and Figure 199 shows the simulated flows at JEI-570. It should be noted that these are daily flows.

5.4.2 Design Storms under Natural Conditions

Next, design storms were simulated using the GSFLOW model with all model parameters set for Natural Conditions. Results for the 5-yr, 25-yr, and 100-yr storm are shown as hydrographs for each gage in the BRC in Figure 200 through Figure 202, respectively. The magnitudes of the flows are lower due to the decrease in runoff under Natural Conditions as well as the lack of contribution from agricultural drainage ditches.

5.4.3 Design Storms under Post Development Conditions

Finally, design storms were run using the GSFLOW model under with all model parameters set for Post-development Conditions. As noted earlier, the model did not assume application of Low Impact Designs (LIDs) in the Post Development Conditions. Results for the 5-yr, 25-yr, and 100 year storm are shown as hydrographs for each gage in the BRC in Figure 203 through Figure 205, respectively. The magnitude of the flows are reduced relative to the Current Conditions despite the increase in imperviousness in the BRC under Post-development Conditions due to the mitigating effects of the storm water lakes and the removal of agricultural drainage ditches in the BRC. These effects are best seen by direct comparison of the hydrographs. Figure 206 shows the hydrographs for the 5-yr storm at JEI-567 under Current, Natural, and Post-development Conditions. Figure 207 compares the 25-yr storms at JEI-567, and Figure 208 compares the 100-yr storms at JEI-567, respectively. Similar figures (Figure 209 through Figure 211) compare the 5-yr, 25-yr, and 100-yr storms at JEI-569, respectively. Figure 212 through Figure 214 compare the hydrographs for the 5-yr, 25-yr, and 100-yr storms at JEI-570, respectively.

Flows were also measured at the downstream ends of Trout, Owl, and Telegraph Creek for comparison under Current, Natural, and Post-development Conditions. Locations are shown in Figure 215. The flow comparison is summarized in Table 3. For all three design storms, the model simulations showed that the Post-development Conditions fall between the Current Conditions and Natural Conditions flows.

7 <u>Limitations</u>

Services performed by Earthfx Inc., et al. were conducted in a manner consistent with that level of care and skill ordinarily exercised by members of the environmental engineering and consulting profession.

This report presents the results of data compilation and computer simulations of a complex geologic setting. Data errors and data gaps may be present in the information supplied to Earthfx, and it was beyond the scope of this project to review each data measurement and infill all gaps. Models constructed from this data are limited by the quality and completeness of the information available at the time the work was performed. It should be recognized that the passage of time affects the information provided in this report. Environmental conditions and the amount of data available can change. Discussions relating to the conditions are based upon information that existed at the time the conclusions were formulated.

All of which is respectively submitted,

EARTHFX INC.



E.J. Wexler, M.Sc., M.Sc. (Eng), P.Eng. Earthfx Inc.

Greg F. Rawl, P.G.

8 References

- American Society for Testing and Materials, 2000, Standard Guide for Subsurface Flow and Transport Modeling (ASTM) D5880-95.
- Anderson, M. P. and Woessner W. W., 1992, Applied Ground Water Modelling Simulation of flow and advective transport: Academic Press, USA.
- Ardaman & Associates, Inc., 2007, Subsurface soil exploration water management lakes, Babcock Ranch, Lee County, Florida, 2007.
- Bear, J., 1979, Hydraulics of Groundwater: McGraw Hill, NY, 567 p.
- BEM Systems, Inc., 2004, Southwest Florida regional model development work order (Hydrology and Hydraulic Modeling Support; WO1, January 2004.
- Berggren, W. A., Kent, D. V., Swisher, C. C., and Aubry, M. 1995, A revised Cenozoic geochronology and chronostratigraphy: in Berggren, W. A. et al., (eds.), Geochronology, Time Scales and Global Stratigraphic Correlation. SEPM Special Publication, 54: 129-212.
- Boggess, D.H., and Watkins, F.A., Jr., 1986, Surficial aquifer system in eastern Lee County, Florida: U.S. Geological Survey Water-Resources Investigations Report 85-4161, 59 p.
- Camp, Dresser, and McKee, 2006, Tidal Caloosahatchee Basin Modification of Hydrologic Model Final Report: July 2006.
- Craig A. Smith & Associates, Inc., 2006, Surface Water Management Plan, Four Corners Area: Prepared for Hendry County and the SFWMD, June 1996.
- Craig A. Smith & Associates, Inc., 2001, County Line Ditch Final Design Recommendation: Prepared for Hendry County and the SFWMD.
- DHI Inc. and Stanley Consultants, Inc., 2005, C-43 Basin Hydraulic and Hydrologic Model C-43 Basin Phase I Storage Reservoir Project Implementation Report: June, 2005.
- DHI Inc. 2009, Comprehensive Hydrological Study of the Lee County Southeastern Density Reduction/Groundwater Resource (DR/GR) Area -- Final Report of the MIKE SHE Model Development and Results, September 2009.
- Duever, Mike, 2009, Southwest Florida Predevelopment Map, SFWMD
- ECT Inc., 2009, Babcock Ranch Preserve Hydrological Analysis Charlotte and Lee Counties, July 2009.
- Florida Geological Survey, 2001, Geology and Hydrogeology of Lee County, Florida: FGS Special Publication 49, Thomas M. Missmer and Thomas M. Scott, ed.
- Harbaugh, A.W., 2005, MODFLOW-2005, The U.S. Geological Survey modular ground-water model—the Ground-Water Flow Process: U.S. Geological Survey Techniques and Methods 6-A16.
- Johnson Engineering, Inc., 2001, Water Resources Assessment Plan Crescent B Ranch, 2001.

- Johnson Engineering, Inc., 2006, Geologist's Log of JE900 Babcock Ranch, 2006.
- Johnson Engineering Incorporated, 2007a, The Babcock Ranch Community, SFWMD Permit Application # 070330-5
- Johnson Engineering Incorporated, 2007b, Surface Water Management Report The Babcock Ranch Community.
- Johnson Engineering, Inc., 2007, 2008 and 2009, Various documents prepared in support of the South Florida Water Management District Conceptual Surface Water Management Permit Application 070330-5.
- Knapp, M.S., Burns, W.S., and Sharp, T.S., 1986, Preliminary assessment of the groundwater resources of western Collier County, Florida: West Palm Beach, South Florida Water Management District Technical Publication 86-1, 106 p.
- Krause, P., Boyle, D.P., and Base, F., 2005, Comparison of different efficiency criteria for hydrological model assessment: assessment: in Advances in Geosciences, V.5, p89–97.
- Leavesley, G.H., Litchty, R.W., Troutman, B.M. and Saindon, L.G. 1983. Precipitation-Runoff Modeling System: User's Manual. Water Resources Investigations Report 83-4283.
- Markstrom, S.L., Niswonger, R.G., Regan, R.S., Prudic, D.E., and Barlow, P.M., 2008, GSFLOW—Coupled ground-water and surface-water flow model based on the integration of the Precipitation-Runoff Modeling System (PRMS) and the Modular Ground-Water Flow Model (MODFLOW-2005): U.S. Geological Survey Techniques and Methods 6-D1, 240 p.
- Merritt, M.L., and Konikow, L.F., 2000, Documentation of a computer program to simulate lake-aquifer interaction using the MODFLOW ground-water flow model and the MOC3D solute-transport model: U.S. Geological Survey Water-Resources Investigations Report 00-4167, 146 p.
- Nash, J. E. and Sutcliffe, J. V., 1970, River flow forecasting through conceptual models, Part I A discussion of principles: in Journal of Hydrology, v.10, p. 282–290.
- Niswonger, R.G., and Prudic, D.E., 2005, Documentation of the Streamflow-Routing (SFR2) Package to include unsaturated flow beneath streams A modification to SFR1: U.S. Geological Survey Techniques and Methods 6-A13, 62 p.
- Niswonger, R.G., Prudic, D.E., and Regan, R.S., 2006, Documentation of the Unsaturated-Zone Flow (UZF1) Package for modeling unsaturated flow between the land surface and the water table with MODFLOW-2005: U.S. Geological Survey Techniques and Methods 6-A19, 74 p.
- Priestley, C.H.B. and R.J. Taylor, 1972, On the assessment of surface heat flux and evaporation using large-scale parameters: Monthly Weather Review v. 100, p. 81-92.
- Quinones-Aponte, Vicente and Wexler, E.J., 1995, Preliminary assessment of injection, storage, and recovery of freshwater in the lower Hawthorn aquifer, Cape Coral, Florida: USGS Water Resources Investigation Report 94-4121, 102 p.
- Rawl, G.F., Earthfx Inc., Voorhees, M.L., and Mades, D, 2008, Analysis of Infiltration and Storm Water Runoff from the Babcock Ranch Community Development, Charlotte and Lee Counties, Florida: September 2008.
- Rawl, G.F., Earthfx Inc., Voorhees, M.L., 2005, Lee County Groundwater Resource and Mining Study Draft for Peer Review: June 2005.

- Reese, R.S., 2000, Hydrogeology and the Distribution of Salinity in the Floridan Aquifer System, Southwestern Florida: U.S. Geological Survey WRIR 98-4253, 86 p., 10 pls.
- Reese, R.S., and Cunningham, K.J., 2000, Hydrogeology of the Gray Limestone Aquifer in Southern Florida: U.S. Geological Survey WRIR 99-4213, 244 p.
- SDI Environmental Services, Inc., BPC Group Inc., and Danish Hydrologic Institute, 2008, Southwest Florida Feasibility Study Integrated Hydrologic Model -- Model Documentation Report: prepared for the South Florida Water Management District, January 2008.
- SDI Inc. 2007, Four Corners/County Line Ditch Preliminary Design Report for the SFWMD, July 2007.
- Suphunvorranop, 1985, Technical Publication No. 85-5, A guide to SCS runoff procedures: St. Johns River Water Management District Project Number 15/20 200 03, July 1985.
- Soil Conservation Service, 1972, National Engineering Handbook, Section 4 Hydrology: U.S. Department of Agriculture –Soil Conservation Service, Washington, D.C.
- Wedderburn, L.A., Knapp, M.S., Waltz, D.P., and Burns, W.S., 1982, Hydrogeologic reconnaissance of Lee County, Florida Part 1 Text: SFWMD Technical Publication 82-1

9 Tables

Table 1: Summary of streamflow monitoring station information.

Station ID	Station Name/ Location	Drainage Area (mi²)	Period of Record for Concurrent Stage and Discharge Measurements (for this study)	Period of Continuous Water Level Measurement (for this study)
JEI-567	Curry Lake Canal at Hercules Grade	8.07	6/2006 - 12/2009	6/2006 - 6/2010
JEI-569	Curry Lake Canal near County line	12.68	6/2006 - 12/2009	4/2006 - 6/2010
JEI-570	Trout Creek near SR78	20.13	6/2006 - 12/2009	4/2006 - 6/2010
JEI-1471	Telegraph Creek at Babcock Ranch Headquarters	24.64	720/06 - 9/2010	2/2008 - 6/2010
JEI-564/JEI-565	Big Island Canal and Telegraph Creek at Big Island Dike	78.09	10/2007 -6/2010	4/2006 - 6/2010
JEI-1495	Big Island Canal at County Line	192 18	7/2006 - 12/2009	8/2008 - 6/2010
JEI-1497	Telegraph Creek at Timber Bridge		7/2006 - 12/2009	10/2008 - 6/2010
022929176	Telegraph Creek at State Highway at Olga	67.4	11/2007 - 6/2010	11/2007 - 6/2010
JEI-1518	Cypress Head / South Lightered Cana		11/2007 - 6/2010	9/2008 - 11/2010
JEI-1502	Cypress Creek Outflow		9/2006 - 6/2010	8/2008 - 10/2010
JEI-1508	Jacks Branch Inflow		10/2007 - 6/2010	11/2008 - 6/2010
JEI-1514	Jacks Branch Outflow		10/2007 - 6/2010	8/0208 - 12/2010

Table 2: Geologic, hydrogeologic, and groundwater model layer in study area (modified from Rawl and others, 2005).

SERIES	GEOLOGIC UNIT		HYD	RO	GEOLOGIC UNIT	Groundwater Model Layers	
HOLOCENE PLEISTOCENE	UNDIFFERENTIATED				SURFICIAL SEDIMENTS	HOLOCENE	
	3		FER	PI	NECREST LIMESTONE	PLIOCENE	
PLIOCENE	TAMIAMI FORMATION		SURFICIAL AQUIFER SYSTEM	ВО	NITA SPRINGS MARL CONFINING BED	(Not Present in Model Area)	
					LOWER TAMIAMI AQUIFER	OCHOPEE	
					U	PPER PEACE RIVER CONFINING BED	UPPER PEACE RIVER CONFINING
PEACE FORMA	PEACE RIVER FORMATION	IATE R I	SANDSTONE AQUIFER		SANDSTONE		
MIOCENE	PEACE RIVER FORMATION ARCADIA	ORN O	MED	BASAL PEACE RIVER CONFINING BED MID-HAWTHORN		BASAL PEACE RIVER CONFINING	
			INTERMEDIATE AQUIFER SYSTEM		MID-HAWTHORN AQUIFER	ARCADIA	
	HA	ARCADIA FORMATION	T .	BA	SAL MID-HAWTHORN CONFINING BED	BASAL MID-HAWTHORN CONFINING	
			Zyl		LOWER HAWTHORN AQUIFER	LOWER HAWTHORN	
OLIGOCENE SUWANNEE LIMESTONE		FLORIDAN AQUIFER SYSTEM		UPPER FLORIDAN AQUIFER	SUWANNEE		

Table 3: Simulated flows at Trout, Owl, and Telegraph Creek in response to design storms under Current, Post-development, and Natural Conditions.

	100	Year, 3-Day	Storm	25 Year, 3-Day Storm			Year, 3-Day Storm 5 Year, 1-Day Storm		
Basin	Cur- rent	Post- Develop- ment	Natural	Cur- rent	Post- Develop- ment	Natural	Cur- rent	Post- Develop- ment	Natural
Trout Creek (cfs)	2,432	1,697	1,196	1,748	1,245	856	699	513	359
Owl Creek (cfs)	440	372	332	328	262	242	166	119	110
Telegraph Creek (cfs)	2,046	1,973	829	1,419	1,367	587	448	442	236

Integrated surface-water/groundwater flow mode	I for the Babcock Ranch Community	Development
--	-----------------------------------	-------------

10 FIGURES

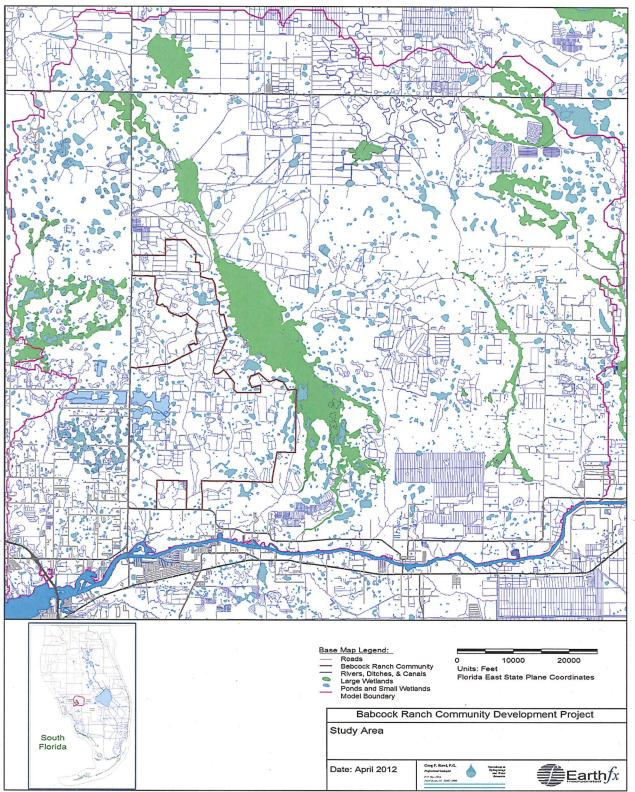


Figure 1: Study area showing Babcock Ranch Community and model extents.

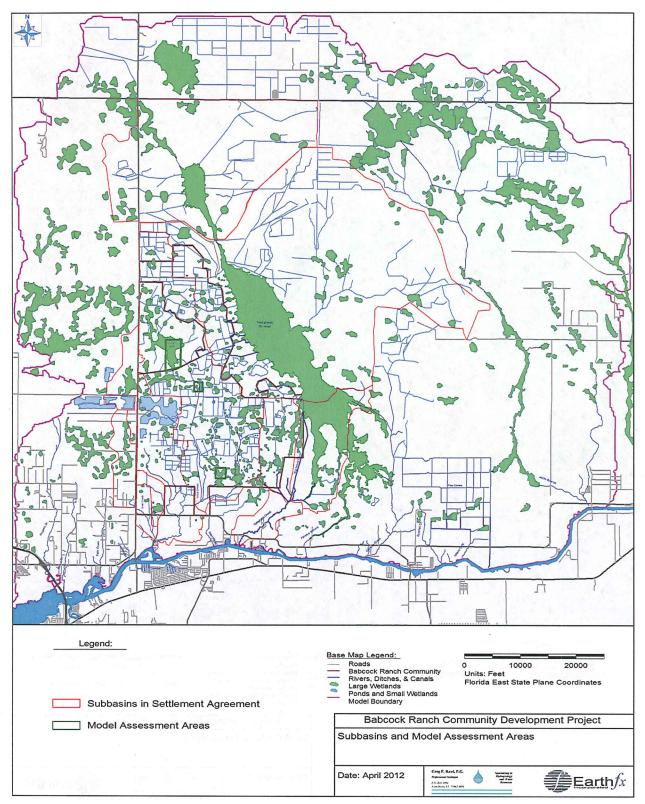


Figure 2: Sub-basins and model assessment areas discussed in the Settlement Agreement.

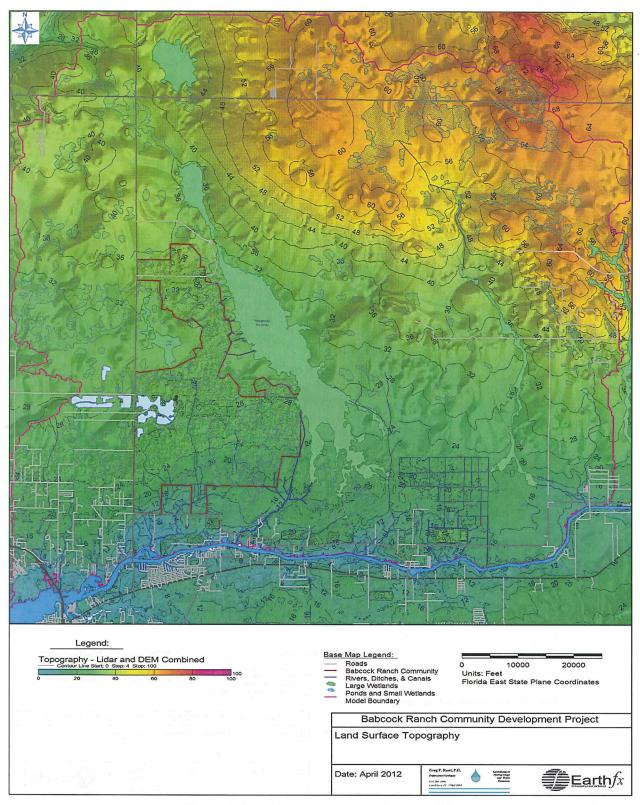


Figure 3: Land surface topography (NGVD).

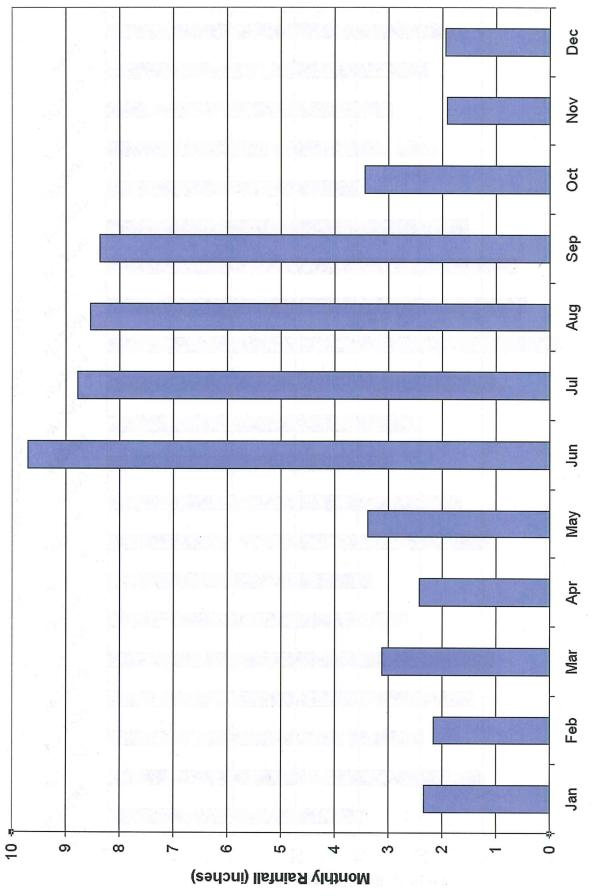
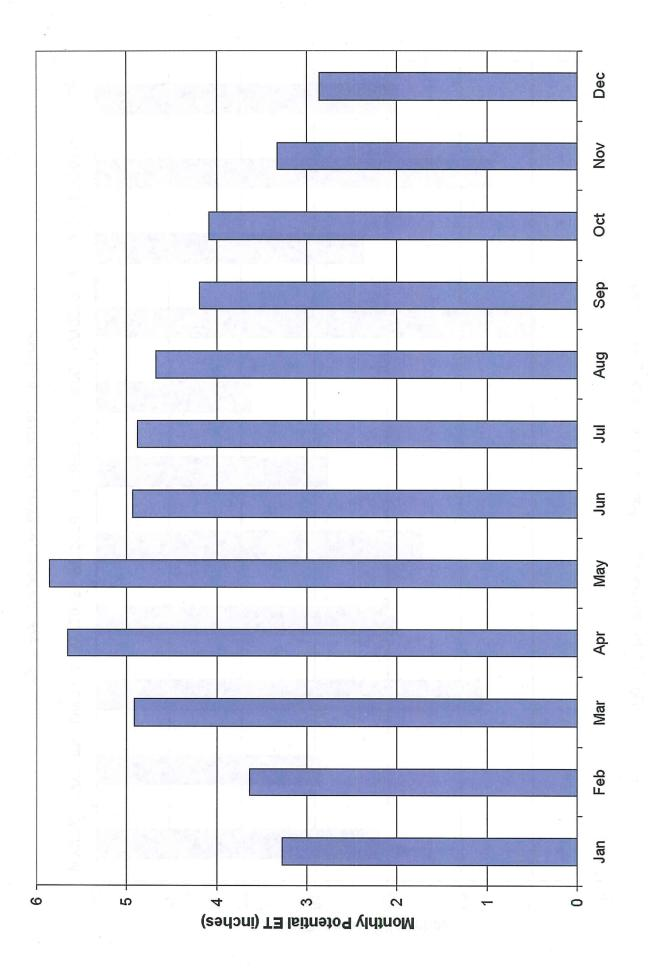


Figure 4: Monthly average rainfall at S-79 (Franklin Lock) based on 1991 to 2010 data.

Figure 5: Annual precipitation at S-79 (Franklin Lock).



Earthfx Inc. and Greg Rawl, P.G.

Figure 6: Monthly potential evapotranspiration at S79 (Franklin Lock).

22

53

54

52

20

51

Annual Potential ET (inches)

49

WY2002 WY2003 WY2004 WY2005 WY2006 WY2007 WY2008 WY2009 WY2010 WY2011 Average

Figure 7: Annual potential evapotranspiration at S79 (Franklin Lock).

48

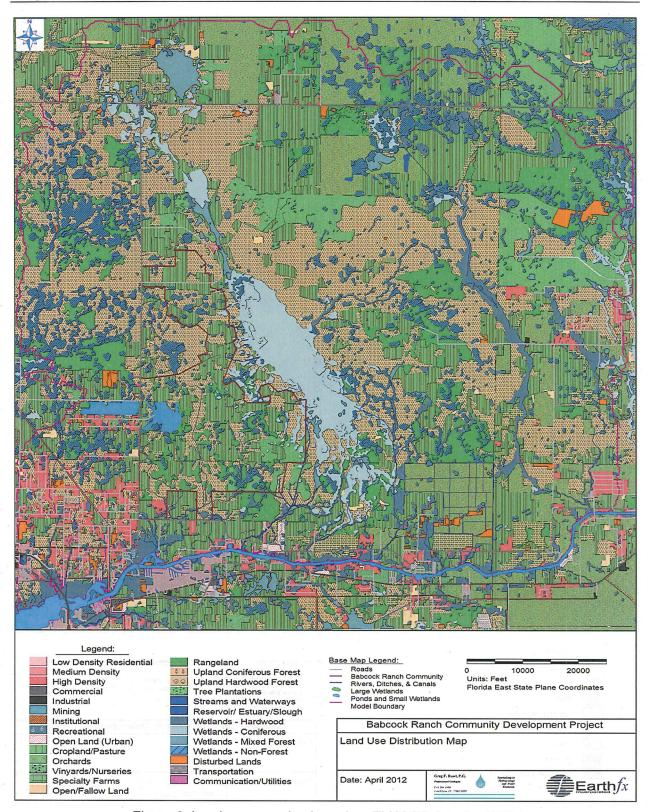


Figure 8: Land use mapping based on FLUCCS data for 2000.

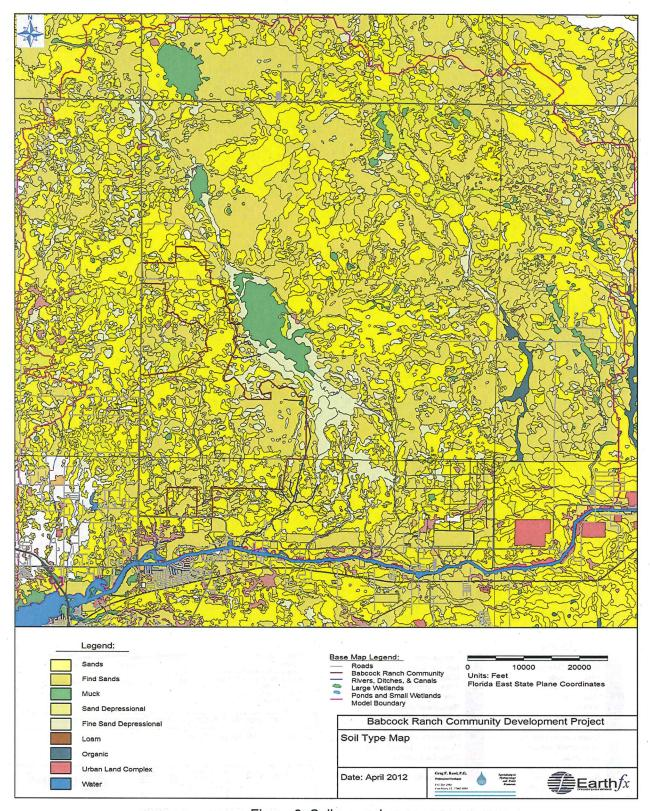


Figure 9: Soils mapping.

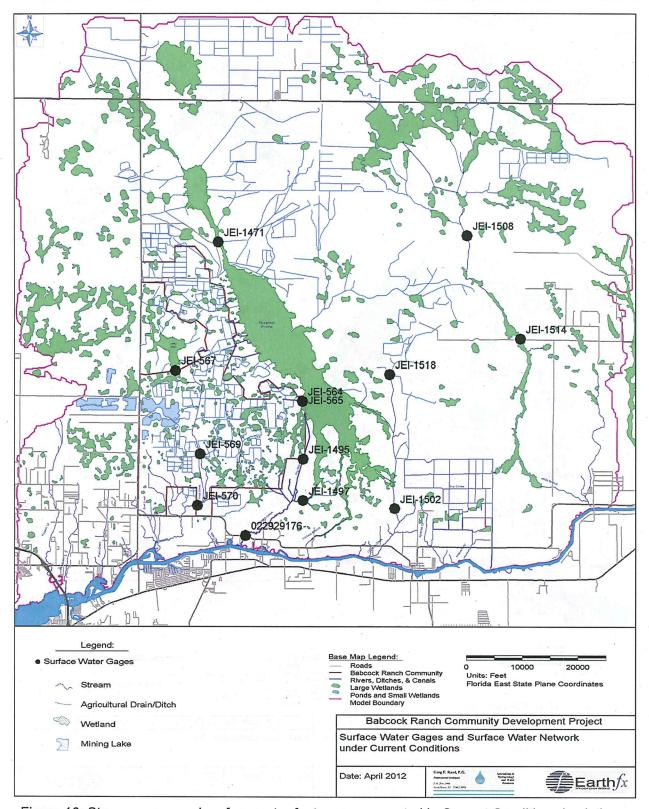


Figure 10: Stream gages and surface water features represented in Current Condition simulations.

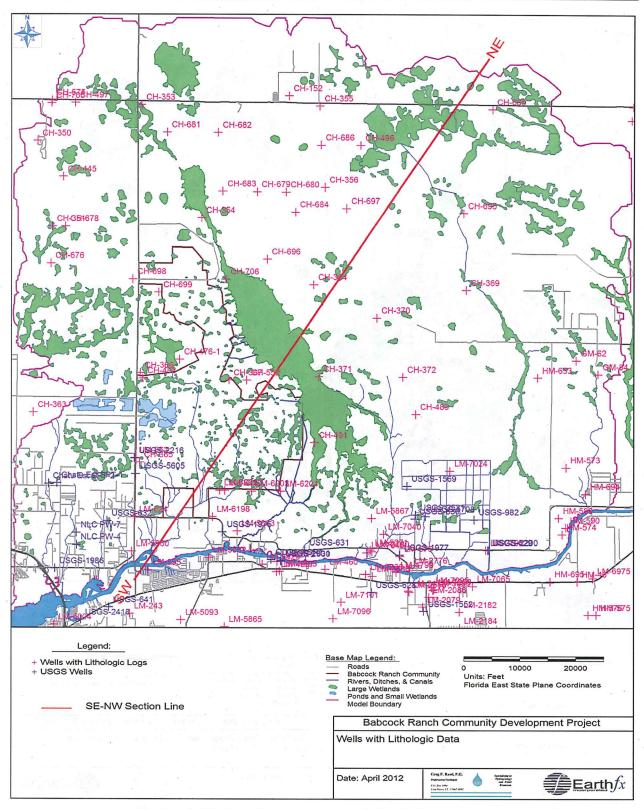


Figure 11: Wells in the study area with lithologic information.

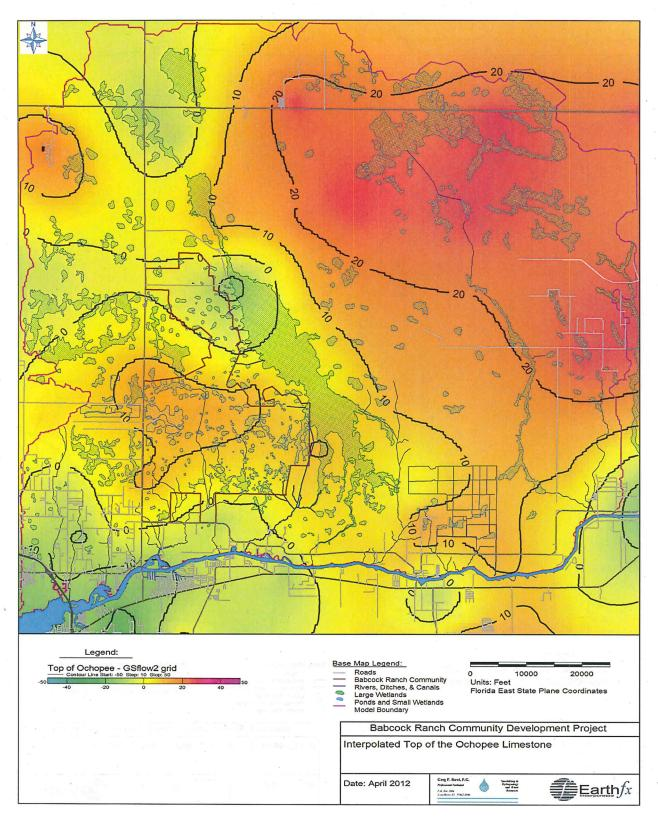


Figure 12: Interpolated top of the Ochopee Limestone (in feet above NGVD).

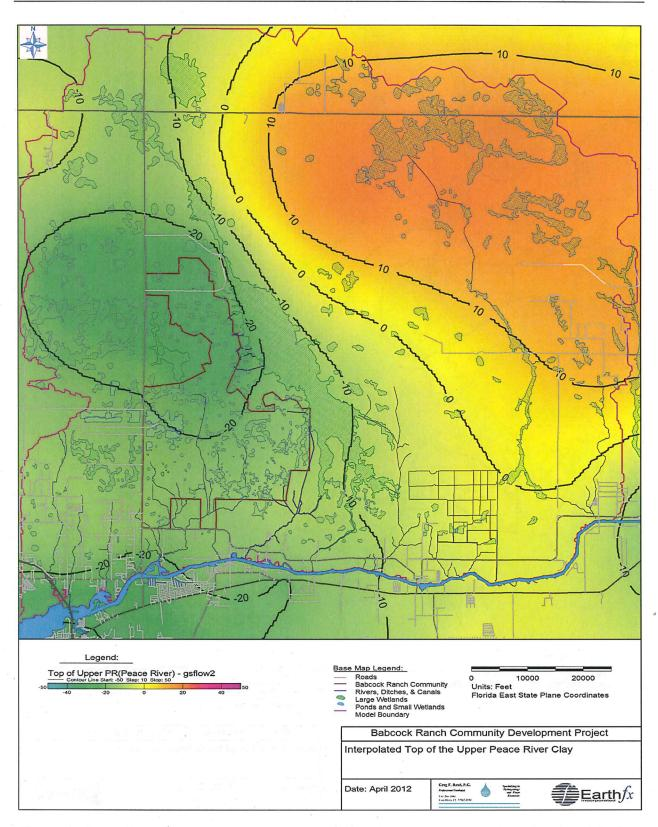


Figure 13: Interpolated top of the upper Peace River clay (bottom of the Ochopee limestone) (in feet above NGVD).

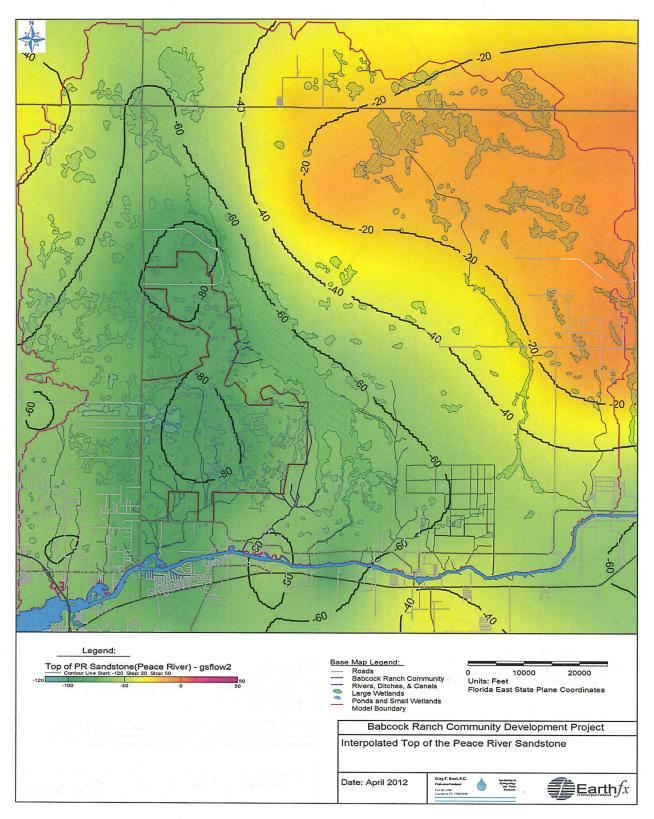


Figure 14: Interpolated top of the Peace River sandstone (in feet above NGVD).

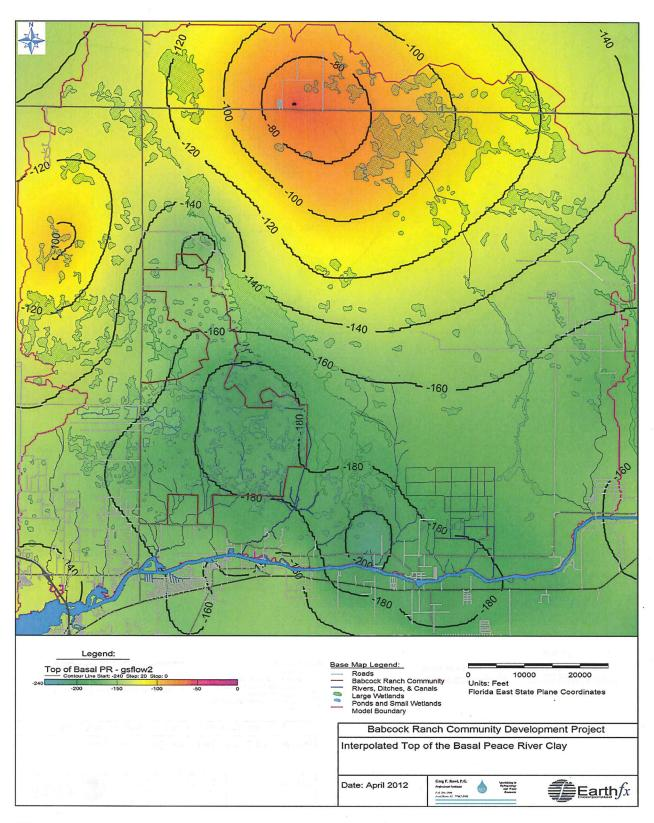


Figure 15: Interpolated top of the basal Peace River clay (bottom of Peace River sandstone) (in feet above NGVD).

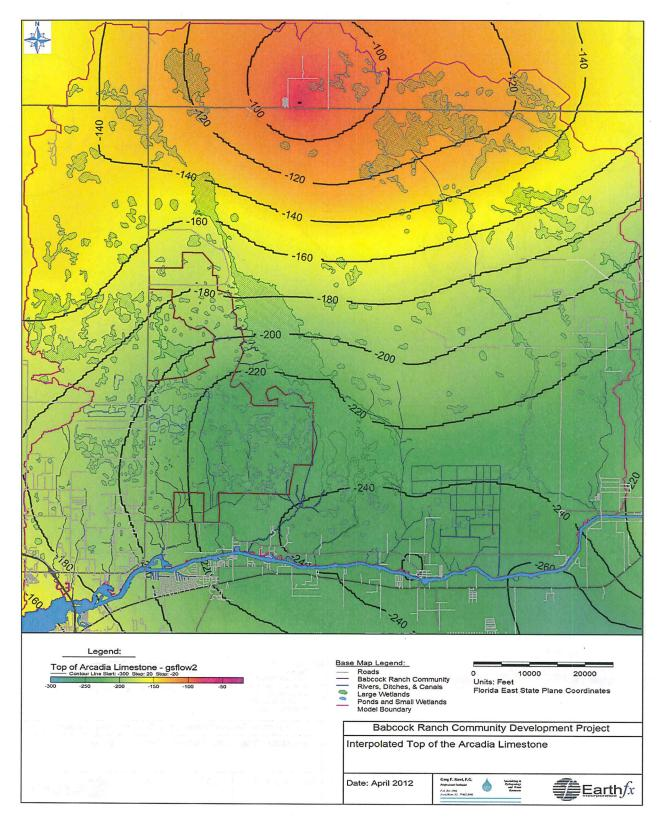


Figure 16: Interpolated top of the Arcadia limestone (in feet above NGVD).

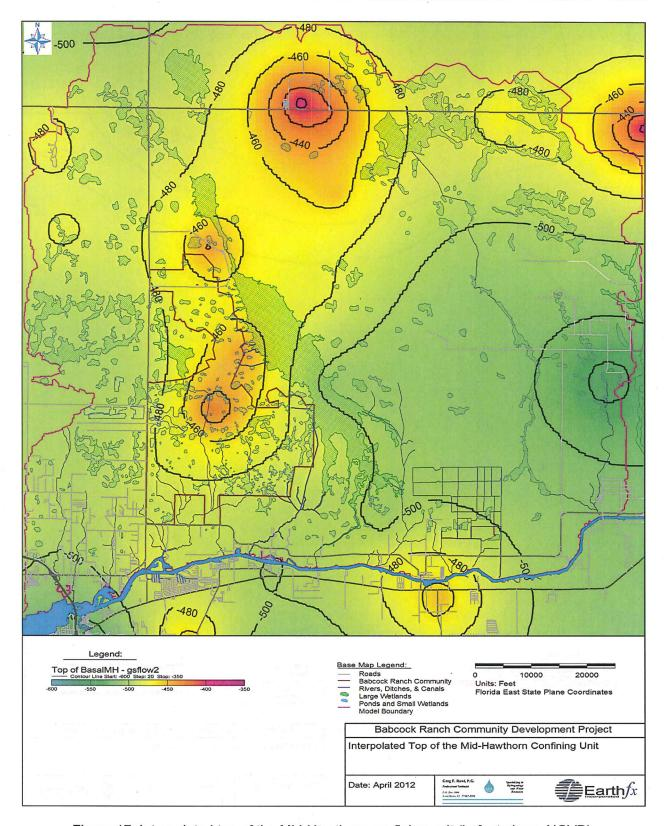


Figure 17: Interpolated top of the Mid-Hawthorn confining unit (in feet above NGVD).

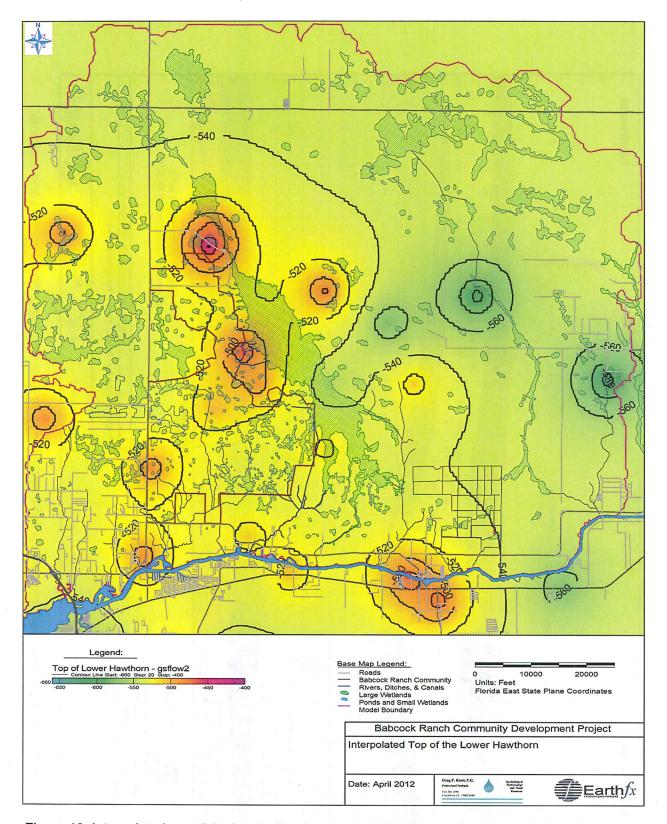


Figure 18: Interpolated top of the Lower Hawthorn unit of the Floridan aquifer (in feet above NGVD).

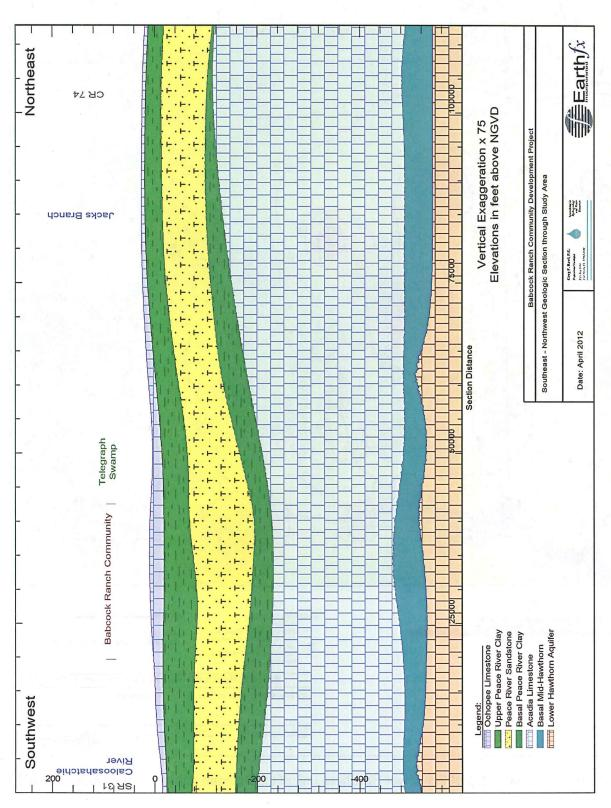


Figure 19: Northeast-Southwest geologic section through the study area showing principal aquifers and aquitards.

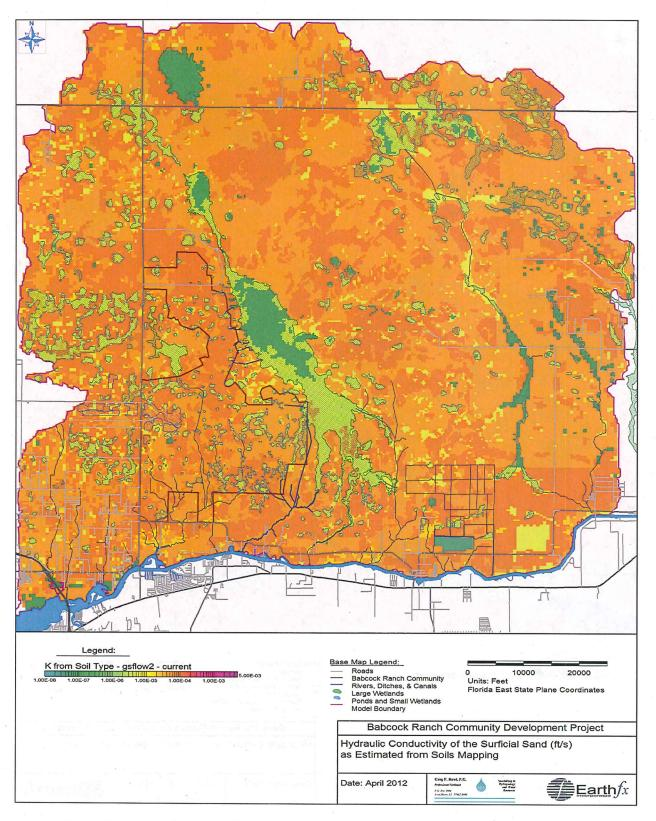


Figure 20: Hydraulic conductivity of the surficial sand as estimated from soils mapping.

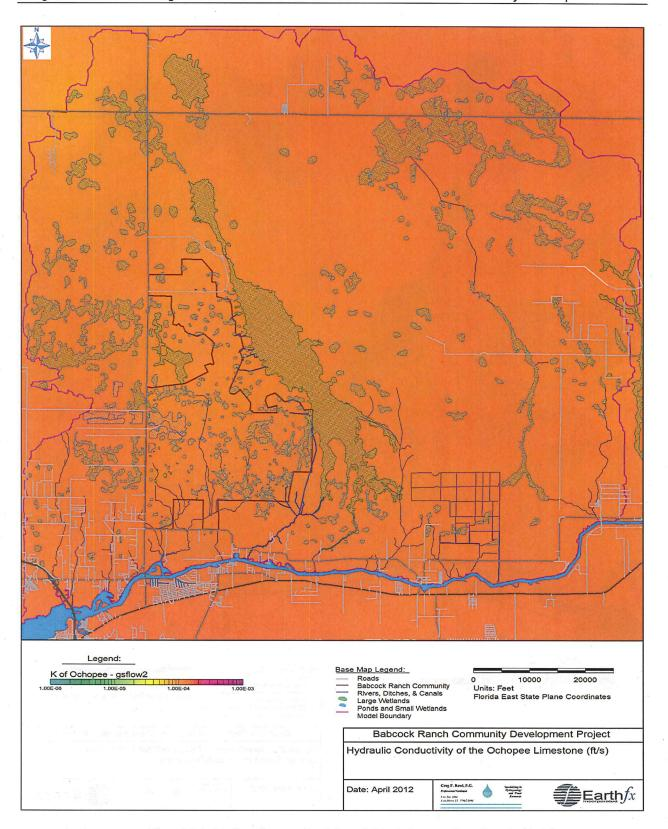


Figure 21: Hydraulic conductivity of the Ochopee limestone.

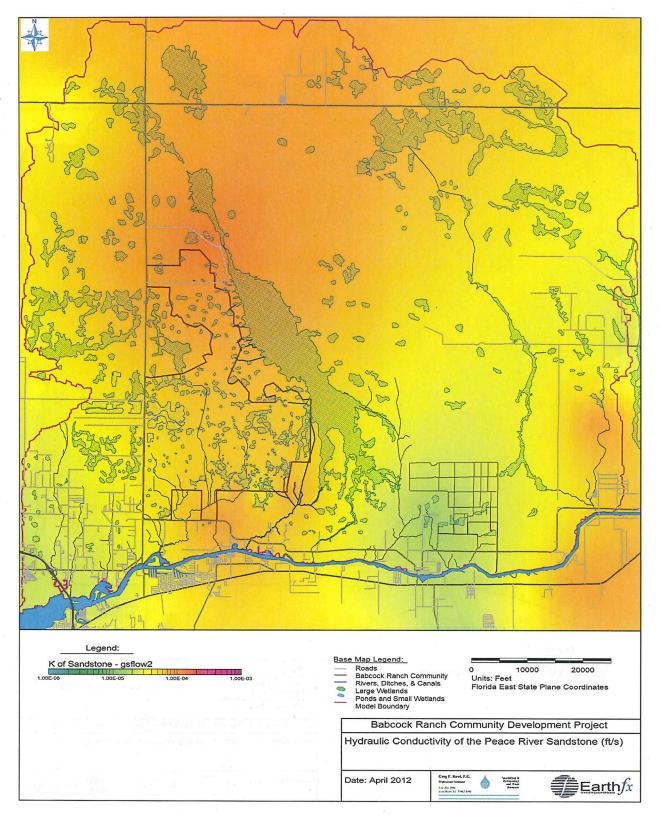


Figure 22: Hydraulic conductivity of the Peace River sandstone.

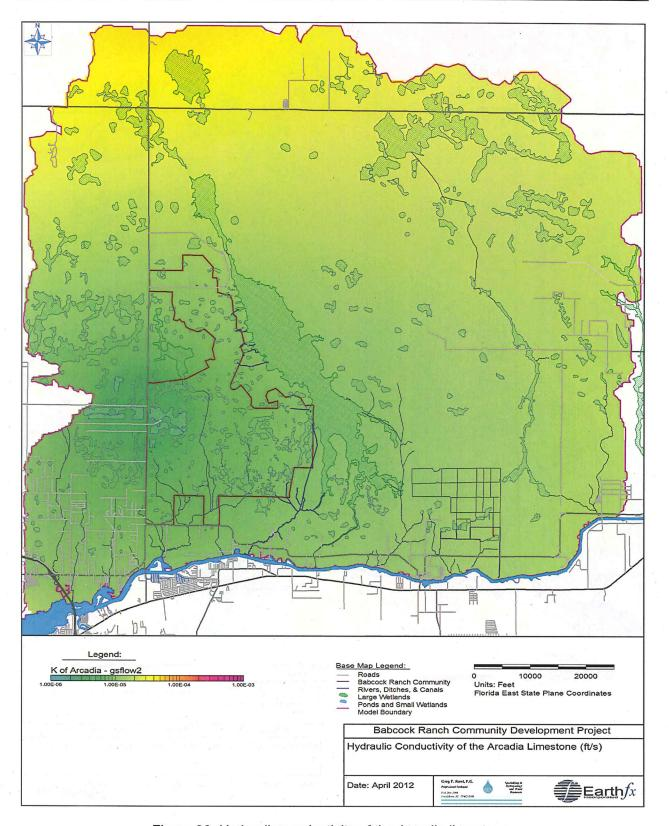


Figure 23: Hydraulic conductivity of the Arcadia limestone.

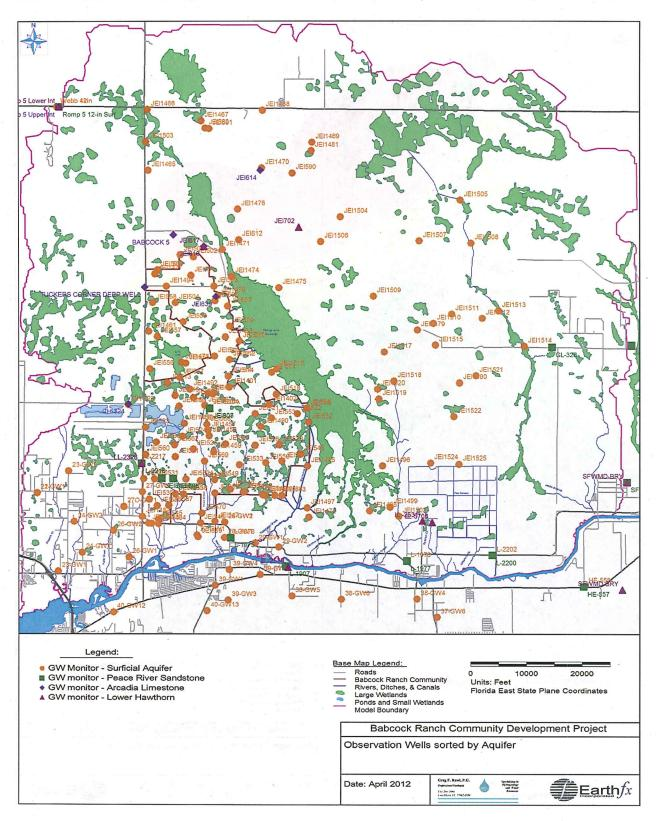


Figure 24: Location of observation wells.

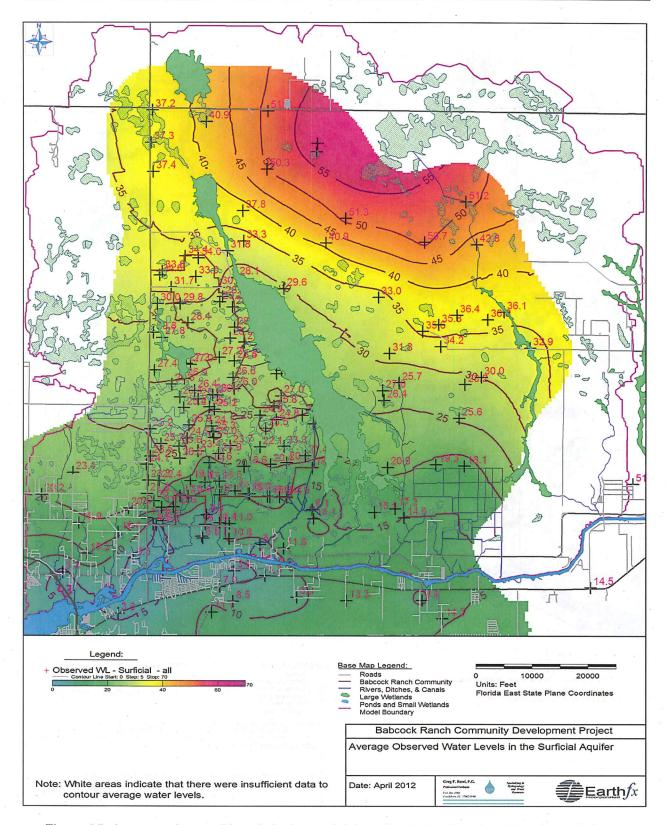


Figure 25: Average observed heads in the surficial aquifer and interpolated heads (in ft above NGVD).

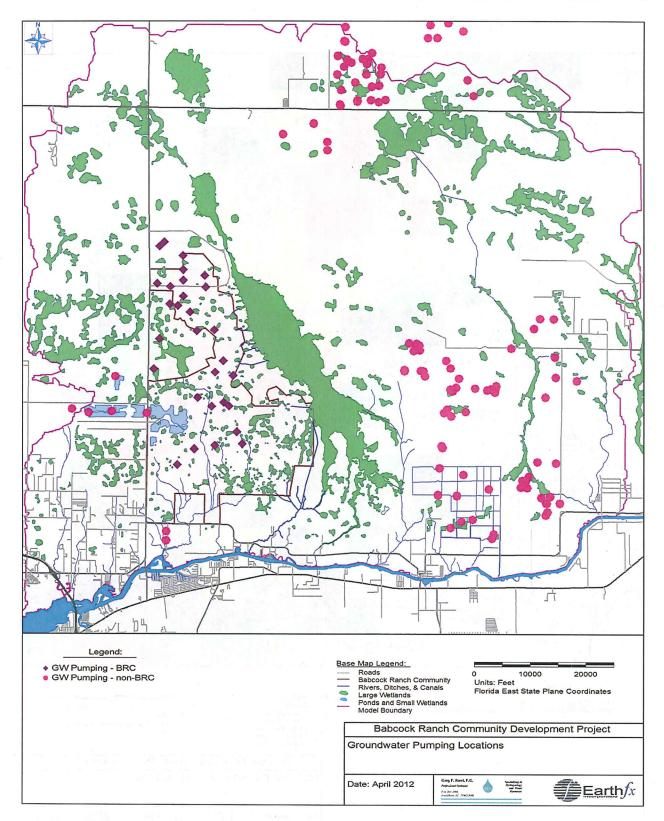


Figure 26: Location of pumping wells simulated in the model.

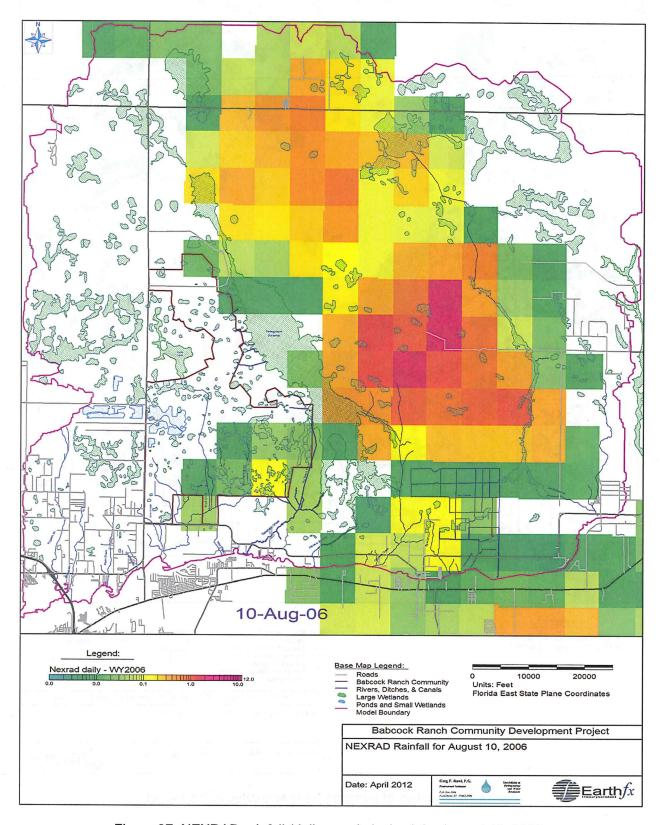


Figure 27: NEXRAD rainfall (daily sum in inches) for August 10, 2006.

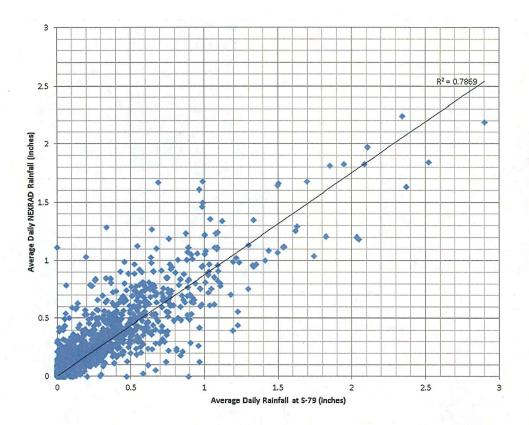


Figure 28: Average daily NEXRAD rainfall versus observed rainfall at S-79 (Franklin Lock).

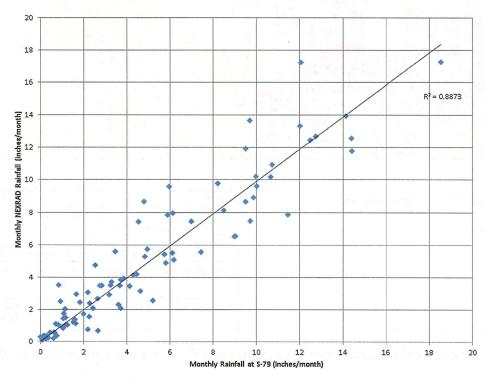


Figure 29: Monthly NEXRAD rainfall versus observed monthly rainfall at S-79 (Franklin Lock).

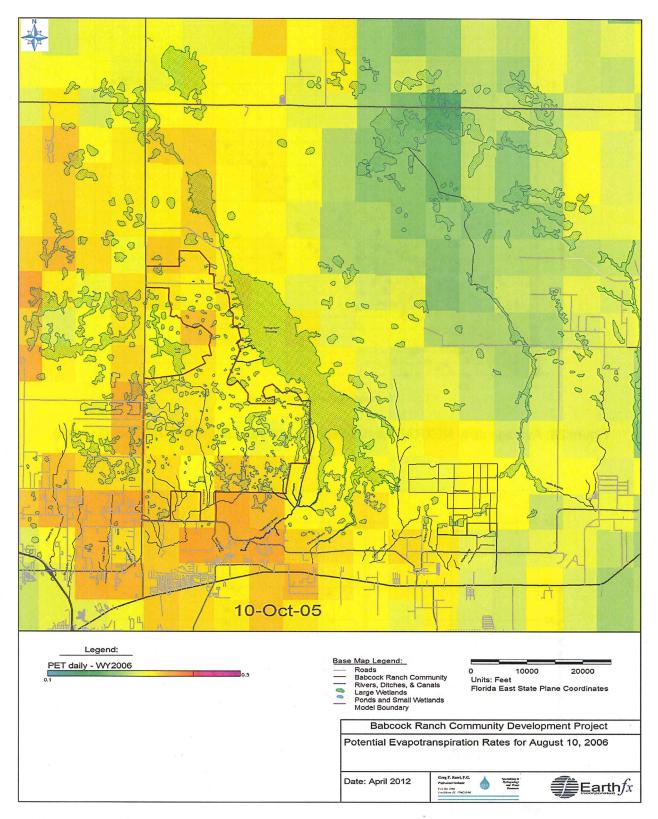


Figure 30: Gridded daily potential evapotranspiration (PET) rates (inches) for August 10, 2006.

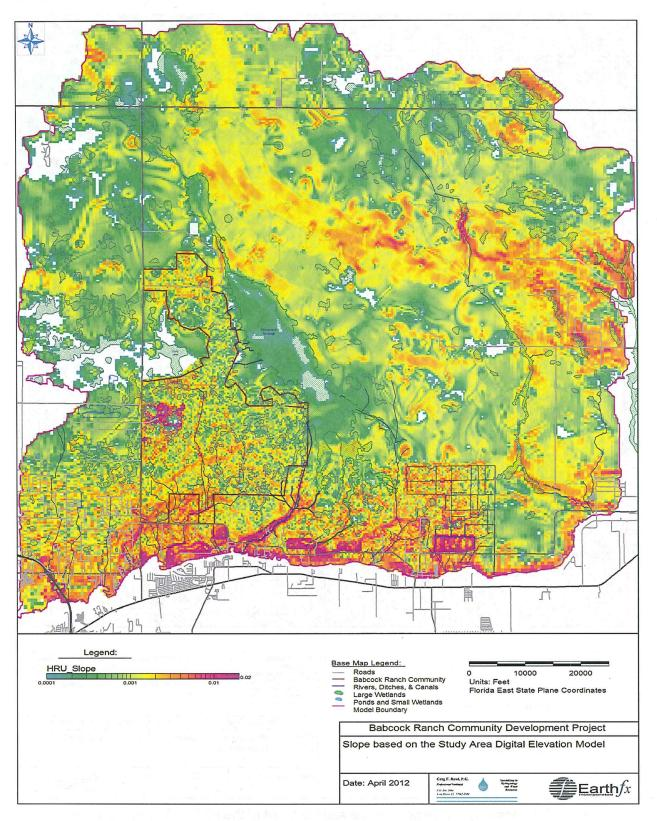


Figure 31: Slope values (decimal fraction) used in the PRMS model.

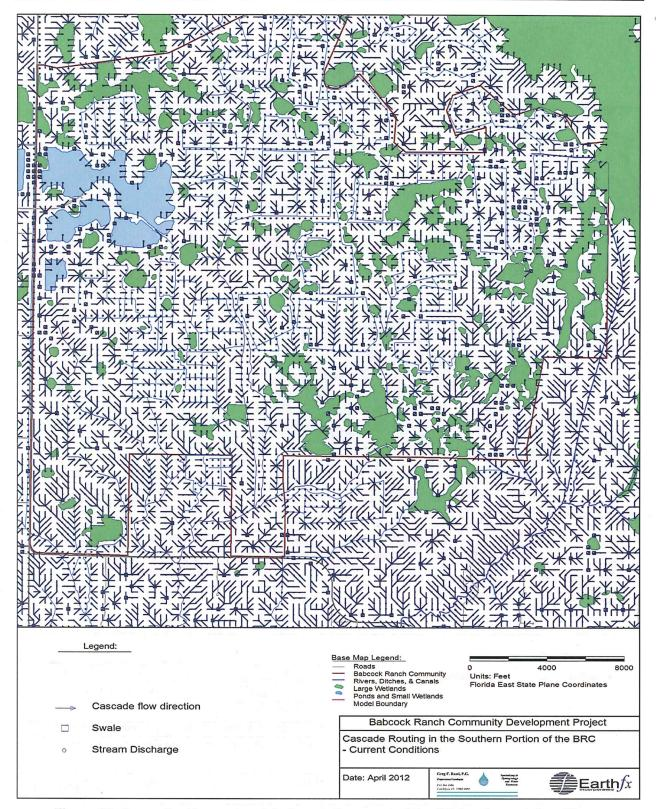


Figure 32: Cascading flow network in the southern part of the BRC – Current Conditions.

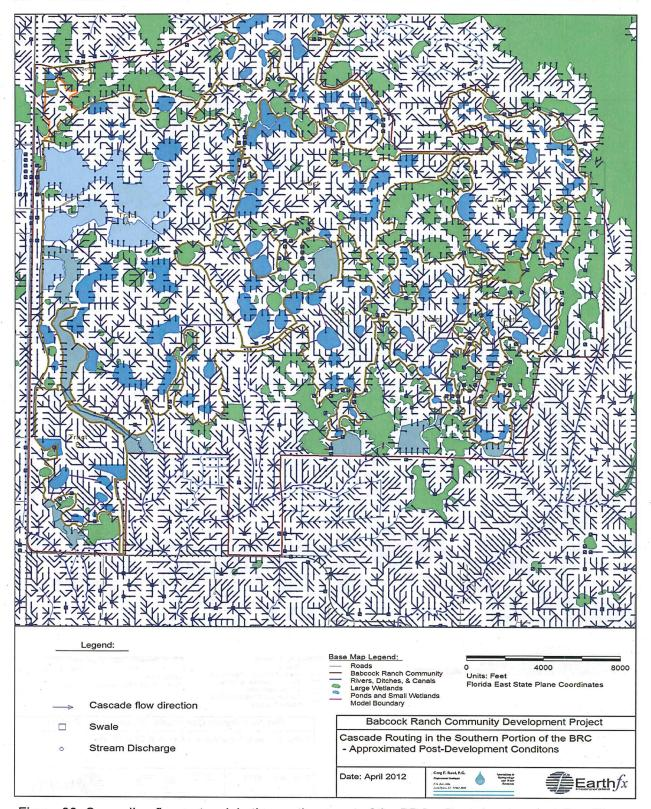


Figure 33: Cascading flow network in the southern part of the BRC – Post-development Conditions.

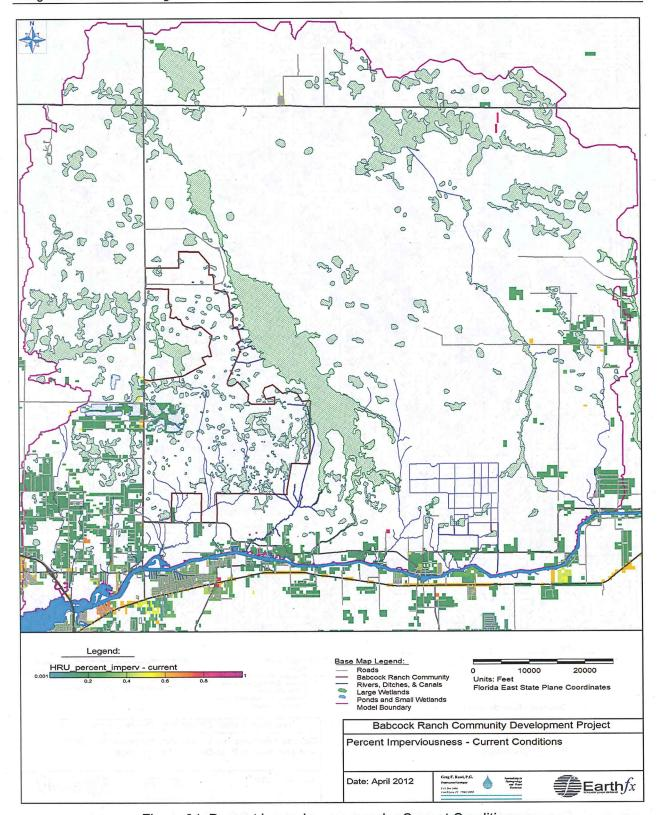


Figure 34: Percent imperviousness under Current Conditions.

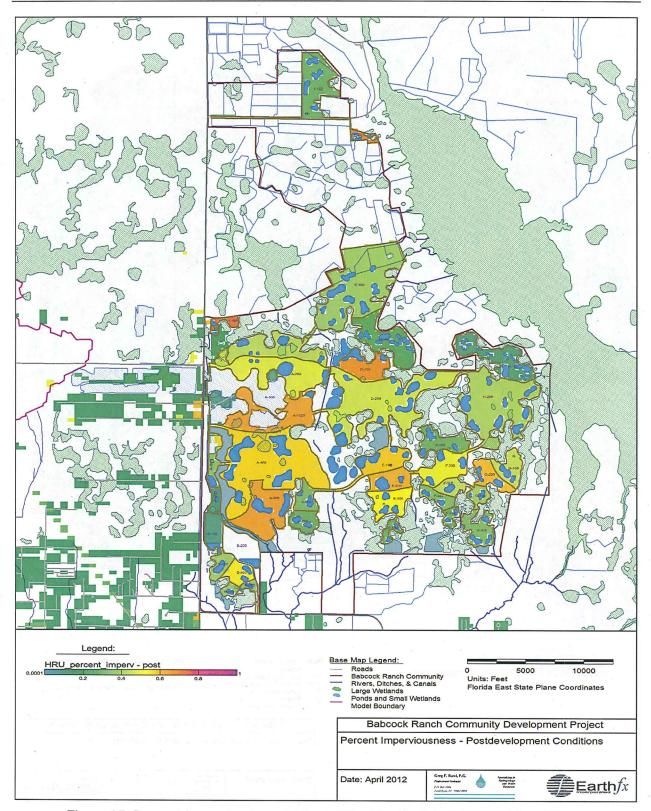


Figure 35: Percent imperviousness in the BRC under Post-development Conditions.

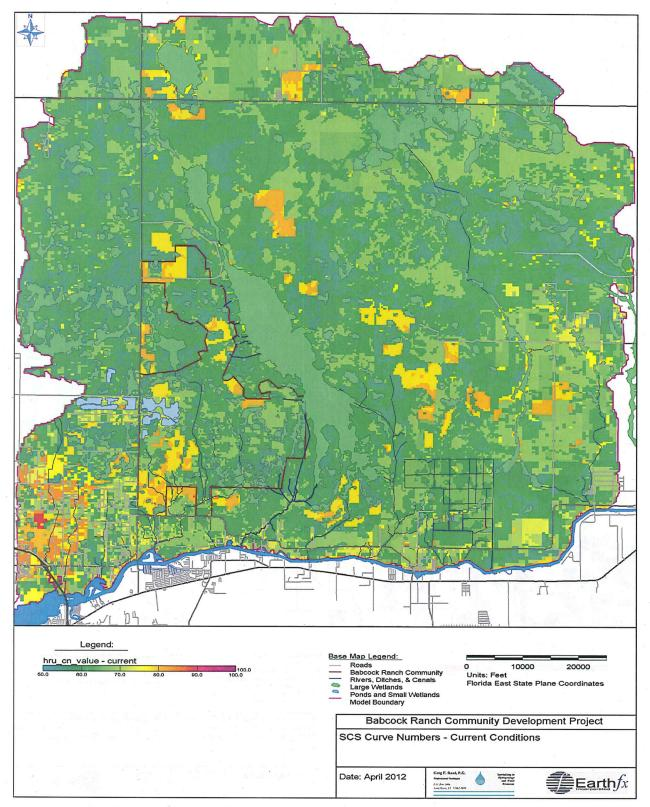


Figure 36: Soil Conservation Service (SCS) curve number (CN) values (AMC II) assigned based on combinations of soil type and Current Conditions land use. Wetland areas have no CN assigned.

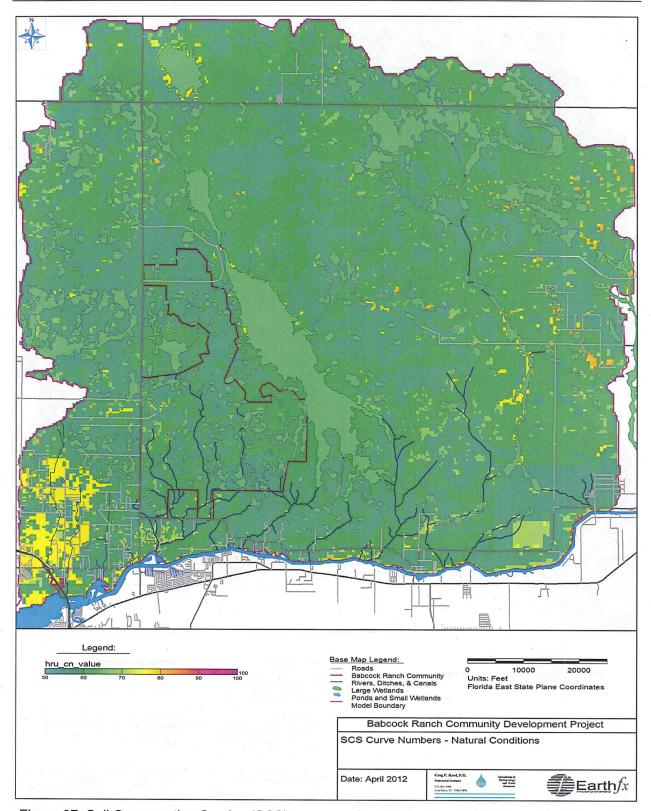


Figure 37: Soil Conservation Service (SCS) curve number (CN) values (AMC II) assigned based on combinations of soil type and Natural Conditions land use.

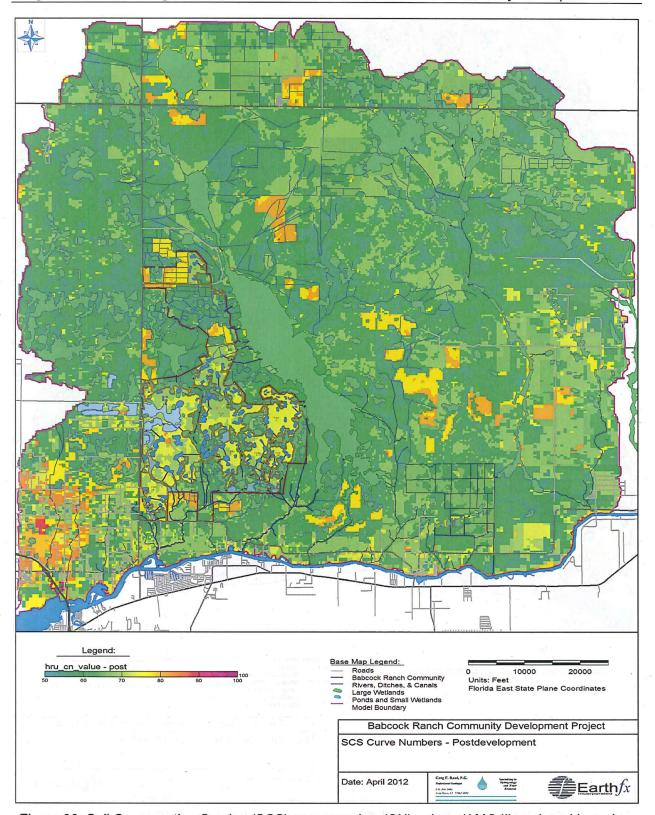


Figure 38: Soil Conservation Service (SCS) curve number (CN) values (AMC II) assigned based on combinations of soil type and Post-development Conditions land use. Wetland areas have no CN assigned.

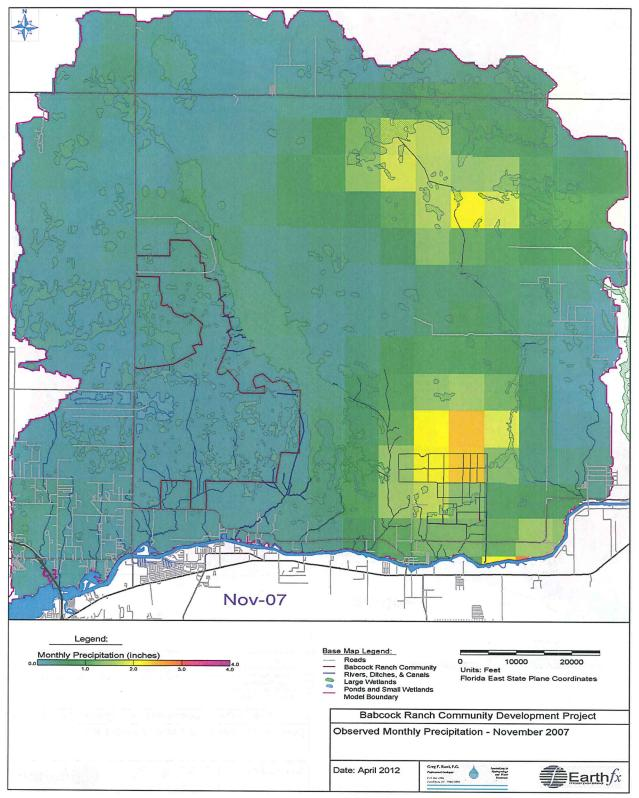


Figure 39: Observed monthly precipitation (inches) in November 2007.

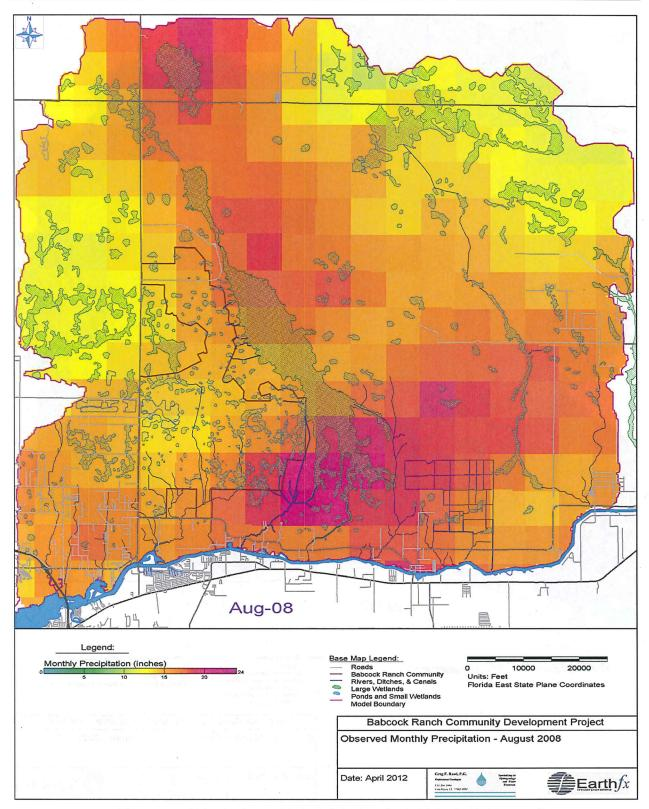


Figure 40: Observed monthly precipitation (inches) in August 2008.

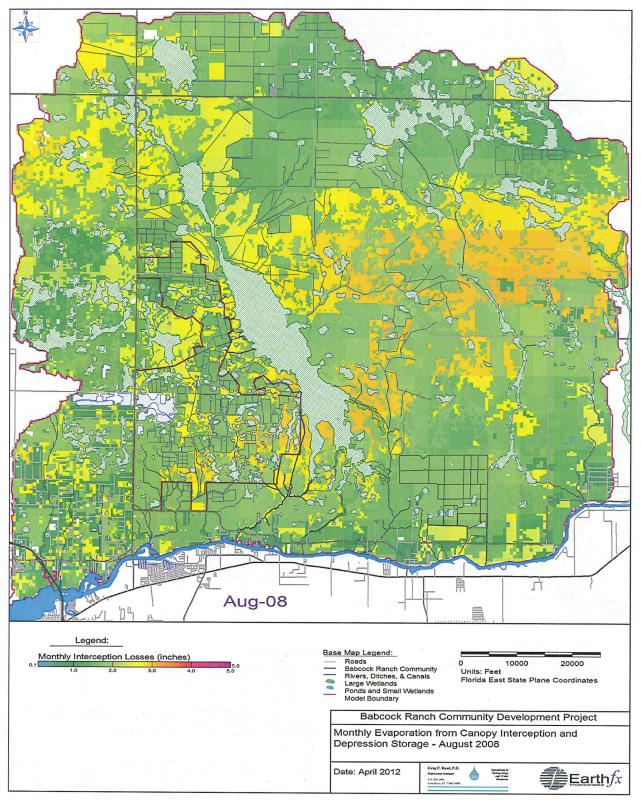


Figure 41: Monthly evaporation from canopy interception and detention storage (inches) in August 2008 under Current Conditions.

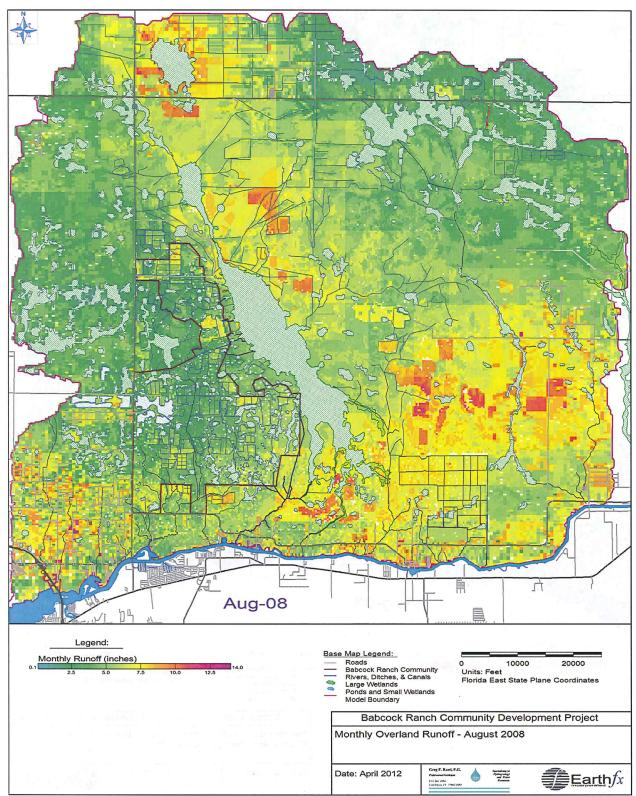


Figure 42: Monthly overland runoff (inches) in August 2008 under Current Conditions.

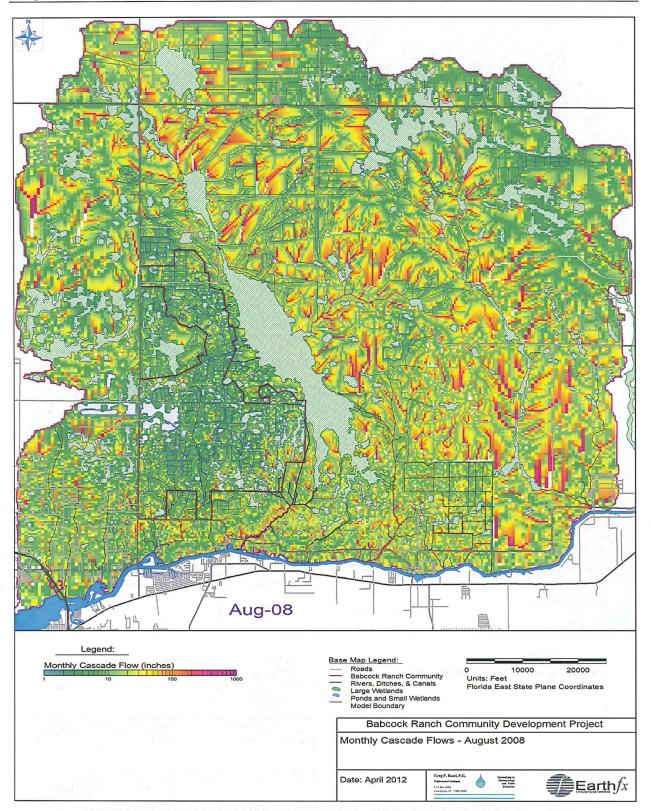


Figure 43: Monthly cascade flows (inches) for August 2008 (inches/month) under Current Conditions. Cascade flows include runoff generated and passing through each cell.

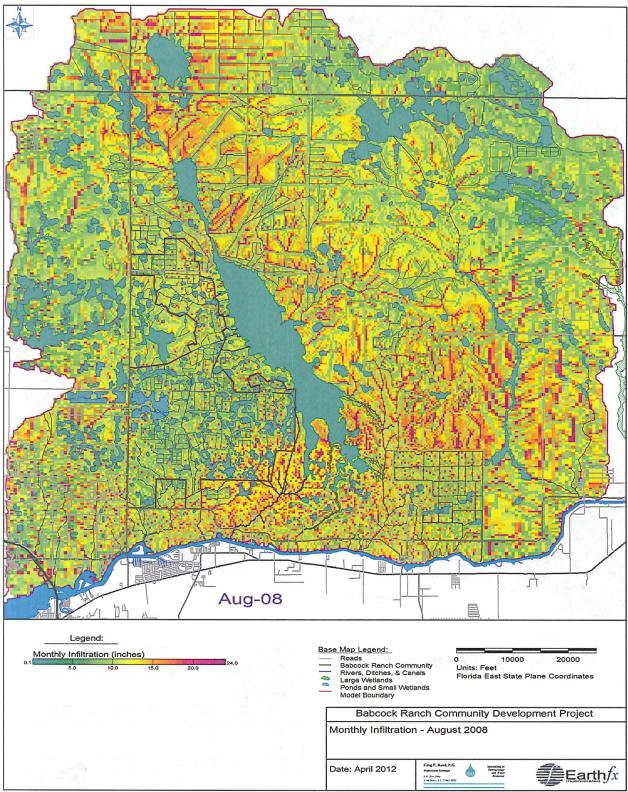


Figure 44: Monthly infiltration (inches) in August 2008 under Current Conditions.

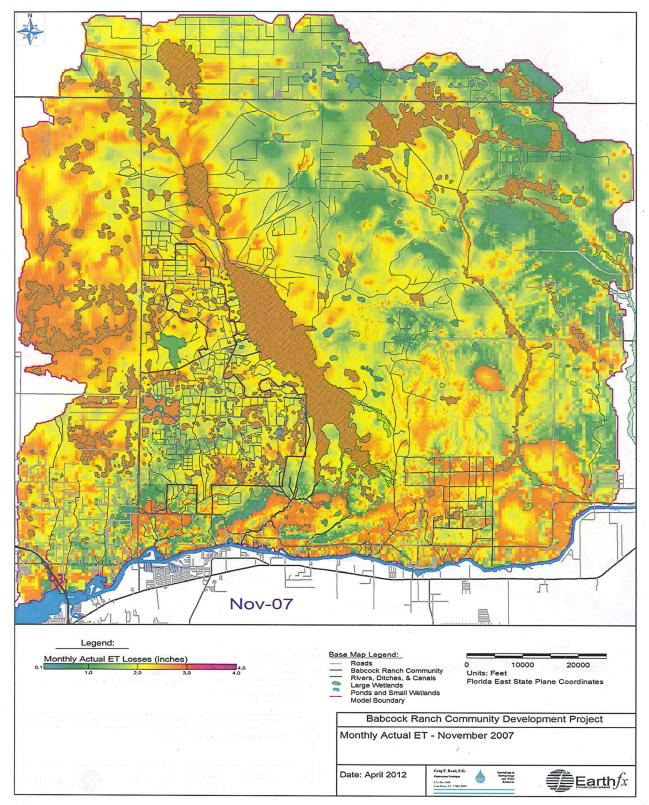


Figure 45: Monthly actual ET (inches) in November 2007 under Current Conditions.

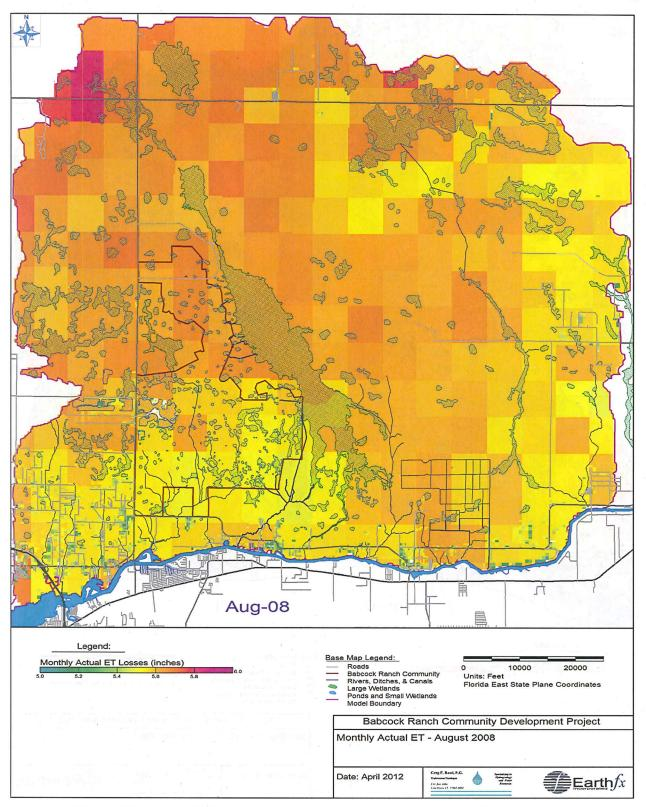


Figure 46: Monthly actual ET (inches) in August 2008 under Current Conditions (note change in scale).

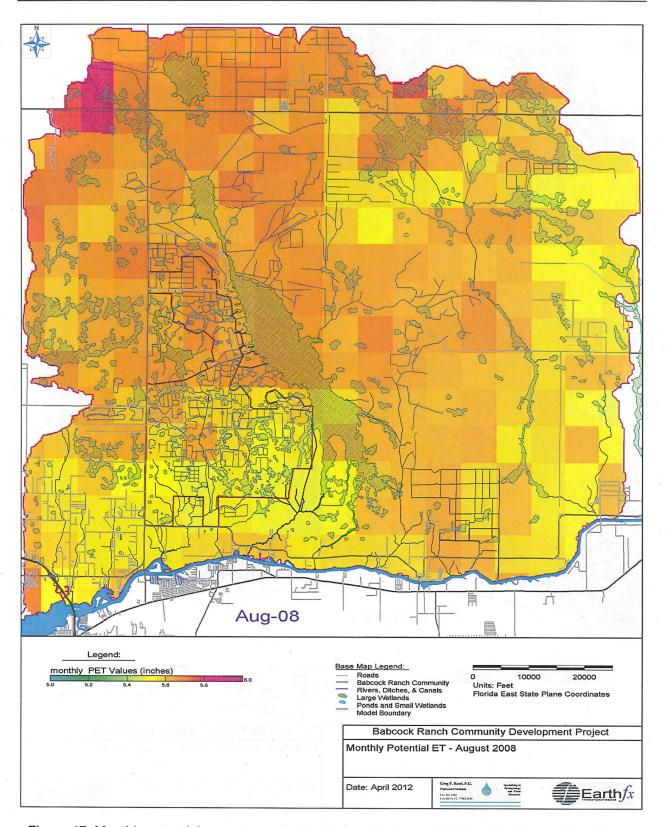


Figure 47: Monthly potential evapotranspiration (inches) in August 2008 under Current Conditions.

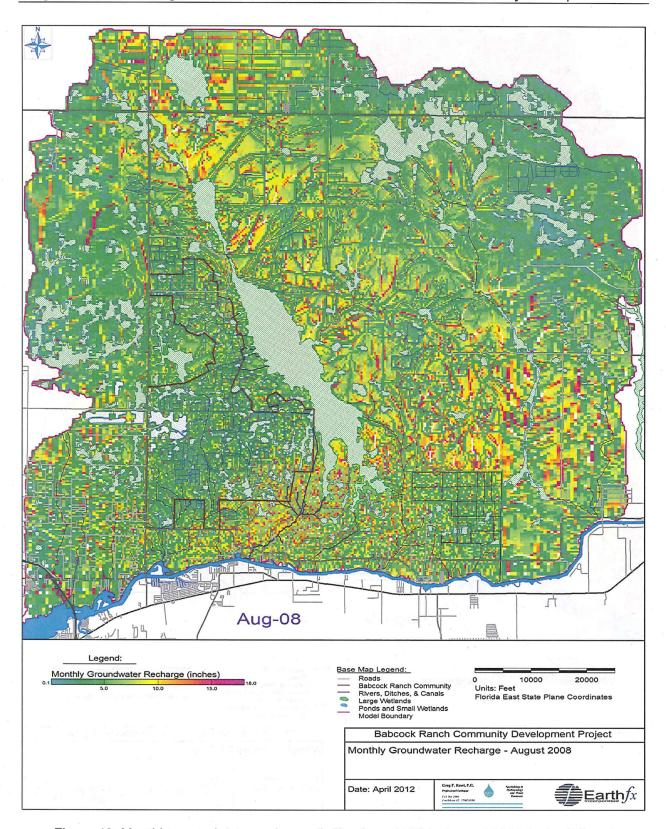


Figure 48: Monthly groundwater recharge (Infiltration - AET) in August 2008 under Current Conditions.

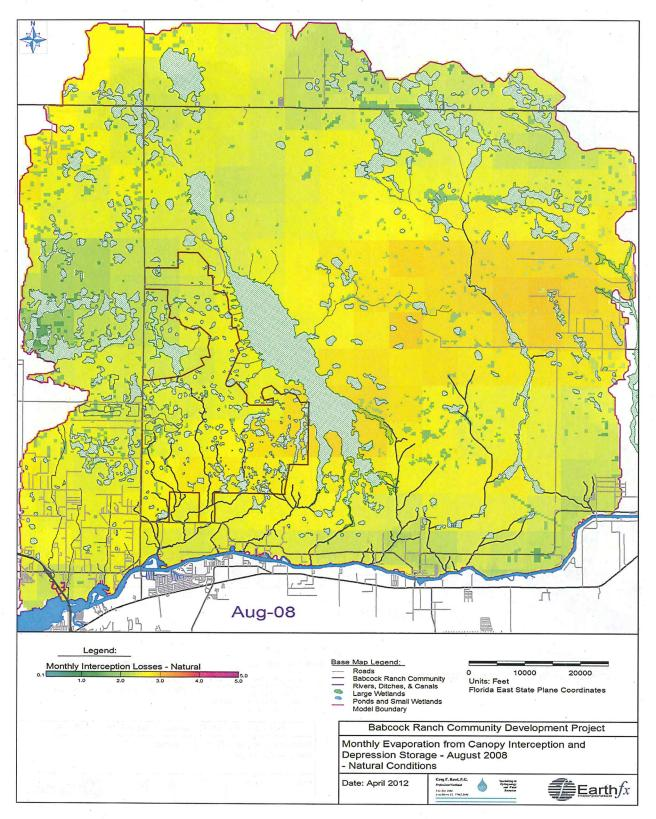


Figure 49: Monthly evaporation from canopy interception and detention storage (inches) in August 2008 under Natural Conditions.

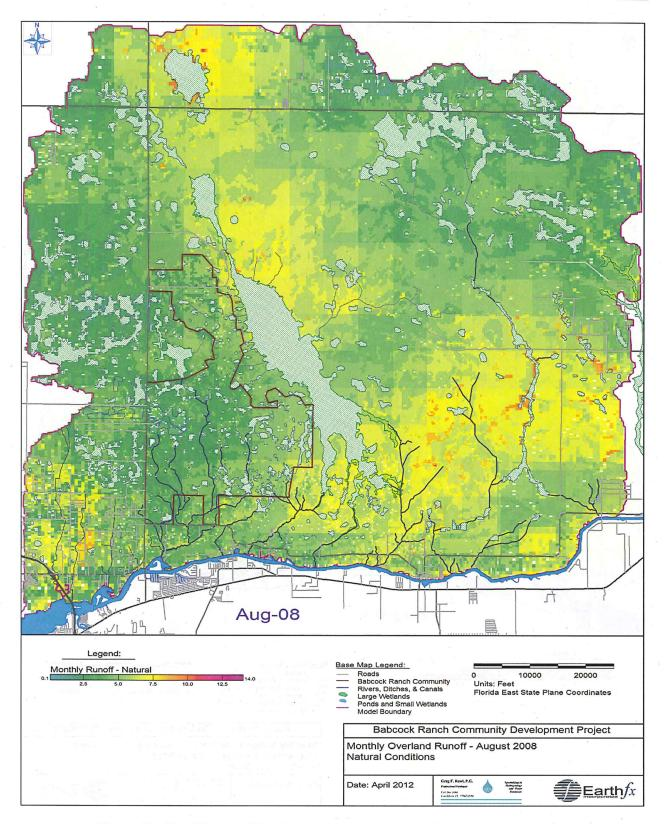


Figure 50: Monthly runoff (inches) in August 2008 under Natural Conditions.

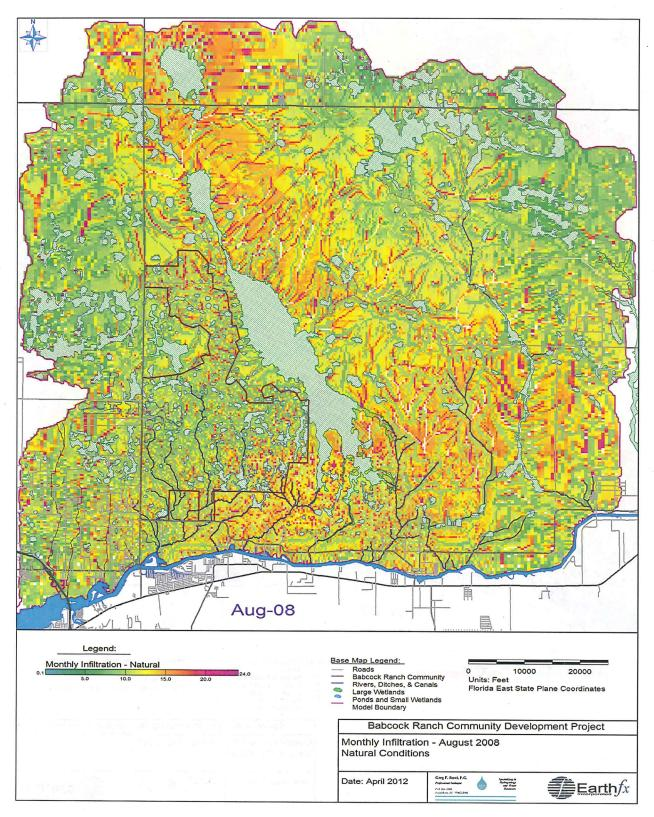


Figure 51: Monthly infiltration (inches) in August 2008 under Natural Conditions.

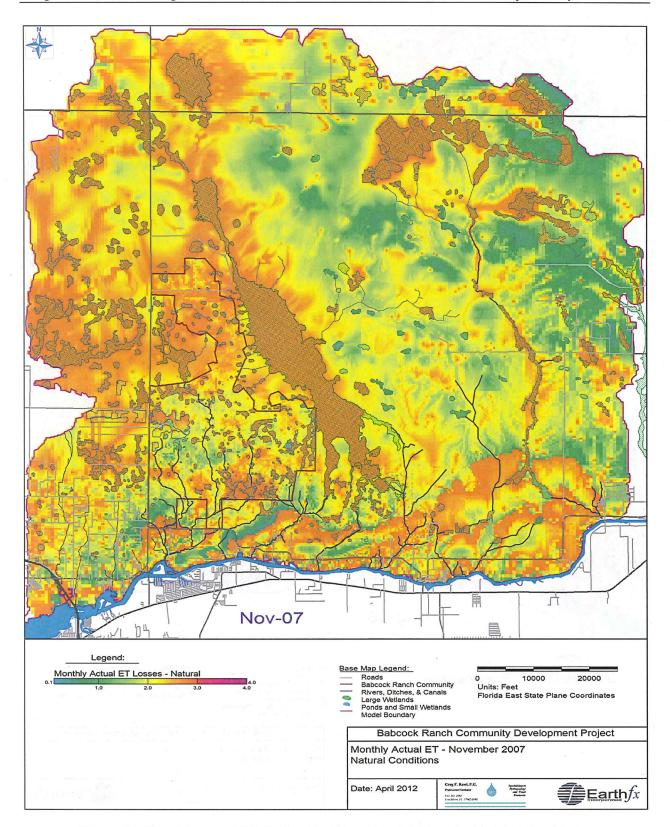


Figure 52: Monthly actual ET (inches) in November 2007 under Natural Conditions.

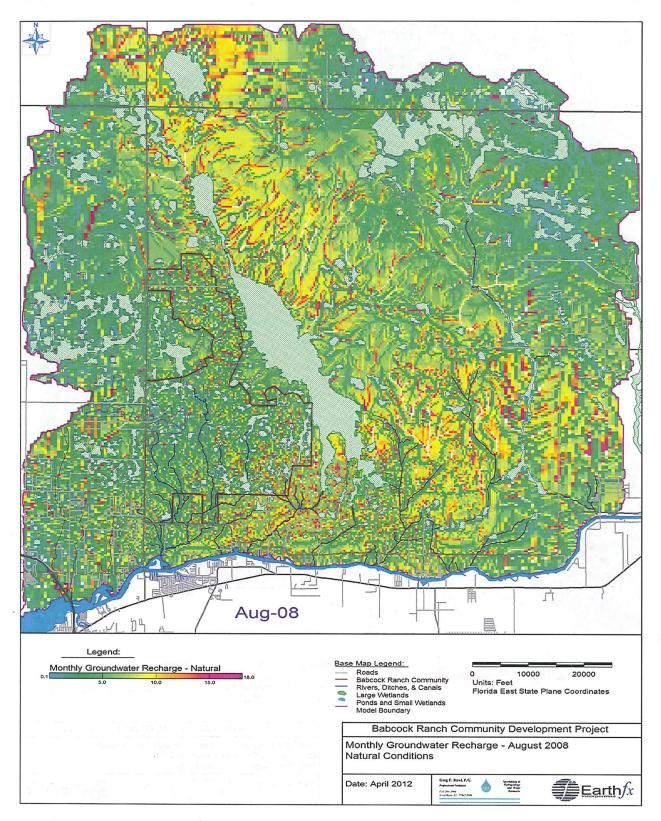


Figure 53: Monthly groundwater recharge (Infiltration - AET) in August 2008 under Natural Conditions.

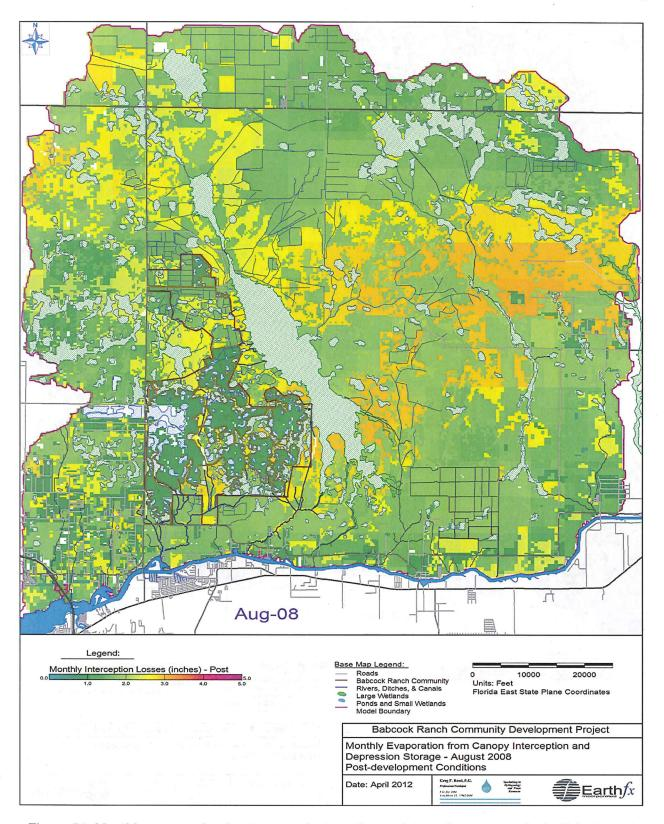


Figure 54: Monthly evaporation from canopy interception and detention storage (inches) in August 2008 under Post-development Conditions.

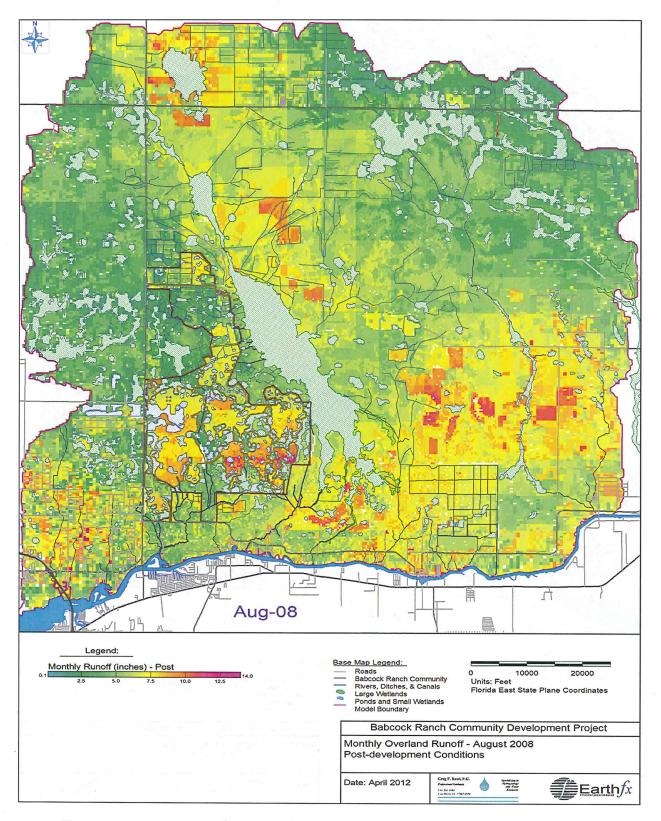


Figure 55: Monthly runoff (inches) in August 2008 under Post-development Conditions.

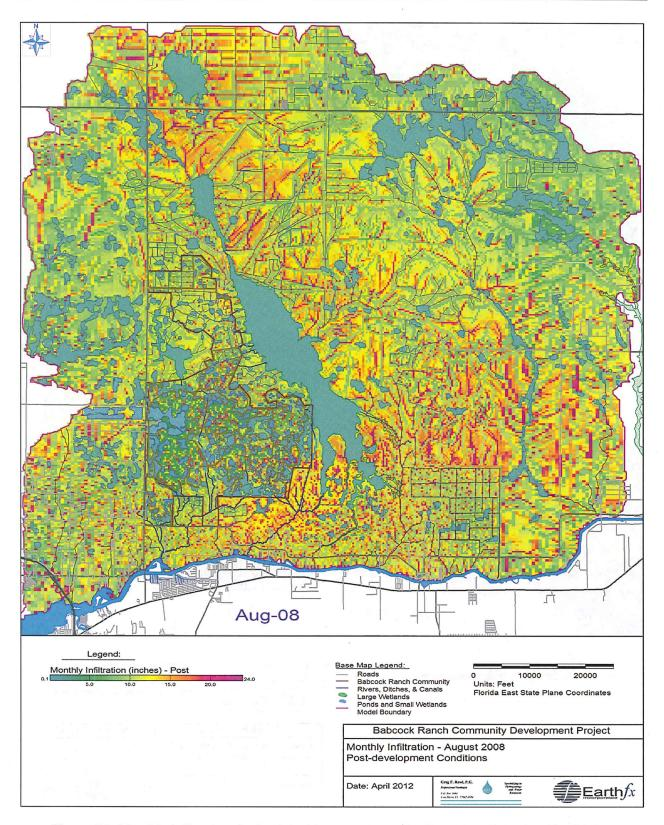


Figure 56: Monthly infiltration (inches) in August 2008 under Post-development Conditions.

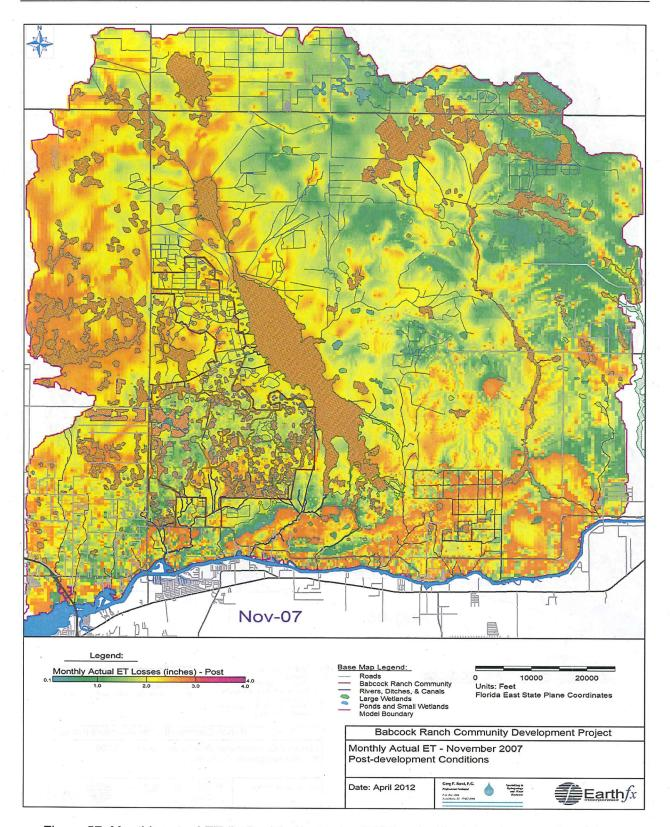


Figure 57: Monthly actual ET (inches) in November 2007 under Post-development Conditions.

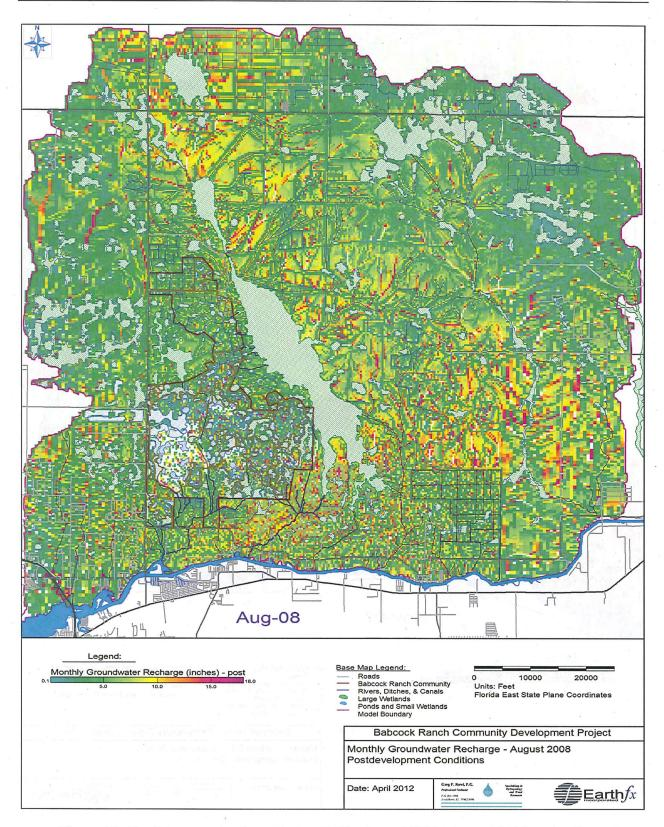


Figure 58: Monthly groundwater recharge (Infiltration - AET) in August 2008 under Postdevelopment Conditions.

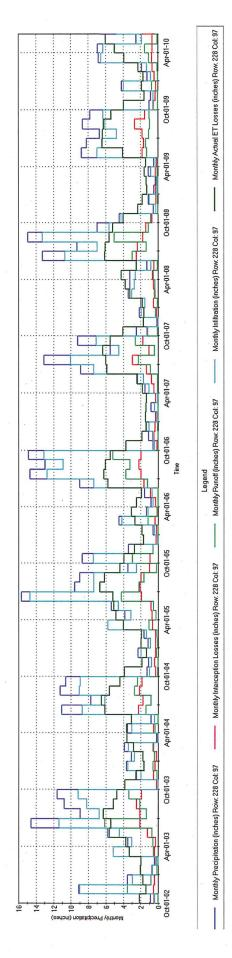


Figure 59. Monthly water budget parameters near well JEI-526 under Current Conditions.

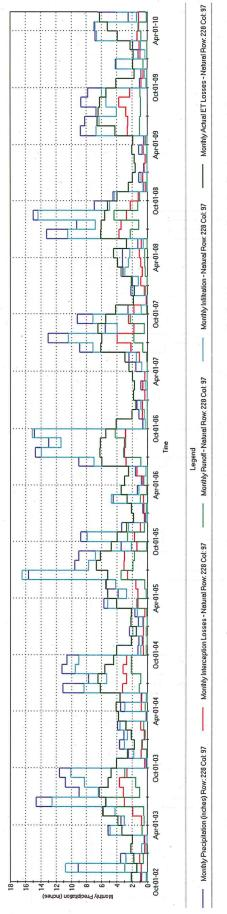


Figure 60: Monthly water budget parameters near well JEI-526 under Natural Conditions.

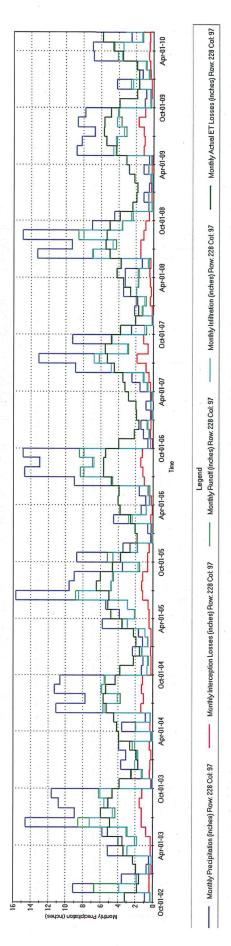


Figure 61: Monthly water budget parameters near well JEI-526 under Post-development Conditions.

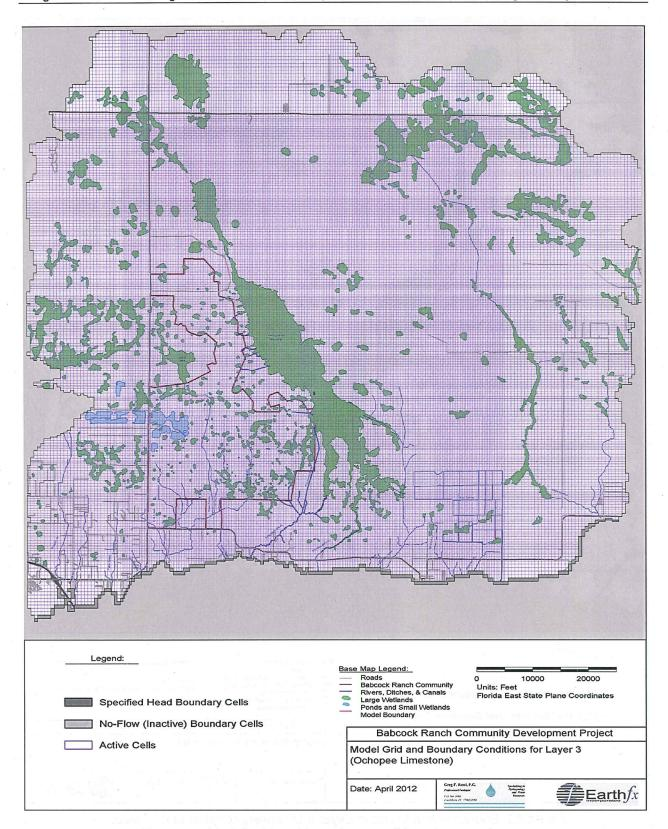


Figure 62: Model grid and boundary conditions in upper layers.

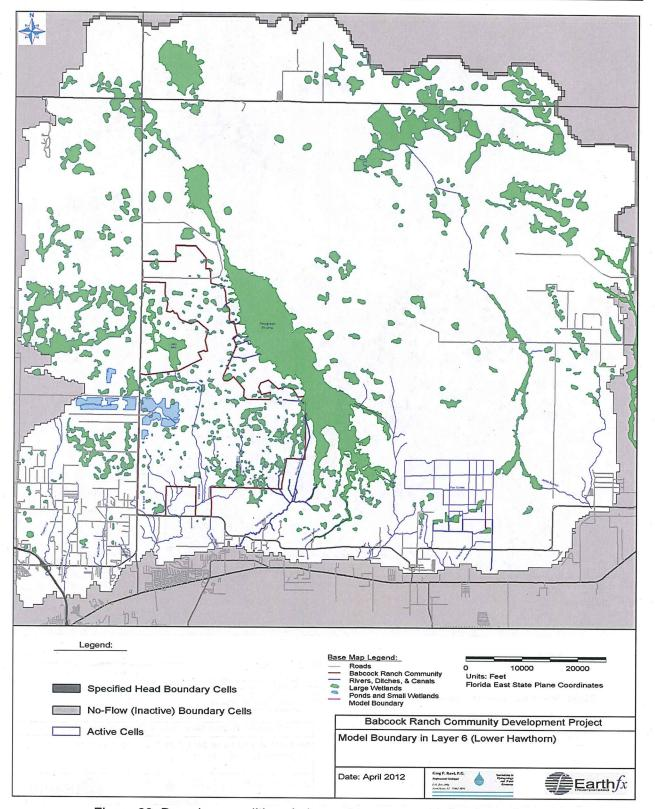


Figure 63: Boundary conditions in Layer 6 to represent inflow in northeast.

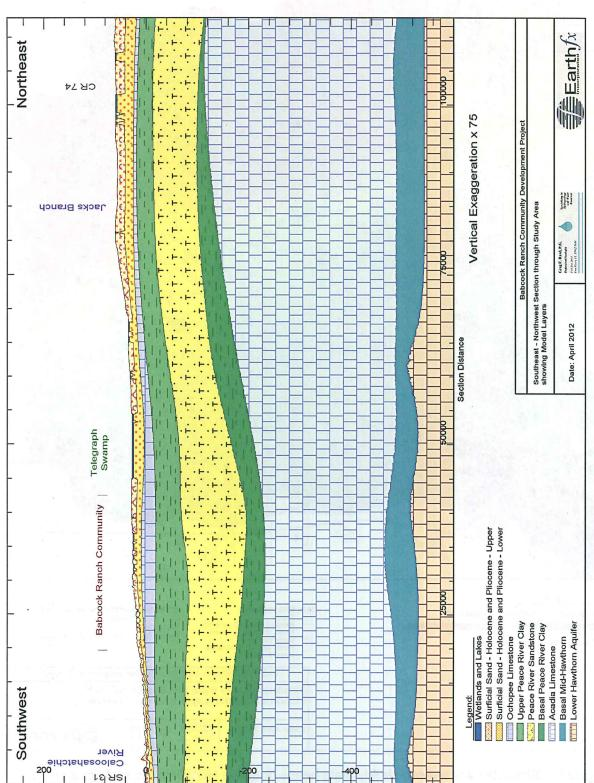


Figure 64: Southwest-Northeast section through study area showing MODFLOW models layers.

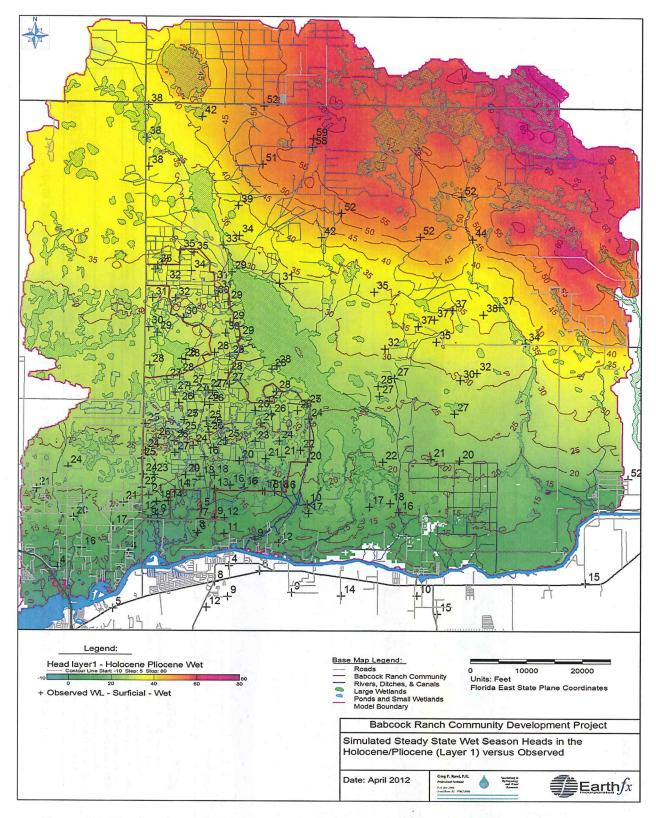


Figure 65: Simulated wet season steady-state heads (ft above NGVD) in the surficial aquifer.

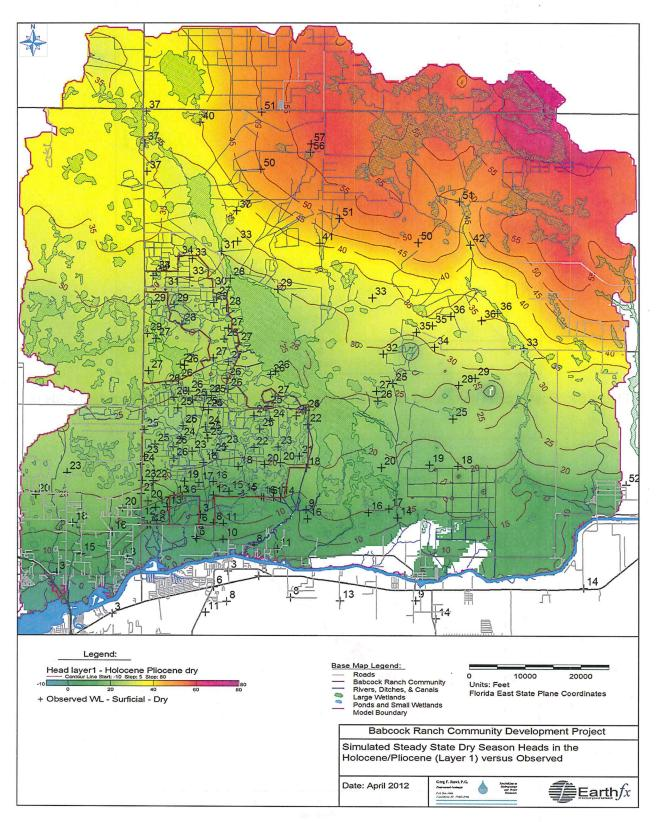


Figure 66: Simulated dry season steady-state heads (ft above NGVD) in the surficial aquifer.

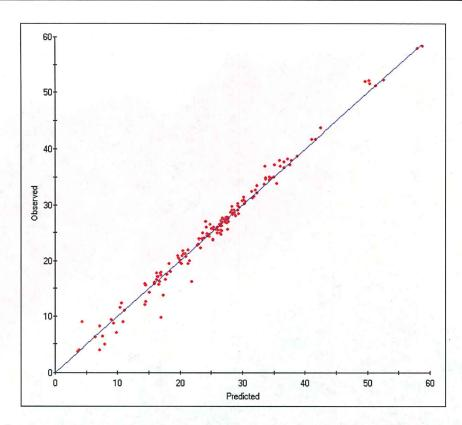


Figure 67: Scattergram comparing observed and simulated wet season surficial aquifer heads (ft above NGVD).

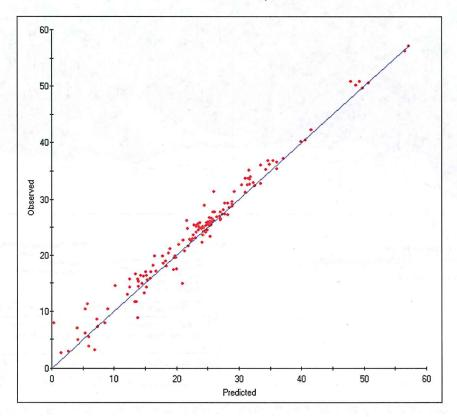


Figure 68: Scattergram comparing observed and simulated dry season surficial aquifer heads (ft above NGVD).

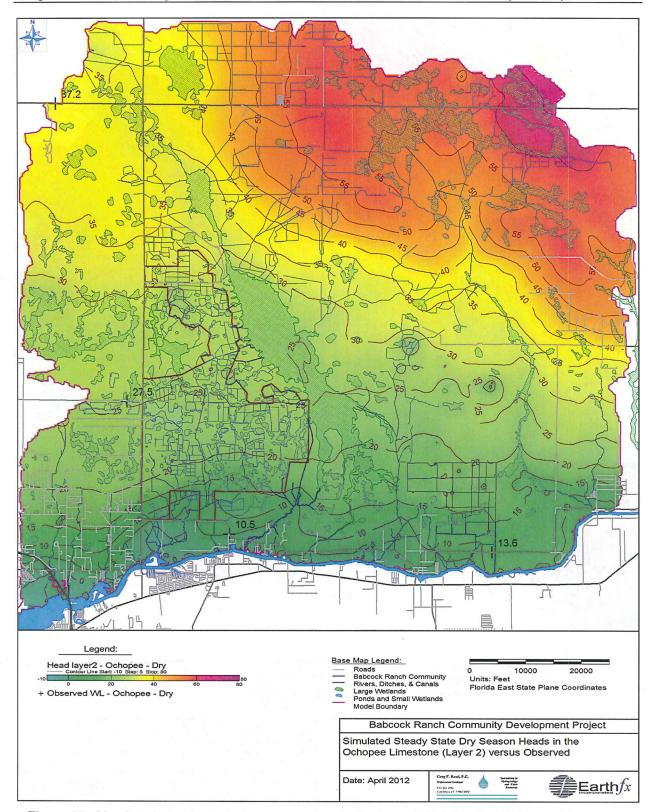


Figure 69: Simulated steady-state dry season heads (ft above NGVD) in the Ochopee Limestone.

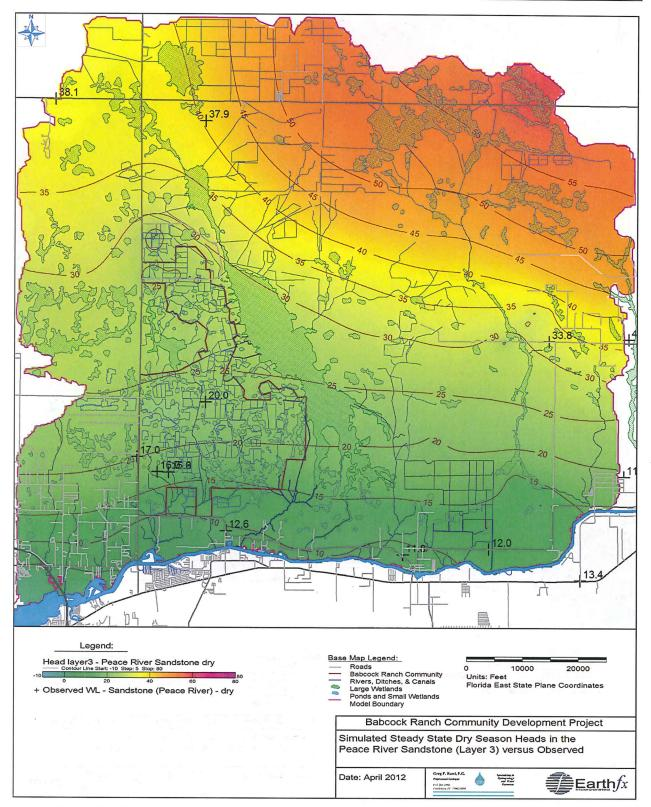


Figure 70: Simulated dry season steady-state heads (ft above NGVD) in the Peace River Sandstone.

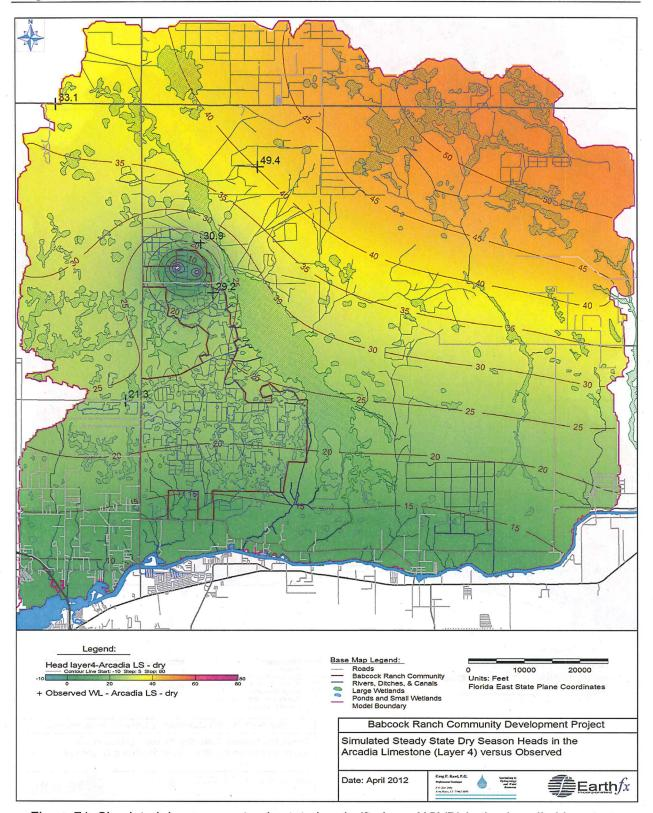


Figure 71: Simulated dry season steady-state heads (ft above NGVD) in the Arcadia Limestone.

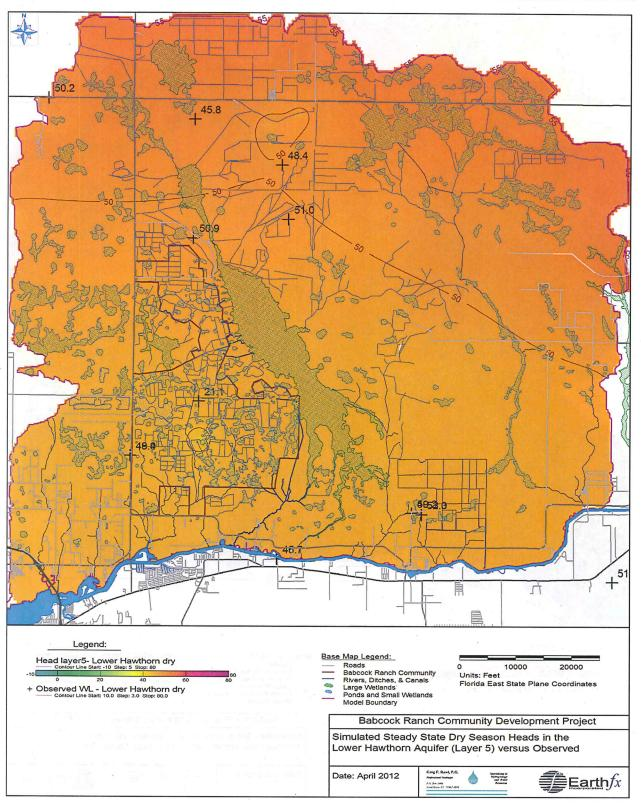


Figure 72: Simulated dry season steady-state heads (ft above NGVD) in the Lower Hawthorn aquifer.

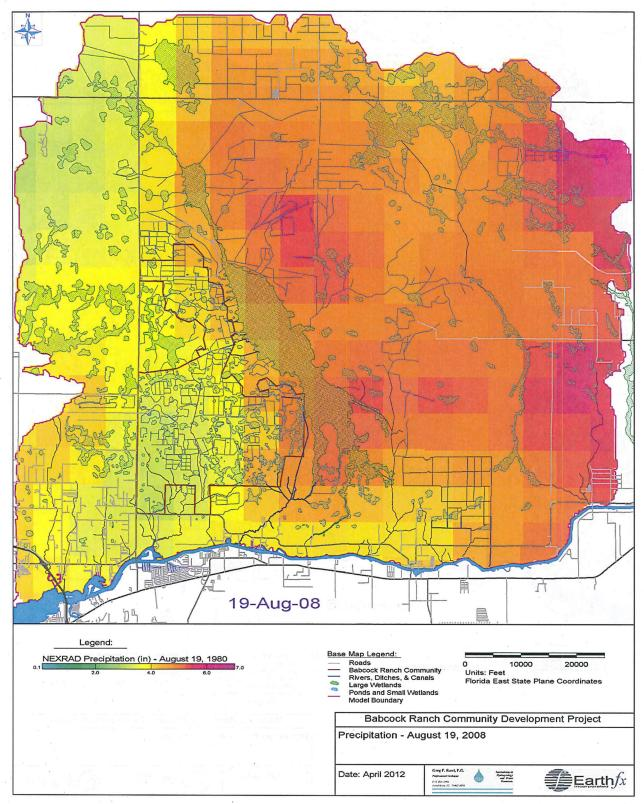


Figure 73: NEXRAD rainfall (inches) for August 19, 2008.

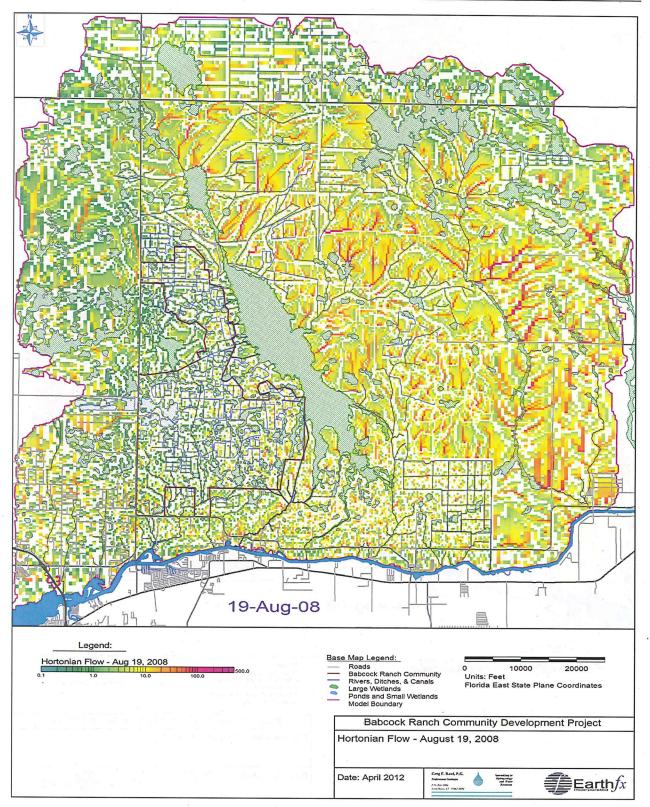


Figure 74: Simulated accumulated Hortonian flow (inches) for August 19, 2008.

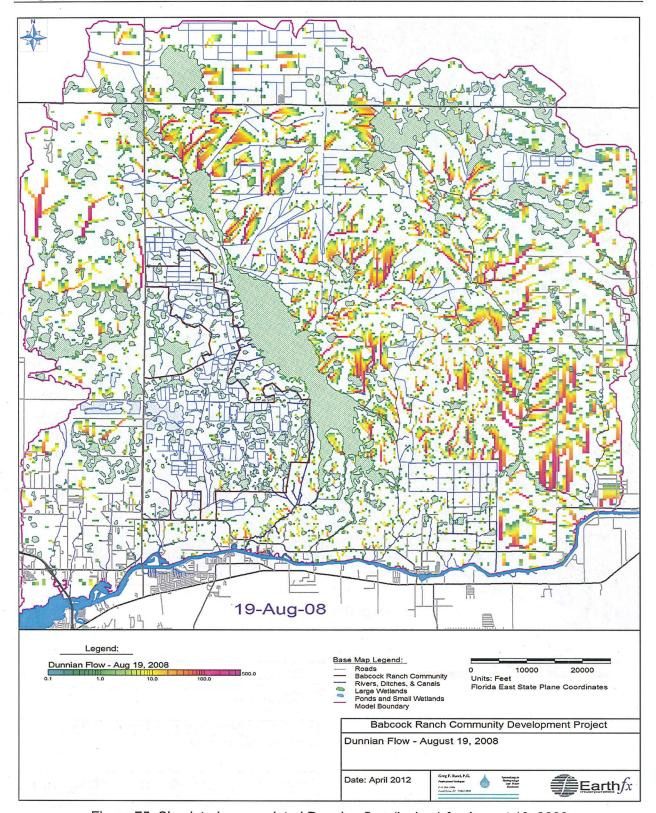


Figure 75: Simulated accumulated Dunnian flow (inches) for August 19, 2008

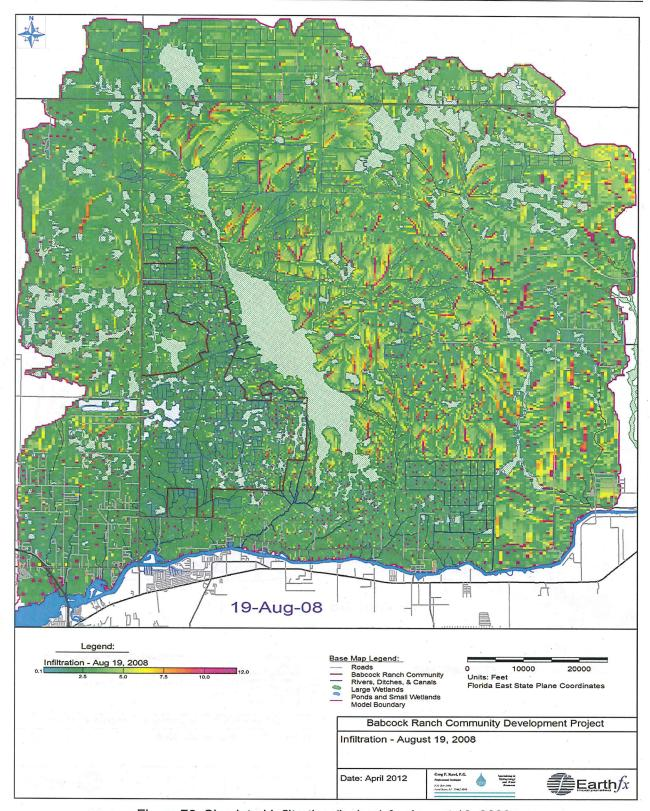


Figure 76: Simulated infiltration (inches) for August 19, 2008.

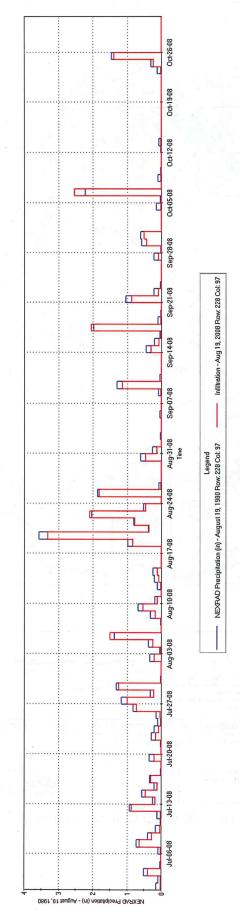


Figure 77: Precipitation and infiltration (inches) at cell 62969 (row 228, col. 97) near JEI-527, for July through October 2008.

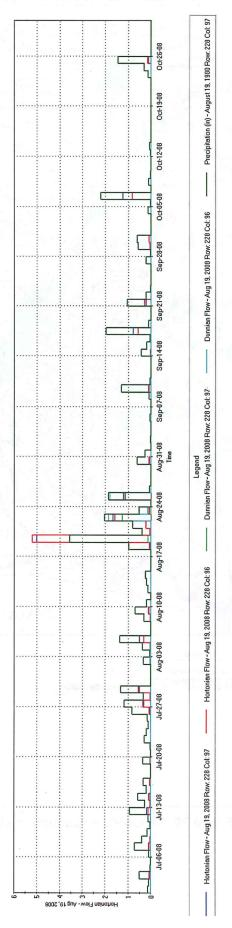


Figure 78: Upslope and downslope Hortonian and Dunnian flows (inches) at cells 62969 for July through October 2008.

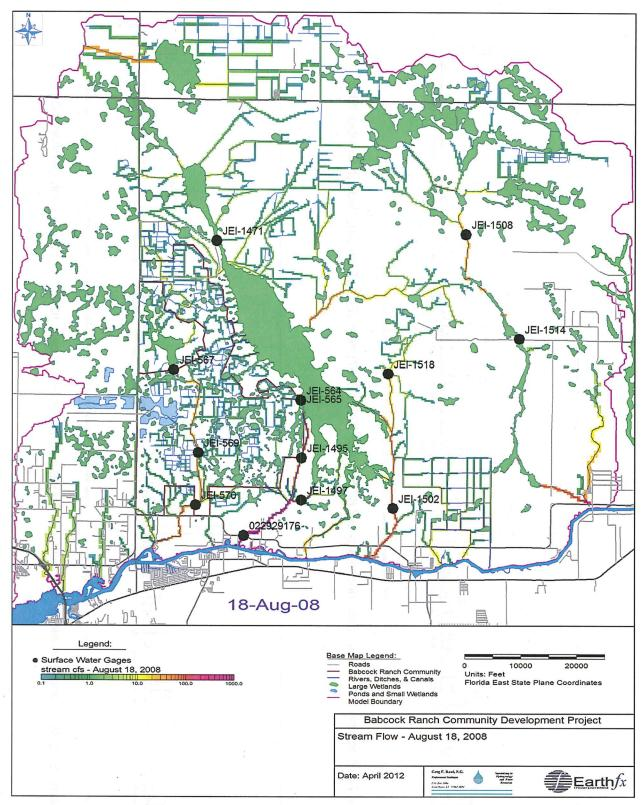


Figure 79: Simulated streamflow (cfs) for August 18, 2008 under Current Conditions.

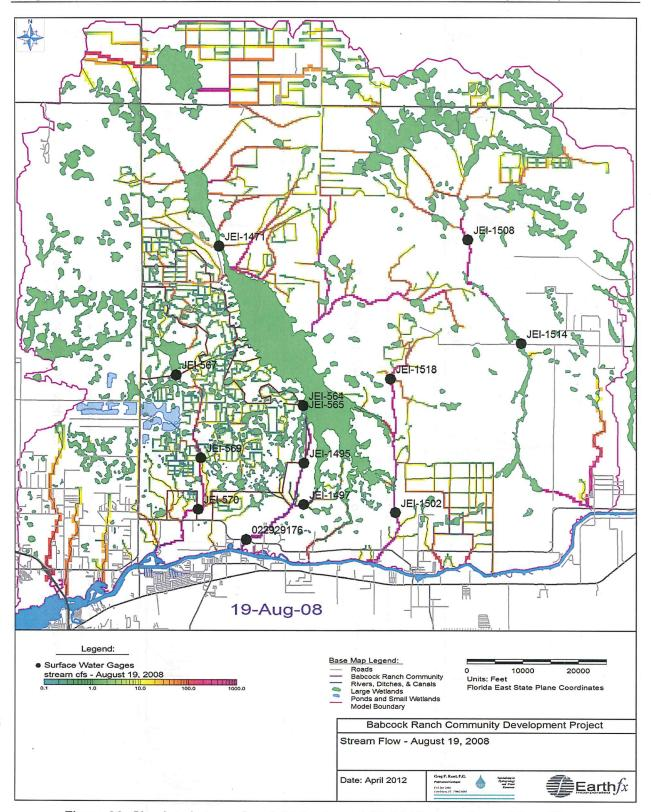


Figure 80: Simulated streamflow (cfs) for August 19, 2008 under Current Conditions.

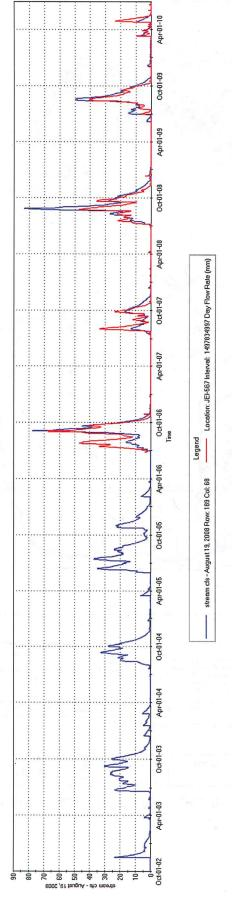


Figure 81: Simulated and observed daily flow (cfs) at gage JEI-567.

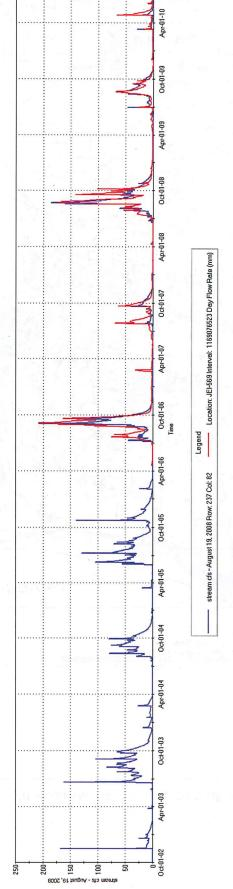


Figure 82: Simulated and observed daily flow (cfs) at gage JEI-569.

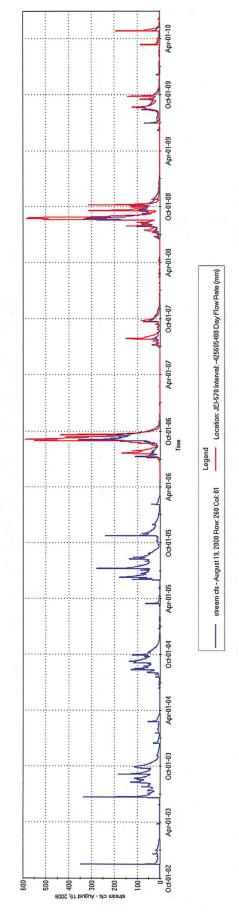


Figure 83: Simulated and observed daily flow at gage JEI-570.

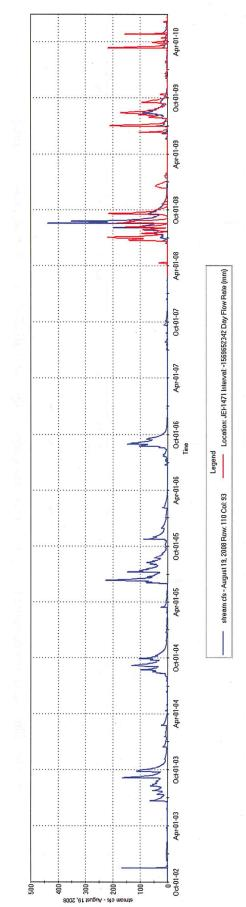


Figure 84: Simulated and observed daily flow (cfs) at gage JEI-1471.

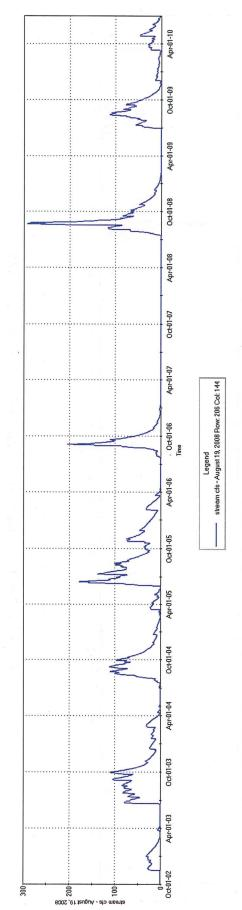


Figure 85: Simulated and observed daily flow (cfs) near gage JEI-564 and JEI-565 (no observed flows at gages).

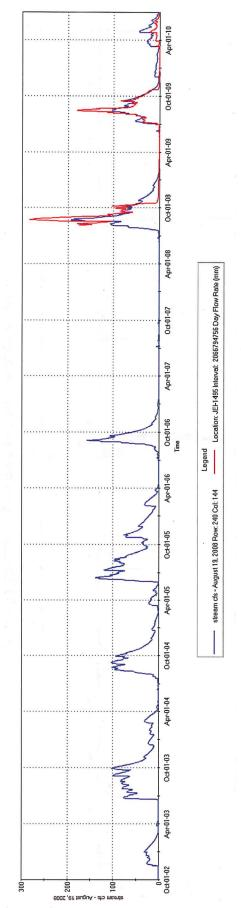


Figure 86: Simulated and observed daily flow (cfs) at gage JEI-1495.

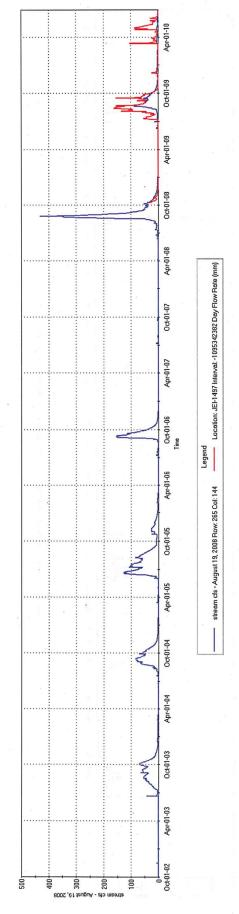


Figure 87: Simulated and observed daily flow (cfs) at gage JEI-1497.

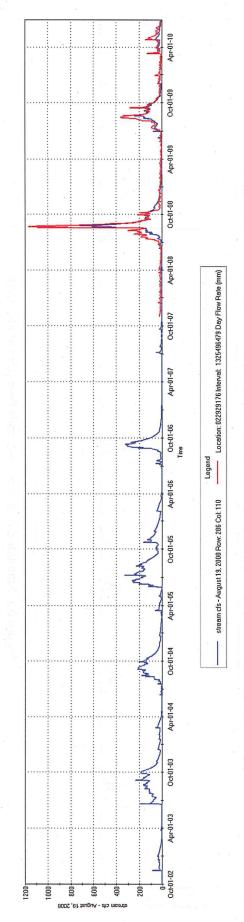


Figure 88: Simulated and observed daily flow (cfs) at the USGS Telegraph Creek gage (0229291).

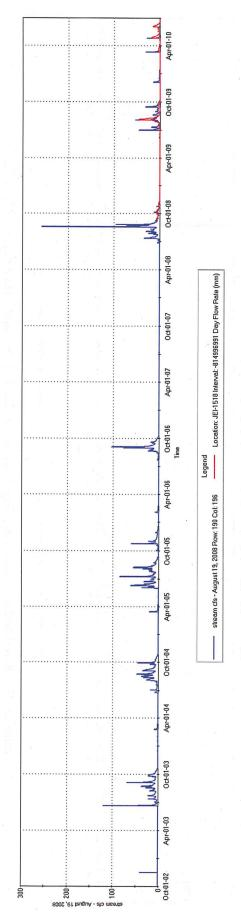
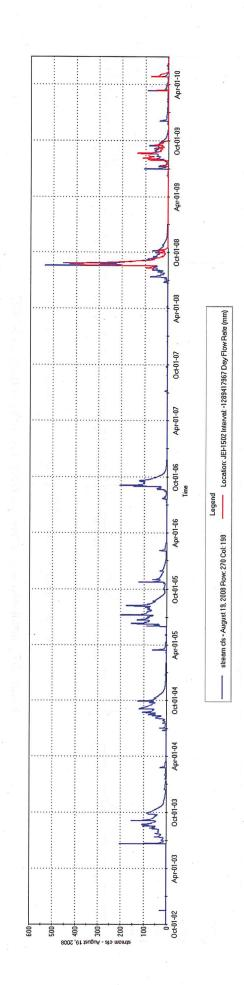


Figure 89: Simulated and observed daily flow (cfs) at JEI-1518.



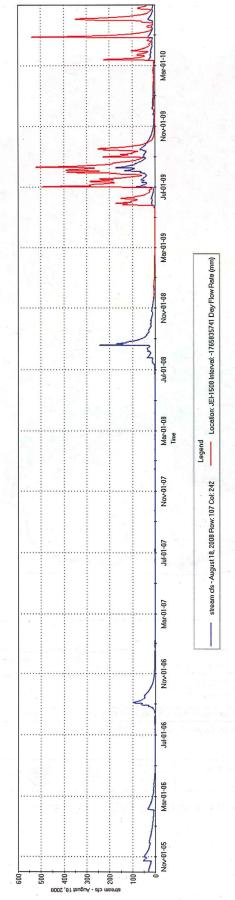


Figure 90: Simulated and observed daily flow (cfs) at gage JEI-1508:

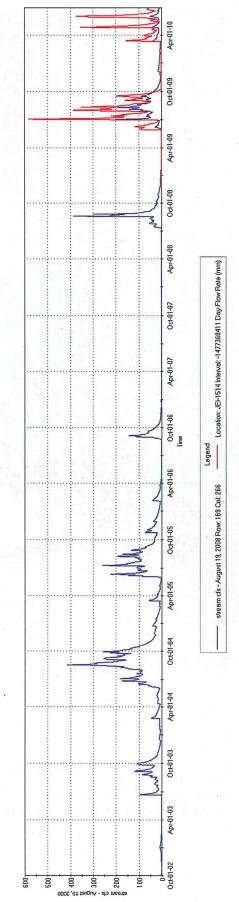


Figure 91: Simulated and observed daily flow (cfs) at gage JEI-1514.

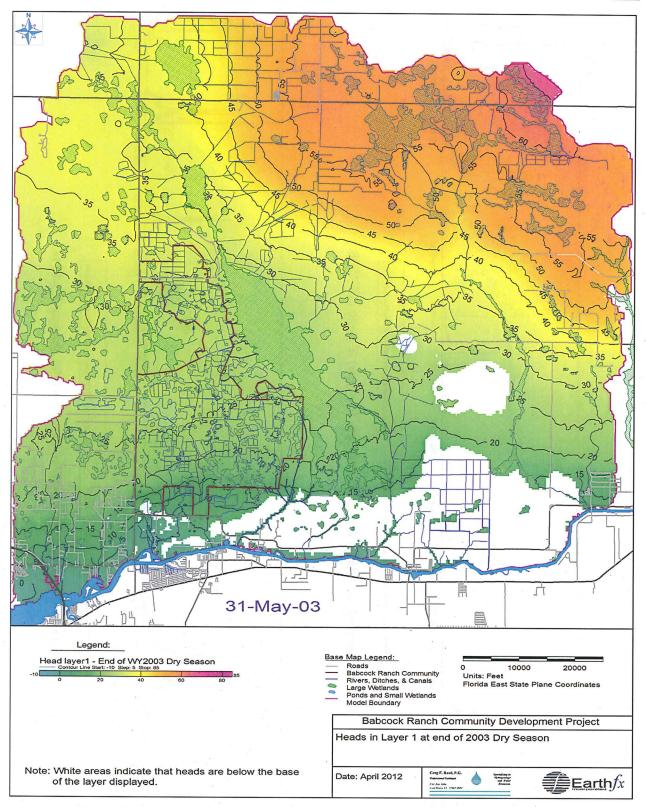


Figure 92: Simulated heads (ft above NGVD) at the end of the 2003 dry season.

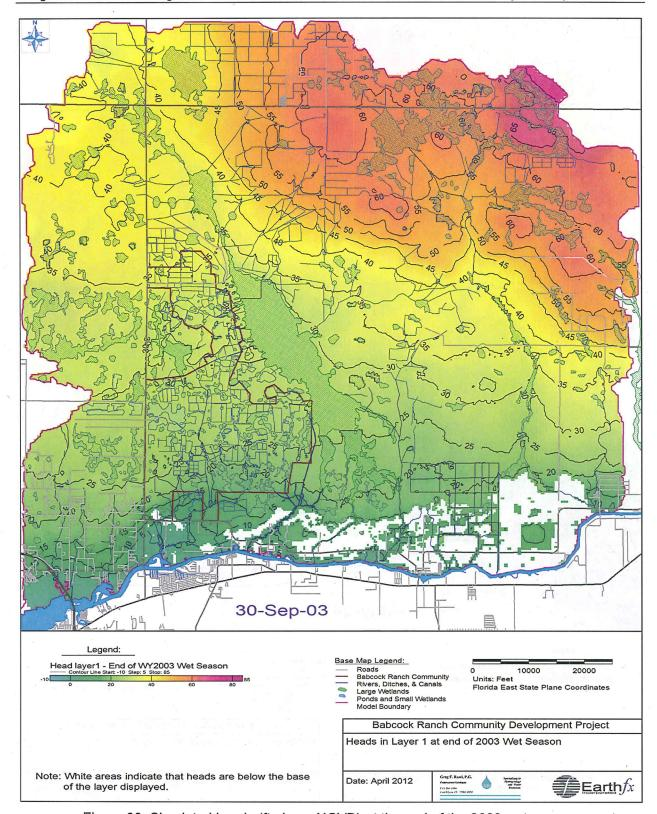


Figure 93: Simulated heads (ft above NGVD) at the end of the 2003 wet season.

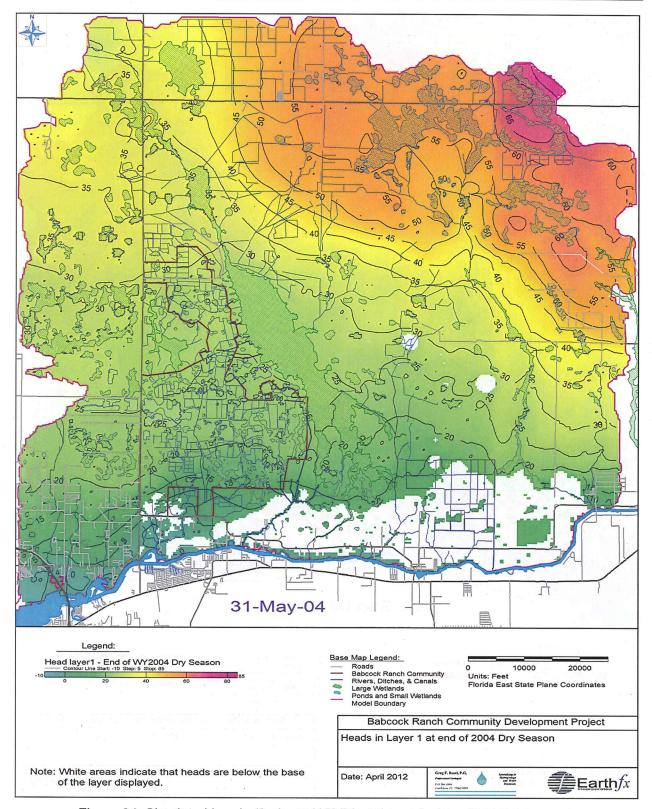


Figure 94: Simulated heads (ft above NGVD) at the end of the 2004 dry season.

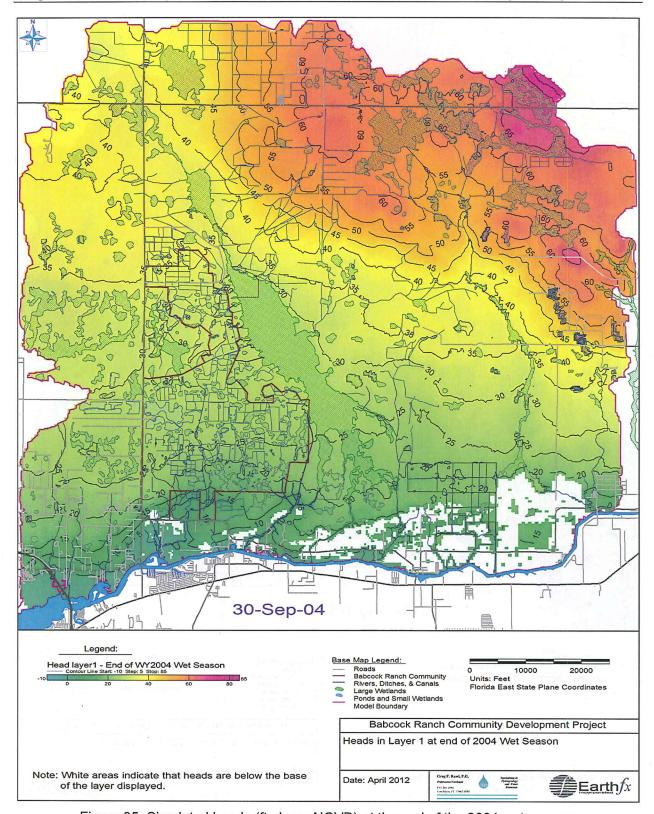


Figure 95: Simulated heads (ft above NGVD) at the end of the 2004 wet season.

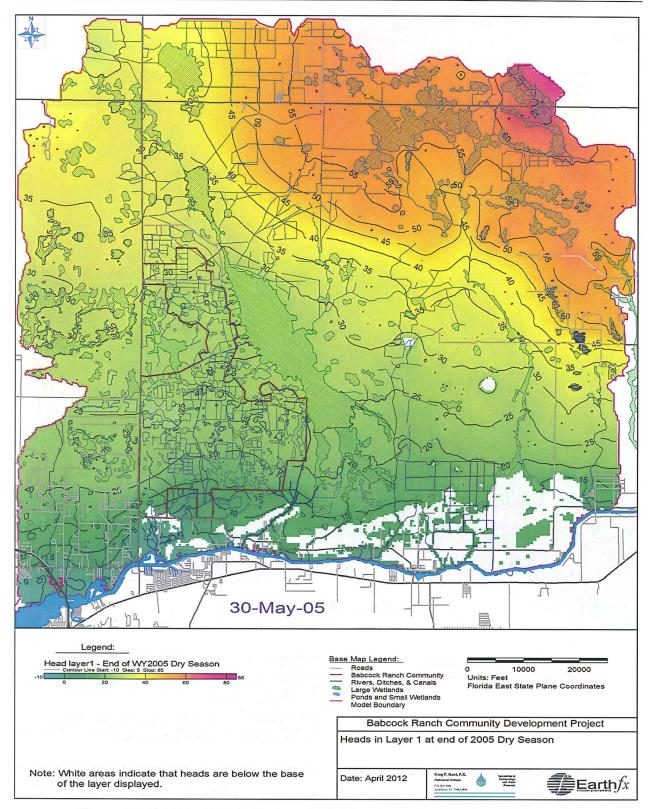


Figure 96: Simulated heads (ft above NGVD) at the end of the 2005 dry season.

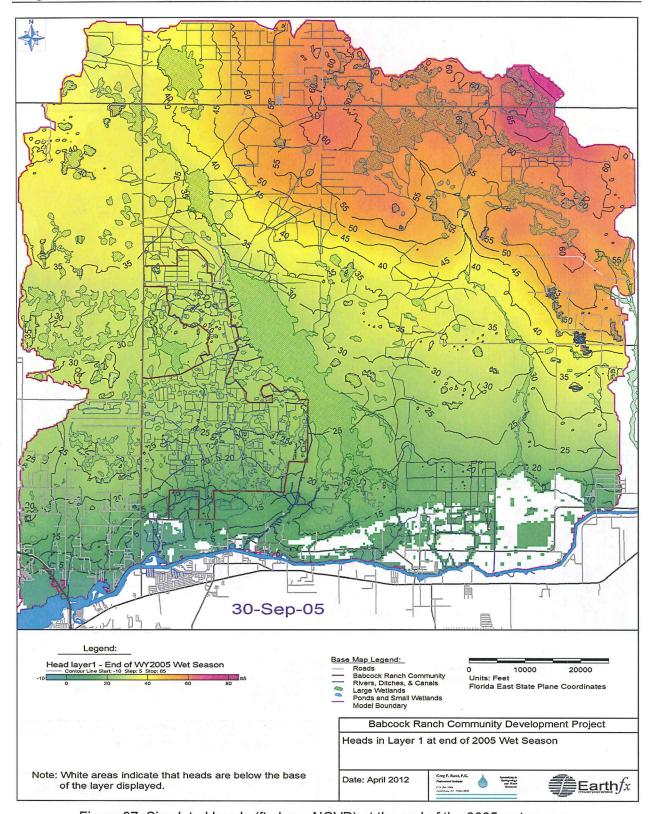


Figure 97: Simulated heads (ft above NGVD) at the end of the 2005 wet season.

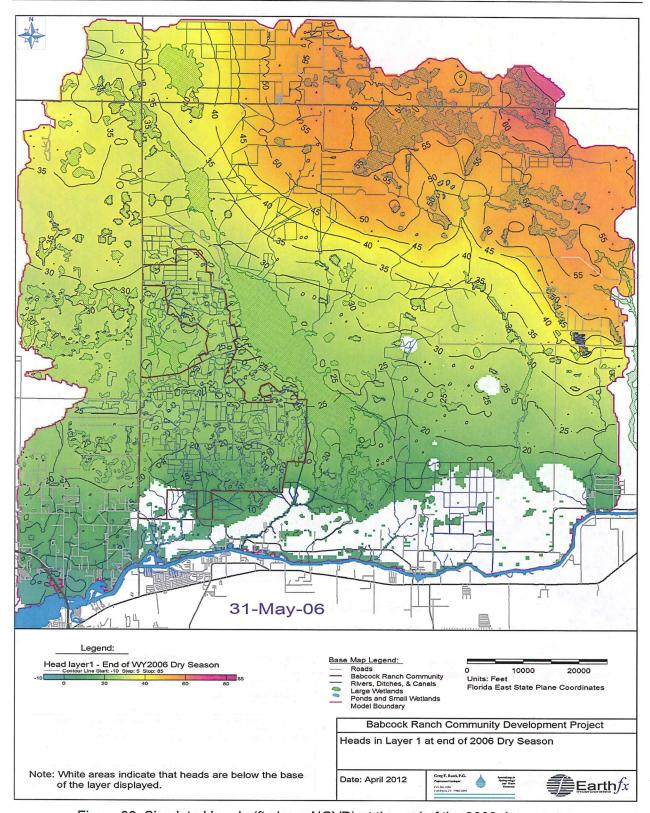


Figure 98: Simulated heads (ft above NGVD) at the end of the 2006 dry season.

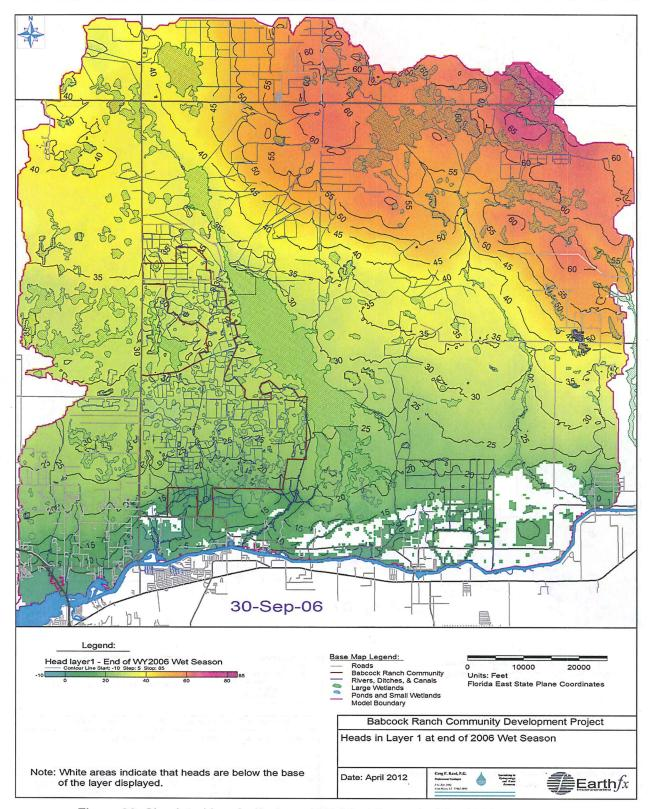


Figure 99: Simulated heads (ft above NGVD) at the end of the 2006 wet season.

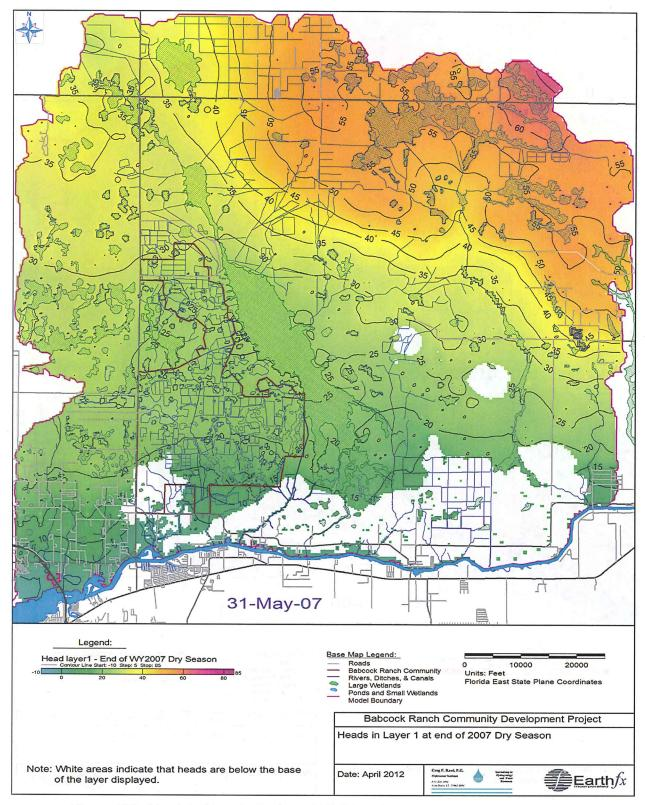


Figure 100: Simulated heads (ft above NGVD) at the end of the 2007 dry season.

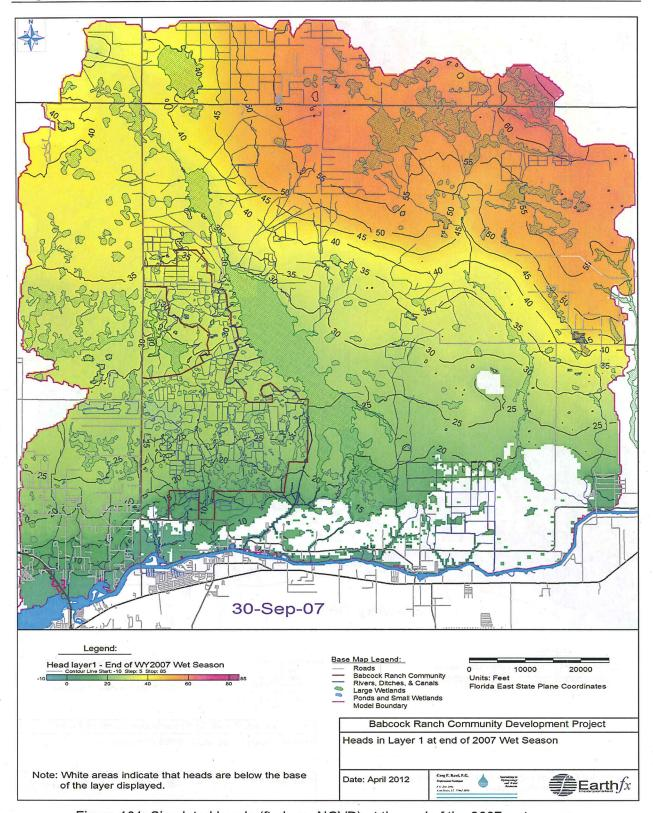


Figure 101: Simulated heads (ft above NGVD) at the end of the 2007 wet season.

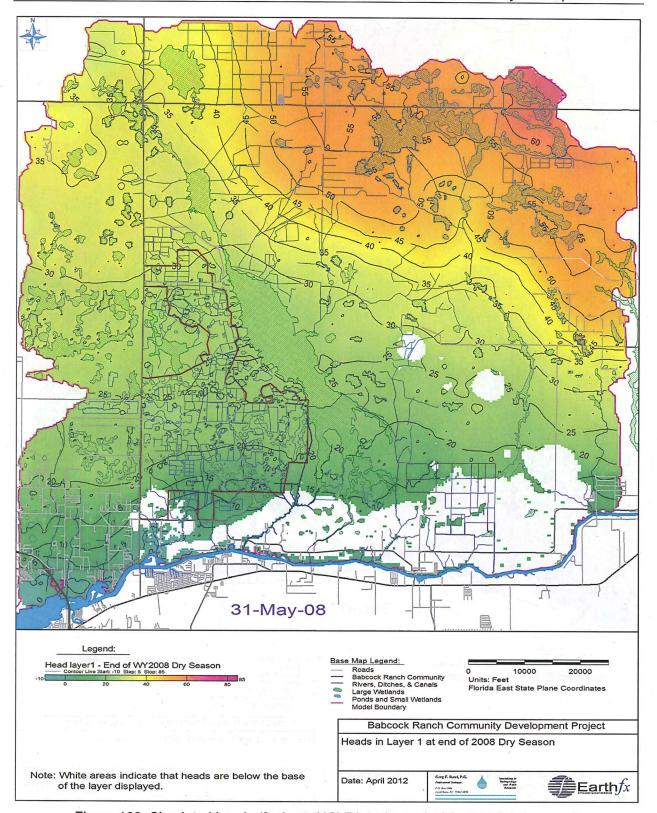


Figure 102: Simulated heads (ft above NGVD) at the end of the 2008 dry season.

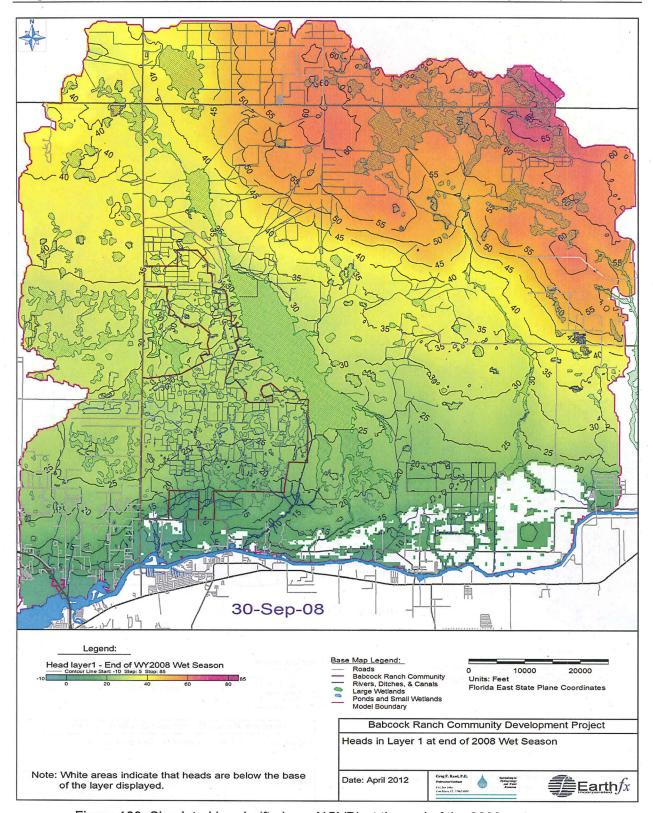


Figure 103: Simulated heads (ft above NGVD) at the end of the 2008 wet season.

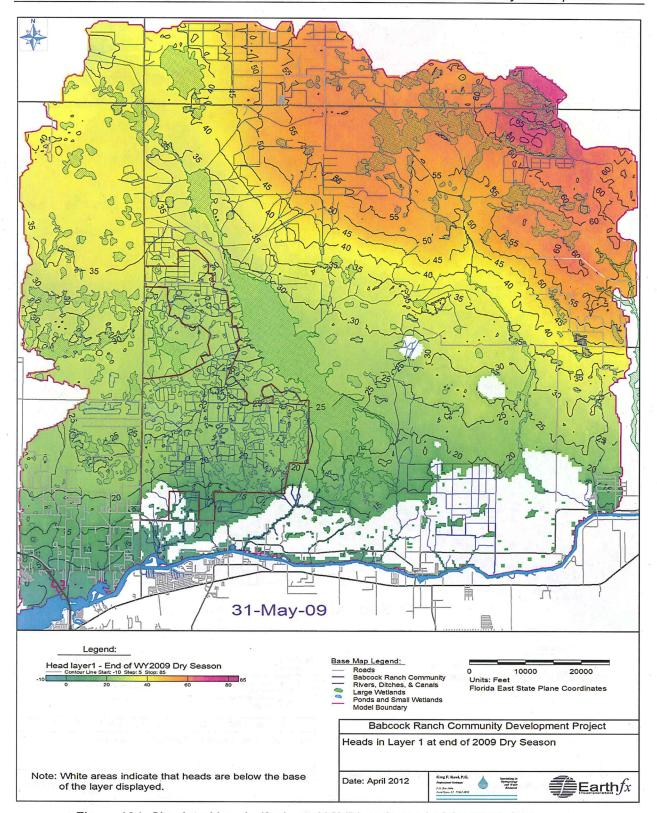


Figure 104: Simulated heads (ft above NGVD) at the end of the 2009 dry season.

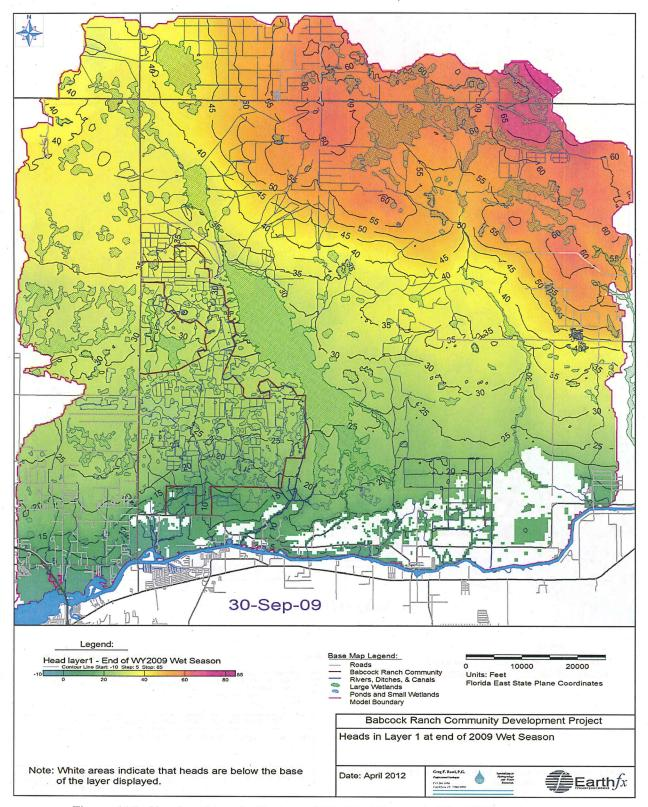


Figure 105: Simulated heads (ft above NGVD) at the end of the 2009 wet season.

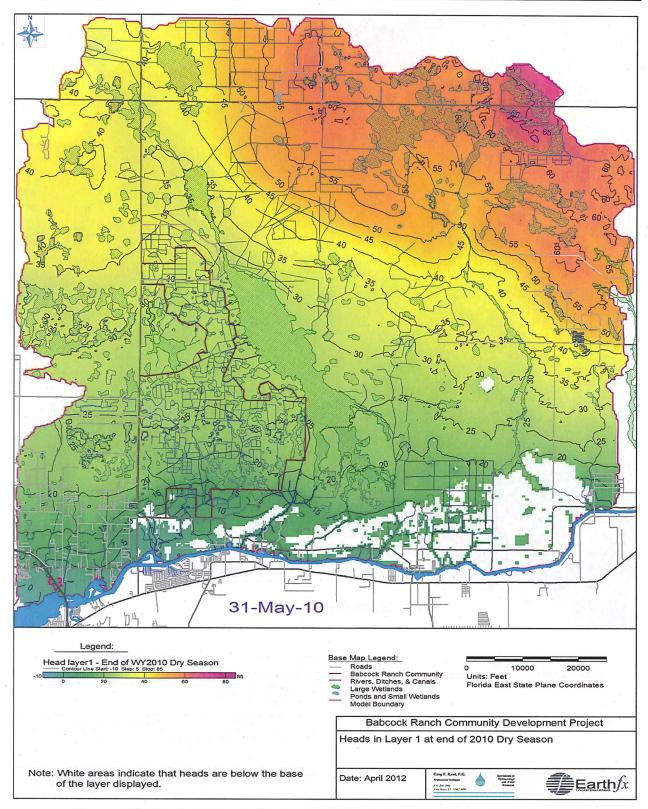


Figure 106: Simulated heads (ft above NGVD) at the end of the 2010 dry season.

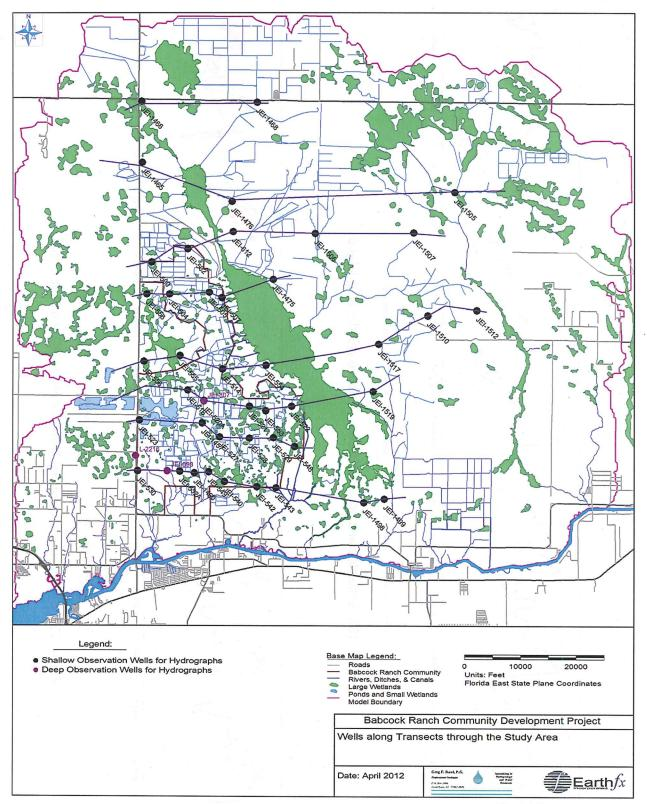


Figure 107: Wells along transects through the study area.

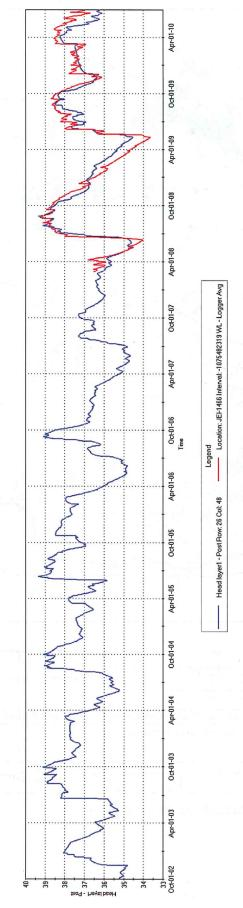


Figure 108: Simulated and observed heads (ft above NGVD) at JEI-1466.

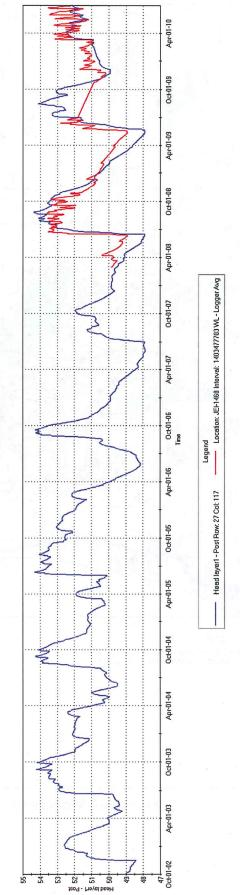


Figure 109: Simulated and observed heads (ft above NGVD) at JEI-1468.

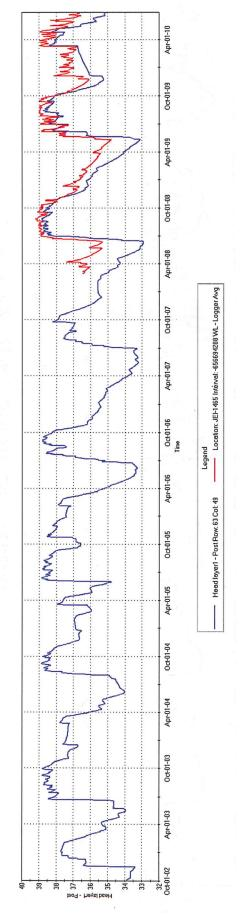


Figure 110: Simulated and observed heads (ft above NGVD) at JEI-1465.

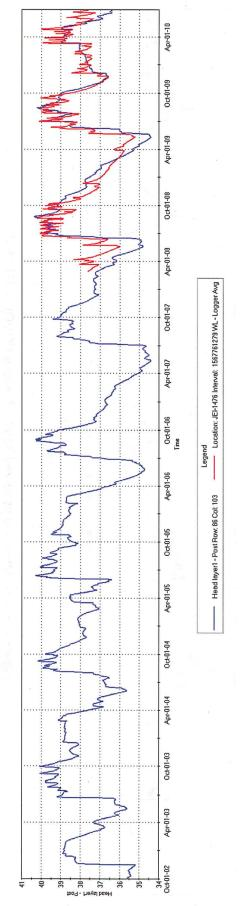


Figure 111: Simulated and observed heads (ft above NGVD) at JEI-1476.

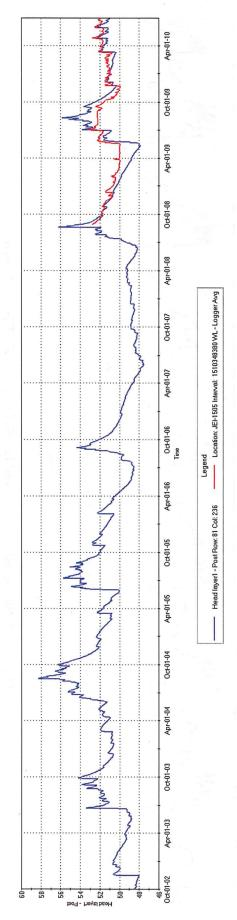


Figure 112: Simulated and observed heads (ft above NGVD) at JEI-1505.

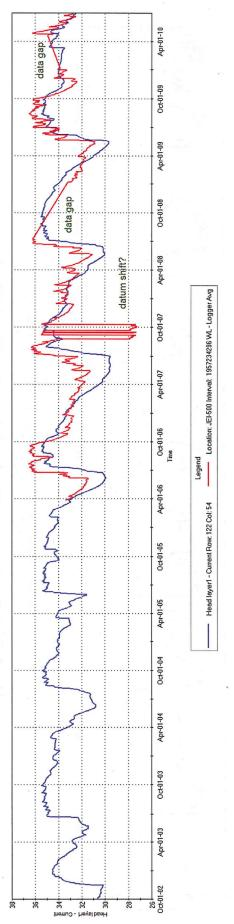


Figure 113: Simulated and observed heads (ft above NGVD) at JEI-500.

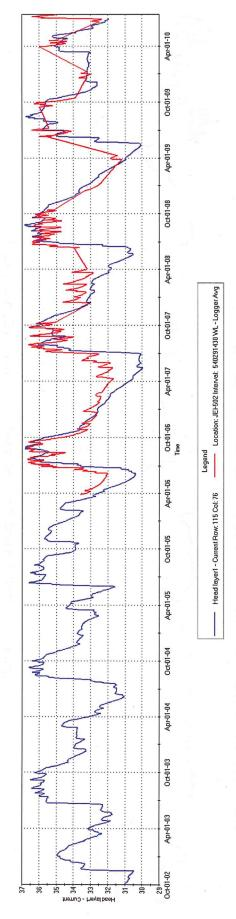


Figure 114: Simulated and observed heads (ft above NGVD) at JEI-502.

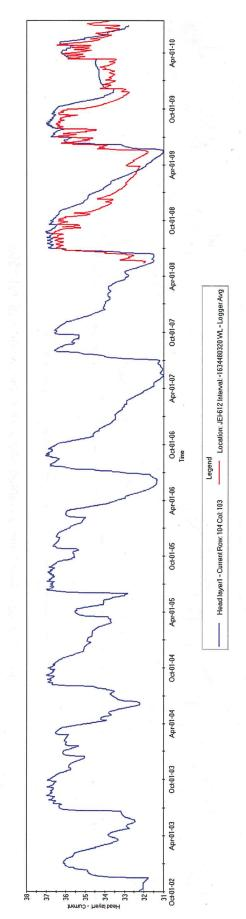


Figure 115: Simulated and observed heads (ft above NGVD) at JEI-612.

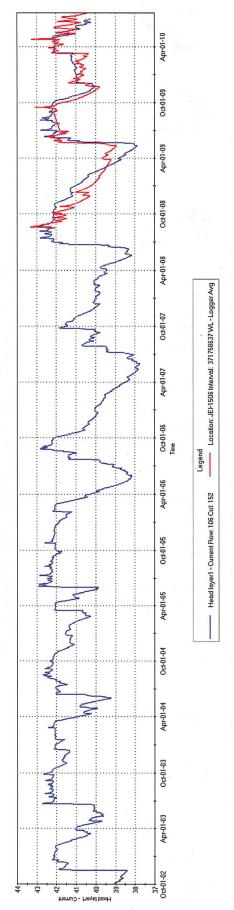


Figure 116: Simulated and observed heads (ft above NGVD) at JEI-1506.

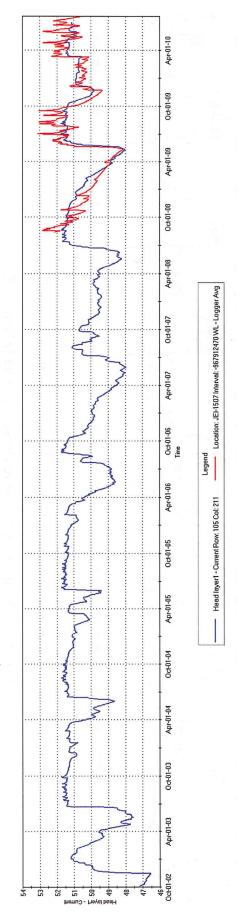


Figure 117: Simulated and observed heads (ft above NGVD) at JEI-1507.

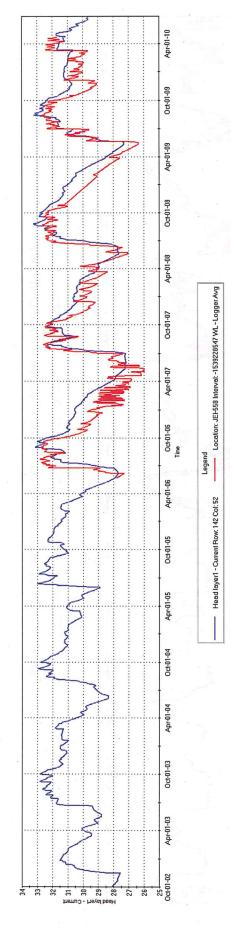


Figure 118: Simulated and observed heads (ft above NGVD) at JEI-558.

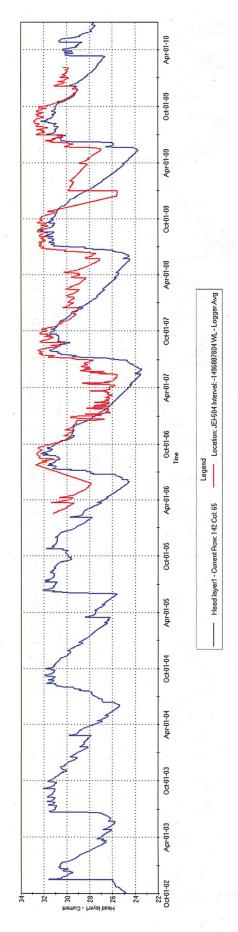


Figure 119: Simulated and observed heads (ft above NGVD) at JEI-504.

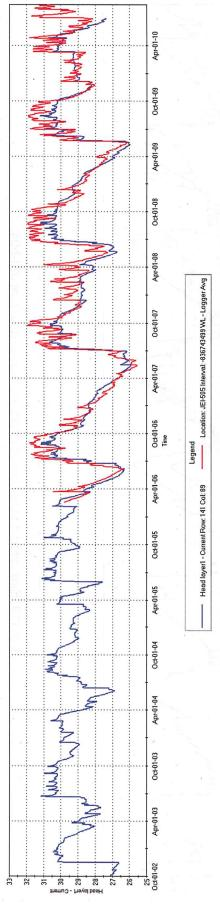


Figure 120: Simulated and observed heads (ft above NGVD) at JEI-505.

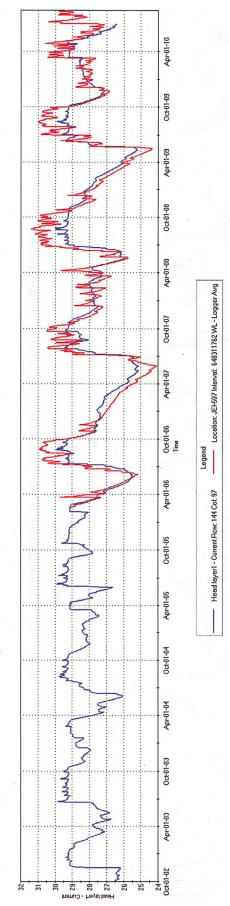


Figure 121: Simulated and observed heads (ft above NGVD) at JEI-507.

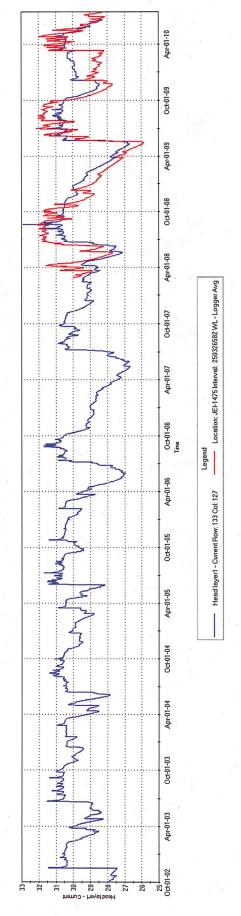


Figure 122: Simulated and observed heads (ft above NGVD) at JEI-1475.

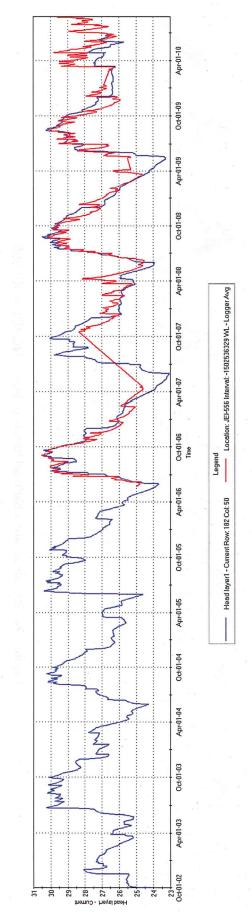


Figure 123: Simulated and observed heads (ft above NGVD) at JEI-556.

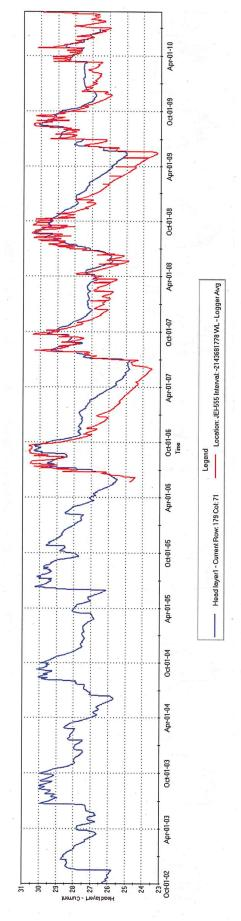


Figure 124: Simulated and observed heads (ft above NGVD) at JEI-555.

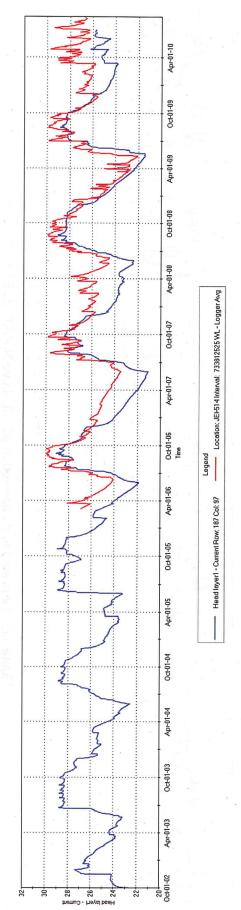


Figure 125: Simulated and observed heads (ft above NGVD) at JEI-514.

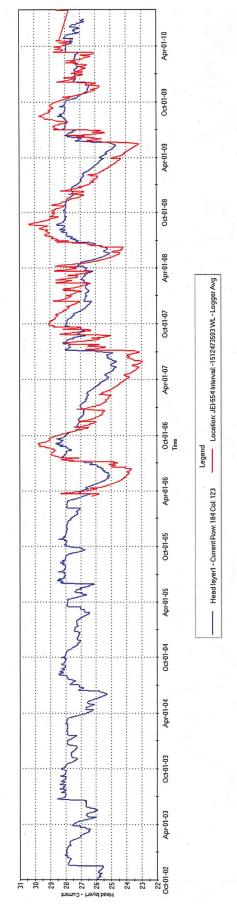


Figure 126: Simulated and observed heads (ft above NGVD) at JEI-554.

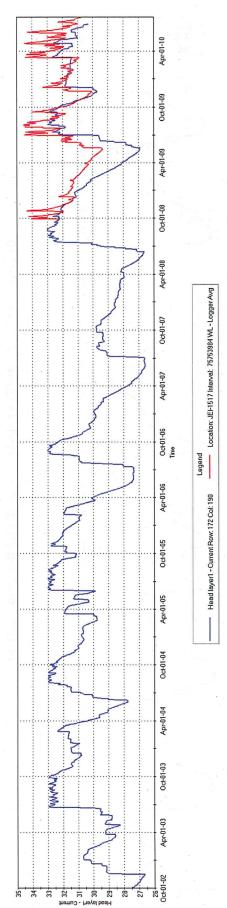


Figure 127: Simulated and observed heads (ft above NGVD) at JEI-1517.

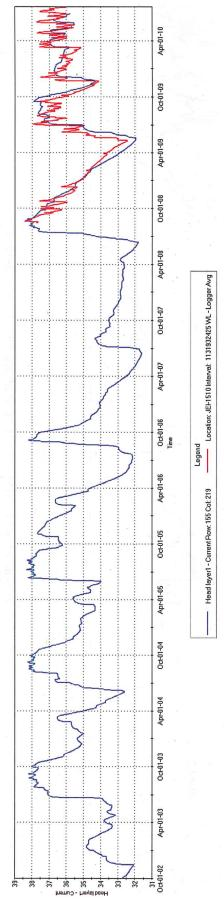


Figure 128: Simulated and observed heads (ft above NGVD) at JEI-1510

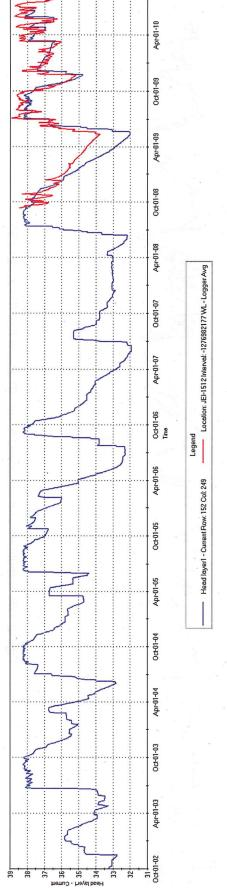


Figure 129: Simulated and observed heads (ft above NGVD) at JEI-1512.

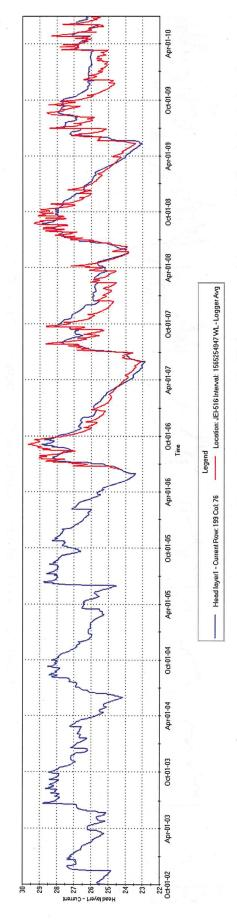


Figure 130: Simulated and observed heads (ft above NGVD) at JEI-516.

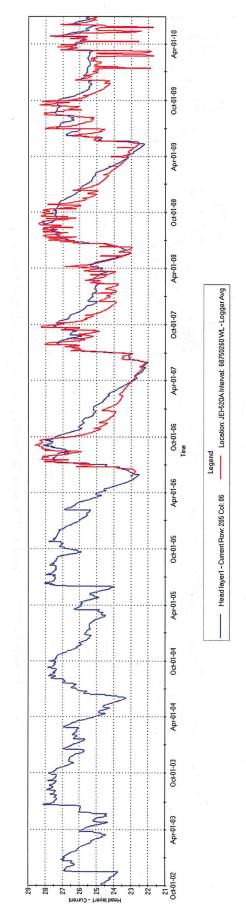


Figure 131: Simulated and observed heads (ft above NGVD) at JEI-520A.

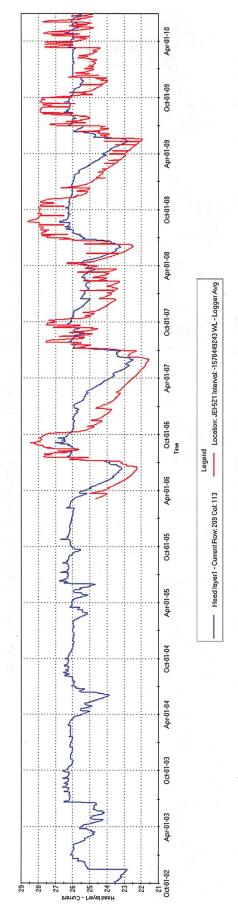


Figure 132: Simulated and observed heads (ft above NGVD) at JEI-521.

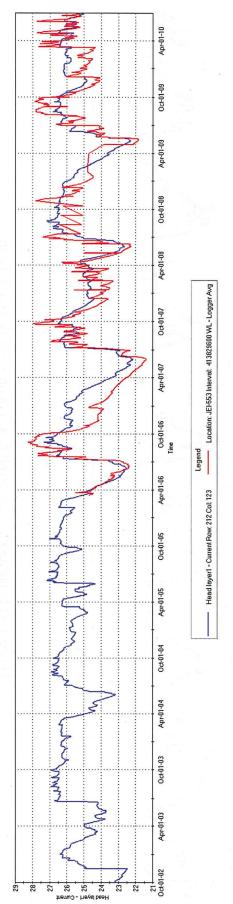


Figure 133: Simulated and observed heads (ft above NGVD) at JEI-553.

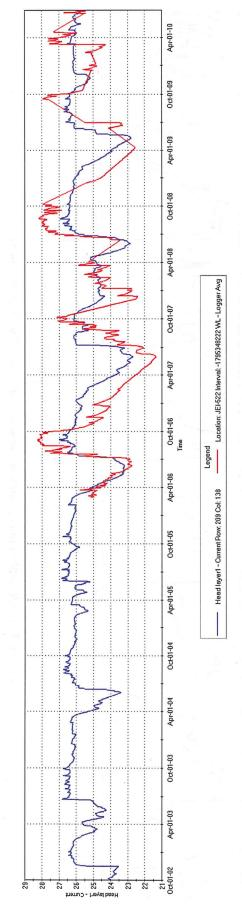


Figure 134: Simulated and observed heads (ft above NGVD) at JEI-522.

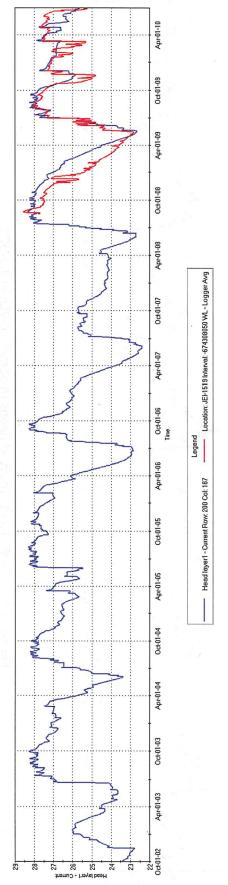


Figure 135: Simulated and observed heads (ft above NGVD) at JEI-1519.

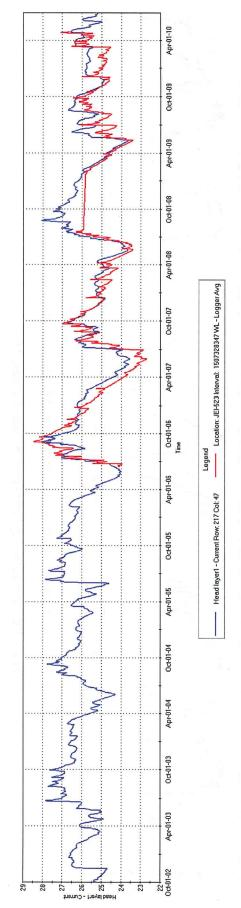


Figure 136: Simulated and observed heads (ft above NGVD) at JEI-523.

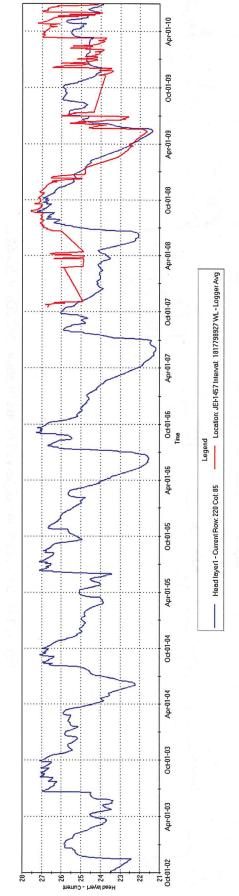


Figure 137: Simulated and observed heads (ft above NGVD) at JEI-1457.

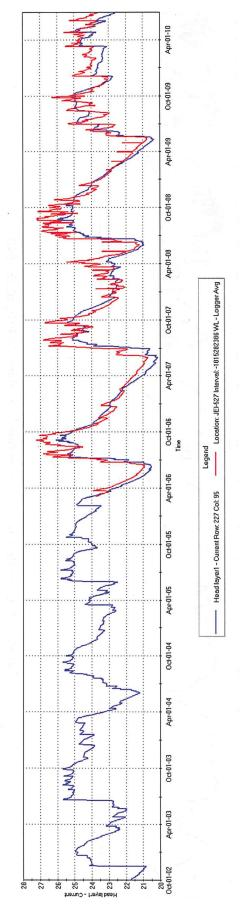


Figure 138: Simulated and observed heads (ft above NGVD) at JEI-527.

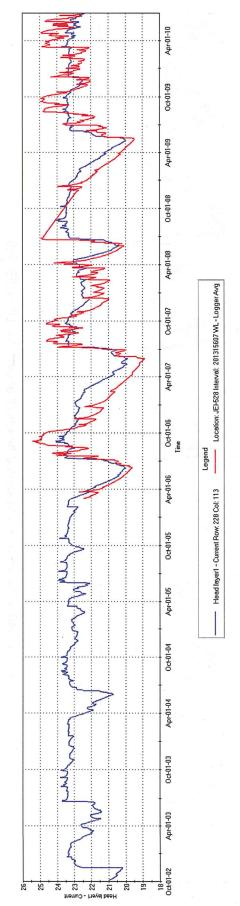


Figure 139: Simulated and observed heads (ft above NGVD) at JEI-528.

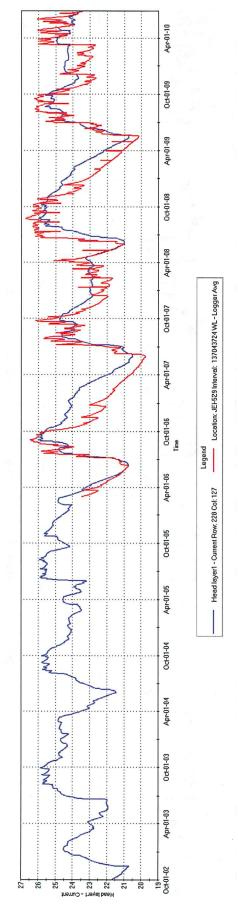


Figure 140: Simulated and observed heads (ft above NGVD) at JEI-529.

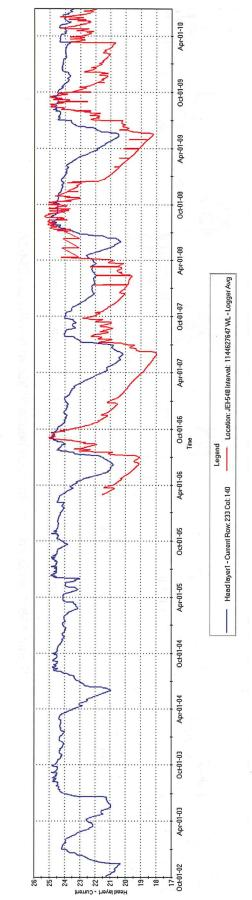


Figure 141: Simulated and observed heads (ft above NGVD) at JEI-548

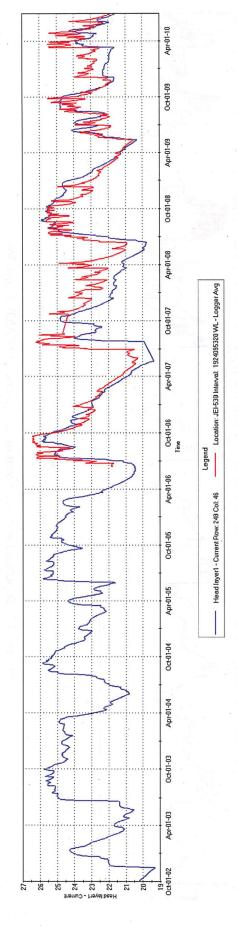


Figure 142: Simulated and observed heads (ft above NGVD) at JEI-530.

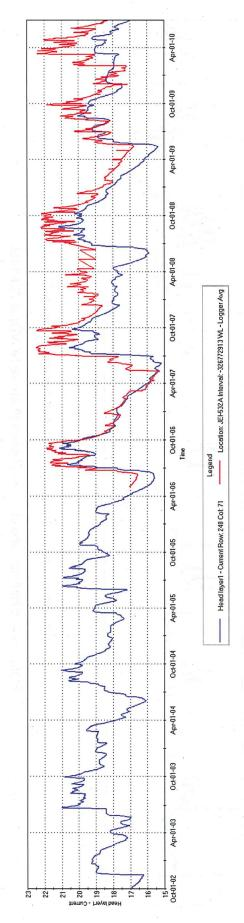


Figure 143: Simulated and observed heads (ft above NGVD) at JEI-532A.

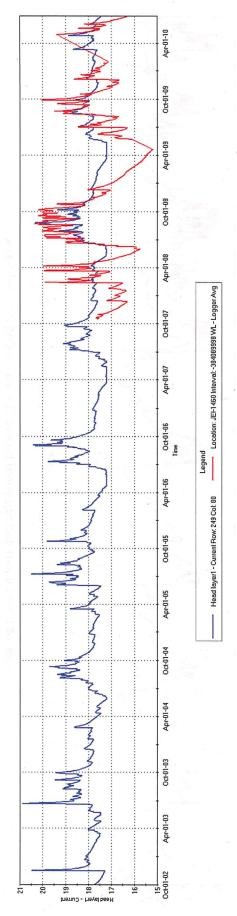


Figure 144: Simulated and observed heads (ft above NGVD) at JEI-1460.

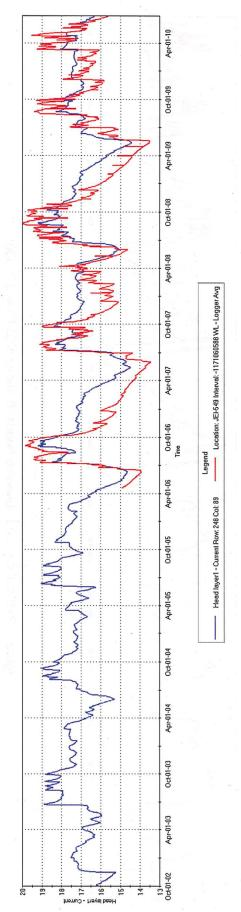


Figure 145: Simulated and observed heads (ft above NGVD) at JEI-549.

Page 183

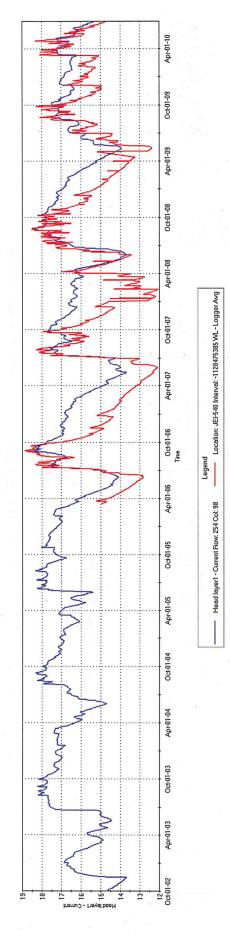


Figure 146: Simulated and observed heads (ft above NGVD) at JEI-540.

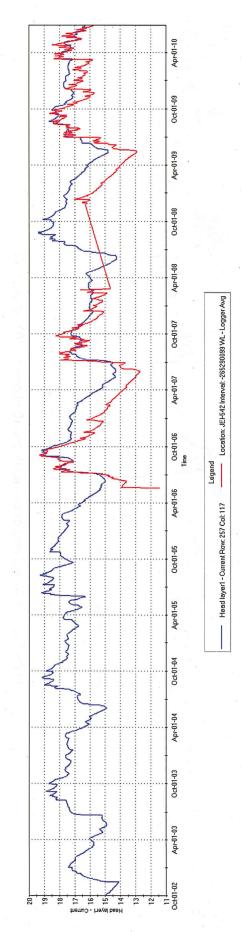


Figure 147: Simulated and observed heads (ft above NGVD) at JEI-542.

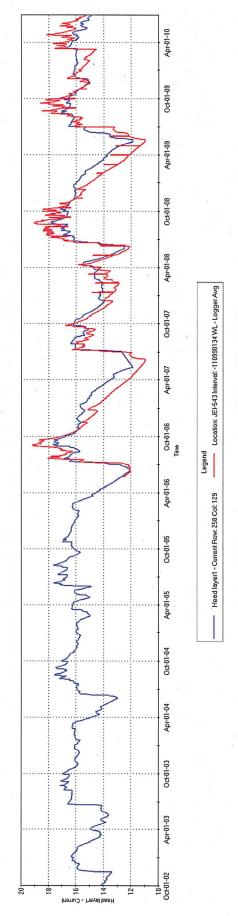


Figure 148: Simulated and observed heads (ft above NGVD) at JEI-543.

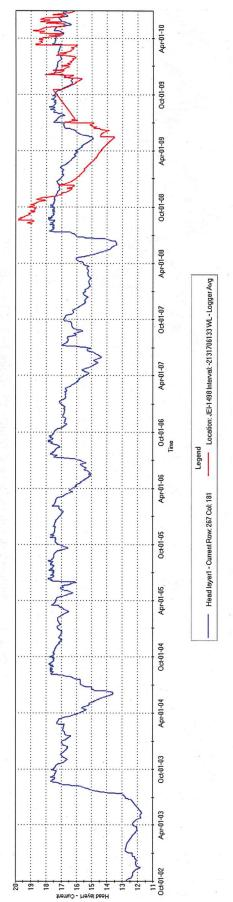


Figure 149: Simulated and observed heads (ft above NGVD) at JEI-1498.

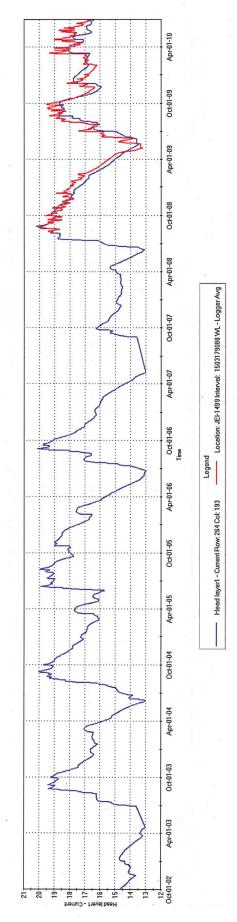


Figure 150: Simulated and observed heads (ft above NGVD) at JEI-1499.

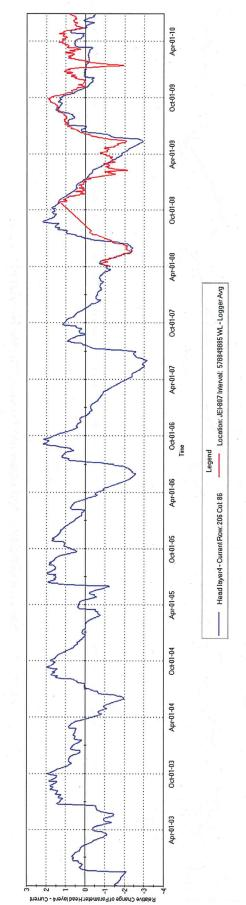


Figure 151: Relative simulated and observed heads (ft above NGVD) at JEI-807.

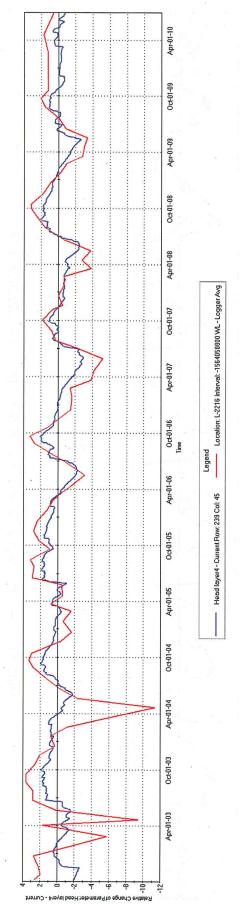


Figure 152: Relative simulated and observed heads (ft above NGVD) at L-2216.

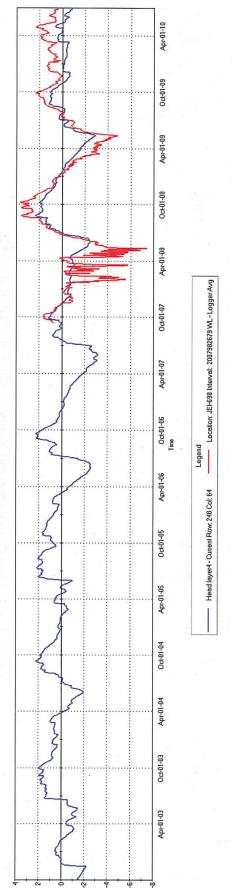


Figure 153: Relative simulated and observed heads (ft above NGVD) at JEI-698.

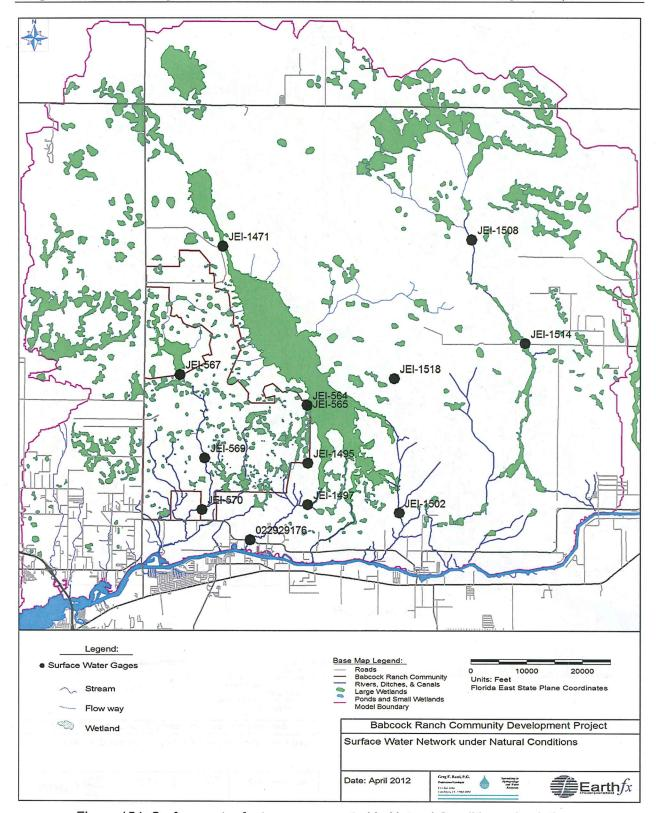


Figure 154: Surface water features represented in Natural Conditions simulations.

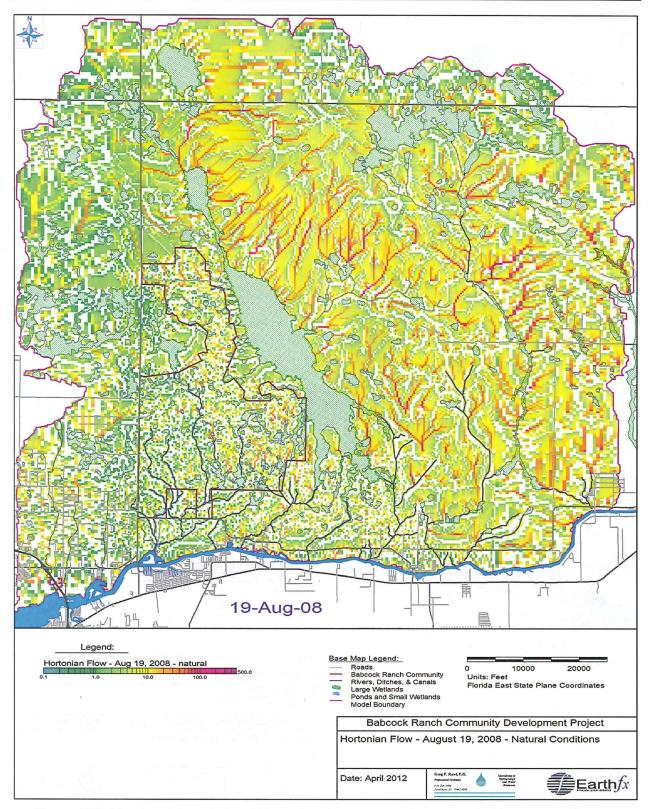


Figure 155: Simulated accumulated Hortonian flow (inches) for August 19, 2008 under Natural Conditions.

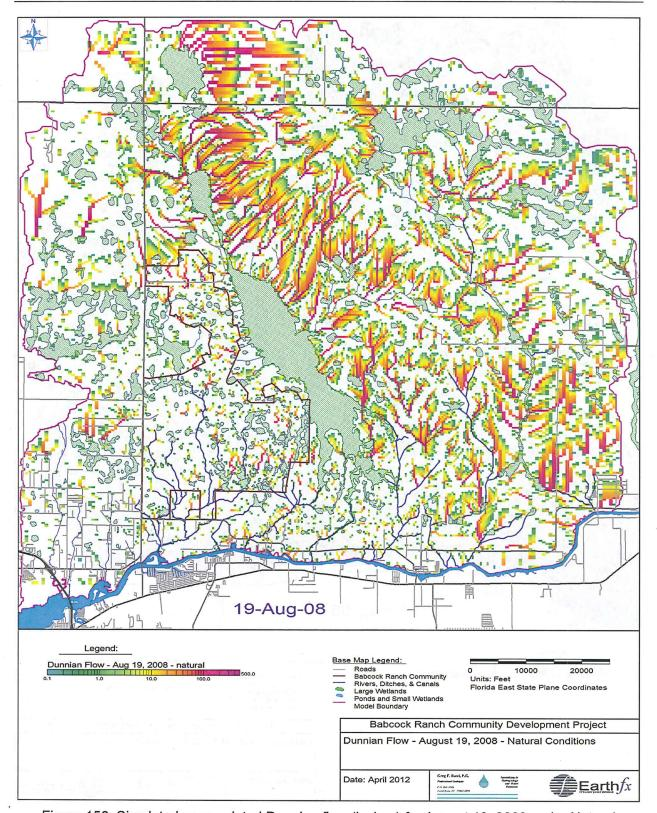


Figure 156: Simulated accumulated Dunnian flow (inches) for August 19, 2008 under Natural Conditions

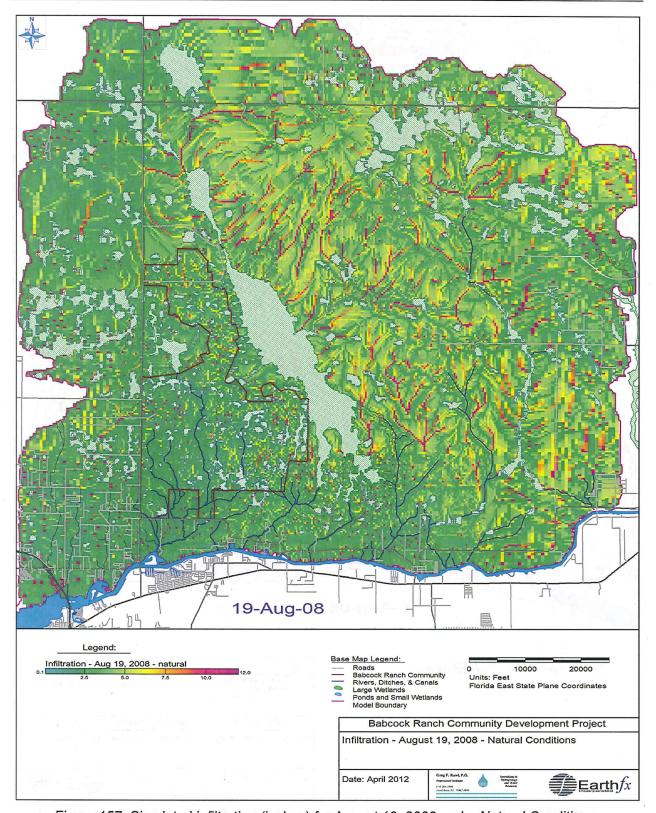


Figure 157: Simulated infiltration (inches) for August 19, 2008 under Natural Conditions.

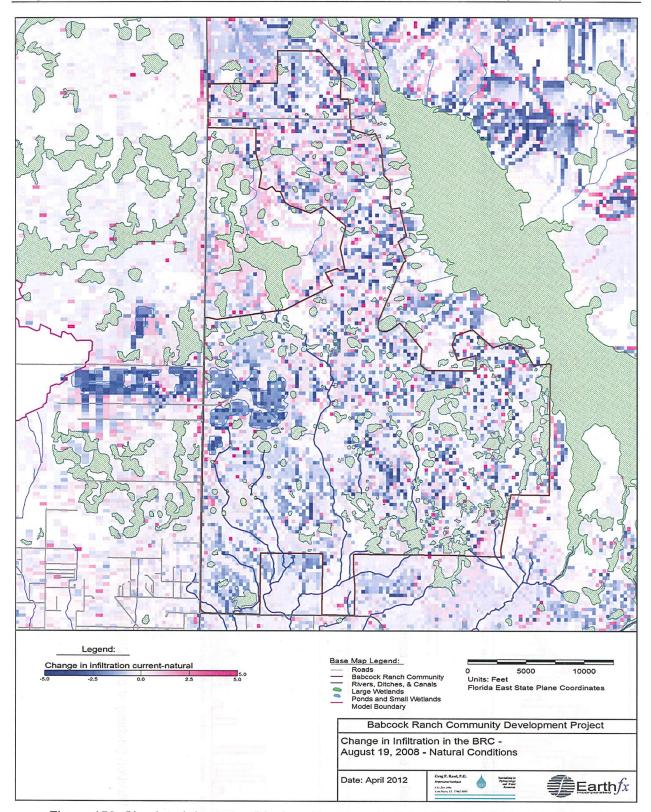


Figure 158: Simulated decrease (blue) and increase (red) in infiltration (Natural to Current Conditions) in the BRC on August 19, 2008.

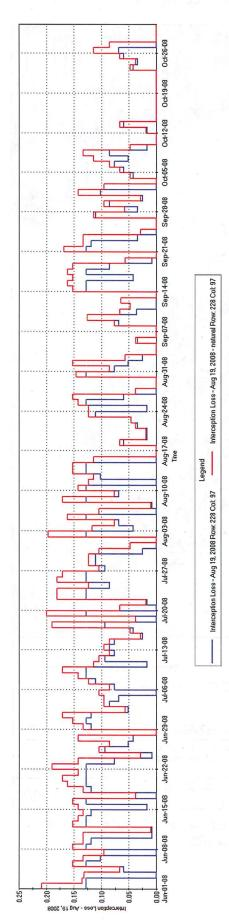


Figure 159: Simulated evaporation from canopy interception (inches) at cell 62969 (r228, c97) for June through October 2008 under Current and Natural conditions.

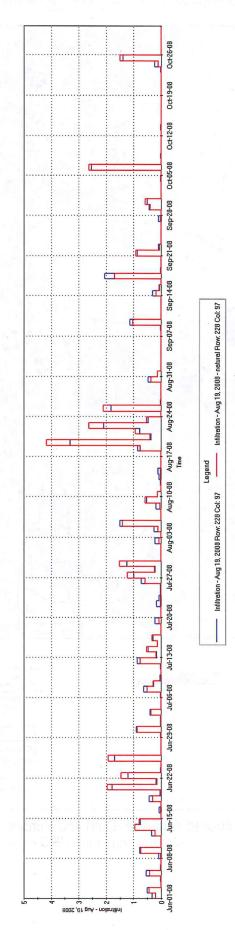


Figure 160: Infiltration (inches) at cell 62969 (r228, c97) near JEI-527, for June through October 2008 under Current and Natural Conditions.

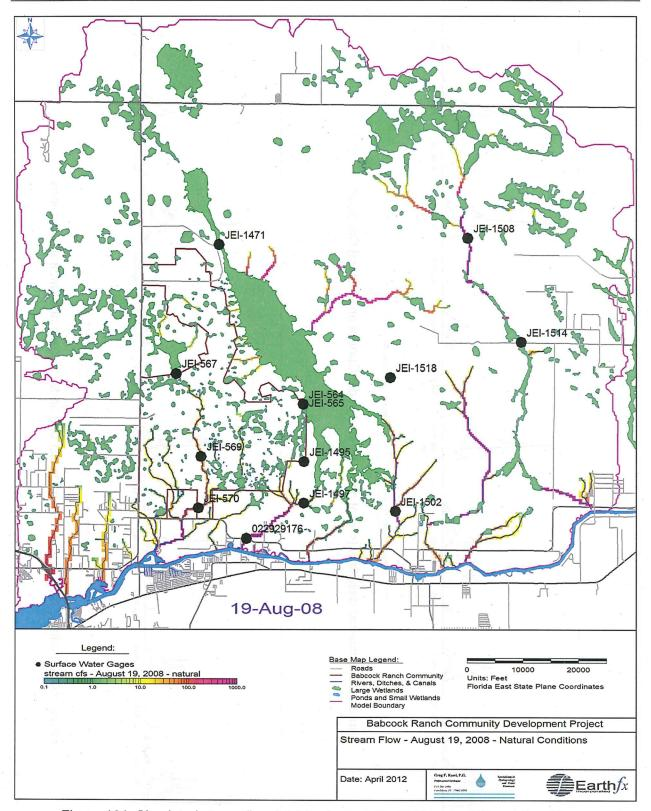


Figure 161: Simulated streamflow (cfs) for August 19, 2008 under Natural Conditions.

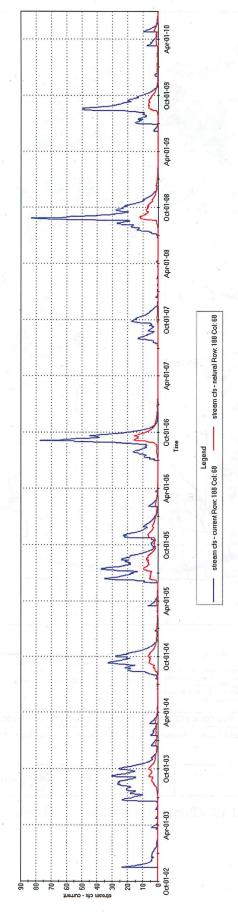


Figure 162: Simulated daily flow (cfs) at gage JEI-567 under Current and Natural Conditions.

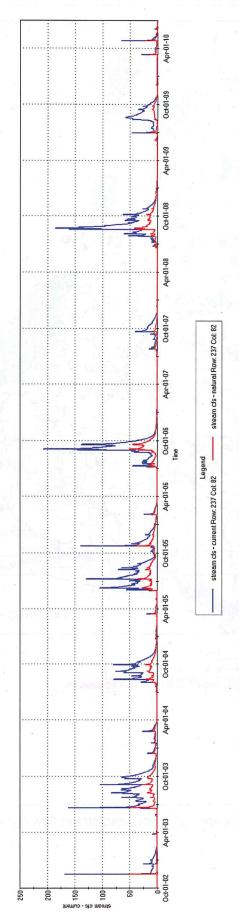


Figure 163: Simulated daily flow (cfs) at gage JEI-569 under Current and Natural Conditions.

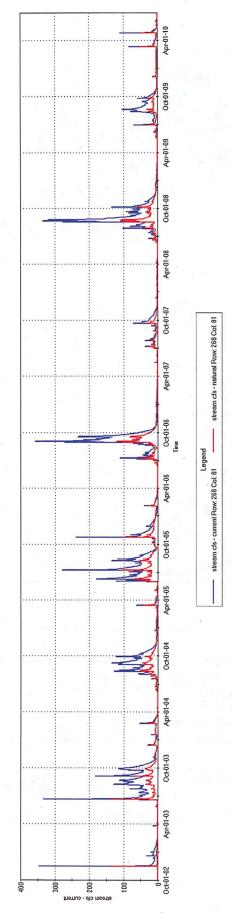


Figure 164: Simulated daily flow (cfs) at gage JEI-570 under Current and Natural Conditions.

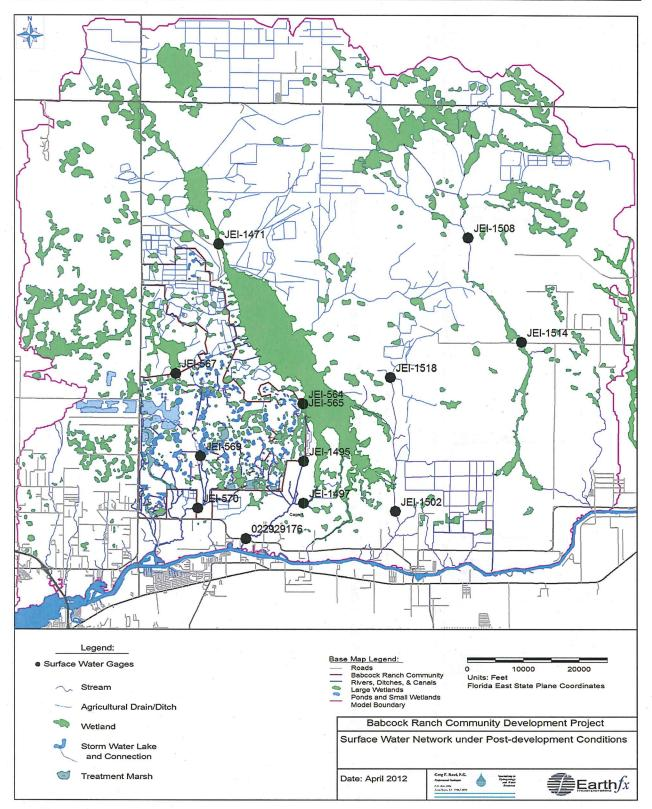


Figure 165: Surface water features represented in Post-development Conditions simulations.

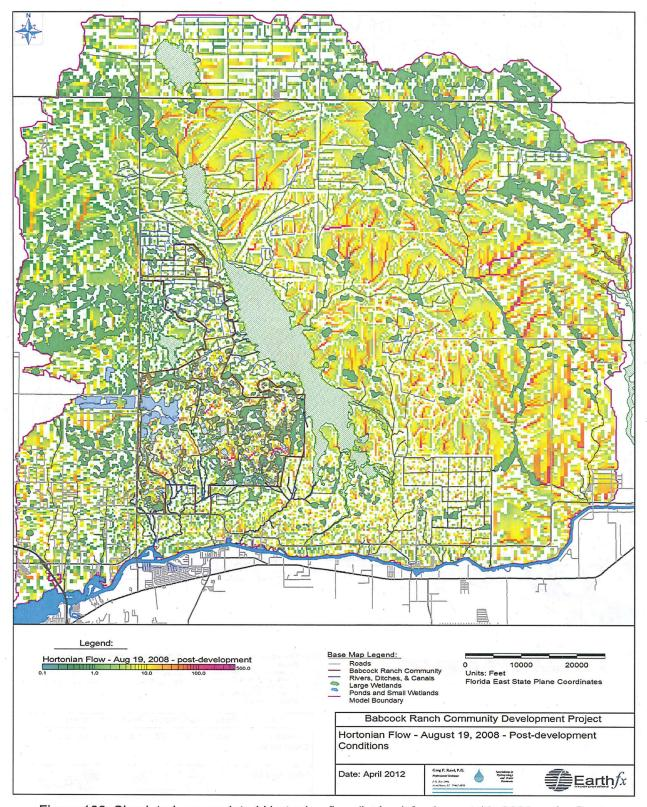


Figure 166: Simulated accumulated Hortonian flow (inches) for August 19, 2008 under Postdevelopment Conditions.

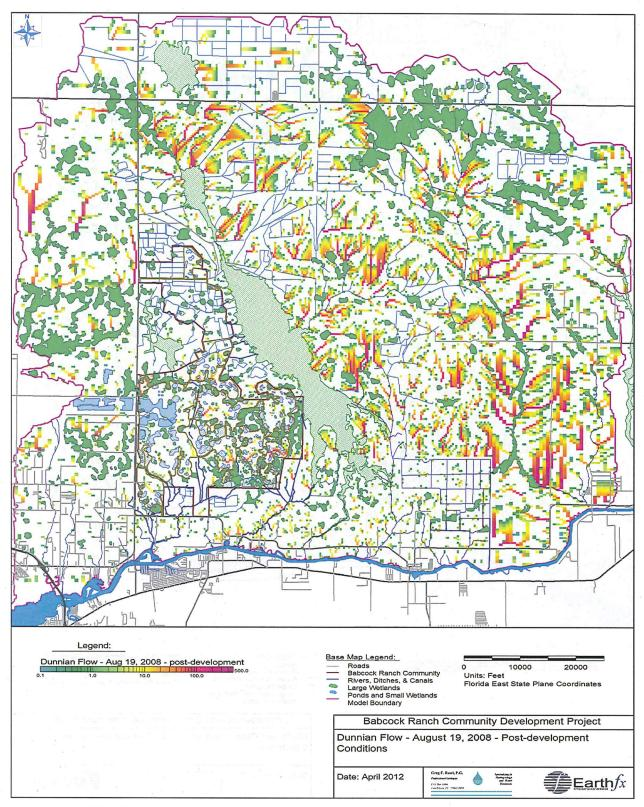


Figure 167: Simulated accumulated Dunnian flow (inches) for August 19, 2008 under Postdevelopment Conditions.

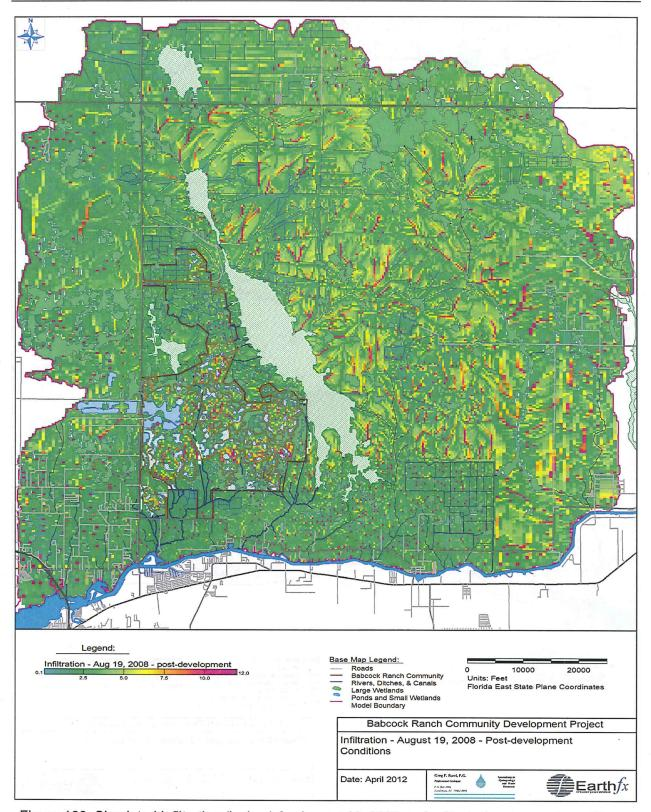


Figure 168: Simulated infiltration (inches) for August 19, 2008 under Post- development conditions.

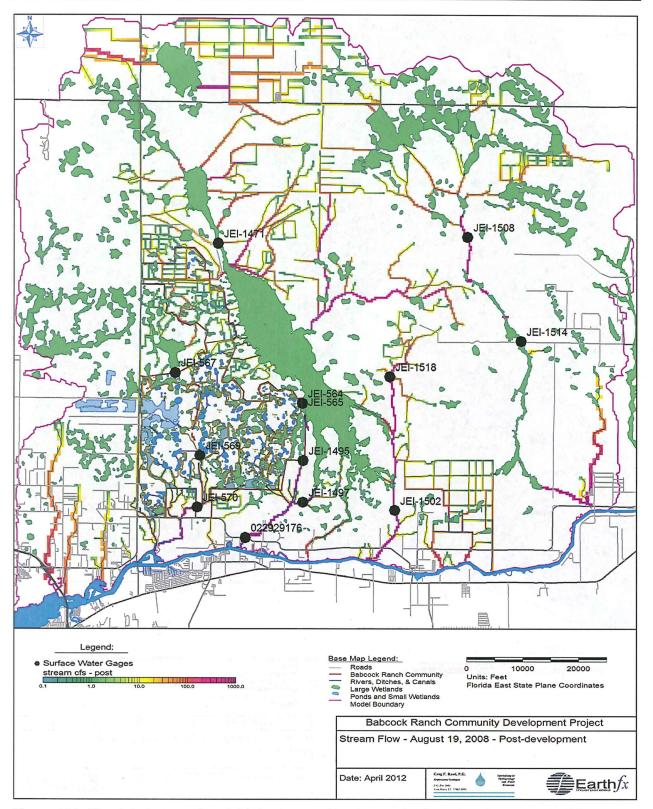


Figure 169: Simulated streamflow (cfs) for August 19, 2008 under Post-development Conditions

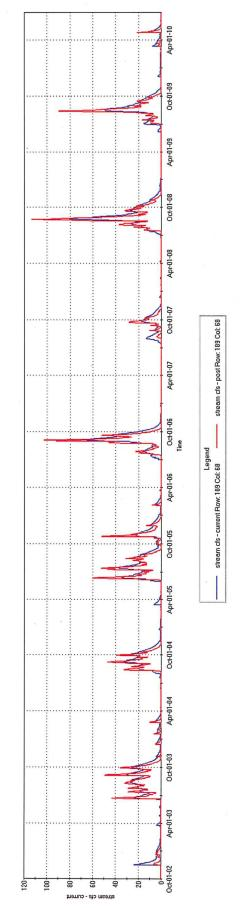


Figure 170: Simulated daily flow (cfs) at gage JEI-567 under Current and Post-development Conditions.

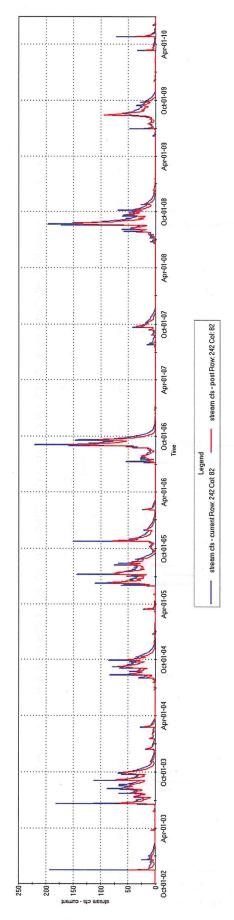


Figure 171: Simulated daily flow (cfs) at gage JEI-569 under Current and Post-development Conditions.

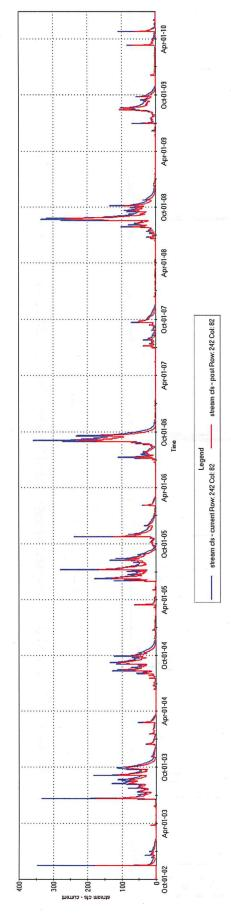


Figure 172: Simulated daily flow (cfs) at gage JEI-570 under Current and Post-development Conditions.

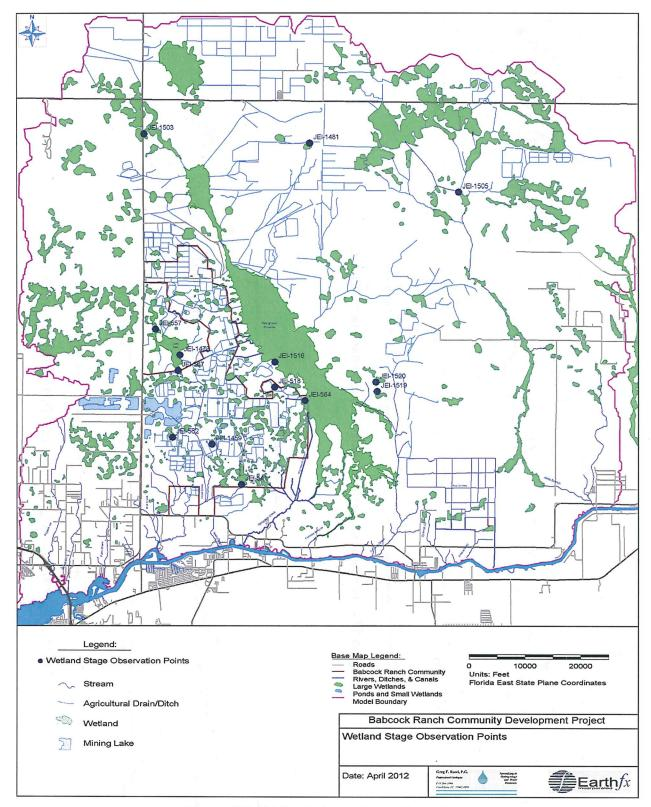


Figure 173: Wetland stage observation points.

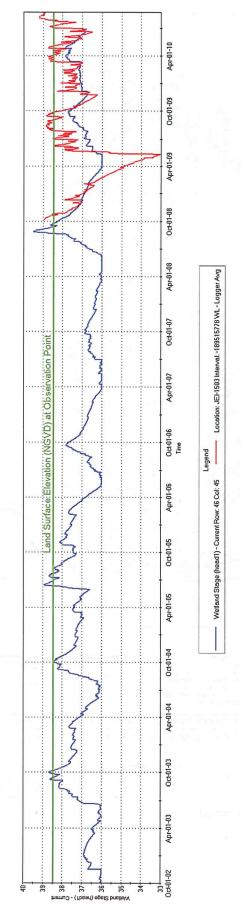


Figure 174: Simulated stage (ft above NGVD) in wetland near JEI-1503.

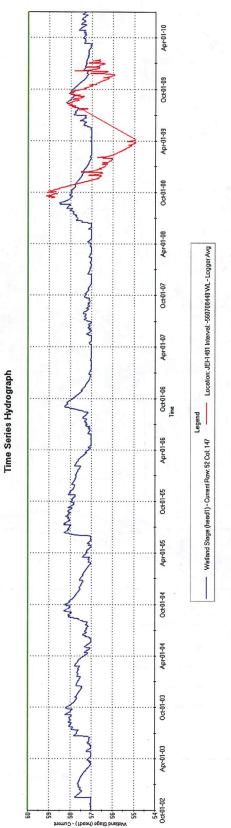


Figure 175: Simulated stage (ft above NGVD) in wetland near JEI-1481.

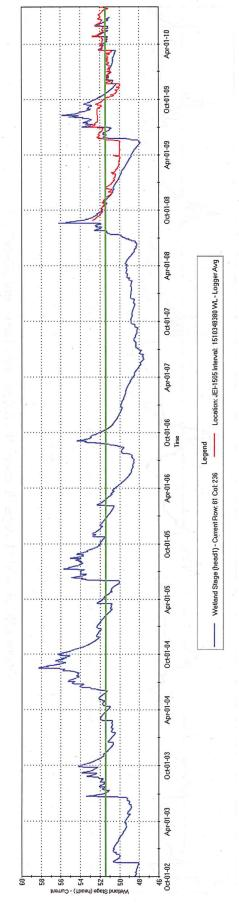


Figure 176: Simulated stage (ft above NGVD) in wetland near JEI-1505.

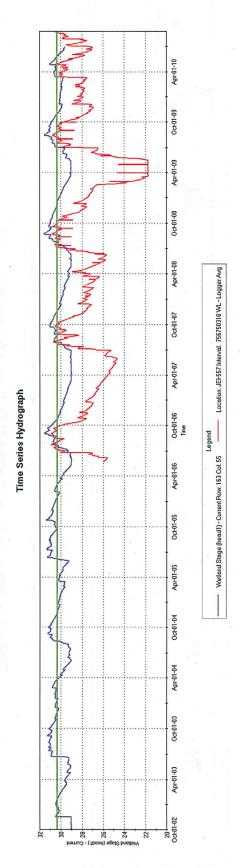


Figure 177: Simulated stage (ft above NGVD) in upper Curry Lake near JEI-557.

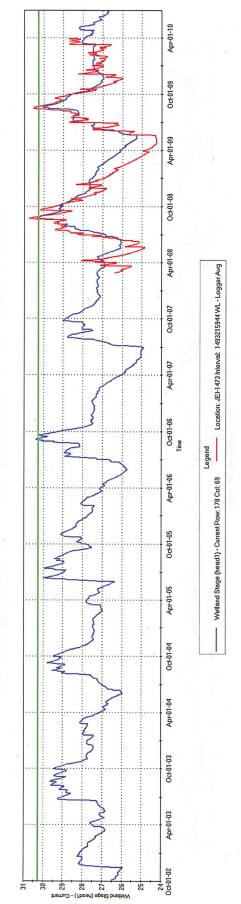


Figure 178: Simulated stage (ft above NGVD) in Curry Lake near JEI-1473.

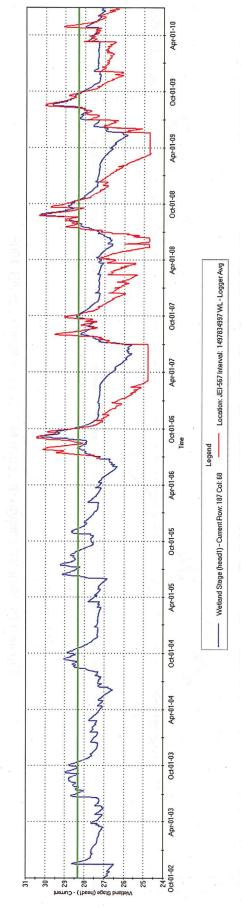


Figure 179: Simulated stage (ft above NGVD) in Curry Lake near JEI-567.

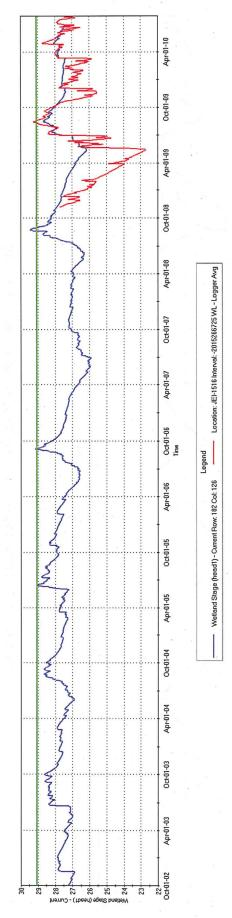


Figure 180: Simulated stage (ft above NGVD) in Telegraph Swamp near JEI-1516.

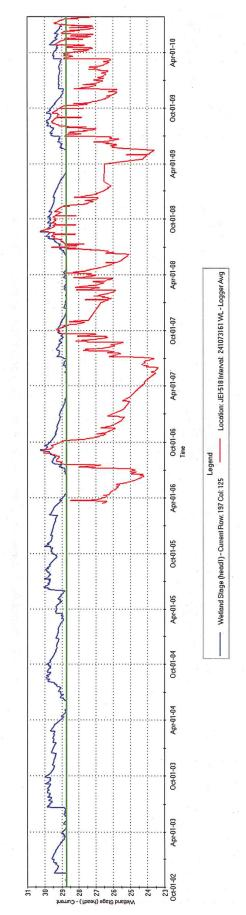


Figure 181: Simulated stage (ft above NGVD) in wetland near JEI-518.

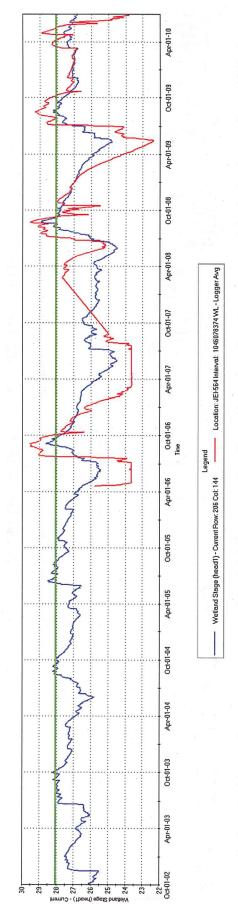


Figure 182: Simulated stage (ft above NGVD) in Telegraph Swamp near JEI-564.

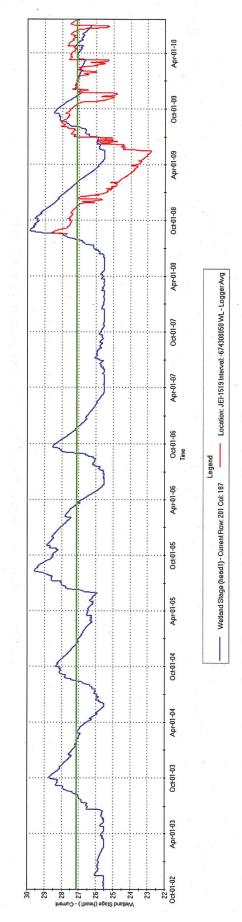


Figure 183: Simulated stage (ft above NGVD) in wetland near JEI-1519.

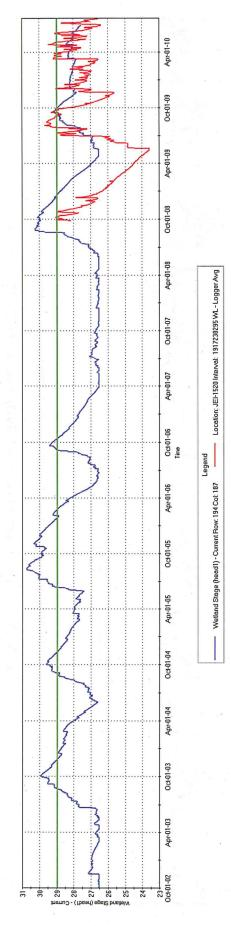


Figure 184: Simulated stage (ft above NGVD) in wetland near JEI-1520.

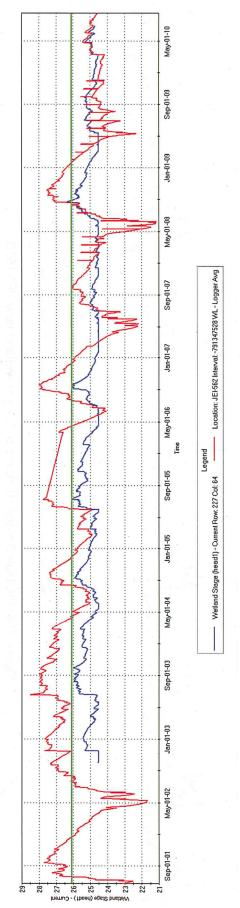


Figure 185: Simulated stage (ft above NGVD) in wetland near JEI-562.

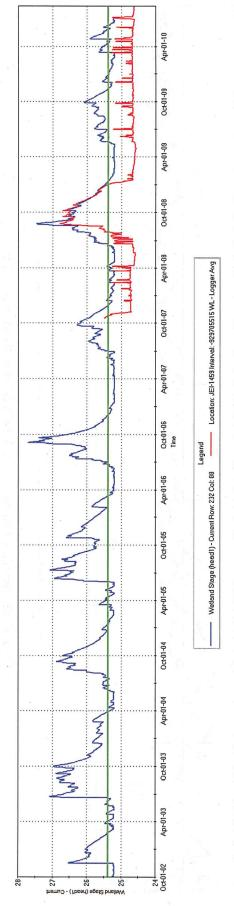


Figure 186: Simulated stage (ft above NGVD) in wetland near JEI-1520.

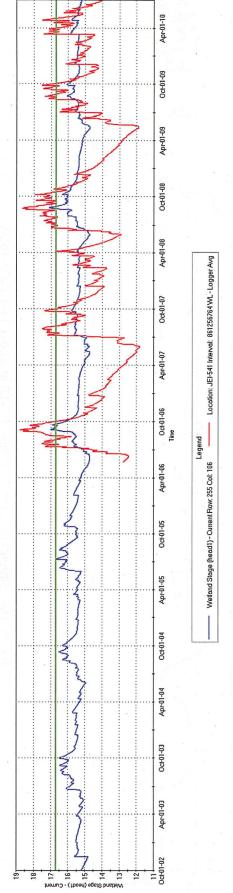


Figure 187: Simulated stage (ft above NGVD) in wetland near JEI-562.

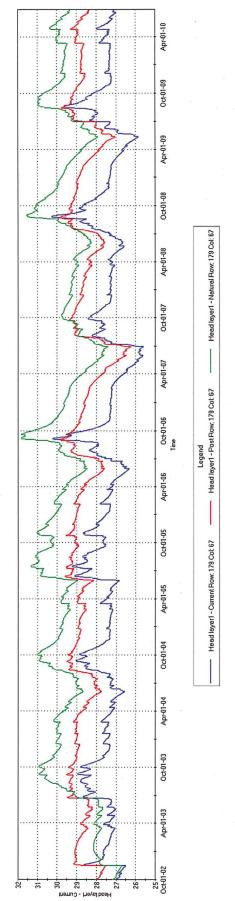


Figure 188: Simulated stage (ft above NGVD) in Assessment Area 1 (Curry Lake) under Current, Natural, and Post-development Conditions.

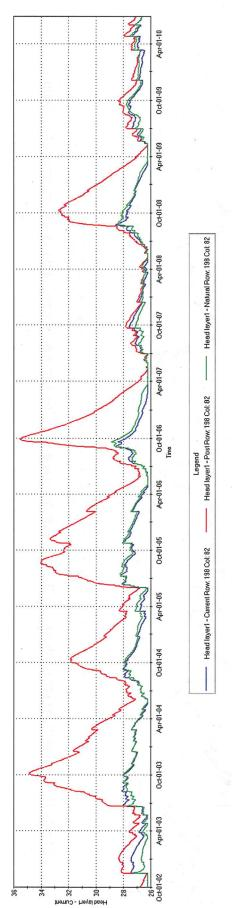


Figure 189: Simulated stage (ft above NGVD) in Assessment Area 2 under Current, Natural, and Post-development Conditions.

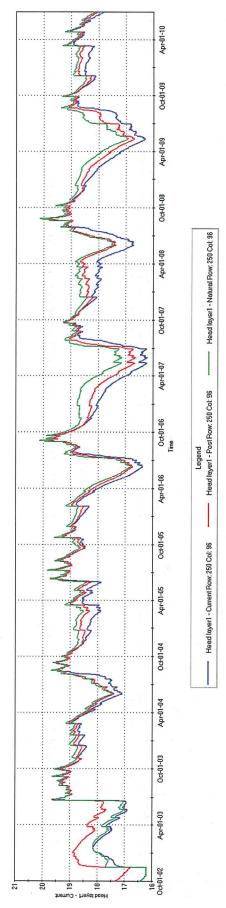


Figure 190: Simulated stage (ft above NGVD) in Assessment Area 3 under Current, Natural, and Post-development Conditions.

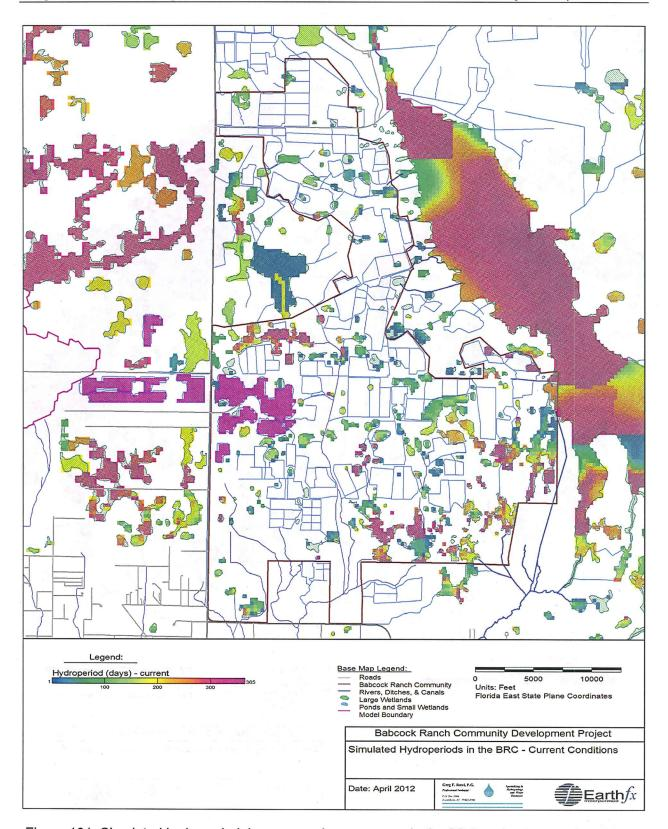


Figure 191: Simulated hydroperiod, in average days per year, in the BRC under Current Conditions.

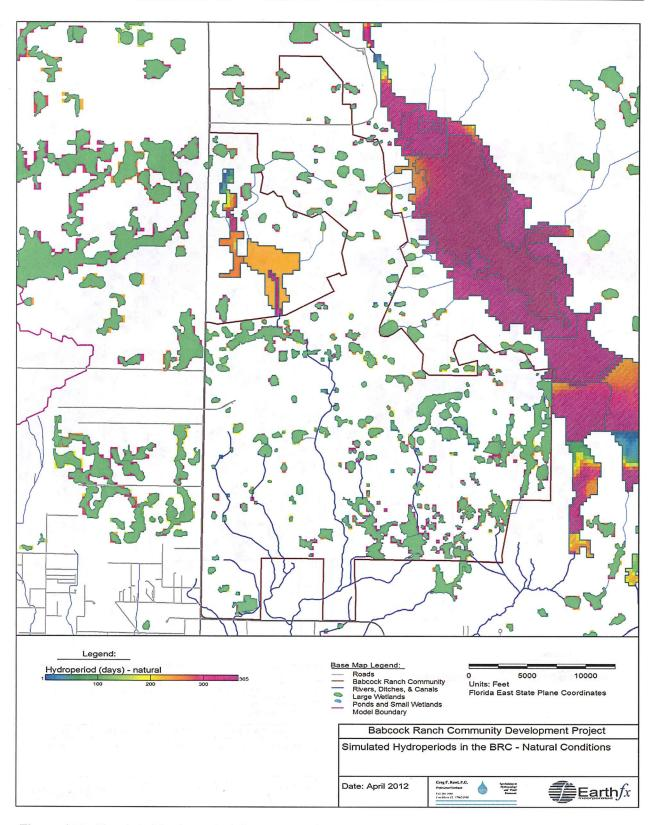


Figure 192: Simulated hydroperiod, in average days per year, in the BRC under Natural Conditions.

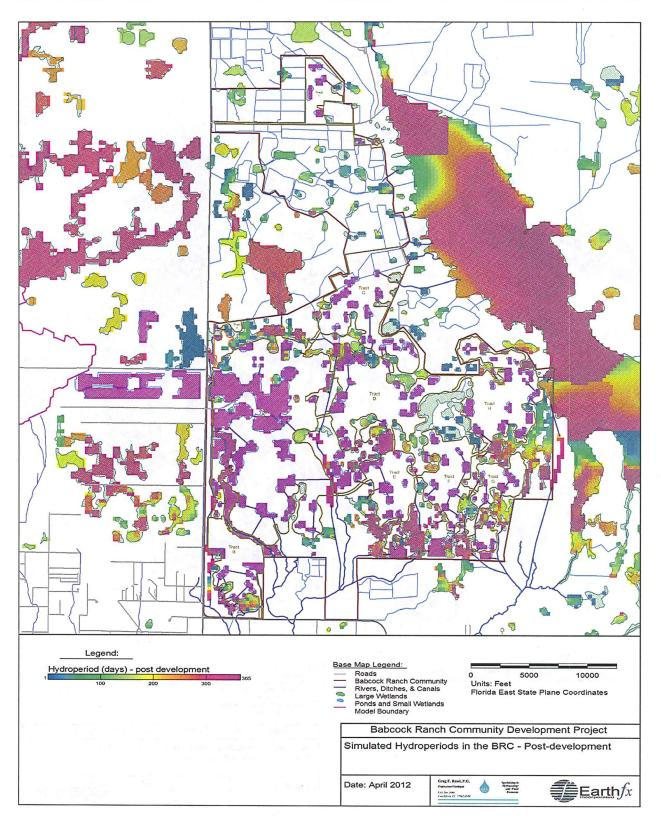


Figure 193: Simulated hydroperiod, in average days per year, in the BRC under Post-development Conditions.

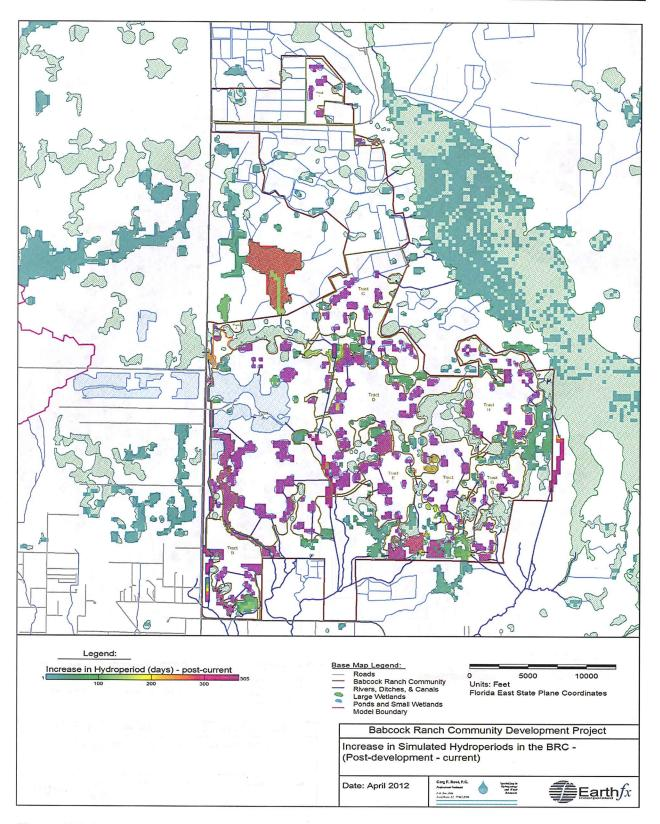


Figure 194: Increase in simulated hydroperiod (Post-development – Current Conditions) in the BRC.

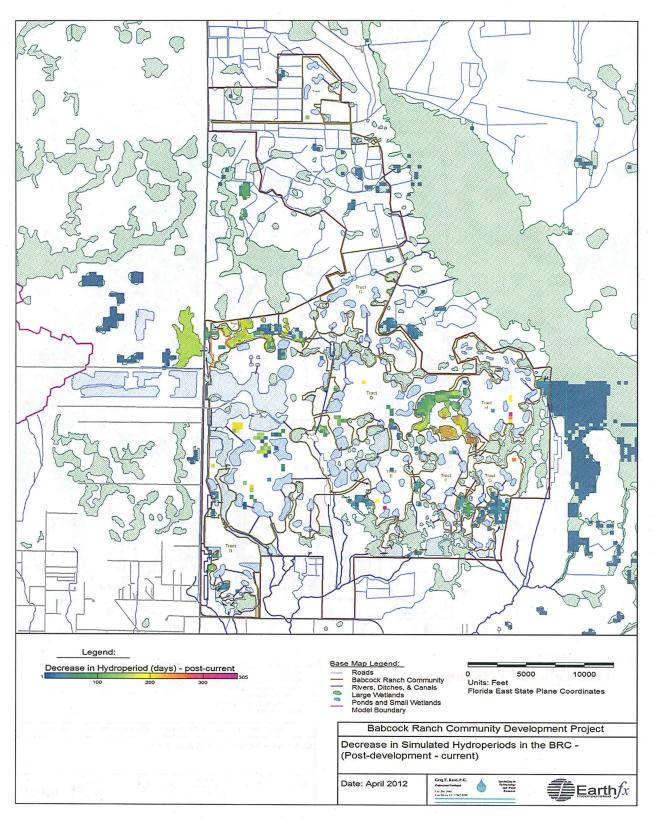


Figure 195: Decrease in simulated hydroperiod (Post-development – Current Conditions) in the BRC.

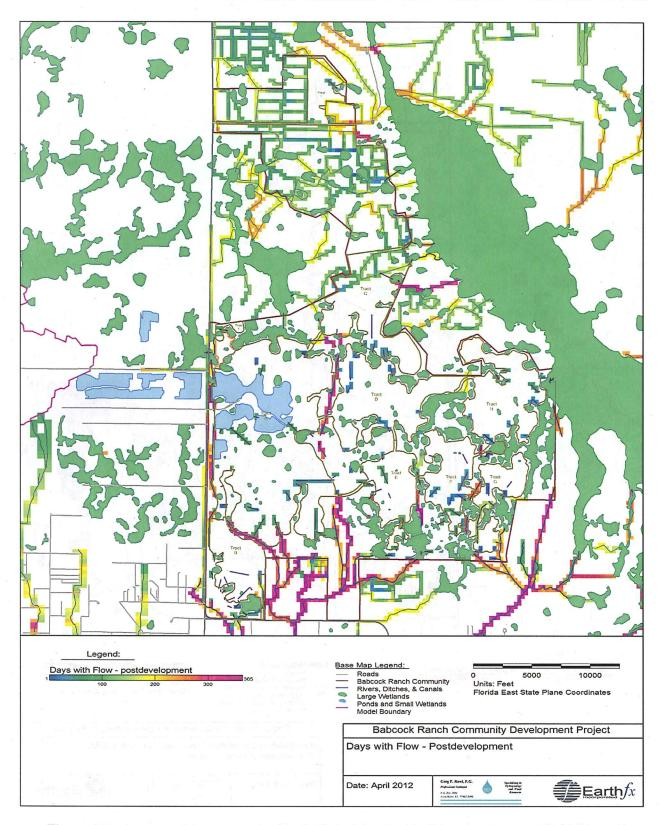


Figure 196: Average days per year with simulated flow under Post-development Conditions.

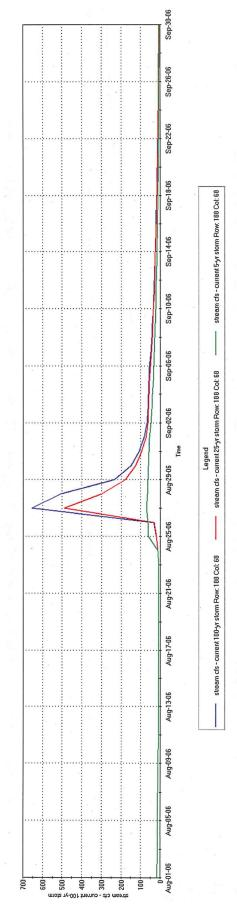


Figure 197: Simulated flow (cfs) versus time for 5-yr, 25-yr, and 100-year storms at JEI-567 under Current Conditions.

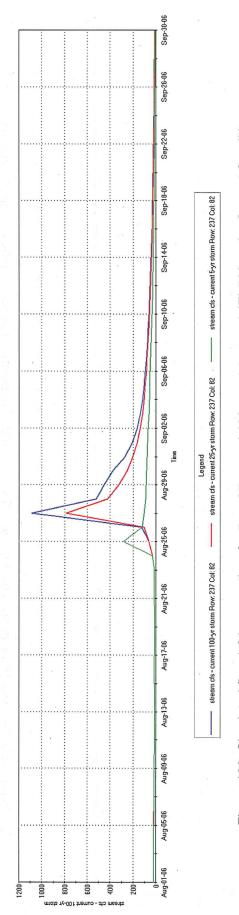


Figure 198: Simulated flow (cfs) versus time for 5-yr, 25-yr, and 100-year storms at JEI-569 under Current Conditions.

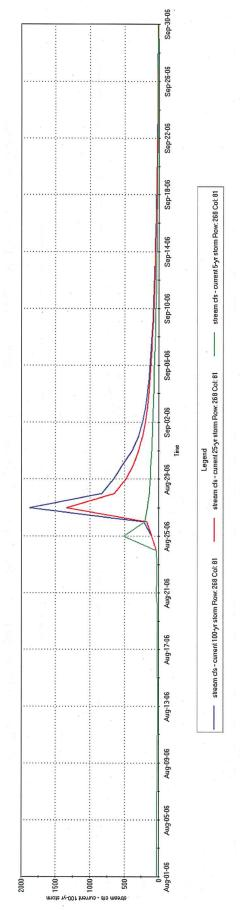


Figure 199: Simulated flow versus time for 5-yr, 25-yr, and 100-year storms at JEI-570 under Current Conditions.

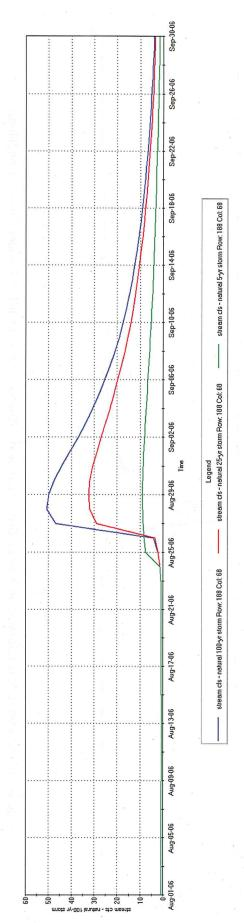


Figure 200: Simulated flow versus time for 5-yr, 25-yr, and 100-year storms at JEI-567 under Natural Conditions.

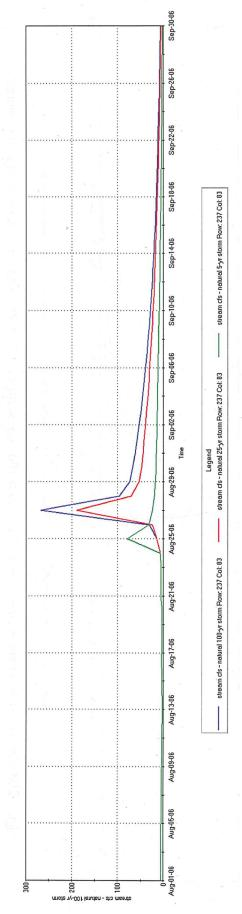


Figure 201: Simulated flow versus time for 5-yr, 25-yr, and 100-year storms at JEI-569 under Natural Conditions.

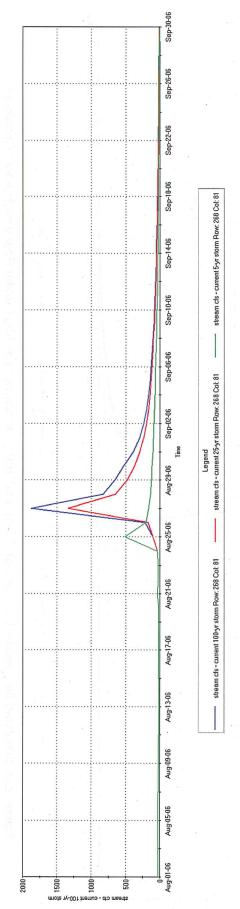


Figure 202: Simulated flow versus time for 5-yr, 25-yr, and 100-year storms at JEI-570 under Natural Conditions.

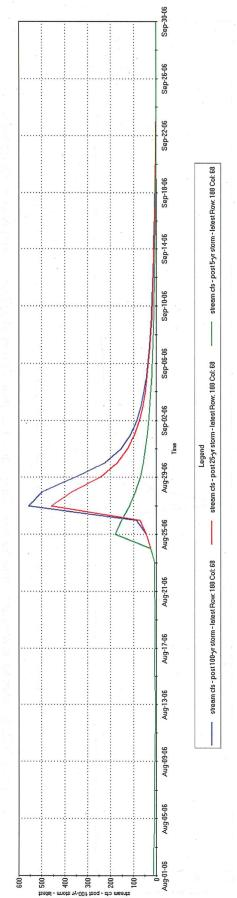


Figure 203: Simulated flow versus time for 5-yr, 25-yr, and 100-year storms at JEI-567 under Post-development Conditions.

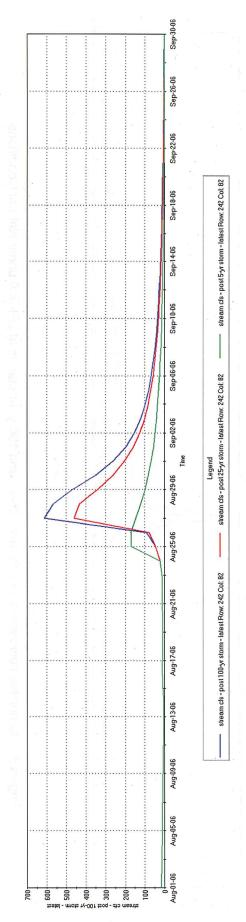


Figure 204: Simulated flow versus time for 5-yr, 25-yr, and 100-year storms at JEI-569 under Post-development Conditions.

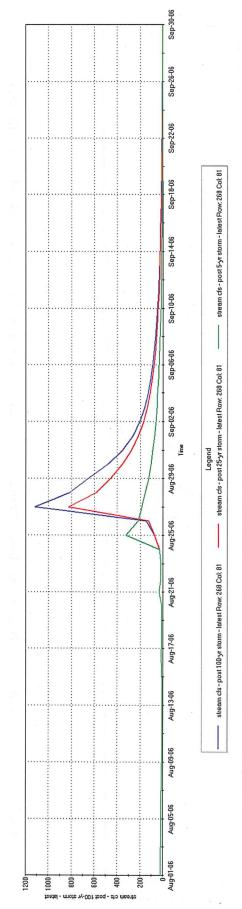


Figure 205: Simulated flow versus time for 5-yr, 25-yr, and 100-year storms at JEI-570 under Post-development Conditions.

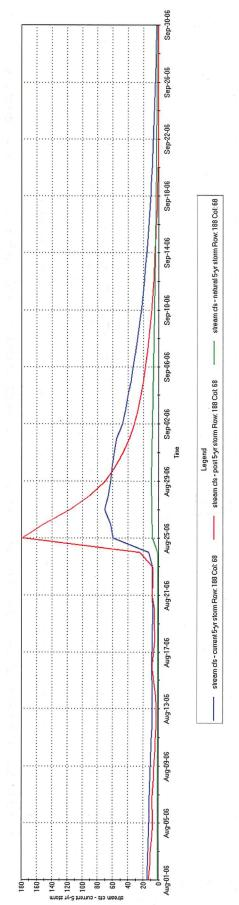


Figure 206: Simulated flow versus time for the 5-yr storm at JEI-567 under Current, Natural, and Post-development Conditions.

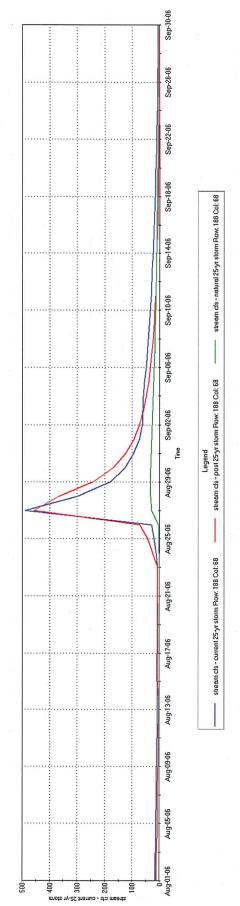


Figure 207: Simulated flow versus time for the 25-yr storm at JEI-567 under Current, Natural, and Post-development Conditions

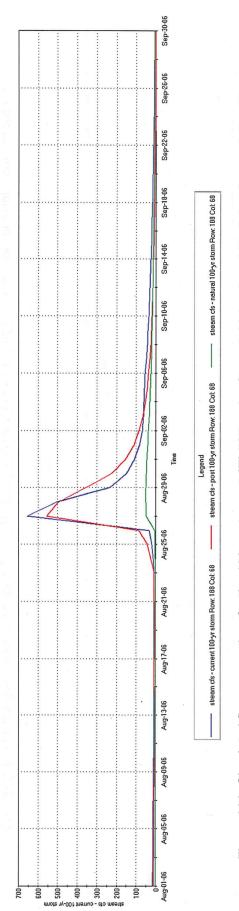


Figure 208: Simulated flow versus time for the 100-yr storm at JEI-567 under Current, Natural, and Post-development Conditions

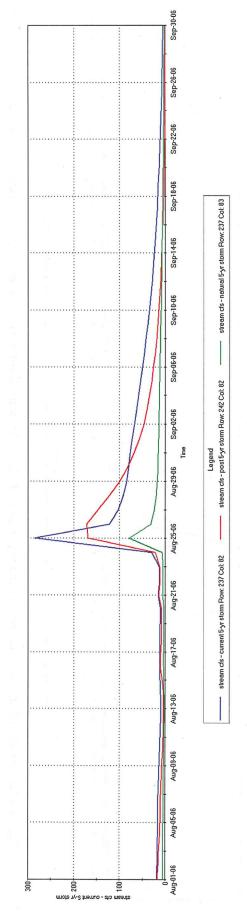


Figure 209: Simulated flow versus time for the 5-yr storm at JEI-569 under Current, Natural, and Post-development Conditions

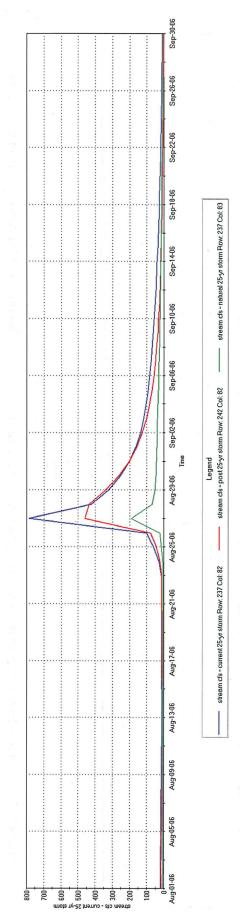


Figure 210: Simulated flow versus time for the 25-yr storm at JEI-569 under Current, Natural, and Post-development Conditions

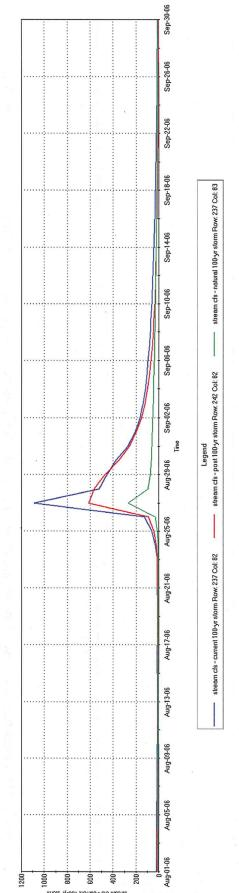


Figure 211: Simulated flow versus time for the 100-yr storm at JEI-569 under Current, Natural, and Post-development Conditions

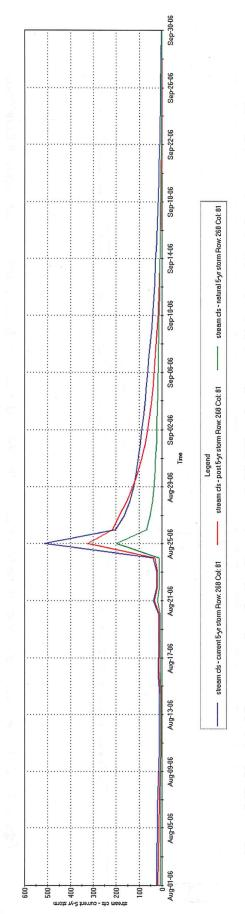


Figure 212: Simulated flow versus time for the 5-yr storm at JEI-570 under Current, Natural, and Post-development Conditions.

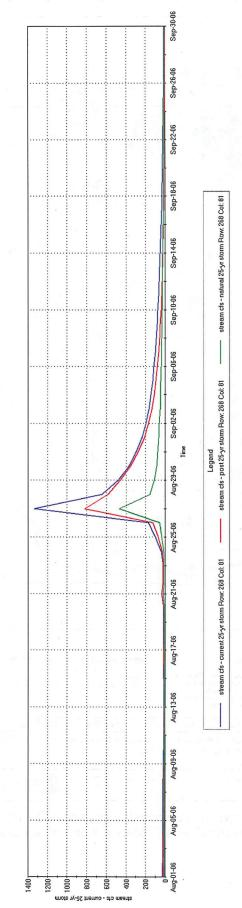


Figure 213: Simulated flow versus time for the 25-yr storm at JEI-570 under Current, Natural, and Post-development Conditions.

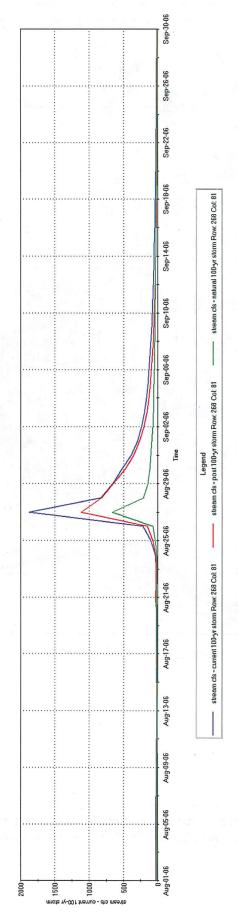


Figure 214: Simulated flow versus time for the 100-year storm at JEI-570 under Current, Natural, and Post-development Conditions.

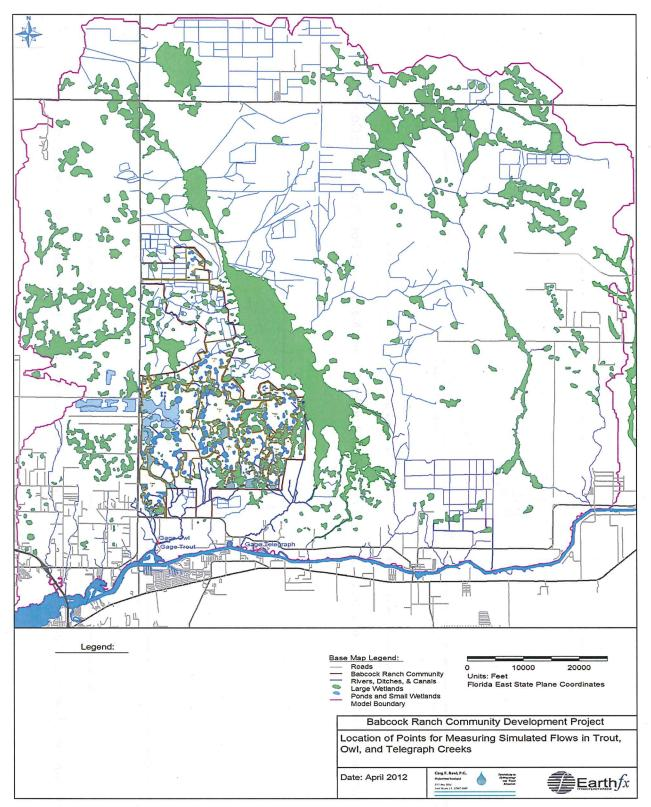


Figure 215: Location of points for measuring simulated flows at the downstream ends of Trout, Owl, and Telegraph Creeks for design storms under Current, Natural, and Post-development Conditions.

Integrated surface-water/groundwater flow model	for the Babcock Ranch	Community Development
---	-----------------------	-----------------------

11 Appendix 1: Streamflow Calculation Methods

11.1 Streamflow Calculation Methods

Stream discharge at the JEI gages was calculated using two methods. A conventional stream-gaging approach based on stage-discharge ratings was used for all stations except JEI-564/565 on Big Island Dike. An empirical approach based on hydrograph comparison was used for JEI-564/565 because insufficient operational data regarding the position of stop logs and gates were available to support the calculation of discharge based on standard ratings for hydraulic structures.

11.1.1 Stage-Discharge Ratings (Stations JEI-567, 569, 570, 1471, 1495, 1497, 1518, 1502, 1508, and 1514:

Numerous concurrent measurements of stage and measurements made by JEI from June 2006 through December 2010 were used to develop stage-discharge ratings to characterize the relationship between stage and flow at the three various gaging stations.

Methodology: Calculations of discharge at 4-hour intervals were prepared using the following four steps:

<u>Step 1:</u> Discharge measurement note sheets prepared by JEI were checked to verify the measured discharges and water-surface elevations reported on the note sheets. Water-surface elevation measurements made by JEI field personnel at the time of discharge measurements and during site visits to check transducer calibrations were compared to data logger readings. Water-surface elevations are referenced to NGVD29. Conversions from NAVD88 elevations reported by JEI to NGVD29 were made by adding 1.2 feet to the NAVD88 elevation.

Step 2: Discharge measurements were evaluated to determine (a) the elevation of zero flow (i.e. PZF) and (b) ratings which characterize the relationship between measured discharges and the concurrently measured water-surface elevations. PZFs were established by evaluating the field measurements made during extremely low flow conditions and the long-term stage hydrographs recorded at each gage. Stage-discharge relationships were determined using the Excel function (SOLVER) to calculate parameters in the generic rating equation (see USGS Water Supply Paper 2175 by Rantz and others, 1982):

$$Q = C(GH - (e-s))^{N}$$

in which

Q = discharge, in cfs;

GH = gage height, i.e. water-surface elevation, in feet NGVD29;

C, e, and N are scaling parameters calculated by minimizing the sum of squared differences between measured and simulated discharges. "N" is constrained to be less than about 3. The parameter "s" represents a time-varying shift in the PZF for channels with an unstable bottom.

Multiple-segment ratings were developed when distinct breaks are apparent in the data to represent low, mid-range and high (over-bank) flow conditions. Residuals from the curve-fitting evaluation were evaluated for a random distribution and trend over time.

Several gages are located on channels with unstable bottoms that are subject to scour and deposition. Gages with residuals that exhibited a long-term trend with time were further evaluated to remove the influence of the apparent long-term shift in channel bottom. The offset "e" for a rating represents the PZF. A linear, time-varying adjustment (termed a "shift") to the PZF was determined for gages with apparent unstable bottoms. The shift is represented by the equation:

s = a(t)

in which

s = shift, in feet;

t = elapsed time since the date of the earliest field discharge measurement used in the rating analysis, in day; and

a = the time-rate-of-change in the shift, in feet/day.

Step 3: The time series of water-level measurements recorded by data loggers at a 4-hour interval were checked for periods of missing, duplicated, or anomalous record. Apparent drift in data logger readings evidenced by differences between the water level measured by the field personnel and recorded by the data logger was corrected by applying a linearly-interpolated adjustment to conditions observed between successive field visits.

The rating curve developed in Step 2 was used to convert the adjusted stage record into discharge at a 4-hour interval. A time series of daily average discharge was calculated by averaging the six 4-hour interval "unit" discharges for each day of record.

<u>JEI-567 – Curry Lake Canal at Hercules Grade:</u> The gage is located on the left (east) edge of a shallow excavated channel within a wide floodplain about 20-feet upstream of two, 2.5-foot diameter corrugated metal culvert-and-rise assemblies under Hercules Grade. The culverts are associated with the HEC-RAS cross section labelled Curry Lake Canal River Station "30160".

The rating (Figure 216) is based in part on discharges measured by JEI personnel at a monthly interval between 6/7/06 and 12/8/09. The point of zero flow (PZF) is 27.10 feet NGVD29 which is the highest of the dual culvert inverts. An analysis for a shift in the channel bottom indicates the PZF for the dual culverts has been increasing in elevation at a rate of 0.078 feet per year since the first rating measurement dated 6/29/06. The shift factor does not apply to flow over the road and flow through the east culvert.

Discharge has been measured using dye-travel time methods during extremely low flow conditions and a current meter for higher flow conditions. Current-meter measurements have historically been made at the inlet (usually) or outlet (occasionally) of each culvert.

Calculated unit discharges are based on data logger records collected from 6/26/06 to 8/12/10. There is no missing stage record for the period of this analysis.

There have been field observations by others of occasional flow over top of Hercules Grade and through another culvert under Hercules Grade 2,700-feet east of the gage, although the extent of the overtopping has not been measured.

The rating represents flow associated with the three conveyances – dual culverts at the gage, the single culvert east of the gage, and flow over Hercules Grade. The stage-discharge rating for the dual culverts is based on discharge measurements. Ratings for the single culvert and weir flow over Hercules Grade are based on the joint consideration of the single culvert and weir geometries and discharge equations utilized in HEC-RAS and GSFLOW models, and professional judgment.

Care should be taken when using the extrapolated high-flow end of a discharge rating. For purposes of calibrating GSFLOW, only a minimal extension of the curve was necessary from the gage height of 30.42 feet NGVD associated with the highest discharge measurement made at JEI-567 to the 30.45 foot maximum recorded during the period of model calibration.

The composite rating is the sum of the following:

Dual Culverts:

For GH \leq 27.10,

Q = 0.0

For GH > 27.10,

 $Q = 12.68*(GH - (27.10-s))^{0.994}$

for which

s = -0.078*(days since 6/26/06)

Single Culvert:

For GH < 28.66,

Q = 0.0

For GH > 28.66,

 $Q = [6.18(GH - 28.66)] + [0.0625(GH - 28.66)^{2.00}]$

Weir (Over-Road):

For GH \leq 30.30, Q = 0.0

For GH > 30.30.

 $Q = 400(GH - 30.29)^{1.50}$

<u>JEI-569 – Curry Lake Canal:</u> The gage is located on a relatively straight reach of Curry Lake Canal on the right (west) bank near the HEC-RAS cross section labeled Curry Lake Canal River Station "10345". The channel is relatively narrow, well incised and has steep sides and a sand bed. The top-bank width-to-depth ratio is about 4:1.

The rating (Figure 217) is based in part on discharges measured by JEI personnel between 6/6/06 and 12/8/09. Discharge has been measured using dye-travel-time methods during extremely low flow conditions. Higher flows are measured using a current meter and wading, or by suspending the current meter from a boat.

The point of zero flow is 14.84 feet. The PZF is a non-specific location on the channel bottom just downstream from the gage. Note that the PZF and historic records of gage height (GH) are relative to a local gage datum that is 4.5-foot lower than NGVD, thus the elevation of channel bottom at JEI569 is 19.0 feet NGVD. An analysis for a shift in the channel bottom indicates the PZF has been increasing in elevation at a rate of 0.042 feet per year since the first rating measurement dated 6/6/06.

Calculated unit discharges are based on data logger records collected from 4/20/06 to 8/5/10. Stage records are missing for the period 1/13/08 through 2/17/08 due to a malfunctioning gaging system.

The rating for this station is represented by two parts as follows:

Low to Medium Flows:

For GH \leq 14.84,

Q = 0.0

For 14.84 > GH < 17.7,

 $Q = 12.1(GH - (14.84-s))^{1.30}$

High Flows:

For GH > 17.7,

 $Q = 3.10(GH - (14.63-s))^{2.50}$

for which

s = -0.042*(days since 6/6/06)

Similar to JEI-567, only a relatively small extension of the rating was needed to calculate discharges used to calibrate GSFLOW. The highest stage recorded at JEI-569 during the calibration period is 20.02 feet, which is 0.33 feet higher than the 19.69 foot stage associated with the highest discharge measurement made at the station.

<u>JEI-570 – Trout Creek:</u> The gage is located on an irregularly shaped reach of Trout Creek on the left (east) bank near the HEC-RAS cross section labelled "Trout-02 River Station "14600". The channel is narrow, well incised and has steep sides and a sand bed. The top-bank width-to-depth ratio is about 3:1. There is an estimated 45-degree bend in the channel towards west about 150-feet downstream from the gage. There is evidence from the cross-section data collected during high-flow measurements of possible bed scour and accretion by as much as about 2 feet at the gage.

The rating (Figure 218) is based on discharges measured by JEI personnel between 6/6/06 and 10/8/08. Measured discharges range between 0.04 and 694 cfs, and no flow was observed on 5 field trips during this period. Discharge has been measured using dye-travel time methods during Earthfx Inc. and Greg Rawl, P.G.

Page 233

extremely low flow conditions. Higher flows have been measured using a current meter and wading, and by suspending the current meter from a boat. Over-bank flow has been measured on several occasions in a heavily vegetated portion of the left-overbank area.

The point of zero flow is 3.00 feet NGVD29. The PZF is a non-specific location on the channel bottom just downstream from the gage. An analysis for shift in channel bottom indicates the PZF has been stable over time.

Calculated unit discharges are based on data logger records collected from 4/20/06 to 12/8/09. There is no missing stage record for the period of this analysis. Some drift in transducer reading is apparent during the dry period from October 2007 to April 2008. Data logger readings were adjusted by as much as 0.38 feet based on the stages measured during monthly field visits.

The rating for this station is represented by three parts as follows:

Low Flows:

For GH \leq 3.00, Q = 0.0

For $3.00 > GH \le 3.80$,

 $Q = 6.56(GH - 3.00)^{1.65}$

Medium to Bank-Full Flows:

For 3.80 > GH < 9.00,

 $Q = 8.24(GH - 3.08)^{1.80}$

High (Over-Bank) Flows:

For GH > 9.00, $Q = 6.58(GH - 3.69)^{2.10}$

The highest stage recorded at JEI-570 during the calibration period is 12.32 feet, which is 0.25 feet higher than the 12.07 foot stage associated with the highest discharge measurement made at the station.

JEI-1471, Telegraph Creek at Headquarters: The rating (Figure 219) is based on discharges measured by JEI personnel between 7/26/06 and 9/9/10. The elevation of the sill elevation on which the stop logs rest is 30.8 feet, and the concrete, fixed-weir crest elevation is 33.8 feet. Calculated unit discharges are based on data logger records collected from 2/28/08 to 7/10/10 during which there is missing record between 4/24/09 and 5/20/09.

Past observations suggest that stop logs are almost always in place; hence water is backed up behind the structure. Varying amounts of leakage have been observed through gaps in the stop logs in addition to weir flow over the stop logs and the concrete crest when upstream stage exceeds these features. No records were made available to identify when stop logs were removed or to define an operating rule for the structure. In addition, the stop logs are not of uniform dimension, hence the elevation of the top of the boards in the individual bays is variable. The measurements of water depth on top of the stop logs made during the monthly field visits represent the most descriptive information available for evaluating discharge at this gage.

The following assumptions were made for purposes of this analysis:

- Stop logs were always in place for the period of analysis.
- Measureable leakage does not occur until the upstream stage exceeds 32.0 feet NGVD.
- Leakage is assumed to be a free-orifice discharge related to the difference between upstream and downstream stage. Since downstream stage is not monitored, the head difference for calculating leakage is estimated as the minimum of either the average head difference historically observed during field visits (i.e. 1.5 feet) or the upstream depth above 32 feet NGVD. A leakage measurement made on 8/7/07 was used to calculate the freeorifice discharge coefficient.
- Field observation indicate that when all boards are in place within an individual bay that the top of the boards is approximately 0.3 feet lower in elevation than the concrete fixed weir.

The rating for this station is represented as: $Q = Q_L + Q_S + Q_C$

For which:

 $Q_L = leakage = 4.48(h_I)^{0.5}$

 $h_L = 0.0,$

when GH < 32.0

 $h_{L} = GH-32$

when 32.0 < GH < 33.5

 $h_L = 1.5$

when GH > 33.5

 Q_S = flow over a <u>single</u> 6-foot wide bay of stop logs = $(2.98)(6.0)(h_S)^{1.5}$

generally when GH < 33.5 unless one or more logs are removed

 $h_S = 0.0,$ $h_S = GH - 33.5,$

generally when GH > 33.5 unless one or more logs are removed

 Q_W = flow over the 85-foot wide, concrete, fixed-weir crest = (3.07)(85.0)(h_W)^{1.5}

 $h_W = 0.0,$

when $GH \le 33.8$

 $h_W = GH - 33.8$, when GH > 33.8

JEI-1495 - Big Island Canal at County Line: The rating (Figure 220) is based in part on discharges measured by JEI personnel between 6/22/06 and 12/8/09. The point of zero flow is 15.98 feet. An analysis for a shift in the channel bottom indicates the PZF has been increasing in elevation at a rate of 0.146 feet per year since the first rating measurement dated 6/22/06.

Calculated unit discharges are based on data logger records collected from 8/5/08 to 8/4/10 during which there is no missing record.

The rating for this station is represented by two parts as follows:

Low to Medium Flows:

For GH < 14.98,

Q = 0.0

For 15.98 > GH < 18.40, $Q = 1.19(GH - (15.98-s))^{3.00}$

High Flows:

For GH > 18.40, $Q = 23.1(GH - (14.56-s))^{1.45}$

for which

s = -0.146*(days since 6/22/06)

<u>JEI–1497, Telegraph Creek at Timber Bridge:</u> The rating (Figure 221) is based in part on discharges measured by JEI personnel between 7/13/06 and 12/8/09. The point of zero flow is 8.73 feet. An analysis for a shift in the rock channel bottom indicates the PZF has been stable since the first rating measurement dated 7/13/06.

Calculated unit discharges are based on data logger records collected from 8/5/08 to 8/4/10 during which there is no missing record.

The rating for this station is represented by three parts as follows:

Low Flows:

For GH < 8.73,

Q = 0.0

For 8.73 > GH < 10.8,

 $Q = 10.2(GH - (8.73-s))^{2.31}$

Medium Flows:

For $10.8 > GH \le 12.0$,

 $Q = 9.57(GH - (8.73-s))^{2.40}$

High Flows:

For GH > 12.0,

 $Q = 156(GH - (10.9-s))^{0.67}$

for which

s = 0.0

Earthfx Inc. and Greg Rawl, P.G.

Page 235

JEI-1518, South Lightered Canal at Cypress Head: The rating (Figure 222) is based in part on discharges measured by JEI personnel between 11/6/07 and 8/3/10. The point of zero flow is 25.06 feet. An analysis for a shift in the channel bottom indicates the PZF has been increasing in elevation at a rate of 0.0467 feet per year since the first rating measurement dated 11/6/07. Calculated unit discharges are based on data logger records collected from 912/08 to 11/17/10 during which there is no missing record.

The rating for this station is represented as follows:

For GH < 25.06,

Q = 0.0

For GH > 25.06

 $Q = 1.16(GH - (25.06-s))^{3.00}$

for which

s = -0.0467*(days since 11/6/07)

JEI-1502, Cypress Creek Outflow: The rating (Figure 223) is based in part on discharges measured by JEI personnel between 9/20/06 and 8/4/10. The point of zero flow is 14.28 feet. An analysis for a shift in the rock channel bottom indicates the PZF has been stable since the first rating measurement dated 9/20/06. Calculated unit discharges are based on data logger records collected from 8/7/08 to 10/6/10 during which there is missing record from October 7-15, 2009.

The rating for this station is represented by two parts as follows:

Low to Medium Flows:

For GH < 14.28,

Q = 0.0

For 14.28 > GH < 15.8,

 $Q = 17.4(GH - (14.28-s))^{1.59}$

High Flows:

For GH > 15.8, $Q = 0.466(GH - (11.65-s))^{3.00}$

for which

s = 0.0

JEI-1508, Jacks Branch Inflow: The rating (Figure 224) is based in part on discharges measured by JEI personnel between 10/9/07 and 8/2/10. The point of zero flow is 41.74 feet. An analysis for a shift in the rock channel bottom indicates the PZF has been stable since the first rating measurement dated 10/9/07. Calculated unit discharges are based on data logger records collected from 11/10/08 to 11/24/10 during which there is no missing record.

The rating for this station is represented as follows:

All Flows:

For GH < 41.74,

Q = 0.0

For GH > 41.74

 $Q = 11.4(GH - (41.74-s))^{3.82}$

for which

s = 0.0

JEI-1514, Jacks Branch Outflow: The rating (Figure 225) is based in part on discharges measured by JEI personnel between 10/9/07 and 8/3/10. The point of zero flow is 32.85 feet. An analysis for a shift in the rock channel bottom indicates the PZF has been stable since the first rating measurement dated 10/9/07. Calculated unit discharges are based on data logger records collected from 10/8/08 to 10/6/10 during which there is missing record between 11/18/09 and 12/31/09.

The rating for this station is represented as follows:

All Flows:

For GH < 32.85,

Q = 0.0

For GH > 32.85

 $Q = 172(GH - (32.85-s))^{1.48}$

Earthfx Inc. and Greg Rawl, P.G.

Page 236

for which

s = 0.0

Empirical Relation (Station JEI-564/565):

<u>JEI-564/565</u>, <u>Big Island Canal at Telegraph Creek at Big Island Dike</u>: Runoff from upper Telegraph Creek passes Big Island Dike at three locations, the eastern most and central of which are stop-log structures similar to that at JEI-1471 and the western most which has a fixed concrete weir and two vertical slide gates. Few records of operational data such as stop-log and gate settings are available to support a hydraulic rating analysis of these structures. Therefore an alternative approach based on hydrographic comparisons was used to determine daily flow records for the canal and creek at Big Island Dike.

The flow records for Big Island Canal and Telegraph Creek at Big Island Dike are based on comparisons of discharge measured during monthly field visits and the daily streamflow records calculated for the downstream stations on Big Island Canal (JEI-1495) and Telegraph Creek at Timber Bridge (JEI-1497). The combined flow in the canal and creek at Big Island Dike is assumed to be proportional to the ratio of the Telegraph Creek drainage area upstream of the dike and the combined drainage areas of the two downstream gages (JEI-1495 and 1497).

Location	Drainage Area (mi²)
Upper Telegraph Creek at Big Island Dike	78.09
Big Island Canal at County line (JEI-1495) and Telegraph Creek at	84.23
Timber Bridge (JEI-1497)	
Ratio	0.93

The combined flow past Big Island Dike into Big Island Canal and Telegraph Creek is represented by the equation:

$$Q_{BID} = 0.93(Q_{JEI1495} + Q_{JEI1497})$$

for which

Q_{BID} = combined discharge through all structures on Big Island Dike, cfs;

Q_{JE11495} = Big Island Canal discharge at County line, cfs; and

Q_{JEI1497} = Telegraph Creek discharge at Timber Bridge, cfs.

The discharge from the cypress bayhead into the upper segment of Big Island Canal at the dike was estimated using on a linear regression of field discharge measurements made concurrently between 6/06 and 10/09 at the west control structure and at the county line gage (Figure 226). The relationship between measured flows at these two locations is:

$$Q_{JE1564/565} = -0.8 + 0.731(Q_{JE11495})$$

for which

Q_{JEI564/565} = Big Island Canal discharge at Big Island Dike, cfs; and

Q_{JEI1495} = Big Island Canal discharge at County line, cfs

During periods when the total discharge past Big Island Dike exceeds the flow past the westernmost structure, the remaining flow is presumably through the middle and/or eastern-most structures on the dike and into Telegraph Creek. Thus the discharge of Telegraph Creek at Big Island Dike $(Q_{TC@BID})$ is represented by:

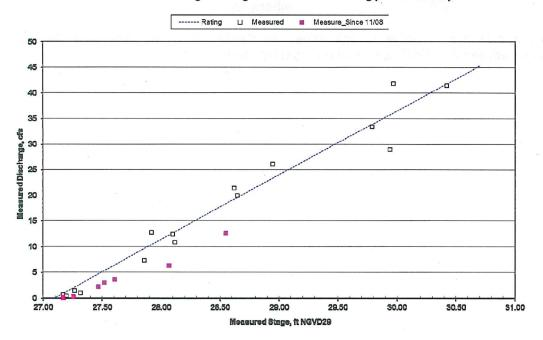
Integrated surface-water/groundwater flow model for the Babcock Ranch Community Development

$$Q_{TC@BID} = Q_{BID} - Q_{JEI564/565} = 0.0$$

when $Q_{BID} \ge Q_{JEI565/565}$ otherwise.

Insufficient data are available to determine the distribution of the estimated Telegraph Creek discharge between the middle and eastern-most structures.

JEI567 Dual Culvert Stage Discharge Measurements and Rating (6/29/06 - 12/8/09)



JEI667 Composite Rating (PZFs = Dual Culverts 27.10'; E Culvert 28.66'; Road 30.29')

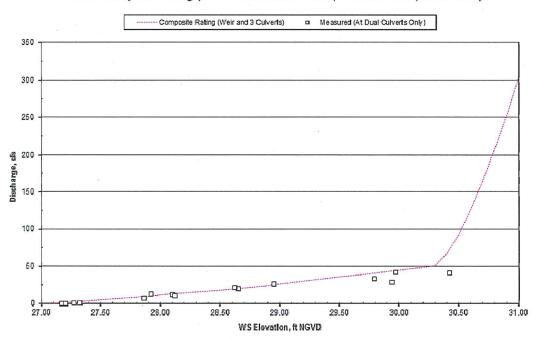


Figure 216: Rating curves for JEI-567.

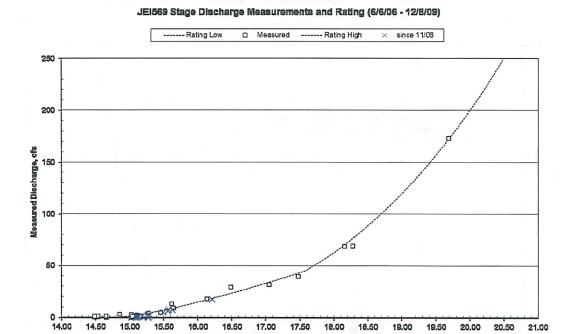


Figure 217: Rating curve for JEI-569.

Measured Stage, ft above -4.5 NGVD29

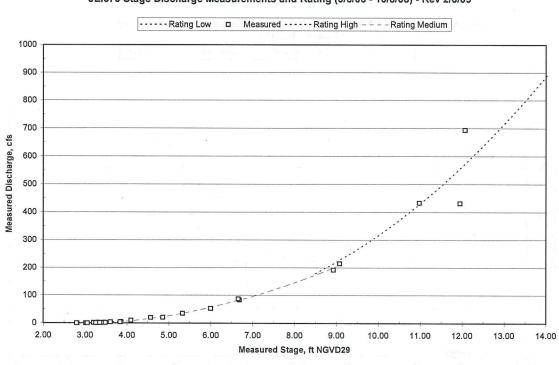


Figure 218: Rating curve for JEI-570.

JEI570 Stage Discharge Measurements and Rating (6/6/06 - 10/8/08) - Rev 2/6/09



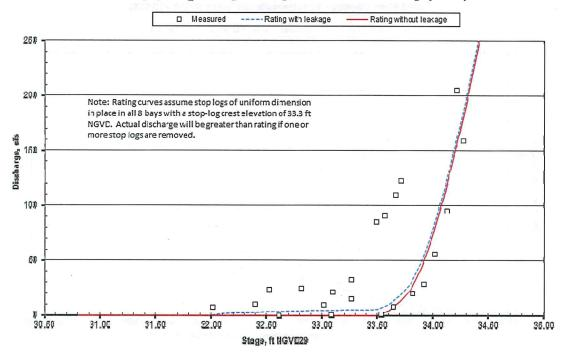


Figure 219: Rating curve for JEI-1471.

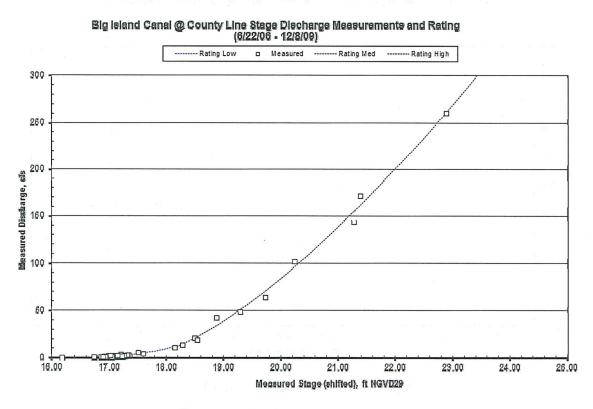


Figure 220: Rating curve for JEI-1495.

Telegraph Cr @ Timber Eridge Stage Discharge Measurements and Rating (12/21/10)

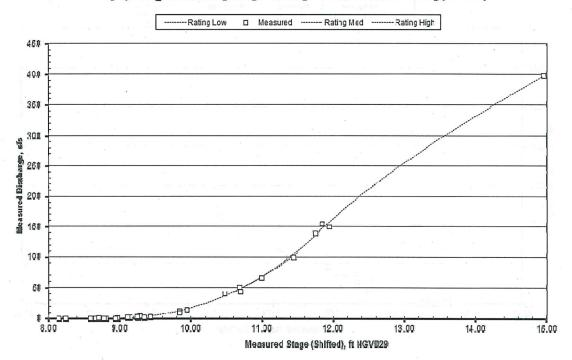


Figure 221: Rating curve for JEI-1497.

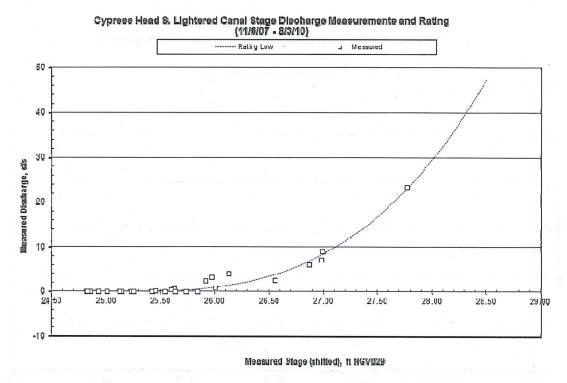


Figure 222: Rating curve for JEI-1518.

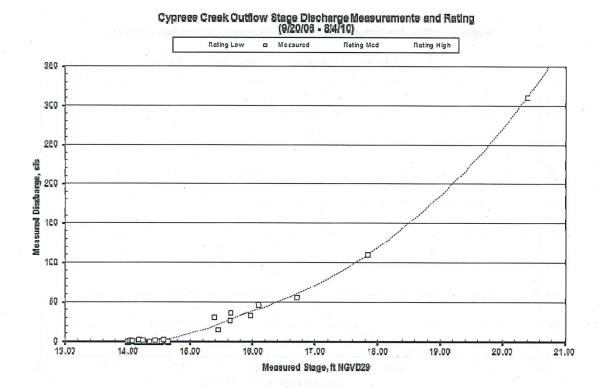


Figure 223: Rating curve for JEI-1502.

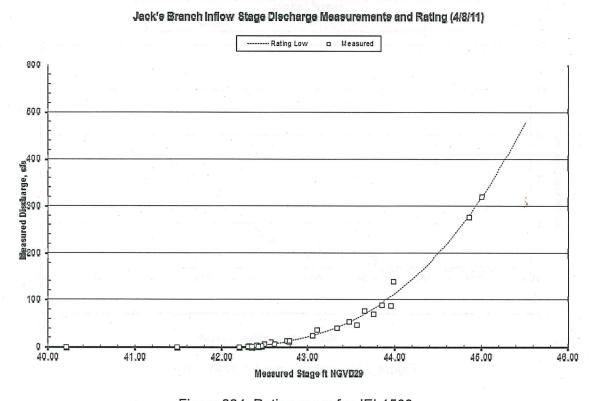


Figure 224: Rating curve for JEI-1508.

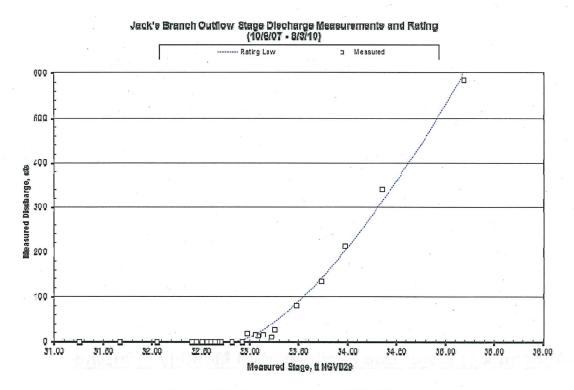


Figure 225: Rating curve for JEI-1514.

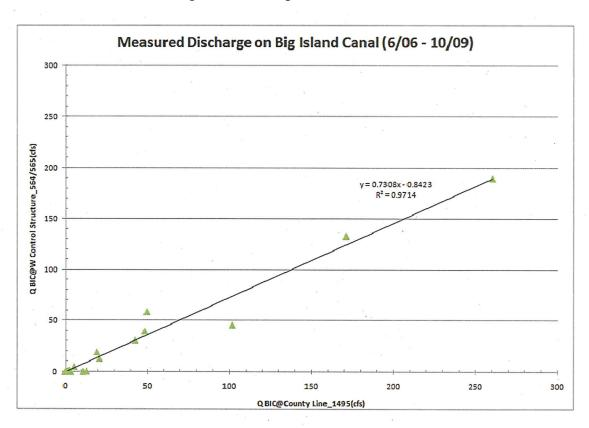


Figure 226: Regression Analysis of Big Island (BI) Canal Discharge at BI Dike and County Line.

	0 0	e e e	2	nmunity Developmen	9
				ll s	
11 100					
	4 107 4 117				
2 Appendix	1: Water Use	<u>Facilities w</u>	<u>ith Monthly P</u>	<u>umping</u>	
	No.				
	20 j				
			* .		
W.		1 · ·			
	2 & W				
		,			
₹					
ř.					
					,
					*
					* : 3 4 4 7 7
					1908 T

12.1 Pumping Data Tables

Table 4: Water use withdrawal facilities with pumping data for Babcock Ranch (SFWMD permit #08-00002-W

Pump ID	Aquifer	East (901)	North (901)
JE-584	Lower Hawthorn	432426	945452
JE-589	Lower Hawthorn	437917	947353
JE-703	mid-hawthorn/arcadia	440365	944051
JE-704	mid-hawthorn/arcadia	440395	942538
JE-633	sandstone	410319	925288
JE-632	sandstone	411150	926085
JE-631	surficial/Ochopee	414500	923558
JE-736 or E-736	sandstone	460985	888999
JE-635	sandstone	409885	918599
JE-630	mid-hawthorn/arcadia	414543	921008
JE-629	sandstone	414533	919154
JE-801	mid-hawthorn/arcadia	418390	920005
JE-628	surficial/Ochopee	412222	918038
JE-769	surficial/Ochopee	413558	914559
JE-770	surficial/Ochopee	414537	916286
JE-637	surficial/Ochopee	412143	914874
JE-785	sandstone	418553	917942
JE-636	surficial/Ochopee	415747	913414
JE-676	surficial/Ochopee	410254	908579
JE-779	surficial/Ochopee	416971	909987
JE-572	surficial/Ochopee	420096	910161
JE-781	surficial/Ochopee	457570	902793
JE-724	surficial/Ochopee	457097	902835
JE-713	surficial/Ochopee	456821	907431
JE-717	surficial/Ochopee	456909	906551
JE-722	Lower Hawthorn	457832	901829
JE-718	surficial/Ochopee	461648	904664
JE-720	surficial/Ochopee	462450	903292
JE-677	surficial/Ochopee	409243	903141
JE-803	surficial/Ochopee	423450	901934
JE-576	surficial/Ochopee	420227	902528
JE-715	surficial/Ochopee	455826	906436
JE-726	surficial/Ochopee	454172	903019
JE-794	surficial/Ochopee	456354	907740
JE-714	surficial/Ochopee	456069	907414
JE-752	surficial/Ochopee	455006	907827
JE-727	surficial/Ochopee	454152	902931
JE-725	surficial/Ochopee	454166	902763
JE-641	surficial/Ochopee	421697	904608
JE-696	surficial/Ochopee	419627	896419
JE-732	surficial/Ochopee	461819	895859
JE-735	surficial/Ochopee	462571	894651
JE-742	surficial/Ochopee	466849	899653

JE-743	surficial/Ochopee	469033	899347
JE-744	surficial/Ochopee	469641	899538
JE-745	surficial/Ochopee	470382	899321
JE-746	surficial/Ochopee	470651	900076
JE-747	surficial/Ochopee	470510	899482
JE-748	surficial/Ochopee	470388	898973
JE-750	surficial/Ochopee	465167	895461
JE-795	Lower Hawthorn	463956	901414
JE-729	surficial/Ochopee	463447	899806
JE-731	surficial/Ochopee	462410	899481
JE-730	surficial/Ochopee	462860	899200
JE-669	surficial/Ochopee	417116	897989
JE-646	surficial/Ochopee	421776	897125
JE-734	surficial/Ochopee	461264	895235
JE-668	surficial/Ochopee	422738	896462
JE-700	surficial/Ochopee	424113	891802
JE-737	surficial/Ochopee	460841	889288
JE-799	surficial/Ochopee	416493	888764
JE-679	surficial/Ochopee	413558	914559
JE-788	Lower Hawthorn	420181	889344
JE-699	surficial/Ochopee	425106	889639
JE-800	surficial/Ochopee	413449	885989
JE-734	surficial/Ochopee	461264	895235
JE-668	surficial/Ochopee	422738	896462
JE-700	surficial/Ochopee	424113	891802
JE-737	surficial/Ochopee	460841	889288
JE-799	surficial/Ochopee	416493	888764
JE-679	surficial/Ochopee	413558	914559
JE-788	Lower Hawthorn	420181	889344
JE-699	surficial/Ochopee	425106	889639
JE-800	surficial/Ochopee	413449	885989

Table 5: Water use withdrawal facilities with pumping data for permitted users.

Aquifer	East (901)	North (901)	Permittee
Holocene/surficial	458369	962647	Berry Grove Charlotte Tract
Holocene/surficial	460082	962674	Berry Grove Charlotte Tract
Holocene/surficial	464710	963887	Berry Grove Charlotte Tract
Holocene/surficial	462032	965364	Berry Grove Charlotte Tract
Holocene/surficial	458822	964990	Berry Grove Charlotte Tract
Holocene/surficial	465478	955143	Berry Grove Charlotte Tract
Lower Hawthorn	445736	951252	Edenbelle Grove
Lower Hawthorn	442747	950513	Edenbelle Grove
Lower Hawthorn	443915	958805	Edenbelle Grove
Lower Hawthorn	449925	956209	Edenbelle Grove
Lower Hawthorn	448368	959983	Edenbelle Grove
Lower Hawthorn	446722	958925	Edenbelle Grove
Lower Hawthorn	443376	957567	Edenbelle Grove

Aquifer	East (901)	North (901)	Permittee
surficial/Holocene	445753	951464	Edenbelle Grove
surficial/Holocene	442630	950751	Edenbelle Grove
surficial/Holocene	442870	953392	Edenbelle Grove
surficial/Holocene	442165	956149	Edenbelle Grove
surficial/Holocene	442265	959484	Edenbelle Grove
surficial/Holocene	444699	958295	Edenbelle Grove
surficial/Holocene	445370	954730	Edenbelle Grove
surficial/Holocene	447346	956187	Edenbelle Grove
surficial/Holocene	447478	958030	Edenbelle Grove
surficial/Holocene	447747	958949	Edenbelle Grove
surficial/Holocene	450064	957404	Edenbelle Grove
Lower Hawthorn	450775	951556	Regina Grove
surficial/Holocene	448181	951503	Regina Grove
surficial/Holocene	448345	953980	Regina Grove
surficial/Holocene	449632	954183	Regina Grove
surficial/Holocene	449594	951174	Regina Grove
Lower Hawthorn	466572	952298	TJ & Mary Chastain
surficial/Ochopee	397540	895303	Coral Rock Mine
surficial/Ochopee	407988	895177	Coral Rock Mine
surficial/Ochopee	401696	895513	Coral Rock Mine
surficial/Ochopee	394576	895951	Coral Rock Mine
surficial/Ochopee	402363	901775	Jay Rock Mine
surficial/Holocene	469910	872800	County Line Drainage District
surficial/Holocene	470215	873610	County Line Drainage District
surficial/Holocene	466427	876221	County Line Drainage District
surficial/Holocene	462475	874744	County Line Drainage District
surficial/Holocene	464403	875855	County Line Drainage District
surficial/Holocene	469304	881632	County Line Drainage District
surficial/Holocene	464745	884225	County Line Drainage District
surficial/Holocene	460480	885400	County Line Drainage District
surficial/Holocene	460197	880601	County Line Drainage District
surficial/Holocene	463606	880454	County Line Drainage District
Sandstone Aquifer	411455	874063	Blackburn Groves
Sandstone Aquifer	411442	872383	Blackburn Groves
Lower Hawthorn	443414	962104	Calusa I
Lower Hawthorn	442671	967120	Calusa I
Lower Hawthorn	442686	969926	Calusa I
Lower Hawthorn	445004	967109	Calusa I
surficial/Holocene	443586	962001	Calusa I
surficial/Holocene	443600	964644	Calusa I
surficial/Holocene	443614	967288	Calusa I
surficial/Holocene	443600	969271	Calusa I
Lower Hawthorn	No Data	No Data	Payson Tract
Lower Hawthorn	No Data	No Data	
Lower Hawthorn	No Data	No Data	Payson Tract
Lower Hawthorn			Payson Tract
Lower Hawthorn Lower Hawthorn	No Data	No Data	Payson Tract
	No Data	No Data	Payson Tract
Lower Hawthorn	No Data	No Data	Payson Tract
Lower Hawthorn	No Data	No Data	Payson Tract

Aquifer	East (901)	North (901)	Permittee
Lower Hawthorn	No Data	No Data	Payson Tract
Lower Hawthorn	No Data	No Data	Payson Tract
Lower Hawthorn	No Data	No Data	Payson Tract
Lower Hawthorn	No Data	No Data	Payson Tract
Sandstone Aquifer	480936	912166	Six L's/Farm 1
Sandstone Aquifer	477404	910422	Six L's/Farm 1
Sandstone Aquifer	473336	906913	Six L's/Farm 1
Sandstone Aquifer	481146	905309	Six L's/Farm 1
Sandstone Aquifer	481285	901614	Six L's/Farm 1
Sandstone Aquifer	479472	898081	Six L's/Farm 1
Sandstone Aquifer	478473	912212	Six L's/Farm 1
Floridan Aquifer System	601855	1043859	Section 6 Citrus Development
Floridan Aquifer System	605370	1043219	Section 6 Citrus Development
Floridan Aquifer System	605448	1044312	Section 6 Citrus Development
Floridan Aquifer System	605655	1040669	Section 6 Citrus Development
Floridan Aquifer System	605547	1042057	Section 6 Citrus Development
Floridan Aquifer System	602298	1042746	Section 6 Citrus Development
Floridan Aquifer System	602396	1041407	Section 6 Citrus Development
SFWMD Canal (C-39A)	606482	1045139	Section 6 Citrus Development
Sandstone Aquifer	481366	886323	Bowen-South
On-site Lake(s)	478037	886524	Bowen-South
Sandstone Aquifer	485073	901022	Muse Farm
Sandstone Aquifer	479682	879135	Kinser Grove
Sandstone Aquifer	479820	877592	Kinser Grove
Sandstone Aquifer	482044	879145	Kinser Grove
Sandstone Aquifer	478741	880118	Kinser Grove
Sandstone Aquifer	475220	882005	Kinser Grove
Sandstone Aquifer	479584	879183	Kinser Grove
Sandstone Aquifer	479538	877035	Kinser Grove
Sandstone Aquifer	476221	881866	Kinser Grove
Sandstone Aquifer	475964	883117	Kinser Grove
On-site Lake(s)	480284	880303	Kinser Grove
On-site Lake(s)	475044	881957	Kinser Grove
On-site Lake(s)	476465	883916	Kinser Grove
Sandstone Aquifer	475330	883173	Dyess Groves